Rapport nr. 90.065
NTNF project no. MB10.20346

GEOCHEMISTRY OF PLATINUM METALS IN OPHIOLITES IN NORWAY

FINAL REPORT

VOL.1

NORGES GEOLOGISKE UNDERSØKELSE

Postboks 3006 - Lade
7002 Trondheim
Tlf. (07) 92 16 11
Telefax (07) 92 16 20

RAPPORT

Rapport nr. 90.065	ISSN 0800-3416	Åpen/Fortrolig til

Tittel:

NTNF project no. MB10.20346 Geochemistry of platinum metals in ophiolites in Norway, Final report.

Forfatter:	Oppdragsgiver:
R.Boyd, L.-P.Nilsson, R.-B.Pedersen, S.Bakke, T.Boassen, T.Grenne, A.Grønlie, G.M. Johannesen	NGU - N-Trøndelagsprogrammet/NTNF/ Universitetet i Bergen
Fylke: Troms, Nordland, N-Trøndelag, S-Trøndelag, Sogn og Fjordane, Rogaland	Kommune: Lyngen, Rødøy, Hattfjelldal, Leka Røros, Vik, Karmøy
Kartbladnavn (M. 1:250 000) Nordreisa, Vega, Mosjøen, Røros, Odda, Haugesund	Kartbladnr. og -navn (M. 1:50 000) 1634 IV Lyngstuva, 1828 II Rødøy, 1926 II Hattfjelldal 2026 III Krutfjell 1725 III Leka, 1720 III Røros, 1316 IV Myrkdalen, 1113 I Haugesund, 1113 II Skudeneshavn
Forekomstens navn og koordinater:	Sidetall: Vol.1: 44 Vol.2: 220 Pris: kr. 300,- Kartbilag:

Feltarbeid utført:	Rapportdato:	Prosjektnr.:	Seksjonssjef:
	31.03.90	67.2437.00/67.1889.79	

Sammendrag:

The project has documented the existence of several previously unknown platinum group element (PGE) mineralizations in Norwegian ophiolites, of a type previously not well-documented anywhere, i.e. stratiform platinum-palladium-gold mineralization in ultramafic cumulates in ophiolites. PGE-bearing podiform chromitite and high level Ni-Cu sulphide mineralizations have also been studied. It has been documented that PGE-enrichment in the ultramafic bodies hosting the podiform chromitites is confined to the chromitite bodies. Both the podiform chromitite and Ni-Cu sulphide mineralizations are of such limted tonnage that they have no economic interest. The stratiform PGE mineralizations found so far, in the Leka and Lyngen ophiolites are submarginal but are sufficiently rich and of sufficient dimensions that they are considered to indicate a possible potential for mineralizations of economic interest in these complexes and in all others with well developed, laterally extensive sequences of olivine-rich cumulates. This conclusion has relevance for prospecting in general for PGE-mineralizations, and could be particularly important if the present supply-demand situation for the PGE were to change.

Emneord	Petrologi	
Platinametaller	Malmgeologi	
Geokjemi		

CONTENTS

Volume 1

Volume 2

Papers published/manuscripts in preparation

The following papers resulted from the pilot project: page

The following papers, published or in preparation, result from/are intimately related to the topics of the present project (with reference to the appropriate chapter in the main report):

1. INTRODUCTION

1.1 Project concept and organization

The current project was preceded by a pilot project entitled: Geochemistry of platinum metals in rocks and ores in Norway: Pilot Project (Barnes et al. 1987). The pilot project involved the analysis of 385 samples from a range of geological environments for platinum group elements (PGE) and gold. The environments included Ni-Cu deposits, of which two in oceanic crustal rocks, chromite deposits in ophiolitic rocks and chromite-bearing rocks from ophiolites.

The most important conclusion reached during the pilot project was that: "Results from only one of the geotopes sampled, ophiolites and related rocks, give an indication of possible economic interest." The following recommendations for further work in this respect were made: "The specific targets located so far considered to merit further study are:

- chromite-olivine cumulates in the Leka ophiolite
- chromite-bearing harzburgites forming isolated ultramafic bodies, i.e. Osthammeren, Skamsdalen, Aurtand and Ørnstolen
- the potential for further Cu-Ni-PGE mineralizations of the Fæøy type in the Karmøy ophiolite.

Critical topics to be examined in the Leka ophiolite will be the lateral and vertical extent of the Os-Ir-Ru enrichment, geochemical variations within the enriched zone, the mineralogical residence of the PGE and the processes leading to their concentration.

In the isolated harzburgite bodies the critical question in an economic evaluation will be whether the PGE are exclusively linked to chromite. All the chromite mineralizations found to date are very small."

The present project was formulated with the aims of examining these topics. It encompasses an evaluation of the processes leading to PGE enrichment, in both petrological and economic-geological contexts.

Organization

Much of the project was carried out through collaboration between the Geological Survey of Norway (NGU) and the Geological Institute, Div. A, University of Bergen (UiB). The project was led from NGU and carried out by workers from NGU (R. Boyd and L.-P.Nilsson) and UiB (R.-B. Pedersen and G.M. Johannesen). The project has thus been able to benefit from the considerable expertise on ophiolites which has been built up at UiB over the last 10-15 years. During the lifetime of this project NGU has carried out work on three scientifically related but organizationally unrelated projects, on parts of the Lyngen ophiolite (T.Grenne), on PGM in heavy mineral concentrates from the Raudberget talc deposit, Vik, Sogn (S.Bakke, T.Boassen, L.-P. Nilsson) and on the Lillefjellklumpen Ni-Cu-PGE mineralization in N-Trøndelag (A.Grønlie): these projects are also covered in this report for the increase in scientific completeness which they allow.

The project has also involved collaboration with geoscientists from the Geological Institute at the University of Trondheim (NTH); Dept. of Earth Sciences, Open University, England; Sciences de la Terre, Universite du Quebec, Canada; Dept. of Earth Sciences, Memorial University of Newfoundland, Canada. Most of the analytical work for PGE and gold was carried out by Sheen Analytical Services, Perth, Australia because methods with the detection levels and precision required were/are not available on a commercial basis, and probably not from research laboratories either, in Europe. Further analytical work was carried out by Caleb Brett Laboratories, St.Helens, UK (Pt,Pd and Au analyses in the pilot project) and by X-Ray Assay and Chemex Laboratories, Toronto, Canada (PGE and Au analyses on Lillefjellklumpen). Control analyses were carried out at Memorial University of Newfoundland.

Scope of the project

The project has, in its broadest sense, i.e. including work not financed by NTNF, encompassed studies of the following:

- isolated ultramafic complexes and related chromitite mineralizations, mainly in the Røros area and in Nordland (Nilsson)
- heavy-mineral fractions from the Raudberget talc deposit,Vik, Sogn (Bakke, Boassen,Nilsson)
- chromitites in dunite/pyroxenite lenses, dykes and veins in the Leka ophiolite (Pedersen, Johannesen)
- ultramafic cumulates and related chromite, sulphide and arsenide enrichments in the Leka ophiolite (Pedersen, Johannesen)
- a reconnaissance of several ultramafic pods and of ultramafic/mafic cumulates in the Lyngen ophiolite (Grenne)
- the Lillefjellklumpen Ni-Cu-PGE mineralization in the Gjersvik island arc complex (Grønlie)
- the PGE geochemistry of the volcanic suites in the Karmøy ophiolite (Pedersen). The Fæøy Cu-Ni-PGE mineralization which is part of the dyke complex in the Karmøy ophiolite was not studied because it is currently the topic of a thesis being carried out at Memorial University.

The location of the areas studied is shown on a tectonostratigraphic base map (modified from Roberts & Gee 1985 and Furnes, Roberts, Sturt, Thon and Gale 1980) in Fig.1 and their position in an idealized ophiolite pseudo-stratigraphy in Fig.2. Fig. 2 also shows the position of certain types of gold mineralization being considered in a parallel NTNF project led by Professor F.M.Vokes, geologisk inst., NTH.

Almost all of the subprojects indicated above will result in manuscripts for publication in scientific journals, some already have. The report has therefor, in order not to delay this process, been compiled largely from manuscripts in varying degrees of readiness for publication. The report has been written in English for this reason, and in order to make the report itself readily accessible to the international prospecting industry. Volume 1 gives brief descriptions of the work carried out, with emphasis on the conclusions reached: the complete papers/manuscripts are given in Volume 2. For certain subprojects such manuscripts have not yet been completed (Karmøy and Lyngen).

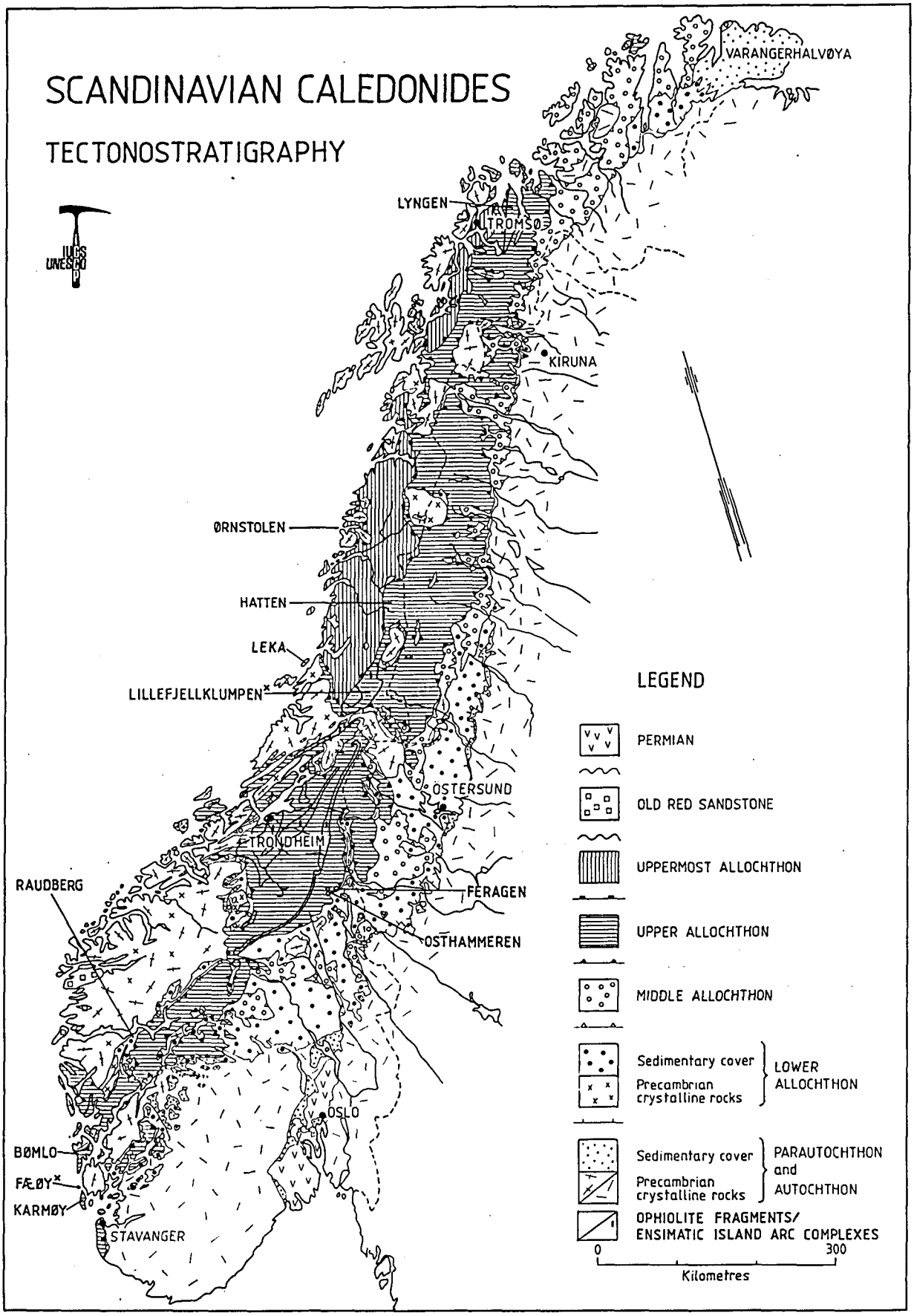

Fig. 1: Tectonostratigraphic map of the Scandinavian Caledonides (Roberts & Gee 1985), showing major ophiolite and ensimatic island arc complexes (modified from Furnes et al. 1980). Complexes/deposits in which noble metal concentrations have been studied are named.

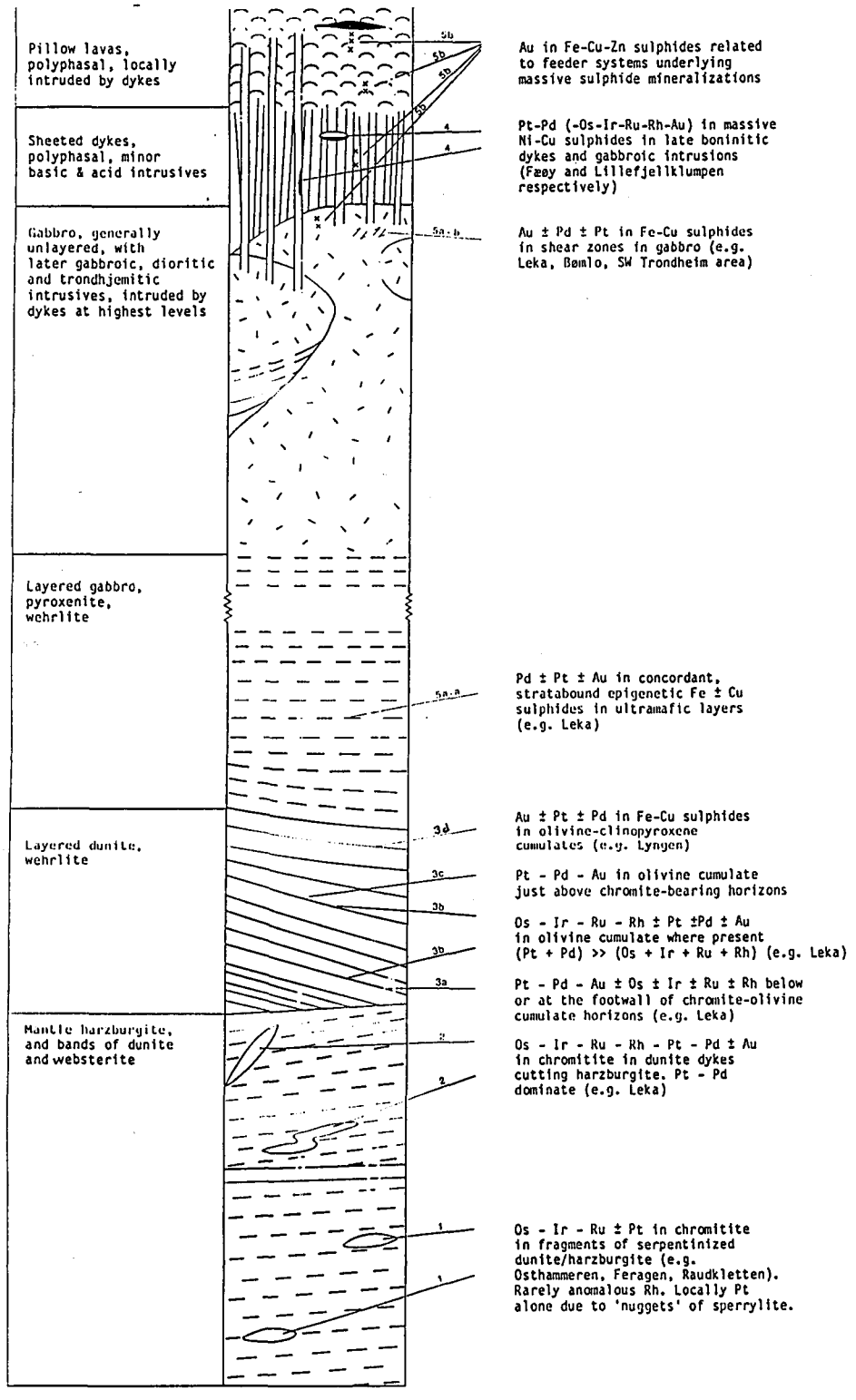

Fig.2: Ophiolite pseudostratigraphy showing the generalized location of noble metal mineralizations found in Norwegian complexes to date.

1.2 Background information on the platinum metal geochemistry of ophiolites

Until the advent of the Inductively Coupled Plasma-Mass Spectrometer (ICP-MS) in the latter half of the 1980s the technology for analysis of all the PGE and gold at, or close to background levels in the rocks of ophiolite complexes was not readily available. Thus Crocket (1981), in an exhaustive survey of the literature to that date, could present only very limited data on the Os,Ru and Rh contents of chromite-free ultramafic rocks in ophiolites and no data for the contents of these elements in sulphide-free mafic rocks in ophiolites. Barnes et al. (1988) presented a summary of analytical data on the PGE-content of several suites of volcanic rocks, showing that the contents of these elements was still only loosely constrained in boninites and ocean floor basalts, both at the lower and upper levels of the assumed range of concentration.

A summary of the data available on the PGE and Au contents of chromite-/sulphide-free rocks from oceanic crustal environments is given in Table 1.

ROCK TYPES	Os	Ir	Ru	Rh	Pt	Pd	Au	n
Boninites	-	<0.01-0.1	-	-	-	6.9-35	0.68-3.3	12
MOR-basalts	<0.086	0.0011-0.116	-	-	-	<0.1-6.29	-	12
Mafic cumulates	0.02	0.017-0.033	-	-	4.5	3.0-3.1	0.17	11
U.mafic cumulates	0.02-0.21	0.05-2.4	-	-	17-28	0.9-29	0.52-2.2	35
Harzburgite	3.95-6.7	2.2-7.29	-	-	4.99-10	2.04-9.5	0.33-1.8	35
Mantle ave.	4.2	4.4	6	2	9.2	4.4	1.4	114

Table 1: PGE and Au contents of rocks in oceanic crustal environments (from Barnes et al.1985: Barnes et al. 1988)

The harzburgites which are assumed to represent tectonized mantle have PGE and Au concentrations of the same order of magnitude as the mantle values which is as to be expected if they can be regarded as undepleted,if tectonized mantle. The ultramafic and mafic cumulates which are specifically not chromite-bearing, are depleted in Os and Ir (and probably also in Ru), i.e.the sub-group of the PGE known as IPGE, which can be explained by the prior fractionation of chromite, in which these elements are enriched.

MOR-basalts are also characterized by a high ratio of PPGE (Rh+Pt+Pd) to IPGE which is again consistent with prior removal of chromite. However normal models for the formation of MORB indicate 10-20% melting of the mantle which would suggest that all sulphide would have melted, with all the PPGE partitioning into the sulphide. This would give a content of PPGE one to three orders of magnitude higher than that which is observed (Barnes et al. 1985). Possible explanations are (Barnes et al. 1985):

- retention of some sulphide (and PPGE) in the mantle.
- prior depletion of PPGE from the mantle from which the MORB melted.

- removal of sulphides from MORB before its extrusion (Czamanske & Moore 1977).

The work done within this project tends to confirm the feasibility of the third explanation.

Available data indicates that boninites have PGE concentrations of the same order of magnitude as MORB but that they are depleted in Cu, Au and possibly Ni relative to MORB (Barnes et al. 1988) which could indicate a prior melting event (Hamlyn et al. 1985). Hypothetical primary magmas of boninitic character have been considered as one of the two magma types involved in the formation of the Bushveld and Stillwater layered intrusions (Irvine & Sharpe 1982)

1.3 Known platinum metal mineralizations in ophiolites

The literature contains documentation of several types of PGE-bearing mineralization in ophiolite complexes. These are:

- podiform chromitites in mantle harzburgite (many examples)
- stratiform chromitite in ultramafic cumulates (two examples)
- stratiform sulphide in ultramafic cumulates (two examples)
- stratiform sulphide in mafic cumulates (one example)
- hydrothermal sulphide/arsenide mineralizations at various levels (several examples)
- massive sulphides at higher levels in ophiolites (several examples).

Podiform chromitites in mantle harzburgite

Among the areas/ophiolite complexes in which podiform chromitites have been analyzed for PGE are southwest Oregon (Page 1969: Page et al. 1975), the Semail Ophiolite, Oman (Page et al. 1979), New Caledonia (Page et al. 1982) and Morocco (Fischer et al. 1988). Chromitites from a number of ophiolites in the Caledonian orogen have been analyzed for PGE: these include the Bay of Islands and White Hills complexes on Newfoundland (Page & Talkington 1984) and the Unst ophiolite on Shetland (Gunn et al. 1985:Prichard et al. 1986). In almost all cases these mineralizations are enriched in IPGE with total PGE rarely exceeding 1 ppm: in a study involving 323 samples from deposits in California and Oregon 10% of the samples were found to have more than 0.17 ppm Ir, 0.32 ppm Ru, 0.026 ppm Rh, 0.064 ppm Pt and 0.01 ppm Pd (Page et al. 1986): the richest individual sample reported from the same study contained 2.93 ppm Ir, 4.93 ppm Ru, 0.074 ppm Rh, 1.18 ppm Pt and 0.005 ppm Pd. The Cliff mineralizations on Unst are an exception in relation to all podiform chromitites described so far in the literature as regards their absolute concentration of PGE (up to >70 ppm PGE) and the predominance of PPGE in relation to IPGE (Pd/Ir ratios of 10-12 while 'normal' podiform chromitites have Pd/Ir ratios of 0.01-0.1).

Numerous papers have described the platinum group minerals (PGM) in podiform chromitite deposits (Chang et al. 1973: Talkington et al. 1984: Legendre & Auge 1986: Prichard et al. 1986: Auge 1988 among others): these show that most deposits, the Cliff type obviously being an exception, are dominated by laurite (RuS_2), IPGE alloys and IPGE arsenides.

Few papers give information on the economic significance or otherwise of the PGE content of the chromitite deposits, some of which reach a size of two million tons (Auge 1988). An exception is Page et al. (1986) who conclude that the potential supply of by-product PGE from mining podiform chromite deposits is small: their estimate of the total world resource of Pt in podiform chromite deposits was roughly one-sixth of the quantity imported annually to the United States. World annual consumption of the IPGE which are predominant in most podiform chromite deposits is met by by-product production from Pt-Pd and Ni-Cu deposits and would probably not justify any additional capacity even if the deposits had tonnages of sufficient grade to be of theoretical interest in relation to the metal prices. An exception again would be mineralizations of the Cliff type, because of their high content of Pt and Pd, if these could be found with an adequate tonnage: indications are that the mineralizations on Unst itself are much to small to be of economic interest in themselves.

Stratiform chromitite in ultramafic cumulates

The first example of this type of mineralization to be described is in the Acoje block of the Zambales Ophiolite in the Philippines (Abrajano & Bacuta 1982: Bacuta et al. 1988). The mineralization was earlier known purely as a stratiform Ni-Cu sulphide mineralization with by-product Pt (Hulin 1950: Parangit 1975). Unfortunately both of the first-mentioned references are abstracts only. The mineralization is described as being a visible Ni-Cu sulphide mineralization associated with stratiform chromitite in dunite-wehrlite cumulates. Its PGE content is given as 30-460 ppb Ir, 830-1100 ppb Ru, 2.6-759 ppb Rh, 2.8-5958 ppb Pt and 2.3-8351 ppb Pd: no indication is given as to values which could be regarded as representative of the deposit as a whole but it is indicated indirectly that the deposit has considerable dimensions and that it is of potential economic interest.

PGE-enrichment in chromite cumulates has also been described from the 3.5 Ga-old Jamestown Ophiolite Complex in S. Africa (de Wit & Tredoux 1988). The mineralization is reported to be enriched in PPGE but it is of extremely limited extent (20-30 cm thick with a strike length of 10m).

Stratiform sulphide in ultramafic cumulates

Orberger et al. (1988: 1989) also describe PPGE enrichment associated with Ni-Cu sulphides in the Acoje block of the Zambales ophiolite: they describe this mineralization however as being independent of any chromite accumulation. It is not entirely clear whether this is a separate mineralization from that described by Bacuta et al. (1988). Afurther example, in the Wadi Onib-Hamisana ophiolite, Sudan, is mentioned in an abstract by Abdelrahman & Matheis (1990): no grades are given.

Stratiform sulphide in mafic cumulates

The one definite example known to the authors is in the Semail ophiolite and was described in a recent abstract by Lachize et al. (1990). It occurs in gabbronoritic cumulates and includes disseminated and massive (30-40%) sulphides. An analysis of "one of the richest layers" gives <8ppb Os, <3ppb Ir, 32 ppb Ru, 4 ppb Rh, 37 ppb Pt, 130 ppb Pd and 150 ppb Au. This implies that the contant of PGE+Au in total sulphides is fairly low; at four times the absolute values it would be 1.4 ppm.

Hydrothermal sulphide/arsenide mineralizations at various levels

This group includes several types of mineralization:

- cobolt-arsenide mineralization in carbonate lenses in serpentinized harzburgite in the Bou-Azzer Ophiolite, Morocco (Fischer et al. 1988): this mineralization is rich in gold (>10 ppm) and generally contains < 100 ppb PGE but locally has values of Pt up to > 2 ppm.
- Cu-Ni-Co sulphide at the periphery of podiform chromite bodies in the Othris Ophiolite (Economou & Naldrett 1984): the analyses show values up to 256 ppb Pt, 213 ppb Ru and 525 ppb Au. Pd is >10 ppb and the high Pt/Pd ratio coincident with a high Cu/Ni ratio is among the factors indicating a hydrothermal origin. The mineralizations are small (the chromite deposits do not exceed 40,000 tons).
- Cu-sulphide in chloritite in shear zones in the Troodos and Leka ophiolites (Vokes 1987). The mineralizations at Leka contain up to 240 ppb Pd (Vokes pers. comm. 1989) but have Au values up to 4.2 ppm.

Massive sulphides at higher levels in ophiolites

Deposits of this type include the Lillefjellklumpen deposit in the Gjersvik Island Arc Complex (Grønlie 1988), the Fæøy deposit in the Karmøy Ophiolite (Boyd et al. 1988) and the Illinois River deposit in Oregon (Foose 1986). All of these are Cu-Ni sulphide deposits with up to several ppm of both Pt and Pd in massive sulphides though they occur at differing positions in the pseudostratigraphy, the Illinois River deposit in mafic cumulates, the Fæøy deposit as a lens in a sheeted dyke complex and the Lillefjellklumpen deposit in a small high-level gabbroic intrusion. All three are small.

2. PLATINUM METALS IN ISOLATED ULTRAMAFIC BODIES AND PODIFORM CHROMITITES

2.1 Summary

Samples of chromitite mineralization and host rock from 39 isolated ultramafic complexes have been analyzed for PGE and Au (Tables 2-5). The anomalous PGE values found are confined to samples from the chromite mineralizations the size of which is such that they are not of economic interest even with the theoretical added value of their PGE-content.

The majority of chromitite deposits sampled and analyzed for all PGE would appear to have weakly or, less commonly, strongly anomalous concentrations of IPGE. A few have, at least locally, anomalous concentrations of PPGE: these include the Osthammeren and Ørnstolen mineralizations which have been studied in detail. The richest single analysis is from a sample of chromitite from the Osthammeren body in the Røros area: it contains 11 ppm total PGE, of which 9.3 ppm Pt. The average of 12 samples from Osthammeren is 1.5 ppm total PGE which is also the highest average for any single field of chromitite deposits.

The chromitites are, in some cases, of considerable mineralogical interest. Numerous platinum group minerals not previously reported in Norway have been found: several of these appear not to have been recorded elsewhere either. The mineralogical studies allow the division of the PGM into primary magmatic or late magmatic/hydrothermal minerals and secondary hydrothermal minerals and increase our knowledge of the degree of solid solution between the PGE-sulpharsenides.

2.2 Platinum-group mineral inclusions in chromitite from the Osthammeren ultramafic tectonite body; south central Norway

This subproject has involved a study of the PGE-geochemistry of the Osthammeren chromitite mineralization and its host serpentinite and a detailed examination of the platinum group minerals: the latter is the main topic of a brief paper which is in press (Nilsson 1990), of which a fuller version, as submitted for publication in Norsk Geologisk Tidsskrift, is included in Vol. 2 of this report.

Twelve samples of chromitite from Osthammeren and ten of the host serpentinite have been analyzed for all the PGE and Au (Table 6), in addition to the initial analysis for Pt, Pd and Au in the pilot project. The average content of PGE+Au in the serpentinite samples was 39.6 ppb while the chromitite samples averaged 1500 ppb. This strong indication that significant PGE enrichment is confined to the chromitite rules out any economic potential in this mineralization.

The contents of the PGE and Au found in the serpentinite are within, or close to the ranges reported for the contents of these elements in mantle harzburgite by Barnes et al. (1985) except for Au which is 3.5 ppb higher at Osthammeren. The contents of the individual PGE in the average of the results from Osthammeren are similar to those reported from several chromitites described in the literature, e.g. Skyros (Economou 1986) and Harold's Grave, Unst (Prichard et al. 1986: Gunn 1989)(see Fig. 9 in the paper in Vol.2). The single sample containing 9.3 ppm Pt is atypical in relation to the other samples.

Table 2 (1)

Content of Au, Pt and Pd (ppb) in chromitite from ophiolite fragments and solitary ultramafic complexes, central Norway.
A compilation of datafrom the pilot project.

Location	Sample No.	Au	Pt	Pd	Ore type
Rødøya ophiolite fragment, Vefsn district:					
1. "Karoline" claim, close to Rødøygårdene	LP 1	28	43	110	massive, with little gangue
2. Top of Rødøyfjellet	LP 2	13	5	12	medium-grained moderate impregnation
Velfjord ophiolite fragment, South Helgeland district:					
3. Claim SW of Nævernes	LP 3	9	9	<2	medium-grained moderate impregnation
4. Claim SW of Nævernes	LP 4	2	22	5	massive ore/very strong impregnation
5. Holmen claim	LP 5	7	26	16	weak impregnation
6. Stort Haab mine	LP 6	2	13	<2	medium-grained strong impregnation
7. Fire Søskende claim	LP 7	2	12	<2	fine-grained impregnation
8. Haabet claim	LP 8	5	16	4	medium-grained strong impregnation
Feragen solitary ultramafite, Røros district:					
9. Forsøket mine	LP 9	41	7	<2	leopard
10. Geitsjøgruva mine	LP 10	5	24	11	massive
11. Skalgruva mine	LP 11	8	<3	<2	massive (very little gangue)
12. Loc. no. 70, mine	LP 12	5	13	5	massive
13. Rødtjerngruva mine	LP 13	5	<3	<2	massive/very strong impregnation
14. Leighgruva mine	LP 14	2	6	<2	fine-grained strong impregnation
15. Røragsgruva mine	LP 15	5	11	<2	leopard (scattered)
16. Loc. 18	LP 16	4	4	<2	leopard (dense)
17. Skalgruva mine	LP 17	4	6	<2	pique-ore
18. Jakobine mine	LP 18	5	<3	<2	fine-grained weak impregnation
19. Amalie mine	LP 19	5	4	<2	schlieren impregnation
20. Rødtjerngruva mine	LP 20	4	<3	<2	fine-grained impregnation/leopard ore
21. Jacobine (?) mine	LP 21	5	<3	<2	pique ore (3 parallel bands)
22. Jacobine (?) mine	LP 22	2	8	<2	fine-grained impregnation/pique-ore
23. Stampen mine	LP 23	5	10	<2	medium-grained strong impregnation/pique ore (dense)
Raudhammeren ultramafite, Røros district:					
24. Loc. 118	LP 24	3	<3	<2	medium-grained strong impregnation/leopard ore
25. Loc. 119	LP 25	16	31	<2	massive ore (cross-cut by late cabonate-serpentine veins)
26. Loc. 121	LP 26	32	15	<2	massive ore
27. Loc. 124	LP 27	3	6	<2	patchy/banded impregnation (very uneven)
28. Loc. 124	LP 28	4	36	2	massive ore
29. Loc. 125	LP 29	2	8	<2	banded ore (mm-cm thick bands)
Storgråberget ultramafite, Røros district:					
30. Loc. 132	LP 30	2	4	<2	massive ore/impregnation ore (very uneven)
31. Loc. 135	LP 31	2	<3	<2	massive ore
Osthammeren ultramafite, Røros district:					
32. Loc. 132	LP 32	8	760	<2	massive ore (very little gangue)
Brorhaugen ultramafite, Røros district:					
33. Loc. 141	LP 33	152	79	<2	massive ore (from vein)
Klettene ultramafite, Røros district:					
34. Loc. 145	LP 34	2	12	3	fine-grained impregnation/patches/ schlieren (very uneven)
35. Loc. 146	LP 35	4	4	<2	massive
36. Loc. 147	LP 36	4	4	<2	massive ore (strongly brecciated by late magnesite-serpentine veins)
Tollefshaugen ultramafite, Grimsdalen,					
37. Loc. 185	LP 37	6	<3	<2	medium-grained patchy/banded impregnation
Raudhamran ultramafite, Haverdalen, Dovre district:					
38. Loc. 186	LP 38	3	5	<2	medium-grained impregnation ore
39. Loc. 187	LP 39	3	<3	2	fine-grained/patchy impregnation in bands
40. Loc. 187	LP 40	2	7	<2	medium-grained patchy impregnation
41. Loc. 190	LP 41	<1	6	<2	fine-grained/medium-grained impregnation
Skamsdalen ultramafite, Lesja district:					
42. Skamsdalen mine	LP 42	4	88	26	medium-grained strong impregnation/massive ore
43. Skamsdalen mine	LP 43	120	178	156	massive ore
Nysetri ultramafite, Lesja district:					
44. Nysetri mines, Loc. 97	LP 44	3	16	<2	medium-grained impregnation ore
45. Nysetri mines, Loc. 95	LP 45	3	16	3	fine-grained to medium-grained patchy impregnation
46. Nysetri mines, Loc. 95	LP 46	3	11	<2	fine-grained to medium-grained patchy impregnation

2
Table (X) cont.

Location	Sample No.	Au	Pt	Pd	Ore type
Lesjehorrungane ultramafites, Lesja district:					
47. Aurtand (= Sjong) mine	LP 47	2	13	2	fine-grained to medium-grained impregnation ore
48. Aurtand (= Sjong) mine	LP 48	5	427	104	medium-grained strong impregnation
49. Severine claim	LP 49	4	<3	<2	medium-grained strong impregnation
50. Severine claim	LP 50	3	12	2	rel. weak impregnation ore/leopard ore
51. Halvfarhøi mine	LP 51	2	4	<2	strong, patchy impregnation ore
Dørkampen ultramafite, Skjåk district:					
52. Dørkampen, loc. 66	LP 52	3	13	<2	impregnation/leopard ore
53. Dørkampen, loc. 68	LP 53	4	9	<2	impregnation/leopard ore
54. Dørkampen, loc. 69	LP 54	2	9	<2	medium-grained strong impregnation/ (compact ore)
Krosshø ultramafite, Grotli area, Skjåk district:					
55. loc. 61	LP 55	3	7	<2	medium-grained impregnation
Feragen ultramafite, Røros district:					
56. Mynta mine	LP 56	<1	<3	<2	leopard ore (coarse patches)
57. Falkestien mine	LP 57	<1	<3	<2	pique ore
58. Skalgruva mine	LP 58	<1	<3	<2	pique ore/leopard ore (dense)
59. Svinet mine	LP 59	<1	<3	<2	medium-grained strong impregnation/pique ore
60. Leigruva mine	LP 60	1	3	<2	leopard ore/banded ore
61. Leigruva mine	LP 61	5	<3	<2	leopard ore (very coarse chr-patches)
62. Liegruva mine	LP 62	2	7	6	pique ore (very weak); i.e. scattered)
63. Rødtjerngruva mine	LP 63	3	3	<2	leopard ore
64. Liegruva mine	LP 64	1	7	3	massive (very little gangue)
Glupen ultramafite, Sunndal district:					
65. Glupen mine	LP 65	<1	6	<2	leopard ore (coarse patches within fine-grained impregnation)
Ørnstolen ultramafite, Selsøy, Rødøy kommune, North Helgeland district:					
66. Ørnstolen claims, loc. 1	AK 1	32	22	74	
67. Ørnstolen claims, loc. 2	AK 2	138	6	<2	
68. Ørnstolen claims, loc. 3	AK 3	11	56	63	
69. Ørnstolen claims, loc. 4	AK 4	718	299	1391	
70. Ørnstolen claims, loc. 5	AK 5	10	7	10	
of the 70 samples 66 are: non-anomalous to weakly anomalous					
Arithmetic mean (n = 66)		9.92	12.02	6.15	
Geometric mean (n = 66)		3.80	6.66	1.80	

where <x is calculated as $\bar{x}^2$
Anomalous samples (No. 32, 43, 48 and 69 are excluded)
Analyst: Caleb Brett Laboratories Ltd., St. Helens, UK (28-07-1986)
Method: Fire Assay and atomic absorption spectrometry.

Content of platinum-group elements (PGE) and Au in ppb in 4 anomalous chromitite samples from a pilot study comprising 70 chromitite samples (ref. Table). In addition analysis of host serpentinite from Osthammeren (sample LPN78-139.

Location	Sample No.	Os	Ir	Ru	Rh	Pt	Pd	Au
1. Osthammeren, Røros district	LPN78-139	5.5	5.2	6.2	0.9	1.7	1.7	11.8
2.	LP32	174.2	674.4	841.	65.2	323.4	2.9	4.9
3.	LPN32-REP	166.3	659.2	835.8	64.9	316.1	3.0	5.2
4. Skarnsdalen, Lesja	LP43	37.2	47.8	128.1	21.7	265.3	157.0	56.2
5.	LP43-REP	36.1	46.7	120.2	20.6	252.6	149.7	52.8
6. Aurtand, Lesja	LP48	20.2	51.8	67.9	36.1	88.9	29.3	6.1
	LP48-REP	20.5	50.4	64.3	34.1	83.5	27.6	8.4
7. Ørnstolen, Selsøy, Rødøy	AK4	10.5	25.0	40.9	9.7	397.7	1621.0	832.4

Analyst: Memorial University of Newfoundland, St. John's, Newfoundland, Canada (ca. Dec. 1987?).
Method: Fire Assay and ICP-Mass Spec'

Table 3

Content of platinum-group elements (PGE) and Au* in ppb in chromitite and host rocks and copper-magnetite mineralizations from solitary ultramafites, central Norway. A compilation of data.

Location	Sample	Os	Ir	Ru	Rh	Pt	Pd	Au	Ore type/host rock
1. Svartåsen, Røros district	Svart-1	40	31	66	6.5	2.5	9.0	4	impregnation ore
2. Kjemsjøfjell, Alvdal v.fjell	Kjems-1	66	37	84	8.5	18	22	<2	strong impregnation, compact ore
3. Raudkletten, Folldal district	Raudk-1	160	100	240	9.0	8.0	15	12	massive ore in small pods
4. " , "	Raudk-2	96	160	230	25	99	5	8	massive ore in small pods
5. " , "	Raudk-4	10	19	53	6.5	1.5	11	<2	massive ore/dense leopard ore
6. Tolgenkletten,Tolga,N-ØsterdalTolge-1		10	7.0	16	2.5	1.0	13	2	schlieren impregnation
7. Fåsteen,Tynset,N.-Østerdal	Fåste-1	34	24	60	18	980	15	16	fine grained strong impregnation
8. " , " , "	Fåste-3	54	38	98	15	84	42	2	massive ore in schlieren
9. " , " , "	Fåste-4	60	31	100	4.5	6.0	9.5	<2	massive ore in schlieren
10. David claim, Feragen,	David-1	450	240	540	19	1.0	9.5	4	massive ore
Røros district	David-1 D	460	210	440	18	1.5	6.0	<2	" "
11. Vinkelen mine, " "	Vinke-1	24	22	80	6.5	2.5	16	6	massive ore
Røros district									
12. Elev claim, " "	Elev-1	20	17	57	5.5	2.0	7.5	4	massive ore
Røros district									
13. Bakos mine, " "	Bako-1	54	30	110	7.0	0.5	9.0	2	massive ore
Røros district									
14. Pikhågen, Selsøy, Rødøy	Pikhå-1	24	21	56	7.5	47	54	<2	impregnation/compact ore
15. Ørnstolen, Selsøy, Rødøy	Ørnst.-1	12	12	42	5.5	4.0	7.0	12	fine-grained impregnation ore
16. " , " , "	Ørnst.-3-1	38	36	54	8.5	160	77	10	fine grained impregnation ore
17. " , " , "	Ørnst.-3-2	10	5.5	25	3.5	16	14	8	serpentinite-tremolite rock
18. " , " , "	Ørnst.-3-3	4	<0.5	6.5	0.5	2.0	12	10	tremolite rich ultramafic rock
19. " , " , "	Ørnst.-3-4	32	27	73	12	5.0	13	4	strong impregnation/ compact ore
20. " , " , "	Ørnst.-6	2	<0.5	2.5	<0.5	3.5	32	2	ultramafic rock
21. " , " , "	Ørnst.-9	62	31	68	9.0	72	32	10	impregnation/compact ore
22. " , " , "	Ørnst.-14	4	<0.5	7.5	1.0	0.5	12	6	ultramafic rock
23. Ørnstolen, Selsøy, Rødøy	Ørnst.-17	<2	<0.5	4.0	2.5	15	37	4	hornblendite
24. Hatten, Hattfjelldal	Hatt-1	2	2.0	<0.5	1.5	160	11	250	copper-magnetite
ore									
	Hatt-1 D	(100)	(10)	2.0	2.5	120	6.5	240	"
25. " , "	Hatt-2	2	1.0	2.0	2.5	<0.5	17	550	"
	Hatt-2 D	(100)	(9)	4.5	4.0	7.5	12	530	"
26. " , "	Hatt-5	<2	0.5	4.0	1.5	2.0	12	200	"
	Hatt-5 DUP	(80)	8.5	4.5	3.5	4.5	11	190	"
27. " , "	Hatt-7	4	2.0	15	1.0	7.0	7.0	6	serpentinite (altered dunite)
28. " , "	Hatt-8	4	2.0	10	2.0	4.5	7.0	<2	" (" harzburgite)
29. Røddiken (Tuva), Hattfjelldal	Rødd-1	6	5.0	4.0	<0.5	2.0	6.0	<2	Cumulate impregnation ore

Analyst: Analytical Services (W.A.) PTY.LTD. Perth, Western Australia (24-05-1988)
Method: Fire Assay and ICP-Mass Spec'.
* Recovery of Au is not quantitative at levels below 500 ppb.

Table 4

Content of platinum-group elements (PGE) and Au* in ppb in chromitite and sulphide mineralizations (No. 14 and 33) from solitary ultramafites, central and northern Norway. A composition of data

Location	Sample No.	Os	Ir	Ru	Rh	Pt	Pd	Au	Ore type/host rock
1. Svarthølhaugen, Oppdal district	-501 B	20	18	35	11	2.5	7.0	<2	impregnation ore
2. " , " "	-501 C/2	36	19	40	9.0	3.5	5.5	2	impregnation ore
3. Vindalskammen, " "	-502 A/6	150	64	250	35	17	32	54	massive ore
4. " , " "	-502 B/2	34	27	45	12	3.0	20	<2	massive ore
5. Koppungen, Sunndal district	-503 A	16	19	24	9.5	3.0	4.0	<2	massive ore
6. Grønvoldsteinen, Sunndal district	-504 A	50	33	82	21	3.0	7.5	<2	massive ore (coarse grained)
7. " , " "	-504 C	760	260	760	41	600	34	58	massive ore (fine grained, strongly magnetic)
8. Storskarhø, " "	-505 C/2	12	17	28	11	4.5	5.5	8	massive/strong impregnation ore
	-505 C/2 DUP	14	17	30	11	4.0	5.0	8	" "
9. " , " "	-505 C/3	6	12	20	6.0	4.0	2.5	8	" "
10. Tronfjell (N-slope), Alvdal	-508 (A)	26	23	38	12	2.0	3.0	<2	strong impregnation/massive ore
11. " ("), "	-508 B	2	5.0	6.0	2.0	8.0	5.0	4	serpentinite/serp.dunite
12. " (Grytåa, SE of top) Alvdal	-509	<2	5.0	4.0	1.5	2.0	3.0	<2	serpentintie/serp.dunite
13. " (S of top) "	-510	<2	2.5	1.5	1.0	0.5	1.5	<2	olivingabbro
14. Hjelmkona, Halsa, Nord-Møre	-511	(62)	8.5	5.5	3.0	11	10	100	sulphide-impregnation (strongly weathered)
15. " , " , "	-512	32	20	40	9.5	6.0	14	6	strong fine grained impregnation/massive ore
16. " , " , "	-513	26	12	26	7.0	4.5	6.5	8	coarse grained, uneven, impregnation ore
17. Sjømæingen, Gjemnes, Nord-Møre	-514 D	44	24	43	11	5.0	5.0	<2	coarse-grained impregnation/ massive ore
18. " , " , "	-514 C/2	6	14	40	9.0	18	18	4	" "
	-514 C/2 DUP	4	12	44	11	22	19	8	" "
19. Holberget, Kolletholen, Folldal	-515 B	50	42	69	18	2.0	2.5	<2	massive ore
20. Rødøya (NE of Skarvhammeren),Vefsn	-516 A	10	13	22	8.0	1.0	4.0	<2	medium grained impregnation ore
21. Rødøya (Rødøyvågen), Vefsn	-516 B	16	4.0	20	7.5	5.5	12	<2	impregnation / massive ore
22. " ("), "	-521 B	8	2.0	12	4.5	10	18	4	massive ore
23. " ("), "	-522	26	14	51	23	9.0	13	6	massive ore
24. " ("), "	-525	12	4.0	22	8.0	6.0	18	<2	massive ore
25. " ("Karoline")	-527	18	5.5	35	15	4.0	12	<2	massive ore
26. Forhågen, Kvaløya, Tromsø	-529	4	1.5	6.0	2.0	2.5	6.0	<2	weak impregnation in serpentinite
27. " , " , "	-531	3	5.5	30	6.5	4.5	10	<2	strong impregnation in serpentinite
28. Kalvholmen, Hestmannøy area	JHLV-1	150	22	78	33	240	630	26	massive ore
29. Raudholmen, "	JHLV-2	6	3.5	16	6.0	5.5	15	24	massive ore
30. Lille Esjeholmen, Nesøy area	JHLV-3	8	3.5	13	6.5	4.5	15	6	massive ore
31. Ramberget, Hestmannøy	AK86-Kr 1B	10	2.0	6.5	3.5	10	15	16	impregnation ore
	" , DUP	12	2.0	7.0	4.0	11	17	10	"
32. " , "	AK86-Kr 2	4	5.0	2.0	7.0	5.5	3.5	4	massive ore
33. "Harsjø"-boulder, Harsjø-farms,	K (ca. 1946)	44	7.0	18	7.0	11	12	10	sulphide boulder with 12 % Cu and 2 % Ni

Analyst: Sheen Analytical Services LTD, Perth, Western Australia (14-04-1989)
Method: Fire Assay and ICP-Mass Spec'.
* Recovery of Au is not quantitative at levels below 500 ppb.

Table 5

TABLE A6

Content of PGE and Au in ppb in chromitites and host serpentinite from the Osthammeren ultramafic tectonite body.

Sample no.	Location (claim no./ loc. no. ref. to Fig. 3)		Os	Ir	Ru	Rh	Pt	Pd	Au	TOT	Ore-type/ host rock	Analyst/ analytical method
LPN78-138/2	9						760	<2	8		massive ore (PGM-anomalous sample)	1
-138/2	9		174.2	674.4	841.0	65.2	323.4	2.9	4.9		massive ore (PGM-anomalous sample)	2
		DUP	166.3	659.2	835.8	64.9	316.1	3.0	5.2			
										2068.5	Average of two analyses	
-139			5.5	5.2	6.2	0.9	1.7	1.7	11.8		serpentinite	
LPN87-1/1	1		62	41	100	8.0	25	9.0	10		transition disseminations/-	3
		DUP	54	39	100	9.0	7.5	30	10		massive ore	
-2	2		130	160	160	130	9300	79	200		massive ore	
		REP	380	73	150	22	39	6.5	8			
		REP	86	79	170	28	49	8.5	12			
-3	3		62	58	140	31	83	11	2		massive ore	
-4/1	4		140	130	230	19	79	28	6		massive ore in veins	
		DUP	130	110	190	28	120	6.0	6		and schlieren	
-4/3	4		120	110	180	17	84	5.0	2		massive ore	
-5	5		530	510	640	63	470	7.0	6		massive ore in vein	
		DUP	130	110	750	78	480	11	10			
-6/1	6		50	54	100	21	1000	19	20		massive ore in vein	
		REP	270	43	97	11	22	10	2			
		REP	44	44	130	13	24	40	2			
-8/1	8		92	90	170	18	72	28	4		transition dissemination -	
		DUP	70	73	150	26	68	27	4		massive ore in fine veins	
-9/1	9		550	420	590	34	160	22	12		massive ore in veins	
		REP	560	290	610	32	120	9.0	6			
		REP	560	430	550	35	190	34	8			
-9/2	9		670	490	640	50	430	20	2		massive ore in veins	
-10/1	10		570	470	520	27	210	8.5	10		massive ore in veins	
-10/2	10		1400	810	1400	73	350	6.0	30		massive ore	
		DUP	1100	610	1100	54	230	8.0	32			
			346	243	396	35	449	17	14	1500	Average of samples 1/1 to 10/2 n = 12	
-1/2	1		6	5.0	4.0	<0.5	2.0	6.0	<2		serpentinite	3
-4/2	4		6	6.5	8.0	1.0	<0.5	8.5	4		"	
-6/2	6		4	3.5	14	1.0	2.5	21	6		"	
-8/2	8		2	4.0	5.5	1.0	7.0	5.5	4		"	
-9/3	9		4	1.5	8.0	2.0	4.5	19	<2		"	
-12	12		2	2.0	5.5	1.0	1.5	4.5	2		"	
-13	13		2	6.0	12	1.5	3.0	15	2		"	
-14	14		2	2.5	35	1.5	7.5	6.0	<2		"	
-15	15		6	4.0	7.0	1.0	3.0	14	24		"	
-16	16		4	3.0	11	1.0	3.0	12	8		"	
			3.8	3.8	11.0	1.1	3.4	11.2	5.3	39.6	Average of samples -1/2 to 16 n = 10	

Analyst:

1 Caleb Brett Laboratories Ltd., St. Helens, UK

2 Memorial University, St. John's, Newfoundland, Canada

3 Analytical Services (W.A.) PTY.LTD, Perth, Western Australia

Method:

Fire Assay and atomic absorption spectrometry

Fire Assay and ICP-Mass Spec'

Fire Assay and ICP-Mass Spec'

The mineralogical studies have revealed the following two assemblages:

1. Os-,Ir-,Ru- and, to a lesser extent, Pt-bearing minerals in primary magmatic, euhedral-subhedral, small (under 20 microns) inclusions in fresh unaltered chromite. These consist of mainly single-phase inclusions of Os-free laurite, Os-laurite, osmiridium and a Pt-Ir-Os-Fe alloy. A few of the inclusions are associated with small blebs of Na-bearing hornblende or phlogopite, indicating the presence of volatiles at an early stage in the formation of the PGM.

2. Secondary PGM occurring as anhedral-subhedral, texturally complex grains or grain-aggregates up to 70 microns across and always found in cracks in chromite, usually in association with ferrite-chromite, a hydrothermal alteration product of chromite. These contain up to eight PGM plus Ni-sulphide and Ni-arsenide. The phases found include Os-free laurite, Os-laurite, erlichmanite, Ir-rich erlichmanite, native Os, iridosmine, osarsite, irarsite, hollingworthite, Rh-rich platarsite, Ru-rich platarsite, sperrylite, (Ir,Rh)SbS, IrSbS, Pd-antimonide (probably stibiopalladinite), (Ir,Pt,Pb)S_2 (possibly a new mineral) and the associated phases, pentlandite, heazlewoodite and niccolite.

2.3 Inclusions of platinum group minerals (PGM), base-metal sulphides (BMS) and sulpharsenide in chromitite and host rocks from the Ørnstolen ultramafic tectonite body, north central Norway

Five chromitite samples from the Ørnstolen ultramafic body were analyzed for Pt, Pd and Au in the pilot project (Table 2). Three samples contained 100-200 ppb Pt+Pd+Au while one contained 299 ppb Pt, 1391 ppb Pd and 718 ppb Au, values later confirmed by reanalysis at Memorial University.

The subproject reported here has included further whole-rock analyses of PGE and Au contents and a mineralogical study. Both are reported in full in a draft manuscript included in Vol. 2 of this report.

A further nine samples were analyzed in the course of this project, four chromitite samples and five samples of the host metaperidotite (see paper in Vol.2). The host rocks contain a prograde metamorphic assemblage consisting mainly of olivine, enstatite and tremolite, the only primary phase being chromite. The metaperidotites proved to have low contents of the IPGE, with an Ir content under half the estimated mantle average (Barnes et al. 1988), while Pt-, Pd- and Au-values, while still low (all single values <100 ppb) are significantly higher than the values reported for mantle harzburgite by Barnes et al.(1985), by a factor of two for Pt and Pd, and a factor of four for Au. None of the chromitite samples yielded values comparable to the richest sample analyzed in the pilot project, the highest values found being 383.5 ppb total PGE+Au, of which 160 ppb Pt. The average of the five chromitite samples is 223.2 ppb total PGE+Au. The strong enrichment in Pt, Pd and Au found in one sample analyzed during the pilot project must be very local. The restriction of the anomalous values to the chromitite precludes any economic potential in the area.

A few small PGM inclusions have been found in chromite grains in the

chromitite samples: the PGM found are laurite, Os-laurite and irarsite. The occurrence of an arsenic-bearing phase in what appears to be an inclusion in chromite is unusual (they are common in later-formed hydrothermal assemblages). A Pd-Bi-bearing phase was found in a sample of metaperidotite. Details of the base metal sulphides and sulpharsenides found are given in the complete report in Vol. 2.

2.4 Hydrothermal gold-enriched iron and iron-copper occurrences in the Hatten ultramafic tectonite lens, Hattfjelldal

Chromitite samples from the Hatten ultramafic body in Hattfjelldal are reported in the literature (Lunde & Johnsen 1928) as containing 0.83 ppm Pt. A reconnaissance of the area was therefore carried out in order to obtain samples of the chromitite: neither the locations nor the dimensions of the chromitite showings are, however described in the above reference and the mineralizations could not be found in the time available. Mineralizations containing magnetite and copper- and iron-sulphides, and located on shear zones, as described by Corneliussen (1891) and Vogt (1894) were however found and sampled.

The mineralizations sampled are of such limited extent that they have no economic significance: they are probably of the same type as the mineralizations described from the Troodos and Leka ophiolites by Vokes (1987), these also, so far as is known of quite limited size. The possibility of finding larger mineralizations of this type in other ophiolite complexes should not be excluded.

Of five samples analyzed for all the PGE+Au three contain Au values between 195 and 540 ppb, one of these also containing 140 ppb Pt (see paper in Vol.2 for complete analytical data): we have no explanation for the elevated Os and Ir contents reported for the three samples which were re-analyzed. Au values are available for a further twelve samples (see Table 3 in the report in Vol. 2): ten of these have values >100 ppb with a maximum of 3260 ppb. An examination of the mineralogy of the samples is in progress.

2.5 Platinum group minerals (PGM), gold and associated minerals in the Raudberg field ultramafic tectonites, Vik, Sogn og Fjordane, western Norway

The Raudberg area contains several ultramafic lenses with a combined surface area of just over 3 sq.km.: they are concentrically zoned from metadunite cores to serpentinite and then soapstone on their margins. The soapstone is being evaluated as a source of talc. The soapstone contains small amounts of sulphide and because of the ease with which these could be beneficiated their mineralogy and chemistry has been studied despite their low abundance.

Seventeen whole rock samples have been analyzed for all the PGE and gold. The results show erratic weak enrichment in several of the elements (see paper in Vol. 2 for complete analytical data). The richest single sample contains 46 ppb Os, 13 ppb Ir, 170 ppb Ru, 41 ppb Rh, 7 ppb Pt, 17 ppb Pd and 2 ppb Au. The highest single values for Pt, Pd and Au are found in a sample with 20, 62 and 16 ppb respectively. Samples of concentrate

prepared by relatively simple methods give enrichment of at least an order of magnitude, the richer of two concentrates giving 2.38 ppm PGE+Au, of which 350 ppb Pt, 580 ppb Pd and 340 ppb Au.

Because of the sparsity of the ore minerals, and of the noble metal-bearing phases within these, the mineralogical studies have been carried out on concentrates and therefore do not include any consideration of textural relationships between ore minerals and silicate matrix. The predominant ore minerals, in addition to chromite, are heazlewoodite and cobaltite in the metadunite, gersdorffite, heazlewoodite, cobaltite and pentlandite in the serpentinite and pentlandite in the soapstone, indicating decreasing As and Ni and increasing S contents from the cores of the bodies outwards. Most of the PGM found, except for irarsite, are alloys of Pt with other PGE. One PGE-telluride, michenerite, has been found and small amounts of non-PGE-bearing tellurium minerals are common.

3. PLATINUM METALS IN PODIFORM CHROMITITE IN DUNITE/PYROXENITE LENSES/DYKES/VEINS IN MANTLE HARZBURGITE IN THE LEKA OPHIOLITE

The mineralizations considered in the above chapter occur in isolated ultramafic lenses most of which are thought to have originated in sub-oceanic mantle or lowermost oceanic crustal rocks (i.e. ultramafic cumulates if they can be identified). By their nature it is not possible to reconstruct their geological environment and their degree of alteration /metamorphism often makes it difficult to determine their original character. The presence of a complete ophiolite stratigraphy with excellent exposure permits a much better understanding of the nature and origin of the mineralizations on Leka.

The lowermost part of the Leka Ophiolite Complex (LOC) consists of mantle harzburgite with a clear tectonic fabric and containing tabular dunite bodies and dykes and veins of dunite and pyroxenite. The latter contain, in many cases, a central zone, generally of disseminated chromite, but locally with massive chromitite zones 10-20 cm thick. These mineralizations do not have dimensions which give them any direct economic significance but they are important for an understanding of the processes controlling the distribution of the PGE in the complex.

Eighteen samples of chromite-free harzburgite, dunite and pyroxenite have been analyzed for all the PGE+Au. They all yielded low values <80 ppb total PGE+Au, compatible in general with the mantle average given by Barnes et al. (1988), except for a slight positive Ru anomaly which could possibly be an analytical artifact. Sixteen chromite-bearing samples were analyzed: they revealed a range from mantle concentration levels up to 8510 ppb, of which 4600 ppb Pt and 2700 ppb Pd. Comparison with Cr analyses shows a strong positive correlation between Cr-content and total PGE+Au-content and PPGE/IPGE exemplified by the Pt/Ir ratio (see Figs. 6 and 7 in the full manuscript in Vol. 2). The enriched samples have PGE contents atypical in relation to most podiform chromitites for which PGE-data is available in their enrichment in PPGE: the distribution pattern of the PGE resembles that found at the Cliff mineralization on Unst though at almost an order of magnitude lower absolute concentration (Fig. 3).

The correlation with Cr-contents indicates that chromite is important for the enrichment of the PGE though probably through the physical process of accumulation rather than through solid substitution in chromite. The two richest samples are from chromitite in pyroxenite dykes while almost all the low-PGE chromitite samples are from dunites: this may indicate that differentiation of the magma in the mantle is important for the formation of PPGE-enriched chromitites in this type of deposit.

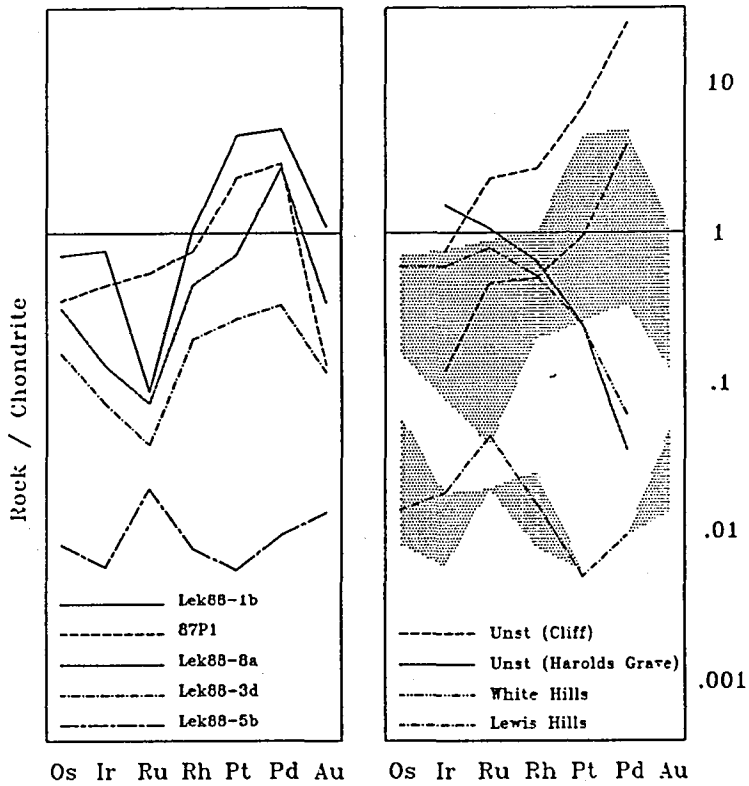

Fig.3: A) Chondrite-normalized PGE patterns of chromitites in dunitic bodies in mantle harzburgite in the Leka ophiolite.
B) Comparison of these with corresponding data from Unst (Prichard et al. 1986) and Bay of Island (Talkington & Watkinson 1986).

4. PLATINUM METALS IN ULTRAMAFIC CUMULATES

4.1 Summary

The platinum metal geochemistry of parts of the sequences of ultramafic cumulates in the Leka and Lyngen ophiolites has been examined. In the case of Leka this study had the advantage of building on a very detailed knowledge of the field geology, mineralogy and petrology of the rocks: the work done on Lyngen must be regarded as a reconnaissance. That stratiform enrichments of Pt,Pd and Au, albeit at subeconomic levels, were found in both complexes after examination of relatively limited parts of them, would seem to indicate a potential for richer mineralizations in both areas and a clear potential for PGE-mineralizations in ultramafic cumulates in ophiolites in general. The paper in Vol. 2 concludes with a model for the formation of the type of PGE-enrichment found on Leka and gives criteria which should be useful in a search for further mineralizations of this type, either in the LOC or other ophiolites. These criteria include association with reversals in the trend of cryptic variation in olivine composition, the actual composition of the cumulus olivines and a stratigraphic position above chromite-bearing horizons.

The stratiform mineralizations found on Leka are:
- Os-Ir-Ru-enriched chromitite with up to 500 ppb PGE+Au
- Pt-enriched olivine adcumulate with up to 1 ppm PGE+Au over 0.5 m
- Pd-enriched olivine adcumulate with up to 1 ppm PGE+Au over 0.5 m and up to 3 ppm in hand samples.

The mineralizations have been followed over a strike length of 1500m and have a probable total strike length of about 3000m. Hand samples from mineralized horizons outside the area studied in detail have also proved to be enriched in Pt, Pd and Au.

The mineralizations found in the Lyngen complex would appear to be of a slightly different type, occurring higher up in the cumulate stratigraphy, in association with Cu-dominated sulphides and without any, even indirect association with chromitite enrichments. They do not appear to have the same stratigraphic regularity as the mineralizations found on Leka. The highest concentration found was 551 ppb, of which 150 ppb Pt, 240 ppb Pd and 150 ppb Au.

4.2 Platinum metal abundances in the ultramafic cumulates of the Leka ophiolite

The examination of part of the sequence of ultramafic cumulates in the LOC represents the largest single subproject reported here. It has built on the work of H. Furnes and R.B.Pedersen and their colleagues at the University of Bergen (see paper in Vol. 2 for reference list) but has involved considerable additional hand sampling, the drilling of over 20 shallow drill holes (down to a maximum depth of 30 m), the analysis of several hundred samples for the PGE and Au, of a lesser number for other elements and a mineralogical study of the PGE-enriched horizons which is still in progress.

Analysis of hand samples collected at intervals of a few metres proved the existence of relatively weak enrichments of the IPGE (of the order of a few hundred ppb) in association with the most prominent chromitite horizon

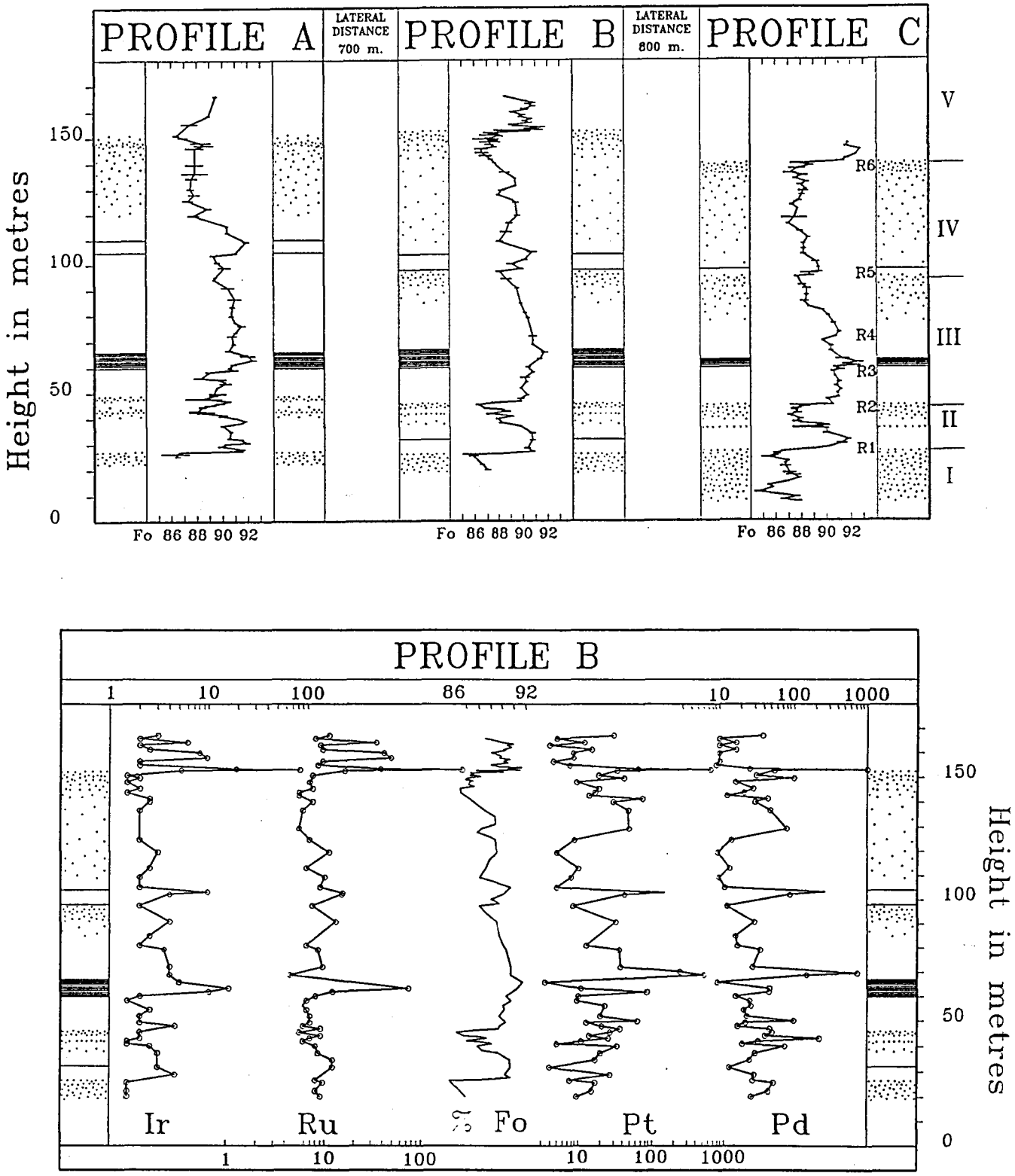

Fig.4: A) Cryptic variation of olivine across part of a sub-zone of olivine cumulates: profiles A,B and C are separated by 700 and 800 m respectively. Cyclic units which can be defined in the field are marked by Roman numerals. Reversals in cryptic variation are marked R1, R2, etc.
B) Variation of PGE content with height in Profile B.

in the sequence (Fig. 4), and with a chromite-bearing horizon at the base of a cyclic unit 100 m higher up in the stratigraphy (R6). The hand samples also indicated the existence of three horizons enriched in the PPGE, of which two contained >1000 ppb Pt+Pd. One of these was found immediately above the main chromitite while the two others were found at the bases of higher cyclic units.

In order to obtain complete intersections of the enriched horizons a number of drillholes (max. depth 30 m) were drilled in three profiles, the profiles having separations of 700 and 800 m (Fig. 5). Analysis of the drillcore (0.5 m lengths) confirmed the existence of the PPGE-enrichment just above the main chromitite (Figs. 4,5), showing that it consisted of two horizons, and showed the presence of PPGE-enriched horizons associated with the bases of the cyclic units immediately below (R2) and immediately above (R4) the main chromitite (itself characterized as R3). The enrichment associated with R6 was also found but the core samples had a maximum content of PGE+Au of 228 ppb, suggesting that the hand sample from this horizon, which contained over 2.2 ppm was collected from the richest part of the horizon. The enrichment found to be associated with R5 from the analysis of the hand samples was not intersected by any of the drillholes.

The richest drillhole intersection is in drillhole 87A1, across the lowermost enrichment above the main chromitite (R3) in profile B (Figs. 4,5). It contains 0.5 m of core with 1099 ppb PGE+Au, of which 140 ppb Pt, 780 ppb Pd and 170 ppb Au, and averages 609 ppb PGE+Au over 1.5 m of core. The last 0.5 m of drillhole 88B1 (Fig. 5) contains 966.5 ppb PGE+Au, associated with the enrichment at R4, and averages 680 ppb PGE+Au over the last 1.5 m of the hole: we do not know the average composition at this locality because the hole stops in the middle of the mineralized zone. Hole 88B2 intersected the PPGE enrichment above R2, which gave 801 ppb PGE+Au, of which 390 ppb Au, over 0.5 m: the following seven samples representing 3.5 m of core averaged over 370 ppb Au but showed only very weak enrichment of Pt and Pd: this Au enrichment is thought to be hydrothermal.

The Pt-Pd-enriched horizons have a PGE-geochemistry similar to that found in stratiform PGE mineralizations such as the Merensky and Johns-Manville reefs, found in large layered intrusions in cratons, though at somewhat lower absolute concentrations (Fig. 6). Further features in common with these mineralizations are very limited thickness, large lateral extent and a close relationship to the bases of cyclic units, i.e. pointing to a genetic link with influx of fresh magma pulses and mixing of these with the magma resident in the chamber. The Leka mineralizations contrast with those mentioned above in that they occur much deeper in the cumulate stratigraphy, in association with olivine adcumulates, while the well-known reefs occur after the crystallization of cumulus plagioclase commences. The variations in composition of the mineralizations on Leka indicate that the Pt-enriched horizons occur just below those that are enriched in Pd and that the former are well-developed close to the presumed magma feeder while the reverse is the case for the Pd-enriched horizons.

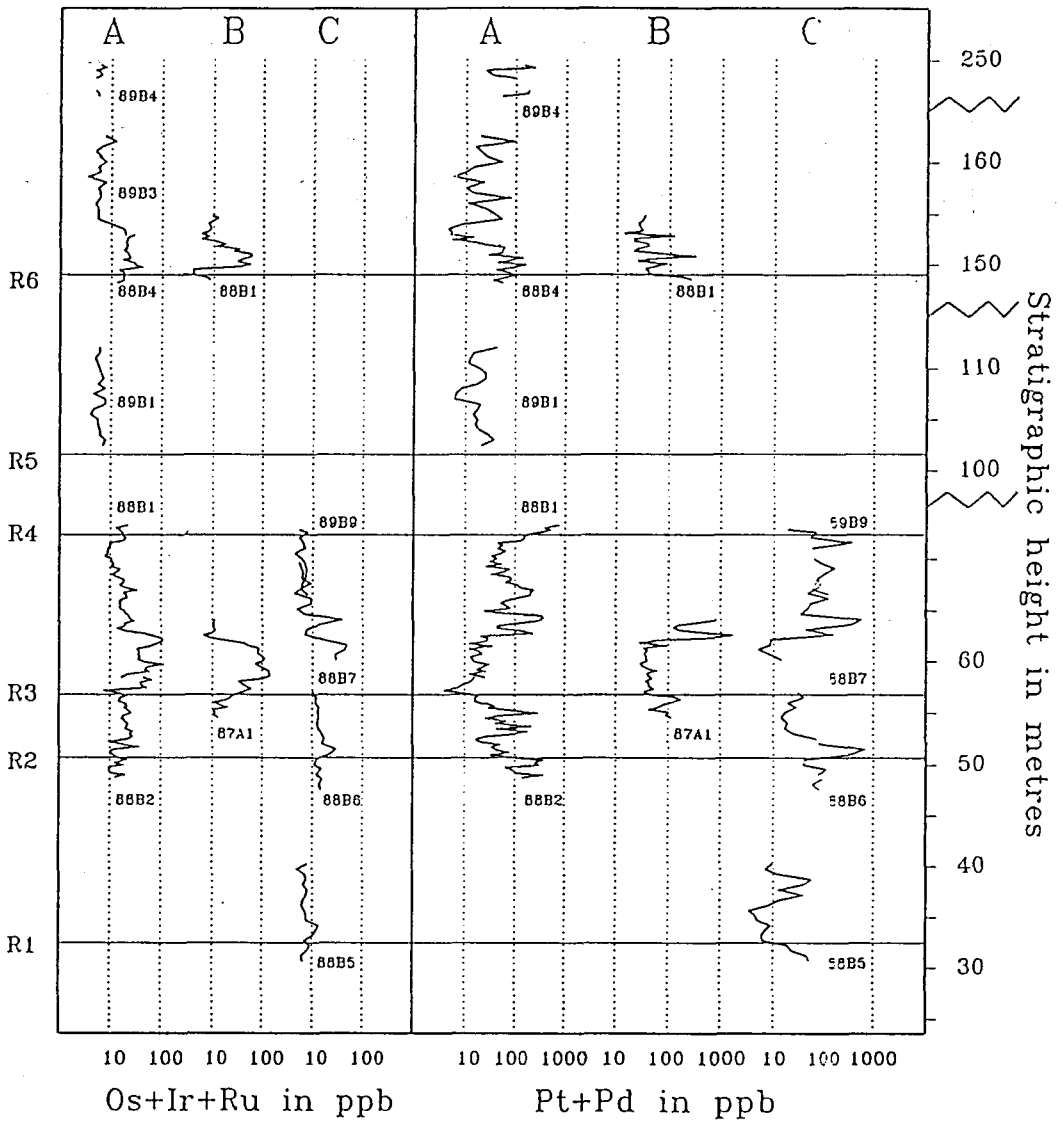

Fig. 5: Relative positions of drillcores through PGE+Au mineralizations in the ultramafic cumulates at Leka with data on IPGE- and PPGE+Au contents.

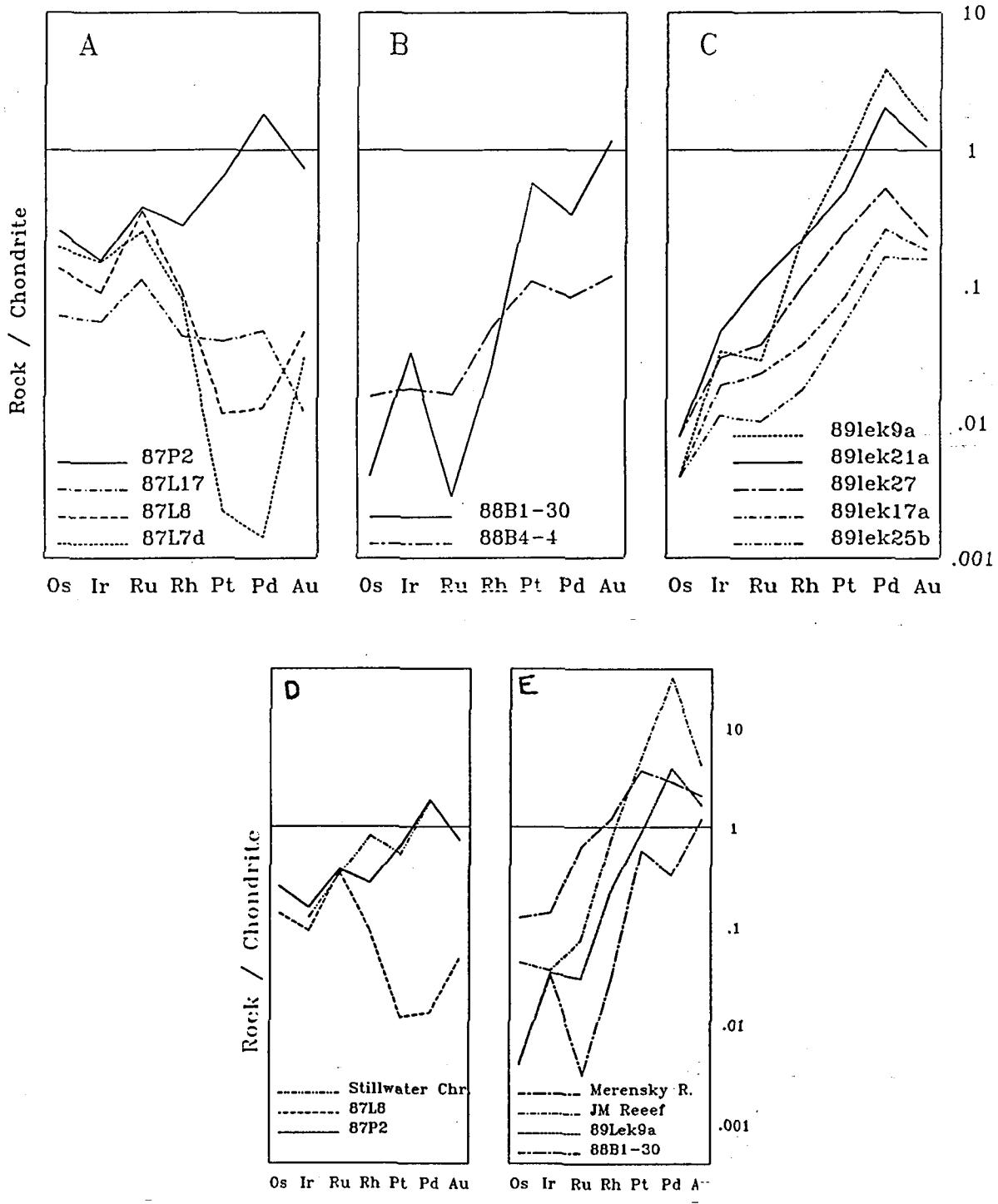

Fig. 6: Chondrite-normalized patterns of PGE and Au contents for: A) IPGE-enriched chromitites, B) Pt-dominated enrichments, C) Pd-dominated enrichments and for D) the IPGE-enriched chromitites and Stillwater chromitites (Page et al. 1976) and for E) the PPGE-enriched horizons and the Merensky and Johns-Manville Reefs (von Gruenewaldt 1979: Barnes & Naldrett 1985).

The occurrence of the PPGE enrichments is related to the mixing of a primitive magma in equilibrium with olivine of composition Fo93-92 with a slightly more evolved magma (in equilibrium with Fo90-85): mixing of the two magmas facilitated the preciptation of both chromite and sulphides /arsenides, a model which builds on the work of Irvine (1977), Campbell et al. (1983) and Naldrett & von Gruenewaldt (1989). Nd-isotope studies of the PGE-enriched cumulates show that they crystallized from a magma with MORB/IAT affinity: calculation of its probable original PGE content suggests that it would be of roughly the same order as that of the boninitic parental magmas postulated for the Bushveld and Stillwater intrusions (Davies & Tredoux 1985: Zientek et al. 1986).

The model should enable the prediction of which type of cyclic unit in the ultramafic cumulates of ophiolites should be favourable for the occurrence of PPGE-enriched horizons: it is probable that further horizons of this type can be found in the Leka ophiolite. It is regarded as highly probable that many such horizons will be found in ophiolite complexes with well-developed sequences of ultramafic cumulates, particularly when the PGE geochemistry of the parts of cyclic units immediately above the chromite horizons or the bases of cyclic units in general, whether marked by chromite enrichment or not, are studied. Among the complexes in which the preconcitions for mineralizations of this type would seem to be present are the Semail ophiolite in Oman (Lippard et al. 1986), the Bay of Islands ophiolite in Newfoundland (Dunsworth et al. 1986) and, of less well-known examples, the Pozanti-Karsanti ophiolite in Turkey (Rahgoshay et al. 1987), which is reported as containing chromite-bearing olivine cumulates over a 2 km thickness with several dm-thick chromitite horizons for every metre.

4.3 Platinum metal abundances in ultramafic cumulates in the Lyngen ophiolite

A reconnaissance of ultramafic bodies in the more accessible parts of the Lyngen ophiolite was carried out in 1987-88 as a collaborative project between Norges geologiske undersøkelse and Troms fylkeskommune. The Lyngen ophiolite is by far the largest in Norway, with a total strike length of over 80 km, but it is also disrupted and strongly deformed and has an incomplete stratigraphy. Mantle harzburgite and ultramafic cumulates are present, but as tectonically emplaced pods of which the largest, at Russelv in the northernmost part of the Lyngen peninsula, is about 6 km long. The ophiolite is delimited to the west by a tectonically disturbed erosional unconformity which is overlain by a sedimentary sequence which contains a series of serpentinite lenses at a specific level just over 1 km above the unconformity.

133 samples from ultramafic bodies on each side of Kjosen, east of Russelv (Fig. 7) and from the serpentinite lenses in the sedimentary sequence overlying the ophiolite were analyzed for PGE+Au. The 9 serpentinite samples gave uniformly low values, <30 ppb total PGE+Au. 73 samples from metadunitic budies, probably originally cumulates, at Kjosen yielded values predominantly <50 ppb PGE+Au, with a maximum of 106.5 ppb PGE+Au, of which 83 ppb Pt. The weak enrichment found in these rocks is consistently of Pt. 51 samples of metamorphosed olivine- and olivine-clinopyroxene cumulates from the Russelv ultramafic body gave more positive results: these rocks locally contain visible chalcopyrite-pyrrhotite

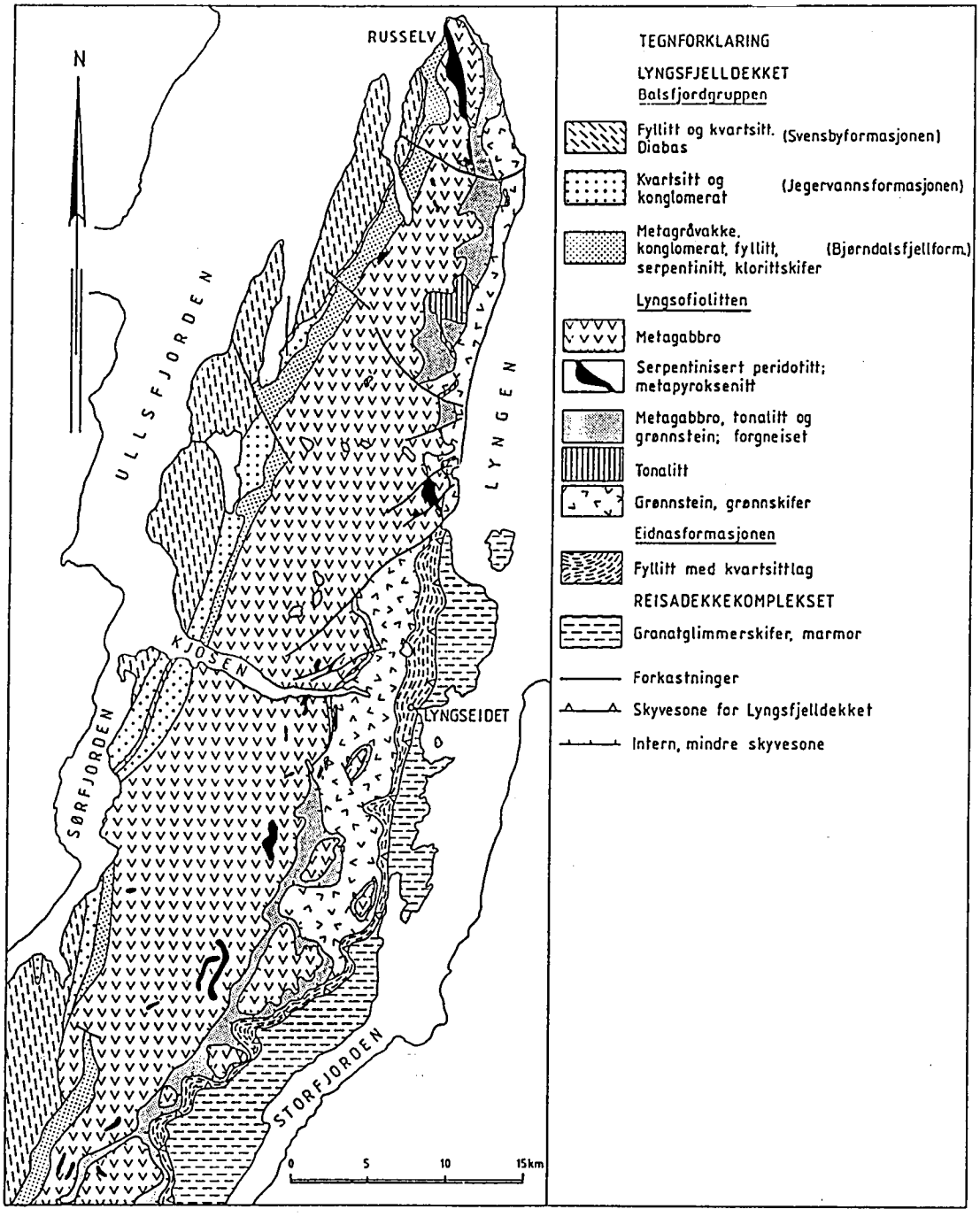

Fig. 7: Geology of the Lyngen peninsula (based on Boyd & Minsaas 1983 a,b)

dissemination, altered to bornite and digenite: there is a positive correlation between noble metal content and sulphide content. The richest samples contain over 100 ppb each of Pt, Pd and Au, with a maximum of 550 ppb PGE+Au. The samples from Russelv have higher Au/Pt and Pd/Pt ratios than those from the Kjosen area. The absolute grades are similar to those reported from a mineralization in mafic cumulates in the Semail ophiolite by Lachize et al. (1990) but the latter has a much higher modal % of sulphides which indicates that the Lyngen mineralization in which the actual volume of sulphides is only a few percent at most, would have a much higher grade of noble metals on 100% sulphide, a frequently quoted

parameter (e.g. Naldrett 1981).

The discovery of noble metal enrichments after such a limited reconnaissance of a small part of the complex indicates that a potential for finding further horizons of this type, possibly at higher levels in the stratigraphy is present and that the possibility of finding richer concentrations cannot be ruled out.

5. PLATINUM METALS IN HIGHER LEVEL MINERALIZATIONS

All the Norwegian ophiolite complexes which have been studied petrologically in any detail have been shown to contain components formed in island arc environments, and are regarded as supra-subduction ophiolites (Pedersen et al. 1988). If the definition of ophiolite is broadened to include predominantly island arc-derived copmlexes, with lesser components formed at ridges, then we have two high level PGE-bearing mineralizations in ophiolites in Norway, the Fæøy deposit in the Karmøy ophiolite, and the Lillefjellklumpen deposit in the Gjersvik island arc complex. Both are deposits of massive Ni-Cu sulphides with associated PGE and small amounts of Au. For both deposits the samples analyzed average 1.8 ppm Pt: the values from Fæøy for Pd average 4.76 ppm while the corresponding average for Lillefjellklumpen is 3.07 ppm. Gold contents average 101 and 219 ppb respectively. The Lillefjellklumpen mineralization is tiny and that at Fæøy, small - its probable original tonnage was of the order of 40,000 tons: no further deposits of this type have been found in Norway and deposits with similar characteristics in ophiolites in other parts of the world also seem to be of very limited size: there would not seem to be a potential for deposits of this type with economically interesting dimensions but should this conclusion prove to be wrong, grades of Pt and Pd of the level found in the two deposits in Norway would make deposits of even a modest size economically attractive.

The Lillefjellklumpen deposit is located in the Gjersvik island arc complex, north-east of Grong in N-Trøndelag (see paper by Grønlie in Vol.2). The host complex is interpreted as an ensimatic island arc, the mineralization itself being associated with a small gabbroic intrusion at the base of the volcanic level of the complex. The mineralization consists of massive sulphide, dominated by pyrrhotite, pyrite, pentlandite and chalcopyrite, with an average grade of 3.6% Ni and 1.2% Cu (Grønlie 1988). The averages of eight samples analyzed for all the PGE+Au are 139 ppb Os, 170 ppb Ir, 189 ppb Ru, 214 ppb Rh, 1799 ppb Pt, 3068 ppb Pd and 219 ppb Au. These values compare closely with those for typical mineralizations at Sudbury (Naldrett 1981). The PGE are hosted in merenskyite, sperrylite, moncheite and temagamite, the mineralization being very unusual in having merenskyite as the dominant platinum group mineral.

Detailed study of the Fæøy deposit has not been given high priority because it has been the topic of an M.Sc. thesis being carried out by a student from Memorial University, Newfoundland: unfortunately the completion of this project has been delayed. The mineralization is a massive sulphide deposit located in the dyke complex of the Karmøy ophiolite. It outcrops at sea-level and most of the workings from mining activity early in this century and late in the last are under water. It is a Cu-Ni deposit but with highly variable Cu/(Cu+Ni) ratios, varying from 0.3 to 0.75. The average of six samples analyzed for PGE+Au is 234 ppb Os, 195 ppb Ir, 219 ppb Ru, 244 ppb Rh, 1794 ppb Pt, 4760 ppb Pd and 101 ppb Au.

6. PLATINUM METAL GEOCHEMISTRY OF SUCCESSIVE MAGMA TYPES IN THE KARMØY OPHIOLITE

The upper levels of the Karmøy ophiolite include volcanic rocks of several different types - mid-ocean ridge basalts (MORB), island arc tholeiites (IAT), boninites, calcalkaline and alkaline basalts. Investigation of the PGE geochemistry of these rocks allows the following conclusions to be drawn:

1) The boninites and calcalkaline basalts have higher PGE-contents than the other series.
2) The boninites show a bimodal distribution of PGE abundance. The PGE-enriched boninites have chondrite-normalized PGE patterns similar to those found in boninites in modern island arcs, while the PGE-depleted boninites have patterns resembling those in the other series (MORB, IAT, alkaline).
3) The bimodal distribution of PGE abundance in the boninites is probably related to sulphur saturation and enrichment of PGE in the sulphides, the Fæøy mineralization probably being a product of this process.
4) The considerable variations in ENd ratio in the boninites indicate that the magma did not differentiate in a large steady-state magma chamber, as did the MORB/IAT series. It would thus seem to be unlikely that large layered intrusions of boninitic parentage and containing stratiform PGE enrichments will be found in the Karmøy or other ophiolite complexes.
5) The apparent difference in PGE-content between MORB/IAT magmas and the PGE-enriched boninites is also ascribed to later sulphur saturation in the latter.
6) Rock complexes with boninitic parental magmas in ophiolites should not be regarded as particularly favourable for PGE-enrichment in relation to others with MORB/IAT parental magmas.

7. CONCLUSIONS

The most important finding within the project is the discovery and documentation of stratiform PPGE mineralizations in ultramafic cumulates in the Leka ophiolite and of indications of similar mineralizations at a stratigraphically higher level in the Lyngen ophiolite. The Leka mineralizations are of a type the existence of which in ophiolites has not been (well) documented before and which has several characteristics in common with stratiform PGE enrichments in large layered intrusions. Though subeconomic, the mineralizations indicate a possible potential for horizons with higher PGE-contents in the two ophiolites examined and a clear potential for PPGE mineralizations in ophiolites with well-developed sequences of ultramafic cumulates in general. The model developed for the mineralizations in the Leka ophiolite (see paper in Vol.2) gives criteria which should assist in the selection of ophiolite complexes with PGE-potential and the location of targets within them.

Samples from numerous podiform chromitite mineralizations have been analyzed and several of the deposits have been studied in detail. Several deposits, including those on Leka, have proved to be enriched in PPGE, unlike most of the examples described in the literature which are enriched in IPGE. The PGE enrichment is confined to chromite-bearing rocks and, at least on Leka, shows a postive correlation with Cr-content: the small size of the chromitite mineralizations precludes any economic potential in the Norwegian examples. The largest examples described in the literature are also relatively small (<5 million tons) which suggests that only the very largest podiform chromitites could be interesting targets for PGE-exploitation and then only if they were enriched in PPGE.

The PGE-enriched massive Cu-Ni sulphide and hydrothermal Cu-sulphide mineralizations examined are also too small to have economic importance.

Studies of the isotope- and PGE-geochemistry of the different volcanic suites in the Karmøy ophiolite and of the cumulates in the Leka ophiolite suggest that rock suites with boninitic parentage should not be regarded as particularly favourable for PGE-enrichment in relation to suites with parental magmas of MORB/IAT affinity.

The project has demonstrated that the availability of new analytical technology (ICP-MS) which allows the rapid analysis of all the PGE at a reasonable cost, can lead to the discovery of new mineralizations and potentially to new mineralizations of economic significance. It shows further the advantages which a well-developed, well-exposed ophiolite complex has as a natural laboratory for the study of the processes controlling PGE-enrichment (as opposed to many layered intrusions in cratons) in that potential magma source rocks, feeder channels and the end products of the magmatic evolution can be sampled as well as the immediate host rocks and the mineralizations themselves.

REFERENCES

Abdelrahman, E.M. & Matheis, G. 1990: Platinum group elements (PGE) with Ni-sulphides in pyroxenites from the Wadi Onib-Hamisana Ophiolite, Red Hills, Sudan. Symp. on Ophiolite Genesis and Evolution of Oceanic Lithosphere, Muscat (abs.)

Abrajano, T.A. & Bacuta, G.C. 1982: Platiniferous Fe-Ni-Cu sulfides in an Alpine terrane, Zambales, Republic of the Philippines, Geol.Soc.Am. Abs. with Programs 429

Auge, T. 1988: Platinum-group minerals in the Tiebaghi and Vourinos ophiolitic complexes: genetic implications. Can. Mineral. 26, 177-192.

Bacuta, G.C., Lipin, B.R., Gibbs, A.K. & Kay, R.W. 1988: Platinum-Group element abundances in chromite deposits of the Acoje ophiolite block, Zambales Ophiolite Complex, Philippines.In: Prichard, H.M., Potts, P.J., Bowles, J.F.W. & Cribb, S.J. (eds.) Geo-Platinum 87, Elsevier, London, 381-382.

Barnes, S.-J., Boyd, R., Korneliussen, A., Nilsson, L.P., Often, M., Pedersen, R.-B. & Robins, B. 1987a: Geochemistry of platinum metals in rocks and ores in Norway: Pilot project. Draft report. Nor. geol. unders., rapport 87.021, 50 pp.

Barnes, S.-J., Boyd, R., Korneliussen, A., Nilsson, L.-P., Often, M., Pedersen, R.B. & Robins, B. 1988: The use of mantle normalization and metal ratios in discriminating between the effects of partial melting, crystal fractionation and sulphide-segregation on platinum-group elements, gold, nickel and copper: examples from Norway. In: Prichard, H.M., Potts, P.J., Bowles, J.F.W. & Cribb, S.J. (eds.) Geo-Platinum 87, Elsevier, London, 113-144.

Barnes, S.-J., Naldrett, A.J. & Gorton, M.P. 1985: The origin of the fractionation of platinum-group elements in terrestrial magmas. Chem. Geol. 53, 303-323.

Barnes, S.J. & Naldrett, A.J. 1985: Geochemistry of the J-M (Howland) Reef of the Stillwater Complex, Minneapolis Adit area. I. Sulphide chemistry and sulphide-olivine equilibrium. Econ. Geol. 80, 627-645.

Boyd, R., Barnes, S.-J. & Grønlie, A. 1988: Noble metal geochemistry of some Ni-Cu deposits in the Sveconorwegian and Caledonian Orogens in Norway. In: Prichard, H.M., Potts, P.J., Bowles, J.F.W. & Cribb, S.J. (eds.) Geo-Platinum 87, Elsevier, London, 145-158.

Boyd, R. & Minsaas, O. 1983: Lyngen, 1634 III, berggrunnskart 1:50 000, foreløpig utgave, Norges geol. unders.

Boyd, R. & Minsaas, O. 1983: Lyngstuva 1634 IV, berggrunnskart 1:50 000, foreløpig utgave, Norges geol. unders.

Cabri, L.J. (ed.) 1981: Platinum-group elements: mineralogy, geology, recovery. Can. Inst. Min. Metall., Spec. vol. 23, 267 pp.

Campbell, I.H., Naldrett, A.J. & Barnes, S.J. 1983: A model for the origin of the platinum-rich sulphide horizons in the Bushveld and Stillwater complexes. J. Petrol. 24, 133-165.

Chang, P.K., Yu, C.M. & Chiang, C.Y. 1973: Mineralogy and occurrence of the platinum-group elements in a chromium deposit in north-western China. Geochimica 2, 76-85 (in Chinese).

Corneliussen, O.A. 1891: Bidrag til kundskaben om Nordlands amts geologi. In: Reusch, H.H.: Det nordlige Norges geologi, Norges geol. unders. 4, 149-189.

Crocket, J.H. 1981: Geochemistry of the platinum-group elements. In: Cabri, L.J. (ed.) 1981: Platinum-group elements: mineralogy, geology, recovery. Can. Inst. Min. Metall., Spec. vol. 23, 47-64.

Czamanske, G.K. & Moore, J.G. 1977: Composition and phase chemistry of sulphide globules in basalt from the Mid Atlantic ridge near 37 N latitude. Geol. Soc. Am. Bull. 88, 587-599.

Davies, G. & Tredoux, M. 1985: The platinum-group element and gold contents of the marginal rocks and sills of the Bushveld complex. Econ. geol. 81, 838-848.

De Wit, M.J. & Tredoux, M. 1988: PGE in the 3.5 Ga Jamestown Ophiolite Complex, Barberton Greenstone Belt, with implications for PGE distribution in simatic lithosphere. In: Prichard, H.M., Potts, P.J., Bowles, J.F.W. & Cribb, S.J. (eds.) Geo-Platinum 87, Elsevier, London, 319-342.

Dunsworth, S., Calon, T. & Malpas,J. 1986: Structural and magmatic controls on the internal geometry of the plutonic complex and its chromite occurrences in the Bay of Islands Ophiolite, Newfoundland. Geol. Surv. Canada Paper 86-1B, 471-482.

Economou, M.I. 1986: Platinum-group elements (PGE) in chromite and sulphide ore within the ultramafic zone of some Greek ophiolite complexes. In: Gallagher, M.J., Ixer, R.A., Neary, C.R. & Prichard, H.M. (eds.) Metallogeny of basic and ultrabasic rocks. IMM, London, 441-453.

Economou, M.I. & Naldrett, A.J. 1984: Sulfides associated with podiform bodies of chromite at Tsangli, Eretria, Greece. Mineral. Deposita 19, 289-297.

Fischer, W., Amosse, J. & Leblanc, M. 1988: PGE distribution in some ultramafic rocks and minerals from the Bou-Azzer Ophiolite Complex (Morocco). In: Prichard, H.M., Potts, P.J., Bowles, J.F.W. & Cribb, S.J. (eds.) Geo-Platinum 87,Elsevier, London, 199-210.

Foose, M.P. 1986: Setting of a magmatic sulfide occurrence in a dismembered ophiolite, southwestern Oregon. U.S.Geol.Survey Bull. 1626-A, 21 pp.

Furnes, H., Roberts, D., Sturt, B.A., Thon, A. & Gale, G.H. 1980:

Ophiolite fragments in the Scandinavian Caledonides. In: Panayiotou, A. (ed.). Ophiolites, Proc. Int. Ophiolite Symp., Cyprus 1979, 582-600.

Grønlie, A. 1988: Platinum-group minerals in the Lillefjellklumpen nickel-copper deposit, Nord-Trøndelag, Norway. Norsk. geol. tidsskr. 68,

Gunn, A.G., Leake, R.C. & Styles, M.T. 1985: Platinum-group element mineralization in the Unst ophiolite, Shetland. Mineral Reconnaissance Programme Rep. Br. Geol. Surv. No. 73, 117 pp.

Gunn, A.G. 1989: Drainage and overburden geochemistry in exploration for platinum-group elemet mineralization in the Unst ophiolite, Shetland, U.K. Journ. of Geochem. Explor. 31, 209-236.

Hamlyn, P.R., Keays, R.R., Cameron, W.E., Warrington, E., Crawford, A.J. & Waldon, H.M. 1985: Precious metals in magnesian low-Ti lavas: Implications for metallogenesis and sulfur saturation in primary magmas. Geochim. Cosmochim. Acta 49, 1797-1811.

Hulin, C.S. 1950: Results of study of Ni-Pt ores and concentrates: Acoje Mining Company, Philippine Island. Philippine Geologist 4, 11-23.

Irvine, T.N. & Sharpe, M. 1982: Source rock compositions and depths of origin of Bushveld and Stillwater magmas. Carnegie Inst. Washington Yb. 81, 294-303.

Ixer, R.A. & Prichard, H.M. 1989: The mineralogy and paragenesis of Pt, Pd, Au and Ag-bearing assemblages at Cliff, Shetland. Abstract, 5th Int. Platinum Symp., Helsinki. Geol. Surv. Finl. Bull. 61, p. 40.

Lachize, M., Juteau, T., Lorand, J.P. & Nehlig, P. 1990: A magmatic sulphide-rich zone in the fossil gabbroic magma chamber of Wadi Haymiliyah (Semail Ophiolite, Oman). Symp. on Ophiolite genesis and Evolution of Oceanic Lithosphere, Muscat (abs.).

Legendre, O. & Augé, T. 1986: Mineralogy of platinum-group mineral inclusions in chromitites from different ophiolite complexes. In: Gallagher, M.J., Ixer, R.A., Neary, C.R. & Prichard, H.M. (eds.) Metallogeny of basic and ultrabasic rocks. IMM, London, 361-372.

Lippard, S.J., Shelton, A.W. & Gass, I.G. 1986: The ophiolite of Northern Oman. Geol. Soc. London Memoir 11, Blackwell, Oxford, 178 pp.

Lunde, G. & Johnsen, M. 1928: Vorkommen und Nachweis der Platinmetalle in norwegischen Gesteinen II. Z. anorg. u. allg. Chem. 172, 167-195.

Naldrett, A.J. 1981: Platinum-group element deposits. In:Cabri, L.J. (ed.) Platinum-group elements: mineralogy, geology, recovery. Can. Inst. Min. Metall., Spec. vol. 23, 47-64.

Naldrett, A.J. & von Gruenewaldt, G. 1989: Association of platinum-group elements with chromitite in layered intrusions and ophiolite complexes. Econ. Geol. 84, 180-187.

Nilsson, L.P. 1990: Platinum-group mineral inclusions in chromitite from the Osthammeren ultramafic tectonite body; south central Norway. Mineral. & Petrol.

Orberger, B., Friedrich, G., Traxel, K. & Woermann, E. 1989: Se- and Pd-concentrations in Cu-Ni-sulfides/alloys from ultramafic rocks in the Acoje ophiolite block, Zambales, Philippines. In: Papunen, H. (ed.): 5th International Platinum Symp. Abstracts, Bull. Geol. Soc. Finland 61, 44.

Orberger, B., Friedrich, G. & Woermann, E. 1988: Platinum-group element mineralization in the ultramafic sequence of the Acoje ophiolite block, Zambales, Philippines. In: Prichard, H.M., Potts, P.J., Bowles, J.F.W. & Cribb, S.J. (eds.) Geo-Platinum 87, Elsevier, London, 361-380.

Page, N.J. 1969: Platinum content of ultramafic rocks. In: U.S.Geol. Survey Heavy Metals Program, Progress Rep. 1968 - Topical Studies, U.S.Geol.Survey Circ. 622

Page, N.J., Johnson, M.G., Haffty, J. & Ramp, L. 1975: Occurrence of and platinum-group metals in ultramafic rocks of the Medford - Coos Bay 2 quadrangles, southwestern Oregon. U.S.Geol.Survey Misc. Field Studies Map MF-694.

Page, N.J., Pallister, J.S., Brown, M.A., Smewing, J.D. & Haffty, J. 1979: Platinum-group metals in chromite-rich rocks from two traverses through the Semail ophiolite, Oman. EOS 60, 963 (abstr.).

Page, N.J., Pallister, J.S., Brown, M.A., Smewing, J.D. & Haffty, J. 1982: Palladium, platinum, rhodium, iridium and ruthenium in chromite-rich rocks from the Semail ophiolite, Oman. Can. Mineral. 20, 537-548.

Page, N.J., Rowe, JJ. & Haffty, J. 1976: Platinum metals in the Stillwater Complex, Montana. econ. geol. 71, 1352-1363.

Page, N.J., Singer, D.A., Morning, B.C., Carlson, C.A., McDade, J.M. & Wilson, S.A. 1986: Platinum-group element resources in podiform chromitites from California and Oregon. Econ. Geol. 81, 1261-1271.

Page, N.J. & Talkington, R.W. 1984: Palladium, platinum, rhodium, ruthenium and iridium in peridotites and chromitites from ophiolite complexes in Newfoundland. Can. Mineral. 22, 137-149.

Parangit, R.U. 1975: Nickel sulfide deposits and exploration works at Acoje Mine, Zambales Province, Philippines. J.Geol.Soc.Philippines 29, 16-27.

Pedersen, R.B., Furnes, H. & Dunning, G.R. 1988: Some Norwegian ophiolite complexes reconsidered. Norges geol. unders. Spec. Publ. 3, 80-85.

Prichard, H.M. & Lord, R.A. 1989: Magmatic and secondary PGM in the Shetland ophiolite complex. Abstract, 5th Int. Platinum Symp., Helsinki. Geol. Surv. Finl. Bull. 61, p. 39.

Prichard, H.M., Neary, C.R. & Potts, P.J. 1986: Platinum group minerals in the Shetland Ophiolite. In: Gallagher, M.J., Ixer, R.A., Neary, C.R. & Prichard, H.M. (eds.) Metallogeny of basic and ultrabasic rocks. IMM, London, 395-414.

Rahgoshay, M., Whitechurch, H. & Juteau, T. 1987: Petrology of the chromite ores in the Tauric and Oman ophiolite complexes. In: Troodos 87, Ophiolites and Oceanic Lithosphere, Geological Survey Department, Nicosia, 154 (abstr.).

Roberts, D. & Gee, D.G. 1985: An introduction to the structure of the Scandinavian Caledonides. In: Gee, D.G. & Sturt, B.A. (eds.), The Caledonide Origin - Scandinavia and Related Areas, J.Wiley and Sons, Chichester, 55-68.

Stockman, H.W. & Hlava, P.F. 1984: Platinum-group minerals in alpine chromitites from southwestern Oregon. Econ. Geol. 79, 491-508.

Talkington, R.W., Watkinson, D.H., Whittaker, P.J. & Jones, P.C. 1984: Platinum-group minerals and other solid inclusions in chromite of ophiolite complexes: occurrence and petrological significance. Tschermaks Mineral. Petrogr. Mitt. 32, 285-300.

Vogt, J.H.L. 1894: Beiträge zur genetisehen Classification der durch magmatische Differentiationsprocesse und der durch Pneumatolyse entstandenen Erzvorkommen. Zeitschr. für prakt. Geol., 381-399.

Vokes, F.M. 1987: Gabbro-hosted mineralization in ophiolites: examples from Troodos and Leka, Norway. In: troodos 87, Ophiolites and Oceanic Lithosphere, Geological Survey Department, Nicosia, 168 (abstr.).

Von Gruenewaldt, G. 1979: A review of some recent concepts of the Bushveld Complex, with particular reference to sulphide mineralization. Can. Mineral. 17, 233-256.

Zientek, M.L., Foose, M.P. & Leung, M. 1986: Palladium, platinum and rhodium contents of rocks near the lower margin of the Stillwater Complex, Montana. Econ. Geol. 81, 1169-1178.

NTNF
Norges Teknisk-Naturvitenskapelige Forskningsråd
Sognsveien 72 - Postboks 70, Tåsen - 0801 Oslo 8
Telefon: (02) 23 76 85. Telex: 76951 ntnf n, Telefax: (02) 18 11 39

Søknadsskjema

Søknad datert. . . . . .

1 Søker: Norges geologiske undersøkelse

NTNF-komite:

NTNF-nr.:

Postadr.: Postboks 3006, 7001 Trondheim

Tlf.:

Prosjekttittel (maks. 64 anslag): Geokjemi av platinametaller i norske ofiolitter

Søkers kontaktperson: Avd.direktør S. Krogh, SINTEF

Faglig hovedansvarlig: forsker R. Boyd, NGU

2 Emneord (4 emneord som karakteriserer prosjektet): Platinametaller/geokjemi/petrologi/malmgeologi

3 Er eller vil det bli søkt om prosjektstøtte fra annen kilde enn NTNF? ☒ Ja ☐ Nei — Hvis ja: Gi opplysninger i pkt. 5 eller i prosjektbeskrivelse

4 Mål

1) Å gjennomføre en første vurdering av potensialet for platinametaller i ofiolitter i Norge
2) Å studere prosessene som styrer fordelingen av platinametallene
3) Å undersøke et fåtall prioriterte områder nærmere

5 Bevilgninger/budsjett for hele prosjekttiden (Alle beløp i 1000 kr.)

	Bevilgninger		Budsjett			
Første år med NTNF-støtte 19	Tidligere år	I år	Søknadsår	Etterfølgende år		
Planlagt siste år med NTNF-støtte 19	19 –19	19	19 87	19 88	19 89	19 – 19
NTNF-midler			400	600	400	
Industrimidler			150	150	150	
Offentlige midler			600	600	600	
Andre midler (spesifisert i vedlegg)						
SUM			1150	1350	1150	

6 Kostnader i søknadsåret (Alle beløp i 1000 kr.)

Nr.	Delprosjekttittel	Ansvarlig	Direkte lønn og felleskostn.	Direkte matr. og utlegg	Kostnader i egne laboratorier	SUM
1)	Rekognoserende undersøkelse m.h.p. platinametaller i norske ofiolitter	R. Boyd NGU-medarb. stipendiat	350	2 185	210 ~~160~~	7 ~~695~~
2)	Oppfølgende undersøkelser i utvalge områder	R. Boyd NGU-medarb. stipendiat	150	75	80	305
SUM			500	360	290	1150
NTNF-andel			230	170		400

NR.5000.mai 84

7 Prosjektsammendrag

Kfr. veiledningen
Skal kunne publiseres direkte i prosjektkatalog

Prosjektet omfatter en vurdering av platinametallinnholdet i bergartskomplekser og malmtyper i ofiolitter i Norge. Prosessene som fører til anriking av platinametaller vil bli studert ut fra både vitenskapelige og økonomisk-geologiske synspunkter. Utvalgte områder vil bli vurdert nærmere. Prosjektet vil være et viktig skritt mot den første moderne oversikt over platinemetaller i berggrunnen i Norge. Arbeidet vil omfatte samarbeid med universiteter og andre geofaglige institusjoner både i inn- og utland.

8 Bakgrunn, behov og nytteverdi

Bakgrunn. Flere geologiske miljø i Norge kan ha et potensial for platinametaller. Disse er: ofiolitter, lagdelte intrusiver, Alaska-type ultramafiske intrusiver og svartskifre. Fra nikkelprospektering, forskning på ofiolitter og kartlegging ellers er det kjent flere ofiolittkomplekser som muligens har potensiale for anriking av platinemtaller. Nylig er platinamineralisering blitt oppdaget i Shetland-ofiolitten som er av samme alder og type som flere norske komplekser.

Behov. EF har gitt prospektering etter platinametaller høy prioritet, og det er interesse for prosjektet i prospekteringsindustrien. Datagrunnlaget som er nødvendig som utgangspunkt for et prospekteringsprogram mangler, bortsett fra i noen få områder.

Nytteverdi. Prosjektet vil føre til en vesentlig utbygging av datagrunnlaget og til forskning basert på resultatene. Dette vil tillate en første vurdering av potensialet for platinametaller i ofiolittmiljøet i Norge. En vesentlig del av innsatsen i prosjektet blir gjennomført av en stipendiat, noe som vil medføre oppbygging av norsk kompetanse på dette området.

9 Brukerkontakt og informasjonstiltak

NGU har uformell kontakt med brukergrupper i industri i Norge og har en utstrakt kontakt med institusjoner som er aktive i forskning innenfor dette området i Europa og ellers. Falconbridge Nikkelverk, Kristiansand vurderer å yte et bidrag på kr. 150.000 til prosjektet.

Resultatene vil bli offentliggjort i form av rapporter, publikasjoner og foredrsag.

10 Organisering av prosjektet

Prosjektledelse, samarbeid, eventuelt kontakt – eller styringsgruppe

Prosjektet tilhører et program som ledes av en styringsgruppe, hvor NGU, SINTEF, industri og universitetene er representert. Prosjektet skal ledes av en person tilknyttet NGU. Innen prosjektet er det tatt kontakt med Universitetetet i Bergen, NTH, Open University, Imperial College og British Geological Survey som ønsker å samarbeide i prosjektet. Det vil videre bli tatt kontakt med universitetene i Aten, København og Southampton og med Grønlands Geologiske Undersøgelse (GGU).

Søkerens underskrift

Faglig hovedansvarlig

Vedlegg: Prosjektbeskrivelse (nye prosjekter)/Fremdriftsrapport (igangværende prosjekter)

LIST OF PAPERS PUBLISHED/PRESENTED ON THE TOPICS OF THE PROJECT

Papers published:

Barnes, S.-J., Boyd, R., Korneliussen, A., Nilsson, L.-P., Often, M., Pedersen, R.B. & Robins, B. 1988: The use of mantle normalization and metal ratios in discriminating between the effects of partial melting, crystal fractionation and sulphide-segregation on platinum-group elements, gold, nickel and copper: examples from Norway. In: Prichard, H.M., Potts, P.J., Bowles, J.F.W. & Cribb, S.J. (eds.) Geo-Platinum 87, Elsevier, London, 113-144.

Boyd, R., Barnes, S.-J. & Grønlie, A. 1988: Noble metal geochemistry of some Ni-Cu deposits in the Sveconorwegian and Caledonian Orogens in Norway. In: Prichard, H.M., Potts, P.J., Bowles, J.F.W. & Cribb, S.J. (eds.) Geo-Platinum 87, Elsevier, London, 145-158.

Grønlie, A. 1988: Platinum-group minerals in the Lillefjellklumpen nickel-copper deposit, Nord-Trøndelag, Norway. Norsk. geol. tidsskr. 68,

Nilsson, L.P. 1990: Platinum-group mineral inclusions in chromitite from the Osthammeren ultramafic tectonite body; south central Norway. Mineral. & Petrol.

Papers presented orally or as posters:

Barnes, S.-J., Boyd, R. & Grønlie, A.: Edelmetallgeokjemi av noen norske Ni-Cu forekomster. NGFs landsmøte, Trondheim, 16-18.01.87.

Barnes, S.-J., Boyd, R. & Grønlie, A.: Noble metal geochemistry of some Ni-Cu sulphide deposits in Norway. EUG IV, Strasbourg, 13-16.04.87, and Geoplatinum 87, Milton Keynes, 23-24.04.87.

Barnes, S.-J., Boyd, R., Korneliussen, A., Nilsson, L.-P., Often, M., Pedersen, R.B. & Robins, B.: The use of mantle normalization and metal ratios in discriminating between the effects of partial melting, crystal fractionation and sulphide-segregation on platinum-group elements, gold, nickel and copper: examples from Norway.Geoplatinum 87, Milton Keynes, 23-24.04.87.

Boyd,R., Pedersen, R.B., Vokes, F.M., Grenne, T., Grønlie, Nilsson, L.P. & Rundhovde, E.: Noble metal mineralizations in Lower Palaeozoic ophiolites in Norway. 5th International Platinum Symposium, Helsinki, 1-3.08.89 and 19. Nordiske Geologiske Vintermøte, Stavanger, 6-9.01.90.

Nilsson, L.P.: Platinum-group mineral inclusions in chromitite from ophiolitic tectonites in the Caledonides of Norway. Troodos 87 Ophiolites and Oceanic Lithosphere, Nicosia, 4-10.10.87.

Nilsson, L.P.: Inneslutninger av platina-gruppe mineraler (PGM) i kromitt fra Osthammeren og Ørnstolen - to ofiolittiske tektonitter i de norske Kaledonider. 18. Nordiske Geol. Vintermøte, København, 12-14.01.88.

Nilsson, L.P.: Tre eksempler på opptreden av platina-gruppe elementer (PGE). Malmgeologisk symposium, Løkken, 12-13.02.88.

Nilsson, L.P.: Platinum-group mineral inclusions in ophiolitic chromitite from the Osthammeren tectonite body, Norway. 5th International Platinum Symposium, Helsinki, 1-3.08.89.

Pedersen, R.B.: PGE-geochemistry of boninitic and basaltic rocks of the Karmøy ophiolite complex, western Norway. 5th International Platinum Symposium, Helsinki, 1-3.08.89.

Pedersen, R.B. & Boyd, R.: PGE-geochemistry of the ultramafic rocks of the Leka ophiolite complex, Norway. 5th International Platinum Symposium, Helsinki, 1-3.08.89.

Volume 2

Papers published/manuscripts in preparation

The following papers resulted from the pilot project: page

The following papers, published or in preparation, result from/are intimately related to the topics of the present project (with reference to the appropriate chapter in the main report):

Barnes, S.-J., Boyd, R., Korneliussen, A., Nilsson, L.-P., Often, M., Pedersen, R.B. & Robins, B. 1988: The use of mantle normalization and metal ratios in discriminating between the effects of partial melting, crystal fractionation and sulphide-segregation on platinum-group elements, gold, nickel and copper: examples from Norway. In: Prichard, H.M., Potts, P.J., Bowles, J.F.W. & Cribb, S.J. (eds.) Geo-Platinum 87, Elsevier, London, 113-144.

Because platinum readily forms arsenides but gold does not, the amount of platinum that can be transported in arsenic-bearing hydrothermal solutions is very low compared to gold.

REFERENCE

Westland, A. D. (1981). Inorganic chemistry of the platinum-group elements. In *Platinum-Group Elements: Mineralogy, Geology, Recovery*, ed. L. J. Cabri, The Canadian Institute of Mining and Metallurgy Special Volume 23, pp. 5–18.

12

The Use of Mantle Normalization and Metal Ratios in Discriminating between the Effects of Partial Melting, Crystal Fractionation and Sulphide Segregation on Platinum-Group Elements, Gold, Nickel and Copper: Examples from Norway

SARAH-JANE BARNES

Sciences de la Terre, Université du Quebéc, 555 Boulevard de l'Université, Chicoutimi, PQ, Canada G7H 2B1

R. BOYD, A. KORNELIUSSEN, L-P. NILSSON, M. OFTEN

Norges Geologiske Undersøkelse, Postboks 3006, N-7002 Trondheim, Norway

R. B. PEDERSEN & B. ROBINS

Geologisk Institutt, Universitet i Bergen, N-5000 Bergen, Norway

ABSTRACT

The distribution of noble metals, Ni and Cu in mafic and ultramafic rocks is thought to be controlled by sulphides, chromite, olivine and platinum-group minerals (PGM). One method for presenting noble metal, Ni and Cu data focuses on the sulphide control by recalculating the data to 100% sulphides and presenting the data chondrite normalized. The relative importance of the influence of sulphides, chromite, olivine and PGM on the noble metals, Ni and Cu is examined here using two alternative methods.

Firstly, the metals can be plotted in the order: Ni, Os, Ir, Ru, Rh, Pt, Pd, Au and Cu and mantle normalized. The noble metals have a much higher partition coefficient into sulphides than Ni or Cu. Therefore, if sulphides have segregated from the magma or are retained in the mantle during partial melting, the magma and all rocks that subsequently form from it will be depleted in noble metals relative to Ni and Cu and the metal patterns will have an overall trough shape. Conversely any rocks containing these sulphides will be enriched in noble metals relative to Ni and Cu and the metal patterns will have an arch shape (characteristic of Pt reefs). Chromite-rich rocks tend to be enriched in the elements Os, Ir and Ru relative to the magma from which they form, therefore if chromite crystallizes from a magma or is retained in the mantle during partial melting, the magma and any rocks that subsequently form from

from Os to Pd, flat from Pd to Cu and have a positive Ni anomaly. The rocks containing cumulate chromite will be enriched in Os, Ir and Ru relative to the other elements and the metal patterns have an overall negative slope with a down turn at Ni (as seen in podiform chromitites). Olivine concentrates Ni and under some conditions Ir. Therefore if olivine crystallizes from a magma or is retained in the mantle during partial melting, Ni and Ir will be depleted in the magma and in any rocks that subsequently form from it. The metal patterns have an overall positive slope from Os to Pd, flat from Pd to Cu and no Ni anomaly. The cumulate will be enriched in Ni and Ir and tend to have a flat metal pattern (e.g. in dunites from komatiites and ophiolites).

A second approach to presenting noble metal, Ni and Cu data is suggested because while the effects of sulphide, chromite and olivine control can be seen on the metal patterns it is easier to distinguish these effects visually using metal ratio diagrams, Pd/Ir versus Ni/Cu and Ni/Pd versus Cu/Ir.

These two approaches are useful petrogenetic and exploration tools. Rocks which have trough-shaped metal patterns formed from magmas which were depleted in noble metals, possibly by sulphide segregation. These rocks do not make good exploration targets although there is the potential of a noble-metal deposit stratigraphically below them. Rocks which are not enriched or depleted in Ni and Cu relative to the noble metals formed from a magma that has not segregated sulphides and therefore a noble metal deposit could lie stratigraphically above these rocks.

INTRODUCTION

Naldrett *et al.* (1979) showed that if noble metal (Os, Ir, Ru, Rh, Pt, Pd, Au) analyses of sulphides are chondrite normalized and then plotted in order of decreasing melting point, smooth curves are obtained. The use of such chondrite normalized curves permits the distinction between sulphides that segregated from primitive magmas such as komatiites, and sulphides which segregated from more fractionated magmas, such as tholeiites. In their review of the noble metal abundance data then available, Barnes *et al.* (1985) were able to extend this approach to silicate rocks. They showed that it is possible to distinguish between noble-metal patterns from silicate rocks thought to represent the upper mantle (flat noble-metal patterns), komatiites (slightly Pd-enriched noble-metal patterns), and podiform chromitites (Os-, Ir- and Ru-enriched noble-metal patterns). However, the noble-metal patterns from; layered intrusions, ocean-floor basalts, continental-flood basalts, alkaline rocks and the non-tectonized portions of ophiolites are not unique and cannot be easily distinguished from each other. This is because the shape of the noble-metal pattern of a rock is influenced by the following factors:

(a) Whether any sulphides are present in the rock: noble metals tend to concentrate in sulphides, therefore the noble-metal pattern of any rock containing sulphides will tend to be dominated by that of the sulphides, which in turn will be similar to that of the liquid at the time of sulphide saturation (Keays, 1982). Thus, despite the fact that the rock may be a cumulate it could have the same shaped noble-metal pattern as the silicate liquid at the time of sulphide saturation.

(b) If no sulphides are present it is important to consider whether the rock represents a cumulate, or liquid, composition. Olivine and chromite cumulates tend to be enriched in Os, Ir and Ru (Agiorgitis & Wolf, 1977, 1978; Keays, 1982; Oshin & Crocket, 1982; Page *et al.*, 1982*a*,*b*; Davies & Tredoux, 1985; Crocket & MacRae, 1986). The mechanism by which this enrichment takes place is a matter of debate. Some authors (e.g. Keays & Campbell, 1981; Barnes *et al.*, 1985; Davies & Tredoux, 1985) suggest that early in the crystallization history of a magma it becomes saturated in Os-, Ru-, Ir-bearing PGM (i.e. at the ppb level) and that these PGM crystallize before the olivine and chromite and are then included within the olivine and chromite. Support is lent to this suggestion by: the observation of Os-, Ir- and Ru-bearing PGM in chromite-rich rocks (Prichard *et al.*, 1981; Stockman & Hlava, 1984; Talkington *et al.*, 1984); the covariance of chromite and laurite compositions in the Bird River Sill (Ohnenstetter *et al.*, 1986) and by the work of Amosse *et al.* (1987) who showed that Ir has a far lower solubility (<50 ppb) than Pt (<600 ppb) in basaltic melts. In contrast some workers (Agiorgitis & Wolf, 1978; Brugmann *et al.*, 1985) suggest that Os, Ir and Ru enter the chromite and olivine by solid substitution. In any event, a rock containing cumulate olivine or chromite may have a less fractionated noble-metal pattern than the liquid from which it formed.

(c) The relative timing of crystal fractionation and sulphide saturation (Keays & Campbell, 1981; Barnes *et al.*, 1985; Lee & Tredoux, 1986; Barnes & Naldrett, 1987). As mentioned above Os, Ir and Ru tend to be enriched in the olivine and chromite cumulates. Therefore, if no sulphide saturation occurs the noble-metal patterns will become progressively fractionated. Once sulphide saturation occurs most of the noble metals will tend to enter the sulphide and any rock containing this sulphide will tend to inherit the noble-metal pattern at the time of sulphide saturation. If sulphide saturation occurs early in the magma's history and the sulphides do not settle out, then the magma is likely to retain a relatively primitive noble-metal pattern despite the fact that the silicate minerals have fractionated.

The simple noble-metal patterns are inadequate for discerning which processes have occurred because they do not show the ratio of Ni and Cu relative to the noble metals. Therefore, two new methods for considering noble metal data have been developed here:

(1) By normalizing the noble metal contents to average mantle values and adding Ni and Cu to either end of the noble-metal pattern the ratio of Ni and Cu to the noble metals may be illustrated. These patterns will be called

mantle normalized metal patterns. Because Ni, Cu and the noble metals have different partition coefficients into sulphides, olivine, chromite and PGM, the relative timing of sulphide saturation, sulphide removal and crystal fractionation may be deduced from the metal patterns;

(2) Although the effects of partial melting, crystal fractionation and sulphide saturation on the metal patterns can be observed, it was found to be easier to separate these effects visually using the metal ratio plots of Pd/Ir versus Ni/Cu and Ni/Pd versus Cu/Ir.

In each case the method will be outlined by using a literature data base and then demonstrated using new data from Norway.

IS NORMALIZATION TO 100% SULPHIDES ALWAYS JUSTIFIED?

Normalization to 100% sulphides assumes that most of the noble metals are present in the sulphide portion of the rock, and such a recalculation allows a more meaningful comparison between rocks with widely differing sulphide contents, by removing the dilution effect of the silicate phases. However, a number of assumptions are inherent in this procedure which are not necessarily valid, particularly in sulphide-poor rocks. Firstly, normalizing to 100% sulphides assumes that durng crystallization of the rocks *all* the noble metals entered a sulphide liquid containing 36–38% sulphur. In rocks containing chromite or olivine some Os, Ir and Ru may be present in the chromite or olivine, or as PGM. Secondly, Ballhaus and Stumpfl (1986) suggest that under certain circumstances the noble metals partition into a fluid phase rather than into sulphides. Thirdly, it assumes that the present sulphur content of the rock represents the original igneous value. Sulphur is an extremely mobile element during hydrous alteration of rocks. Gain (1985) has suggested that sulphur was removed from the UG-2 reef of the Bushveld during cooling of the intrusion, so even rocks that do not contain hydrous minerals may have suffered sulphur loss. Therefore, in order to avoid the potential errors that can arise from recalculation to 100% sulphides the data in this work has not been recalculated.

THE ORDER OF THE ELEMENTS ON A METAL DIAGRAM

Naldrett and Barnes (1986) added Cu and Ni next to Au on the chondrite normalized noble-metal pattern (e.g. Fig. 1(a)). It is suggested here that Ni values be placed to the left of Os, rather than to the right of Cu (Fig. 1(b)). Ni is compatible with most early crystallizing phases (e.g. olivine, pyroxene, spinel), Os, Ir and Ru tend to be enriched in olivine- and chromite-rich rocks, therefore, it is logical that Ni should be placed on the left-hand side of the diagram. Cu, on the other hand, is a relatively incompatible element in mafic rocks, and hence the position of Cu to the right of Au.

THE ADVANTAGE OF MANTLE NORMALIZATION OVER CHONDRITE NORMALIZATION

Simply moving Ni to the left of Os, however, does not produce a smooth chondrite normalized curve for mantle lherzolites (Fig. 1(b)) because the ratio of Ni and Cu in the mantle to C1 chondrites is approximately 0·13 and 0·17 respectively, and the ratio of Ir and Pd in the mantle to Ir and Pd in C1 chondrites is about 0·008 15 (4·4/540). Therefore, if the metal values for a mantle derived rock are chondrite normalized the Ni chondrite values will tend to be 16 times (0·13/0·008 15) the Ir values and the Cu values will tend to be 21 times the Pd values, this gives rise to the trough-shaped metal pattern in Fig. 1(b). As most terrestrial rocks are derived from the mantle, it would be more realistic to normalize to mantle values than C1 chondrites. The argument against mantle normalization has been that there is no

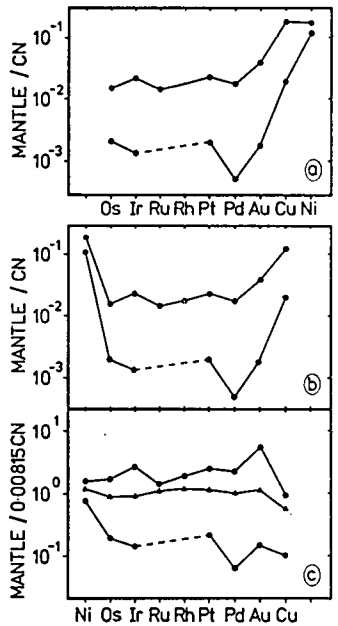

FIG. 1. (a) Conventional chondrite normalized metal patterns showing the range of rocks representing mantle (sources for mantle indicated in Appendix). Note that from Au to Ni the pattern is not flat. (b) Metal pattern of mantle fragments with Ni to the left of Os and Cu to the right of Au; chondrite normalized. Note the peaks at Ni and Cu which reflect the fact that there is 10–20 times more Ni and Cu chondrite normalized in the mantle than there are noble metals. If metal diagrams from ultramafic and mafic rocks are chondrite normalized they too will have peaks at Ni and Cu because they are mantle derived. (c) Revised metal pattern for the range of rocks representing mantle normalized to 2000 ppm for Ni 28 ppm for Cu and 0·008 15 × chondrites for the noble metals. Note that the metal patterns are now flat (triangles indicate the average value from the data base).

TABLE 1
Metal values

Location	Rock type	$\bar{x}^a$	n	Ni %	Cu	S	Os (ppb)	Ir	Ru	Rh	Pt	Pd	Au
World	Mantle fragments	[b]	114	0·2	0·002 8	0·020	4·2	4·4	6	2	9·2	4·4	1·4
Estimate of mantle 0·00815 × CI[c]							4·2	4·4	5·6	1·6	8·3	4·4	1·2
Komatiites													
Karasjok	Volcaniclastics	a	24	0·12	0·012 4	0·081	2·1	1·5	<10	<2	11	11	6
		g	24	0·11	0·005 0	0·056	1·8	1·3	<10	<2	10	10	1·6
Rombak	Chlorite–actinolite Fels	a	7	0·10	0·001 9	0·017	<5	1·2	<10	1·6	<13	15	0·8
		g	7	0·085	0·001 3	0·015	<5	0·8	<10	1·3	<13	14	0·7
Caledonide ophiolites													
Norway	Normal podiform chromitites	a	64	0·13	0·001 9	0·122	n.d.	n.d.	n.d.	n.d.	11	1·6	4
		g	64	0·07	0·000 6	0·080	n.d.	n.d.	n.d.	n.d.	8	0·8	2·5
Norway	Enriched podiform chromitites	a	4	0·13	0·005 6	0·130	n.d.	n.d.	n.d.	n.d.	416	413	248
		g	4	0·12	0·004 4	0·111	n.d.	n.d.	n.d.	n.d.	362	82	43
Leka	Stratiform chromitite		1	0·19	0·003 0	0·559	1070	1760	770	40	<10	<10	8
Leka	Chromite-rich dunite	a	15	0·20	0·002 7	0·303	7·2	7·8	24	2·4	11	17	2·9
		g	15	0·19	0·001 8	0·241	4·5	3·3	17	2	10	15	1·5
Færøy	Ni-rich sulphides	a	6	2·27	1·55	44·92	221	205	203	187	1 503	4 066	34
			6	2·27	1·41	44·92	203	167	186	240	1 450	3 986	23
	Cu-rich sulphides	a	4	1·34	8·28	44·07	252	211	247	235	2 230	5 800	201
		g	4	0·99	7·09	43·95	170	103	177	149	1 630	5 432	163
	Weighted mean		10	2·10	2·69	44·77	225	206	210	195	1 626	4 360	62
Small possibly drift-related intrusions													
Reinfjord	Tholeiitic dykes	a	10	0·10	0·016 4	0·338	<2	0·5	<10	<2	5·3	6·4	1·2
		g	10	0·07	0·013 9	0·263	<2	0·3	<10	<2	3	6	1
Melvann	Alkaline dykes	a	12	0·08	0·024 2	0·615	<2	0·4	<10	<2	6·4	5	1·3

		g	12	0·08	0·014 4	0·241	<2	0·3	<10	<2	6	4	1·2
Lille Kufjord	Ultramafics	a	6	0·08	0·020 6	0·270	<2	0·6	<10	<1	<10	7	3
		g	6	0·07	0·020 0	0·270	<2	0·5	<10	<1	<10	6	1·4
Hosanger	Ni-rich sulphides	a	7	3·15	0·350	34·2	27·8	20·8	39	8	71	105	8·7
		g	7	2·96	0·280	33·9	25	19	37	7	63	92	6
	Cu-rich sulphides	a	3	0·62	7·72	30·96	28	23	62	<20	120[d]	[d]	341
		g	3	0·59	6·79	29·63	25	21	47	<20	60[d]	[d]	116
	Weighted mean		10	2·72	0·93	33·47	25	19·2	38	<8·3	62·7	[d]	17
Flåt	Ni-rich sulphides	a	6	2·90	0·27	35·47	26	29	38	11	78	87	19·6
		g	6	2·06	0·19	35·2	22	27	35	7	50	70	18
	Cu-rich sulphides	a	5	1·50	11·71	34·9	20	22	29	16	159[d]	151[d]	578
		g	5	1·07	8·40	34·8	20	22	22	6	40[d]	100[d]	441
	Weighted mean		11	1·94	1·22	35·15	22	26	33	7	49	74	71
Ertelien	Ni-rich sulphides	a	8	2·12	0·35	42·5	9·4	6·5	14	10	9	198	45·9
		g	8	1·76	0·23	42·3	2	1·7	8·8	6	7	179	17·5
	Cu-rich sulphides	a	7	0·91	10·24	35·57	<5	0·65	<10	7·7	603[d]	135[d]	1 319
		g	7	0·68	5·40	34·8	<5	0·6	<10	2	65[d]	70[d]	591
	Weighted mean		15	1·59	1·00	42·5	<2·5	1·5	<9	5·6	16	163	104
Large proterozoic layered intrusion													
Jotunheim	Pyroxenites	a	14	0·01	0·025	0·164	<2	0·3	<10	1	31	154	18·7
		g	14	0·01	0·023	0·136	<2	0·25	<10	0·9	30	150	16

[a] Because noble metals tend to have a log-normal distribution both arithmetic (a) and geometric (g) means are listed.
[b] Ni and Cu values from Sun (1982). S and noble metals from the sources listed in the appendix.
[c] CI values listed in Naldrett (1981).
[d] Because of analytical difficulties the Pt and Pd numbers for these samples are not reliable.
n.d. = not determined.

reliable estimate of the mantle abundances for noble metals, and the mantle is heterogeneous so that any value chosen to represent it is somewhat arbitrary. Despite these drawbacks, the advantages from mantle normalization (i.e. normalizing to the probable source material) are significant. There are now over 100 published analyses, from 22 localities around the world, for the Ir and Pd contents of samples which are thought to represent mantle material. The average noble metal content of all the mantle material that has been analysed (spinel lherzolites, garnet lherzolites and harzburgites) is close to 0·008 15 × C1 chondrite (col. 1, Table 1). This value is similar to, but slightly higher than, the values obtained by Morgan (1986) for his estimate of the Os, Ir, Pd and Au contents of the upper mantle based on spinel lherzolites. Furthermore, 0·008 15 × C1 chondrite is also surprisingly close to Chou *et al.*'s (1983) estimate that the mantle has experienced an addition of 0·74% chondrite material by bombardment from meteorites after formation of the core. Therefore the mantle normalizing factors for noble metals used in this work are 0·008 15 times chondrite (row 2, Table 1). The mantle abundances for Ni and Cu quoted by Sun (1982) were used for these elements.

The result of this mantle normalized approach can be seen by comparing Figs 1(a), (b) and (c). Figure 1(a) shows the range of metal patterns for the mantle presented in the conventional fashion, note the sharp change in the slope of the curve at Cu. Figure 1(b) shows the metal pattern, still chondrite normalized but with Ni next to Os. Note the enrichment of Ni and Cu relative to the noble metals. Figure 1(c) shows the same metal patterns but normalized to mantle, note that the patterns are now smooth and almost flat.

In Fig. 2 the range of mantle normalized curves for the various rock types is shown. The range was defined by drawing an envelope around the values from the literature (see Appendix for the sources used).

The metal patterns for komatiites (Fig. 2(a)) are only slightly fractionated (Pd/Ir = 5–10) with the Ni and Cu mantle normalized values (mn) close to the mantle normalized values for noble metals (Ni/Ir_{mn} = 1·5–2; Cu/Pd_{mn} = 0·75–0·9). This produces a fairly smooth metal pattern. The very wide range (0·5–500 times mantle) of metal patterns for komatiites arises because the lower limit of the komatiite field is defined by olivine-spinifex textured komatiites (Munro Township and western Australia; Crocket & MacRae, 1986; Keays, 1982) which lack sulphides, whereas the upper limit is defined by massive sulphides in equilibrium with komatiites (Abitibi Greenstone Belt, Green & Naldrett, 1981).

High-MgO basalts (Fig. 2(b)) in this work are regarded as rocks derived from magmas containing 12–18% MgO. This division includes komatiitic basalt, high-MgO basalts and tholeiites but not boninites which have been included with low-TiO_2 basalts Fig. 2(e). The lower limit of the field is defined by the chill zone of Fred's Flow (a komatiitic basalt, Crocket & MacRae, 1986), and the upper limit is defined by the sulphides from Katiniq, Cape Smith Fold Belt (Barnes *et al.*, 1982); the Katiniq sulphides are thought to have formed in equilibrium with a komatiitic basalt. The noble metal portion of the patterns is slightly more fractionated (Pd/Ir = 20–30) than the komatiite curves (compare Figs 2(a) and (b)); the Ni/Ir_{mn} and Cu/Pd_{mn} ratios are close to 1 and produce an overall smooth metal curve.

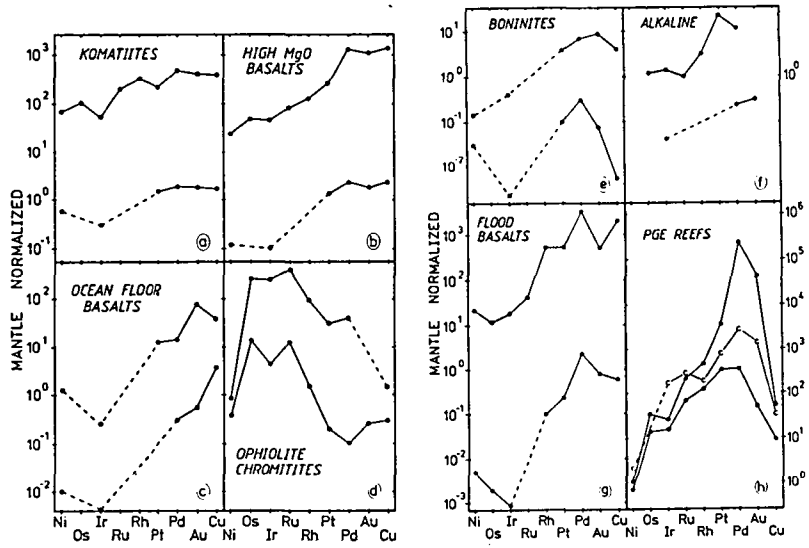

FIG. 2. Range of mantle normalized metal patterns for a variety of rock types using data from the literature: sources are indicated in the Appendix. (a) Komatiites and the sulphides associated with them. (b) High-MgO basalts and sulphides associated with them. (c) Ocean floor basalts. (d) Podiform chromitites from ophiolites. (e) Boninites and low-TiO_2 basalts. (f) Alkaline rocks. (g) Flood basalts and sulphides associated with them. (h) PGE reefs (with the Pt-enriched chromites from the Cliff locality of the Unst ophiolite shown as curve c).

Ocean floor basalts in this work include basalts from ridges, triple junctions and 'type I' lavas from the Thetford ophiolite (all the samples have flat or LREE depleted REE patterns). Metal patterns from ocean floor basalts (Fig. 2(c)) cover the range 0·003–3 times mantle. This range may be too narrow, because none of the samples from the localities considered here contain appreciable amounts of sulphides and none are from primitive ocean floor basalts (highest MgO content 9·2%). The noble metal portion of the patterns shows variable degrees of fractionation with Pd/Ir ratios from 20 to 200; Ni is enriched relative to Ir (Ni/Ir_{mn} = 2–7) and Cu is enriched relative to Pd (Cu/Pd_{mn} = 10–50). Consequently, unlike the metal patterns for more primitive rocks, ocean floor basalts do not have smooth metal patterns, but are trough shaped. This suggests that either some sulphides have been retained in the mantle during partial melting and these have preferentially retained the noble metals over Ni and Cu (Hamlyn *et al.*, 1985), or some sulphides segregated from the magma en route to the surface and these preferentially removed the noble metals (Hertogen *et al.*, 1980). If Hamlyn *et al.* (1985) are correct, then all ocean floor material should be depleted in noble metals. If Hertogen *et al.* (1980) are correct ocean floor basalts that have not segregated sulphides, possibly primitive ocean floor basalts, should not be noble metal depleted.

The wide range in Pd/Ir ratios from ocean floor basalts may be caused by the

removal of Os, Ir and Ru either as PGM or by chromite crystallization, as has been suggested by Hertogen *et al.* (1980) and Oshin and Crocket (1986). The most remarkable feature of metal patterns from ophiolite chromites (Fig. 2(d)) is that they are strongly enriched in Os, Ir, Ru and have Pd/Ir ratios of 0·01–0·1 and cover the range 0·1–200 times mantle. Thus, the complementary metal patterns of ophiolite chromitites and ocean floor basalts can be understood if the chromitites represent the cumulate portion and the ocean floor basalt the fractionated silicate melt portions of a primitive mantle melt.

Some ocean floor material (e.g. the 'type I' basalts at the Thetford ophiolite) that has experienced chromite and olivine fractionation has relatively unfractionated metal patterns (Pd/Ir = 10–15). If sulphide saturation occurs early in the magma's history (i.e. before appreciable chromite or PGM crystallization), then the magma will inherit a primitive metal pattern. However, if chromite (or PGM) crystallization occurs before sulphide saturation, then the chromite or PGM will preferentially remove Os, Ir and Ru from the magma to produce a fractionated liquid and an Os–Ir–Ru-enriched cumulate. Using this reasoning the contradictions between the fractionated silicate geochemistry and the unfractionated noble metal patterns of Thetford 'type I' basalts, may be explained by sulphide saturation before chromite crystallization.

Boninites and low-TiO_2 lavas (Fig. 2(e)) exhibit a variable degree of noble metal fractionation (Pd/Ir ratio = 20–200) and cover the range 0·002–10 times mantle. Ni tends to be enriched relative to Ir, Ni/Ir_{mn} = 2–10 and Cu is depleted relative to Pd, Cu/Pd_{mn} = 0·01–0·7. Irivine and Sharpe (1982) suggest that one of the initial magmas to the Bushveld Complex was boninite-like. Hamlyn *et al.* (1985) have drawn attention to the similarity in the depletion of Cu relative to Pd in boninites and the Merensky reef. They suggest that the Cu depletion results from a previous melting event and that this is important in generating the type of magma from which Pt-reefs such as the Merensky reef of the Bushveld complex form.

Alkaline rocks (Fig. 2(f)) have relatively unfractionated metal patterns (Pd/Ir = 10–20), but the full shape of the metal pattern curve is not known because Ni and Cu values are not available for the samples in which the noble metal levels have been determined. Furthermore, the range of values indicated here may be too small as the data base consists of only 3 localities. The upper limit is based on kimberlites (Kaminskiy *et al.*, 1975) and the lower limit on basanites (Mitchell & Keays, 1981).

Flood basalts (Fig. 2(g)) tend to have fairly fractionated metal patterns (Pd/Ir = 100–200). The curves show a tendency towards enrichment of Ni and depletion in Cu relative to the noble metals. The lower limit is defined by the international standard BCR-1 (Govindaraju, 1984), and the upper limit by sulphides from Nor'ilsk (Naldrett, 1981). However, not all flood basalt related material is as fractionated, the Insizwa Intrusion is associated with the Karroo flood basalts, but the metal pattern is less fractionated than most other flood basalt related intrusions (Pd/Ir = 20, Lightfoot *et al.*, 1984). This anomaly may be explained by suggesting that the Insizwa magma became saturated in sulphides early in its history and that consequently the sulphides froze in the unfractionated metal pattern of the Insizwa magma.

The metal patterns for Pt-reefs are shown in Fig. 2(h). The UG-2 and Merensky reefs of the Bushveld Complex, the JM reef of the Stillwater Complex and the Roby zone of the Lac des Iles Intrusion are all considered in this group. Pt-reefs have also been reported from the Penikat intrusion in Finland (Alapieti & Lahtinen, 1986) and from the Great Dyke of Zimbabwe (Wilson & Prendergast, 1987), but insufficient noble metal data were available to include these localities here. The metal patterns show a variable degree of fractionation in the noble metals; from the UG-2 reef which is the least fractionated (Pd/Ir approximately 20) to the JM reef (Pd/Ir approximately 8000). The most distinctive feature of these metal patterns is the overall arched shape, which is a result of the sharp down turn at each end of the pattern at Ni and Cu respectively. One of the most distinctive features of Pt-reefs is the low ratio of Ni and Cu to noble metals (Ni/Ir_{mn} <0·05, Cu/Pd_{mn} <0·02). Interestingly one other rock type has metal patterns similar to Pt-reefs and this is the Pt-enriched chromitites from the Cliff locality of the Unst ophiolite (c on Fig. 2(h)).

METAL RATIO DIAGRAMS

An alternative approach to presenting noble metal data is to use metal ratio plots. If two metal ratios are plotted against each other, e.g. Pd/Ir versus Ni/Cu, then it is not necessary to recalculate the data to 100% sulphides nor to normalize the data to mantle or chondrite values.

Pd/Ir versus Ni/Cu

Figure 3(a) outlines the fields covered by the major magma suites on a plot of Ni/Cu versus Pd/Ir. Because the number of samples for which the noble metals and Ni and Cu have been determined is small the shape of these fields may change as more data are obtained. Nonetheless this diagram was found to be useful in outlining the processes that may effect the distribution of the noble metals, Ni and Cu. These two particular ratios were chosen because the metal patterns indicated that the Pd/Ir ratio increases as the magma suite becomes more evolved, while the Ni/Cu decreases (Figs 2 (a–g)). Therefore, a plot of these two ratios against each other produces a separation of the various magma suites with the most primitive (mantle material), at one end and the most evolved (continental flood basalts) at the other. The effect of variations in the degree of partial melting and the variations in composition of the source material on the Pd/Ir and Ni/Cu ratios may be estimated empirically by drawing a line through mantle, komatiites, high-MgO basalts, ocean-floor basalts, boninites and continental flood basalts. More detailed possible numerical models are presented elsewhere (Naldrett & Barnes, 1986; Barnes, 1987).

The fields for layered intrusions, and for the intrusive portions of ophiolites are also shown on Fig. 3(a). The effect of crystal fractionation on the Pd/Ir and Ni/Cu ratios can be examined by considering the komatiite and ophiolite data. Some olivine cumulates from komatiite flows (B on Fig. 3(a)) have lower Pd/Ir and higher Ni/Cu ratios than the lavas from which they crystallized. Olivine concentrates Ni in

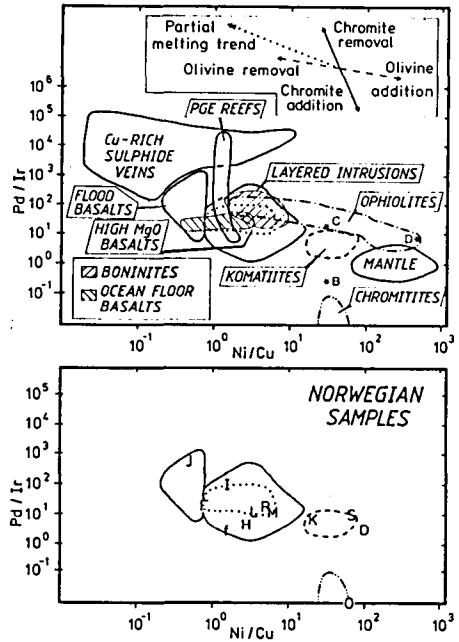

FIG. 3. (a) Metal ratio diagram of Pd/Ir versus Ni/Cu based on literature data for discriminating between the compositional fields of: mantle, komatiites and sulphides associated with them, high MgO-basalts and associated sulphides, ocean-floor basalts, boninites and low-TiO_2 basalts, flood basalts and sulphides associated with them, ophiolites, podiform chromitites from ophiolites, Pt-reefs, layered intrusions of unknown affinity, and Cu-rich sulphides. D = dunites from Thetford ophiolite, B = B-zones of komatiites and C = Cliff locality from Unst. The inset shows the displacement vectors on the diagram for the effects of partial melting of the mantle (dotted), olivine removal or addition (dashed) and chromite removal or addition (solid). (b) Diagram of the Pd/Ir and Ni/Cu ratios of Norwegian mafic and ultramafic rocks compared with selected compositional fields (others left out for the sake of clarity) from Fig. 3(a). Symbols: D = dunites from Leka; K = Karasjok komatiites; S = Rombak komatiites; O = Leka ophiolite chromitite; F = Fæøy ophiolite sulphides; R = Reinfjord Tholeiitic Intrusion; M = Melkvann Alkaline Intrusion; L = Lille Kufjord Tholeiitic Intrusion; J = Jotun pyroxenites; H = Hosanger sulphides; f = Flåt sulphides; I = Ertelien sulphides.

preference to Cu, therefore the higher Ni/Cu ratio in olivine-enriched portions of the flows is reasonable. Some of the olivine cumulates are enriched in Ir, thus the net effect of olivine crystallization is to displace the cumulate samples towards lower Pd/Ir and higher Ni/Cu ratios and to displace the fractionated liquid towards higher Pd/Ir ratios and lower Ni/Cu ratios (Fig. 3(a)).

Chromite crystallization has an effect similar to, but more intense than, olivine crystallization. The difference can be seen by examining the relative positions of chromitites and dunites within ophiolites. The dunites (D) show a large change in

Ni/Cu ratio from the initial liquid (presumed to lie in ocean floor basalt field) but a relatively small change in Pd/Ir ratio, the chromitites show a large change in Pd/Ir ratio and a small change in Ni/Cu ratio. Most of the variation in Pd/Ir and Ni/Cu ratios for komatiites, ophiolites, boninites, flood basalts, high-MgO lavas and layered intrusions may be accounted for by variation in conditions of partial melting and olivine or chromite crystallization.

Cu-rich sulphide veins commonly occur as footwall veins associated with Ni-Cu sulphide deposits, as at Sudbury (Hoffman *et al.*, 1979) and Kambalda (Lesher & Keays, 1984), but they may also occur as veins within the main ore zone as at Katiniq (Dillon-Leitch *et al.*, 1986) or Rathburn Lake (Rowell & Edgar, 1986). Cu-rich sulphide veins tend to be enriched in Au, Pd and at some localities Pt, but depleted in Os, Ir and Ru relative to the bulk composition of the Ni–Cu sulphide deposits with which they are associated. Consequently, the Cu-rich sulphide veins have low Ni/Cu ratios, high Pd/Ir ratios and form a distinct field on Fig. 3(a). Most authors consider these veins to have formed by hydrothermal remobilization of Cu, Au and Pd from the associated Ni–Cu sulphide deposit. However, the situation is complicated by the fact that many Ni–Cu sulphide deposits exhibit an internal compositional zonation with a Cu, Au, Pd, Pt enriched portion and a separate Os, Ir, Ru enriched portion (Kambalda, Keays *et al.*, 1981; Strachona & Leveck West, Naldrett *et al.*, 1982; Insizwa, Lightfoot *et al.*, 1984; Alexo, Barnes & Naldrett, 1986; Lillefjellklumpen, Grønlie, in press). The Cu-rich ore is displaced relative to the bulk ore in the direction of the Cu-rich sulphide veins but does not usually plot in Cu-rich sulphide vein field. Naldrett *et al.* (1982) suggested that at Sudbury the Cu-rich ore is partly fractionated sulphide liquid produced after the crystallization of monosulphide solid solution from an Fe–Ni–Cu sulphide liquid, and furthermore, that the Cu-rich sulphide veins are the final fractionated product. In contrast Keays *et al.* (1981), suggest that the compositional zonation observed in the Ni–Cu sulphide ores at Kambalda is the result of hydrothermal remobilization. Regardless of which hypothesis is correct, it should be remembered when using these metal ratio plots that the composition of Cu-rich ores tends to be displaced towards lower Ni/Cu ratios and higher Pd/Ir ratios on Fig. 3(a) relative to the bulk ore.

The Pt-reefs show a narrow range of Ni/Cu ratios but have a wide range in Pd/Ir ratios. Although the Ni/Cu and Pd/Ir ratios of Pt-reefs from the Bushveld Complex lie in the field of layered intrusions, the JM-reef of the Stillwater Complex and the Roby zone of Lac des Iles Intrusion are extremely Pd-enriched and overlap with a field of Cu-rich sulphide veins. If Cu-rich sulphide veins form by hydrothermal remobilization, then the overlap of the JM reef and Roby zone with the field of Cu-rich sulphide veins could be interpreted as evidence of hydrothermal action in the formation of these rocks. However, as will be discussed below the Ni/Pd and Cu/Ir ratios of the JM reef and Roby Zone do not support such an interpretation. The Pt-enriched chromitites of the Unst ophiolite do not plot in the field of Pt reefs on this diagram (C on Fig. 3(a)), but in the field of ophiolites, which is consistent with their geological setting. The main difference between the Unst rocks and Pt reefs is the higher Ni/Cu ratio of the Unst rocks.

Ni/Pd versus Cu/Ir

Ni and Cu both have similar partition coefficients into sulphide liquid (Rajamani & Naldrett, 1978), therefore the segregation of a sulphide liquid from a silicate magma does not effect the Ni/Cu ratio of either the remaining silicate magma or of a cumulate which contains some sulphides. Partition coefficients for Pd and Ir into a sulphide liquid are unknown; estimates range from 1000 to 100 000 (Campbell & Barnes, 1984), but the partition coefficients are usually assumed to be similar. Therefore, as in the case of the Ni/Cu ratio, the Pd/Ir ratio of the silicate magma, or cumulate is not changed by the segregation of a sulphide liquid. For this reason the effect of sulphide removal from the silicate magma, or sulphide addition to the cumulate during the crystallization of a magma, is not visible on Fig. 3(a). In order to study the effect of sulphide saturation the Ni and Cu to noble metal ratio must be considered. Figure 4(a) shows the fields for some rock types on a plot of Cu/Ir versus Ni/Pd.

Because the partition coefficients for Cu and Ni into sulphides are much less than for noble metals, the segregation of sulphides from a silicate magma causes the silicate liquid to become depleted in noble metals relative to Ni and Cu; thus any cumulate containing these sulphides is enriched in noble metals relative to Ni and Cu. The Ni/Pd and Cu/Ir ratios of the remaining silicate magma increase, and the composition of any rocks that subsequently form from it are increased (Fig. 4(a)). The composition of the complementary cumulates containing the sulphides tend to be displaced to lower Ni/Pd and Cu/Ir ratios. However, the decrease in Ni/Pd and Cu/Ir ratios in the sulphides is also dependent on the amount of sulphides that segregate (i.e. the *R*-factor) as discussed by Keays and Campbell (1981) for Cu and Pd and Campbell and Barnes (1984) for Ni and Pt. If a small amount of sulphides segregates, then the Ni/Pd and Cu/Ir ratios in the sulphides are lower than those of the melt, but if a large amount of sulphides segregates the Ni/Pd and Cu/Ir ratios of the sulphides approach but never exceed those of the melt from which they formed. Thus any samples that plot above the fields outlined by the extrusive rocks on Fig. 4(a) probably formed from magmas that have segregated sulphides. These rocks will not make good exploration targets for noble metals.

The effect of variations in the conditions of partial melting on the Ni/Pd and Cu/Ir ratios, as illustrated by the trend of komatiites, high-MgO basalts, ocean-floor basalts and flood basalts is to decrease the Ni/Pd ratio and to increase the Cu/Ir ratio with decreasing degrees of partial melting. More detailed numerical modelling for partial melting may be found in Naldrett and Barnes (1986) and Barnes (1987).

Olivine crystallization increases the Ni/Pd ratio and decreases the Cu/Ir ratio of the cumulates (Fig. 4(a)). The fractionated liquid shows a complementary trend of an increase in Cu/Ir and decrease in Ni/Pd ratios. Chromite crystallization does not appreciably change the Ni/Pd ratio of the magma but it does increase the Cu/Ir ratio of the magma from which it fractionated because chromite or the PGM associated with it preferentially removes Ir from the liquid. Therefore chromite crystallization displaces the composition of the cumulate to lower Cu/Ir ratios but similar Ni/Pd ratios and the liquids to higher Cu/Ir ratios (Fig. 4(a)).

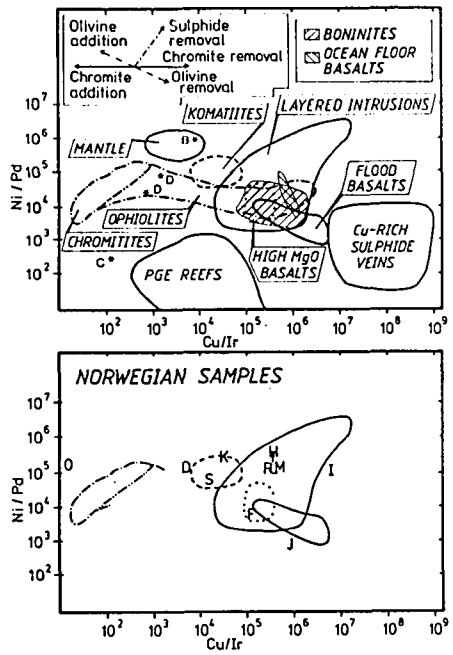

FIG. 4. (a) Metal ratio diagram of Ni/Pd versus Cu/Ir based on the literature data base. Compositional fields are, as on Fig. 3(a), distinguished, but notice the clear separation of PGE reefs and Cu-rich sulphides on this diagram. Inset shows the displacement vectors for olivine removal or addition (dashed), chromite removal or addition (solid) and sulphide removal (dot-dash), the partial melting trend has been left off for clarity. Symbols as on Fig. 3(a). (b) Diagram of the Ni/Pd and Cu/Ir ratios of Norwegian mafic and ultramafic rocks compared with selected compositional fields (others left off for clarity) based on the literature data shown on Fig. 4(a). Symbols as for Fig. 3(a).

The Cu-rich sulphide veins are enriched in Cu and Pd but depleted in both Ir and Ni, and plot in a distinct field on Fig. 4(a). However, on this diagram there is no overlap between the Cu-rich veins and the Pt-reefs as there was on the Ni/Cu versus Pd/Ir plot. The most distinctive feature of the Pt-reefs, their low base to noble metal ratio, is clearly illustrated on Fig. 4(a). Interestingly, the Pt-rich material from Unst ophiolite (C) plots close to the Pt-reef field.

THE NORWEGIAN EXAMPLES

Analytical Methods

For noble metal analysis the samples were divided into two categories based on the amount of chromite they contain. Samples containing <10% chromite were

TABLE 2
Comparison of metal values obtained for standards in this study with previously determined values

	Tv-84			*Ax-26*			*SARM7*	
Source	E	A	B	C	A	B	D	B
n	2	1	4	10	1	1	—	2
Os ppb	<2	n.d.	<2	<5	n.d.	<2	63	62
Ir	0·1	n.d.	0·23	2	n.d.	2·2	74	73
Ru	<10	n.d.	<10	<18	n.d.	<10	430	470
Rh	0·6	n.d.	<1	8·5	n.d.	9	240	204
Pt	2	<3	<10	51	43	35	3 740	3 475
Pd	<20	<2	<10	73	110	87	1 530	1 565
Au	5·9	10	1·2	12	28	8·8	310	275

A: Caleb (this work).
B: Becquerel (this work).
C: Barnes and Naldrett (1987).
D: Steele *et al.* (1975).
E: Barnes (1987).

analysed for noble metals by neutron activation analysis (NAA) after preconcentration into a Ni-sulphide bead by Becquerel of Toronto. Samples containing >10% chromite are not suitable for analysis by NAA because not all of the chromite melts during a normal fire assay and because incompletely dissolved Cr results in interference during the NAA. Those samples containing >10% chromite were analysed by atomic absorption using electrothermal atomization after preconcentration in a silver–lead bead, by Caleb Brett Ltd. This method is only suitable for the elements Pt, Pd and Au. Three samples were used to assess the performance of the laboratories. Tv-84 contains extremely low levels of all the noble metals: Becquerel and Caleb found this sample to contain noble metal levels at, or close to, their detection limit (Table 2) indicating that no significant contamination occurred. Ax-26 contains intermediate noble metal contents and the agreement between Becquerel and Caleb values and previously determined values is reasonable (Table 2). SARM7 contains high levels of the noble metals and Becquerel's values agree with the accepted values to within 10% for Os, Ir, Ru, Pt, Pd and to within 20% for Au and Rh (Table 2).

In NAA Cu can interfere with Pd and Rh determinations and the Crompton edge from Au with Pt determinations. Therefore, in Cu-rich samples, which are also Au-rich, it was not always possible to determine Rh, Pt and Pd.

Ni and Cu were determined by X-ray fluorescence for the komatiites, the Jotun pyroxenites and the Lille Kufjord rocks. For all other rocks Ni and Cu were determined by atomic absorption. S was determined by X-ray fluorescence.

Presentation of the Data

Table 1 presents the arithmetic mean for noble metals, Ni, Cu and S at each of the Norwegian localities considered here. However, noble metals tend to have a log-normal rather than a Gaussian distribution and therefore the geometric means

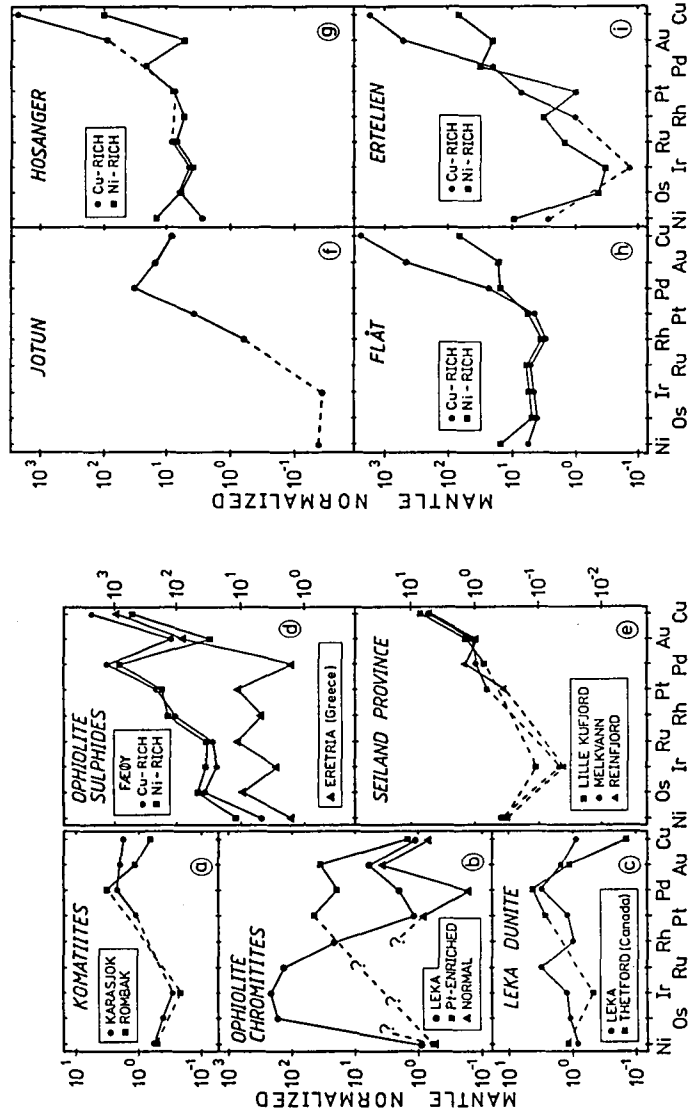

FIG. 5. Mantle normalized metal patterns for the Norwegian rocks sampled: (a) komatiites; (b) chromitites from ophiolites; (c) dunites from the Leka ophiolite compared with the dunite from Thetford mine ophiolite (Oshin & Crockett, 1982); (d) sulphides from ophiolites Faedy compared with Eretria (Economou & Naldrett, 1984); (3) Seiland Province Intrusions; (f) Jotun; (g) Hosanger; (h) Flåt and (i) Ertelien.

are also presented in Table 1. On Figs 3(b), 4(b) and 5 the geometric means have been plotted. Ni, Cu and S were present in all rocks at greater than the detection limits, but this was not the case for the noble metals in some samples. At localities where some samples contained noble metals at less than the detection limit, the geometric mean was estimated using log-probability paper, and the arithmetic mean calculated using a standard statistical formulae (Bury, 1975 p. 279 eqn (8.8)).

At all of the Ni–Cu sulphide deposits two types of ore were found to be present, i.e. Cu-rich and Ni-rich. The mean for each of these ore types at each deposit is presented in Table 1 and plotted in Fig. 5. A simple average of the samples is probably not representative of the sulphide deposits as a whole. The weighted mean for each locality was calculated by weighting the two types of ores such that the Ni/Cu ratio of the weighted mean is the same as that reported for each sulphide deposit when it was mined (Boyd & Nixon, 1985). At most deposits the weighting was 90% Ni-rich ore 10% Cu-rich ore.

Komatiites

Pyroclastic komatiites of Proterozoic age (2085 ±85 Ma Sm/Nd; Krill *et al.*, 1985; Often, 1985) from the Karosjok Greenstone Belt of northern Norway (Fig. 6) have been analysed for noble metals (Table 1). The noble metal portion of the metal pattern is relatively flat (Pd/Ir = 8) and Ni and Cu are not fractionated relative to the noble metals, thus the overall shape of the metal pattern is smooth (Fig. 5(a)). Since these rocks are pyroclastic, the noble metal content of the rocks should be similar to that of the magma. It is interesting to note that the Karasjok komatiite metal patterns closely resemble the spinifex-texture komatiite metal patterns both in shape and level (compare lower curve on Figs 2(a) and 5(a)). Similarly the Ni/Cu, Pd/Ir, Ni/Pd and Cu/Ir ratios are similar to komatiites from the literature and on the metal ratio plots the Karasjok komatiites plot in the field of komatiites (K on Figs 3(b) and 4(b)). Noble-metal patterns from Proterozoic komatiites have been reported previously (Katiniq, Barnes *et al.*, 1982). These patterns are more fractionated than the Karasjok komatiites (compare upper curve on Figs 2(c) and 5(a)). The difference in metal patterns could be because the Karasjok komatiites formed from a magma containing approximately 25% MgO (the average MgO content of the Karasjok samples), whereas the Katiniq komatiites formed from a liquid containing 18% MgO. Tredoux *et al.* (1986) have also noted an antipathic relationship between MgO content and Pd/Ir ratio in lavas from the Kaapvaal craton.

In the eastern volcanosedimentary belts of the early Proterozoic Rombak window in northern Norway (Fig. 6) there are some discontinuous lenses of massive ultramafic rocks of unknown origin (Korneliussen, in preparation). The rocks presently consist of serpentine, chlorite and actinolite. The mean metal pattern (Fig. 5(a)) for the Rombak rocks is similar in shape and level to that of komatiites (Fig. 2(a)), except for a Au and Cu depletion in the Rombak samples. The overall similarity of the Rombak metal pattern with komatiite metal patterns suggests that these lenses may represent deformed and metamorphosed komatiites. Furthermore, the Rombak ultramafic rocks plot in the komatiite field on metal ratio plots (S on Figs 3(b) and 4(b)).

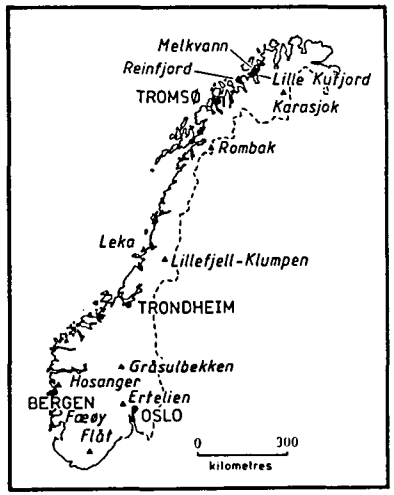

FIG. 6. Map showing the location of the Norwegian samples.

Caledonide ophiolites

Chromitites. High PGE values from podiform chromitites in ophiolites have been reported from Shetland (Gunn *et al.*, 1985; Prichard *et al.*, 1984, 1986), Ray-Iz and Kempirsay, USSR (Khvostova *et al.*, 1976). Ophiolite fragments are present throughout the Upper and Uppermost Allochthon of the Norwegian Caledonides (Gee *et al.*, 1985). Podiform chromitites from 19 of these ophiolite fragments (details of each locality are described in Nilsson, 1980) were analysed for Pt, Pd and Au. Only partial metal patterns can be drawn for the chromitites (Fig. 5(b)).

Chromitites from 15 of the fragments appear to contain noble metal levels similar to chromitites from around the world; the portion of the metal pattern that can be drawn has a similar shape to, and falls within, the range of podiform chromites from the literature (compare normal chromites on Figs 5(b) and 2(d)). These chromitites probably also exhibit the classic chromitite pattern with enrichment in Os, Ir and Ru.

However, chromitites from 4 localities contain Pt and Pd at >100 ppb which are much higher than that normally observed in podiform chromites from around the world (Fig. 2(d), and Pt-enriched on Fig. 5(b)). The shape of the available portion of the metal pattern resembles both the Pt-enriched metal pattern found in the podiform chromitite from the Cliff locality in the Shetland ophiolite and the Pt-reefs (Fig. 2(h)). The distinctive feature of these patterns is their arch shape which is a result of the high noble metal/base metal ratio. It is tempting to suggest that the overall metal pattern from these 4 Norwegian chromitites may have a similar shape and thus that they belong to the class of Pt-enriched podiform chromites.

Sixteen samples of chromite-rich dunites from the intrusive portion of the Leka ophiolite were analysed. Fifteen of the samples contain noble metal levels at 1–3 times mantle level and have essentially flat metal patterns (Fig. 5(c)). The overall shape and level of the metal pattern is similar to that observed for the dunite from the Thetford ophiolite of Quebec (Fig. 5(c)). These rocks are cumulates and therefore the flat metal pattern is not simply the result of sampling mantle; nor do the patterns represent trapped intercumulus liquid because that would be expected to resemble ocean-floor basalt which has Pd-enriched patterns (Fig. 2(c)). The metal patterns from the Leka chromite-rich dunites could represent the sum of the chromite pattern which is Os, Ir and Ru enriched and the ocean-floor basalt pattern (Pd-enriched). The presence of the cumulus olivine lowers the overall level of the pattern for all the elements except Ni. This interpretation is supported by the Pd/Ir versus Ni/Cu metal ratio diagram. The dunites plot on the Ni enriched side of the tie line between chromite and ocean floor basalt (D on Fig. 3(b)). The presence of cumulate olivine could have displaced the samples towards the Ni enriched side of the tie-line.

One sample from Leka which contains approximately 30% chromite has high values of Os, Ir and Ru; this sample exhibits a classic chromitite pattern with enrichment of Os, Ir and Ru (Fig. 5(b)). It is assumed that the metal pattern of this sample is dominated by the chromite. On the metal ratio diagrams this sample plots close to or within the field of chromites from ophiolites (O, Figs 3(b) and 4(b)).

Sulphides. There are two localities in Norway where massive sulphides associated with ophiolites contain ore grade levels of Pt. Both of these localities are too small to represent mineable deposits, but processes leading to their formation are of interest. Lillfjellklumpen is a massive sulphide lens lying concordantly between primitive MORB-type metabasalts and metagabbro in the allochthonous Gjersvik island arc complex (Grønlie, in press). Fæøy is a massive sulphide lens in the sheeted dyke complex of the Karmøy ophiolite (Boyd & Nixon, 1985). Only the Fæøy data will be discussed here as the Lillefjellklumpen data are presented elsewhere and are similar to the Fæøy data.

The massive ore at Fæøy contains two types of ore: Ni-rich and Cu-rich (Table 1). The metal patterns from both types are similar (Fig. 5(d)). Both increase steadily from Ni at 10 times mantle to Cu at 1000 times mantle and both have large negative Au anomalies. The Cu-rich ore is enriched in Cu, Au, Pd and Pt relative to the bulk ore. The metal patterns do not resemble any other metal patterns so far reported from ophiolites; in particular when compared with other ophiolites enriched in Pt (e.g. Cliff from the Shetland ophiolite, C on Fig. 2(h)) the Norwegian sulphides lack the characteristic arch shape. Neither do the Fæøy metal patterns resemble those of sulphides from the Erteria ophiolite, which have been attributed to hydrothermal action (Fig. 5(d); Economou & Naldrett, 1984). The Fæøy metal patterns closely resemble metal patterns from the sulphides which formed in association with komatiitic basalts (Katiniq sulphides from the Cape Smith Fold Belt of Canada, upper curve on Fig. 2(b)). Similarly, on the metal ratio diagrams the Fæøy sulphides plot in the field of high-MgO basalts (F on Figs 3(b) and 4(b)).

Massive sulphides within the intrusive portions of ophiolites are uncommon, but

two possible mechanisms for their formation are: (a) they formed by hydrothermal fluids; (b) the sulphides segregated from the magma during cooling. The suggestion that the Fæøy sulphides formed from hydrothermal fluids may be discarded on the grounds that the metal patterns do not resemble metal patterns from hydrothermal sulphides (Eretria, Fig. 5(d); see also discussion by Grønlie, in press). At Fæøy there are two types of dykes present (Pedersen, in preparation), ocean ridge basalts and boninites. If hypothesis (b) is true it would be anticipated that the sulphides which formed in equilibrium with such magmas should have a metal pattern similar to those found in ocean floor basalts or boninites. The Fæøy metal patterns are not trough-shaped like ocean-floor basalt metal patterns (compare Figs 2(c) and 5(d)) or Cu-depleted like the boninites. This might be taken as evidence that they did not segregate from an ocean floor basalt or boninite. This contradiction may be resolved by suggesting that the material that erupts on the ocean floor may be depleted in noble metals by the prior (i.e. pre-eruption) removal of these elements in sulphides. The metal patterns from primary ocean floor magmas may in fact be less fractionated than those shown in Fig. 2(c) and primary ocean floor magmas may well resemble the metal patterns of high-MgO basalts.

Small possibly rift-related intrusions

Seiland Province rocks. The early Caledonide (500–550 Ma, Sturt & Roberts, 1978) Seiland Province intrusions range in composition from tholeiitic to alkaline in composition. These intrusions are thought to be related to the rifting phase of the Caledonide event (Pedersen *et al.* (submitted)).

Samples from three of these intrusions were analysed: Reinfjord, a tholeiitic intrusion; Melkvann, an alkaline intrusion and Lille Kufjord, an intrusion thought to represent alkaline magma that reequilibrated at high levels in the mantle to generate a late tholeiitic intrusion in the area where alkaline rocks predominate; Bennett *et al.* (1986) describe the Reinfjord and Melkvann intrusions in more detail. These intrusions present an opportunity to examine noble-metal patterns in rocks derived from partial melting of the mantle under various conditions.

The Reinfjord samples are wehrlites, pyroxenites and troctolites principally from dykes and the marginal zones of the intrusion. The Lille Kufjord samples are peridotites and pyroxenites. The samples from Melkvann are peridotites and pyroxenites principally from dykes. Approximately 0·5% S is present in all these rocks and the noble metal, Ni and Cu content of the rocks is probably controlled by these sulphides and the Ni content probably also depends on the cumulate olivine. Because the Reinfjord and Melkvann samples are mainly from dykes and the marginal zones of intrusions it is assumed that their metal patterns are similar to that of the magma which intruded. The metal patterns from all three intrusions are similar (Fig. 5(e)). The noble metals are relatively unfractionated with Pd/Ir ratios of 12–20. Ni is slightly enriched relative to Ir (Ni/Ir_{mn} = 3–6) and Cu is enriched relative to Pd (Cu/Pd_{mn} = 3–6). The level and shape of the noble metal portion of the metal patterns resembles that of high-MgO basalt (compare Figs 5(e) and 2(b)), but with Ni and Cu enriched. Similarly, on a plot of Pd/Ir versus Ni/Cu the Seiland intrusions plot in the field of high-MgO basalts (R, M and L on Fig. 3(b)),

but on the Cu/Ir versus Ni/Pd plot the Seiland intrusion plots above the field of high-MgO basalts. The combination of high Ni/Pd and high Cu/Ir ratios suggests that the noble metals have been scavenged from the magma prior to the development of the present rocks, possibly by sulphides segregated from the magma earlier. The combination of low Pd/Ir ratios and high Ni/Cu ratios and high Ni/Pd and Cu/Ir ratios in the Seiland intrusions suggests that they formed from fairly primitive magmas that had experienced sulphide segregation prior to the development of these rocks.

The metal patterns for samples from the Reinfjord and Lille Kufjord Intrusions suggest that these rocks formed from magmas similar to high-MgO basalts and this is geologically reasonable since these intrusions are tholeiitic. However, the Melkvann intrusion is thought to have formed from an alkaline magma, and therefore, should be compared with a similar type of intrusion. There are, as yet, no noble-metal patterns available in the literature with which to compare it. Rocks of the alkaline family that have been analysed are: kimberlites from the USSR, which show similar PGE fractionation to the Melkvann samples, but at levels an order of magnitude higher (upper curve on Fig. 2(f)); and basanites (lower curve on Fig. 2(f)) from western Australia which also show a relatively unfractionated noble-metal pattern, but at levels slightly lower than the metal patterns from the Melkvann intrusion.

Despite the difference in partial melting conditions postulated for these three intrusions by Robins and Gardner (1975) their metal patterns are remarkably similar. This relationship confirms the conclusion, based on the rather limited data from the literature, that there is no obvious difference between the metal patterns from primitive alkaline rocks and those from high-MgO magmas (compare Figs 2(b) and 2(f)). Hence, primitive mantle melts whether tholeiitic or alkaline in composition have similar metal patterns.

Hosanger. The Hosanger intrusion is a sill of norite which may be part of the Anorthosite Complex within the Bergen Arc System (Boyd & Nixon, 1985). The sulphides occur either as matrix sulphides towards the base of the intrusion (Lien and Litvann ore) or as sulphide veins cutting the norite and gneissic country rock (Nonås ore). The ore from all three localities is similar, except for the presence of some Cu-rich ore from Nonas. In common with most Cu-rich ores the Nonas ore is enriched in Cu and Au relative to the bulk ore. Because of the analytical problems associated with Cu- and Au-rich samples it is not possible to say whether the Cu-rich ore is also enriched in Pt and Pd.

The noble metal portion of the metal patterns is relatively unfractionated Pd/Ir ratios 5–10. However, Cu and Ni are enriched relative to the noble metals (Ni/Ir_{mn} = 4, Cu/Pd_{mn} = 5) which gives the patterns their trough shape. The metal patterns resemble those of the Seiland intrusions and so are interpreted to have formed in the same fashion, that is by segregation from a high-MgO basalt that had not experienced olivine or chromite fractionation, but that had previously segregated some sulphides.

Ertelien and Flåt. The Ertelien deposit occurs at the margins of a small (600 m × 450 m) norite intrusion, located 40 km NW of Oslo (Fig. 6). The Flåt deposit occurs within a diorite dyke (4 × 2 km), 170 km SW of Oslo (Fig. 6). Neither intrusion has been dated, but on the basis of stratigraphic relationships they are thought to be part of a series of mafic intrusions emplaced into the gneissic craton between 1200 and 1370 Ma, possibly as the early rifting phase of Sveconorwegian Orogeny (900–1100 Ma) (Oftedahl, 1980). More details concerning the deposits are given in Boyd & Nixon (1985).

Both Ni-rich and Cu-rich ore types are present at Flåt. The Cu-rich ore is part of the massive sulphides. In common with most Cu-rich ores the Flåt Cu-rich ores are enriched in Cu, Au and Pd relative to bulk ore. The Pd value may not be reliable, because it was possible to determine Pd on only 2 of the 5 Cu-rich samples. The Flåt PGE are remarkably unfractionated (Pd/Ir = 2–5). However, as with the Seiland Province rocks, the Flåt patterns are enriched in Ni and Cu relative to the noble metals (Ni/Ir_{mn} = 1–2, Cu/Pd_{mn} = 4–132) which gives the metal patterns an overall trough shape. On the Ni/Pd versus Cu/Ir plot (Fig. 4(b)) the Flåt ore (f) plots above the fields of the extrusive rocks which indicates some sulphides were removed prior to the formation of the Flåt sulphides. The Flåt metal pattern does not resemble the metal patterns from any common magma type (compare Figs 2 (a–h) and 5(h)). The distinctive feature of the Flåt metal pattern is its low Pd/Ir ratio, this ratio is even lower than that found in komatiite magmas. On the Pd/Ir versus Ni/Cu diagrams (Fig. 3(b)) the position of the Flåt ore (f) suggests that the Flåt samples are enriched in chromite and/or olivine. But, the Flåt samples are massive sulphides which do not contain any olivine or chromite. The reason for the low Pd/Ir ratio is not clearly understood. Overall the Flåt metal pattern suggests that the Flåt sulphides formed in equilibrium with a magma that had not experienced olivine or chromite fractionation but that had experienced sulphide segregation.

At Ertelien both Ni-rich and Cu-rich ores are present: the Cu-rich ore is part of the massive sulphides and is enriched in Cu, Au and Pt and depleted in Ir relative to the bulk ore. The noble metal portion of the metal patterns is fractionated (Pd/Ir = 100–120) (Fig. 5(i)). Both ore types are enriched in Ni and Cu relative to noble metals (Ni/Ir_{mn} = 20–25, Cu/Pd_{mn} = 35–120) such that the metal patterns have a trough shape, similar to that observed in Seiland. The Ni/Cu ratio of the weighted mean of the Ertelien sulphides is higher than that of flood basalt related material but, on the other hand, the Pd/Ir ratio is higher than the ocean floor basalts, thus the Ertelien ore plots in neither field (I on Fig. 3(b)). The position of the Ertelien sulphides suggests that they formed from a primitive magma that had crystallized some olivine and chromite prior to the development of these sulphides. The trough shape of the metal pattern suggests that sulphides have been removed from this magma. This suggestion is reinforced by the position of the Ertelien ore (I) on the Ni/Pd versus Cu/Ir plot (Fig. 4(b)) where the Ertelien ore plots above the fields of extrusive rocks, suggesting that sulphides have been removed from the magma.

A remarkable feature of all these intrusions is the depletion of noble metals relative to Ni and Cu. This is interpreted as suggesting that sulphides have been removed from the magma, either by retention in the mantle during partial melting, or by segregation from the magma en route to surface. The authors favour the latter model and suggest that during early rifting, magmas may not have easy access to the

surface and may pause often during emplacement into the crust; at each pause it is possible that sulphides could segregate from the magma. Another feature that these intrusions have in common is their small size. It is possible that small volumes of magma have difficulty intruding into the crust and therefore pause often allowing, at each pause, segregation of sulphides.

The Jotun Complex—a Large Mid-Proterozoic Mafic Intrusion

The Jotun Complex in southern Norway is a large (100 × 200 km) mafic intrusion of mid-Proterozoic age. It was metamorphosed to granulite facies between 900 and 1100 Ma and implaced in its present position during the Caledonide Orogeny (400 Ma) (Oftedahl, 1980). The size, age and mafic nature of this intrusion make it a target for a Pt-reef-type deposit. The target zone for finding a Pt-reef would usually be considered to lie near the boundary between the ultramafic and mafic zones of the intrusion. However, the polydeformed and polymetamorphosed nature of the Jotun Complex make it difficult to define the stratigraphy of the body, and hence, difficult to define any target zones. Magnetite-rich pyroxenites occur as small lenses 10–100 m across in the metagabbros of the north east portion of the intrusion. Fourteen samples of magnetite-rich pyroxenite from the area of Gråsulbekken have been analysed for noble metals (Table 1).

The noble metals from the pyroxenites are extremely fractionated (Pd/Ir ratio 770), but the pattern is enriched in PGE relative to Cu. The overall shape of the pattern most resembles that of flood basalts (compare Figs 2(f) and 5(f)). On the metal ratio diagrams the Jotun pyroxenites (J on Figs 3(b) and 4(b)) plot close to, or within, the field of flood basalts. The high Pd/Ir ratio of the Jotun pyroxenite rocks suggests that the liquid from which they formed was depleted in Ir, possibly by earlier chromite removal. Although the level (200 ppb) of PGE present in these rocks is an order of magnitude less than ore grade, the low Ni/Pd and Cu/Ir ratios suggest that no sulphides have segregated from the magma, hence the noble metals have not been scavenged from the magma and any sulphides that later segregated could be rich in noble metals, indicating that the Jotun Complex warrants further exploration.

CONCLUSIONS

By adding Ni to the Os end of a noble metal pattern and Cu to the Au end and then mantle normalizing the data rather than chondrite normalizing, the resulting metal patterns become powerful tools for investigating the following petrological problems in ultramafic and mafic rocks.

(1) If the rock represents mantle, a chromitite from an ophiolite, a Pt-reef, or if the rock formed from an unfractionated mantle derived melt, the metal patterns are distinctive and the origin of the rock can be established.
(2) Because the partition coefficient of Ni and Cu is lower than the noble metals into sulphides the separation of sulphides from a magma will produce a cumulate enriched in noble metals relative to Ni and Cu, leaving the magma depleted in noble elements relative to Ni and Cu. Consequently, the cumulate will have arch-shaped metal patterns and the fractionated magma trough-shaped metal patterns. Any rock that subsequently forms from this fractionated magma will also have trough-shaped metal patterns.
(3) Chromite and, to a lesser extent, olivine both tend to concentrate Os, Ir and Ru, possibly as PGM inclusions, therefore the crystallization of chromite and olivine from a magma produces a cumulate enriched in Os, Ir and Ru and a magma depleted in Os, Ir and Ru. Any rock that subsequently forms from this fractionated magma will have metal patterns with steeper positive slopes than the original liquid (i.e. higher Pd/Ir ratios).

Because some workers may feel that the mantle abundance of the noble metals are poorly constrained they may object to the mantle normalization procedure to produce metal patterns. Furthermore, the presence of sulphides in a rock presents the dilemma of whether to recalculate the data to 100% sulphides or not. Both of these difficulties can be overcome by using the metal ratio diagrams Pd/Ir versus Ni/Cu and Ni/Pd versus Cu/Ir. These diagrams successfully separate rocks representing mantle, komatiites, high-MgO basalts, flood basalts, Pt-reefs, ophiolite chromitites and Cu-rich sulphide veins. The diagrams show the effects of Os, Ir and Ru removal by crystal fractionation. The Ni/Pd versus Cu/Ir diagram also shows the effects of sulphide removal as a trend markedly oblique to that due to olivine and chromite trends.

The combined use of mantle normalized metal patterns and metal ratio diagrams allows the effects of partial melting, sulphide segregation, chromite and olivine crystallization to be clearly recognized.

ACKNOWLEDGEMENTS

The analytical work for this project was financed by the EEC Raw Materials Program and Norges Geologiske Undersøkelse. Professor Frank Vokes kindly allowed access to the petrographic collection at the Technical University of Norway (NTH), Trondheim for samples from Ertelien, Fæøy, Flåt and Hosanger. Dr E. W. Sawyer is thanked for numerous corrections and suggestions to the various drafts of the text.

REFERENCES

Agiorgitis, G. & Wolf, R. (1977). The distribution of platinum, palladium and gold in Greek chromites. *Chem. Erde.*, **36**, 349–51.
Agiorgitis, G. & Wolf, R. (1978). Aspects of osmium, ruthenium and iridium contents in some Greek chromites. *Chem. Geol.*, **23**, 267–72.
Alapieti, T. & Lahtinen, J. (1986). Stratigraphy, petrology and platinum-group element mineralization of the early Proterozoic Penikat layered intrusion. *Econ. Geol.*, **81**, 1126–37.
Amosse, J., Allibert, M., Fischer, W. & Piboule, M. (1987). Etude de l'influence es fugacities

d'oxygene et de soufre sur la differenciation des platinoides dans les magmas ultramafiques. Resultats preliminaires. *C.R. Acad. Sci. Paris*, t304 Seri II, **19**, 1183–5.
Ballhaus, G. G. & Stumpfl, E. F. (1986). Sulfide and platinum mineralization in the Merensky Reef: evidence from hydrous silicates and fluid inclusions. *Contrib. Mineral. Petrol.*, **94**, 193–204.
Barnes, Sarah-Jane (1987). Unusual nickel and copper to noble-metal ratios from the Råna Layered Intrusion, northern Norway. *Norsk geol. Tidsskrift*, **67**, 215–32.
Barnes, Sarah-Jane & Naldrett, A. J. (1987). Fractionation of the platinum-group elements concentrations in the Alexo Mine komatiite, Abitibi Greenstone Belt, northern Ontario. *Geol. Mag.*, **123**, 515–24.
Barnes, Sarah-Jane & Naldrett, A. J. (1987). Fractionation of the platinum-group elements and gold in some komatiites of the Abitibi greenstone belt, northern Ontario. *Econ. Geol.*, **82**, 165–83.
Barnes, Sarah-Jane, Naldrett, A. J. & Gorton, M. P. (1985). The origin of the fractionation of platinum-group elements in terrestrial magmas. *Chem. Geol.*, **53**, 303–23.
Barnes, Stephen J. & Naldrett, A. J. (1985). Geochemistry of the J-M reef of the Stillwater Complex, Minneapolis Adit Area. I Sulfide chemistry and sulfide-olivine equilibrium. *Econ. Geol.*, **80**, 627–45.
Barnes, Stephen J., Coats, C. A. J. & Naldrett, A. J. (1982). Petrogenesis of Proterozoic nickel sulfide–komatiite association: the Katiniq Sill, Ungava, Quebec. *Econ. Geol.*, **77**, 413–29.
Becker, R. & Agiorgitis, D. (1978). Iridium, osmium and palladium distribution in rocks of the Troodos Complex, Cyprus. *Chem. Erde.*, **37**, 302–6.
Bennett, M. C., Emblin, S. R., Robins, B. & Yeo, W. J. A. (1986). High-temperature ultramafic complexes in the north Norwegian Caledonides: I—Regional setting and field relationships. *Norges. Geol. Unders. Bull.*, **405**, 1–40.
Boyd, R. & Nixon, F. (1985). Norwegian nickel deposits: A review. *Geol. Surv. Finland, Bull.*, **333**, 364–94.
Brugmann, G. E., Arndt, N. T., Hofmann, A. W. & Tobschall, H.-J. (1985). Precious-metal abundances in komatiites and komatiitic basalts: implications for the genesis of PGE-bearing magmatic sulfide deposits. *Can. Mineral.*, **23**, 293–321.
Bury, K. V. (1975). *Statistical Models in Applied Sciences*. John Wiley, New York, 625 pp.
Campbell, I. H. & Barnes, Stephen J. (1984). A model for the geochemistry of the platinum-group elements in magmatic sulfide deposits. *Can. Mineral.*, **22**, 151–60.
Campbell, I. H. & Naldrett, A. J. (1979). The influence of silicate:sulfide ratio on the geochemistry of the magmatic sulfides. *Econ. Geol.*, **74**, 1503–5.
Chang, P.-K., Yu, C. M. & Chiang, C. Y. (1973). Mineralogy and occurrence of platinum-group elements in chromium deposits of northwest China. *Geochimica*, **2**, 76–85 (in Chinese).
Chou, C. L., Shaw, D. M. & Crocket, J. H. (1983). Siderophile trace elements in the earth's oceanic crust and upper mantle. *J. Geophys. Res.*, **88**, A507-518.
Clark, T. (1985). Precious metals in New Quebec. Ministere de l'Energie et des Res Quebec. Document de promotion.
Cowden, A., Donaldson, M. J., Naldrett, A. J. & Campbell, I. H. (1985). Platinum-group elements in komatiite-hosted Fe–Ni–Cu sulfide deposits at Kambalda, western Australia. *Econ. Geol.*, **81**, 1226–34.
Crocket, J. H. (1981). Geochemistry of the platinum-group elements. *Can. Inst. Min. Metall., Spec. Iss.*, **23**, 47–64.
Crocket, J. H. & Chyi, L. L. (1972). Abundances of Pd, Ir, Os and Au in an alpine ultramafic pluton. *24th Inter. Geol. Cong.*, Section **10**, 202–9.
Crocket, J. H. & MacRae, W. E. (1986). Platinum-group element distribution in komatiitic and tholeiitic volcanic rocks from Munro Township, Ontario. *Econ. Geol.*, **81**, 1242–52.
Crocket, J. H. & Teruta, Y. (1977). Palladium, iridium and gold contents of mafic and ultramafic rocks drilled from the Mid-Atlantic Ridge, leg 37, Deep Sea Drilling Project. *Can. J. Earth Sci.*, **14**, 777–84.

Czamanske, G. K., Haffty, J. & Nabbs, S. W. (1981). Pt, Pd and Rh analyses and beneficiation of mineralized mafic rocks from the La Perouse Layered Gabbro, Alaska. *Econ. Geol.*, **76**, 2001–11.
Davies, G. & Tredoux, M. (1985). The platinum-group element and gold contents of the marginal rocks and sills of the Bushveld Complex. *Econ. Geol.*, **80**, 838–48.
Dillon-Leitch, H. C. H., Watkinson, D. H. & Coats, C. (1986). Distribution of platinum-group elements in the Donaldson West Deposit, Cape Smith Fold Belt, Quebec. *Econ. Geol.*, **81**, 1147–59.
Economou, M. I. & Naldrett, A. J. (1984). Sulfides associated with podiform bodies of chromite at Tsangli, Eretria, Greece. *Mineral. Deposita*, **19**, 289–97.
Fominykh, V. G. & Khvostova, V. P. (1970). Platinum content of Ural dunite. *Doklady Akad. Nauk. SSSR*, **191**, 443–5.
Gain, S. B. (1985). The geological setting of the platiniferous UG-2 chromitite layer on the farm Maandagshhoek, Eastern Bushveld. *Econ. Geol.*, **80**, 925–43.
Gain, S. B. & Mostert, A. B. (1982). The geological setting of the platinoid and base metal sulfide mineralization in the Platreef of the Bushveld Complex north of Potgietersrus. *Econ. Geol.*, **17**, 1395–1404.
Gee, D. G., Guezou, J.-C., Roberts, D. & Wolff, F. C. (1985). The central-southern part of the Scandinavian Caledonides. In *The Caledonide Orogen—Scandinavia and Related Areas*, ed. D. Gee & B. A. Sturt. John Wiley, New York, pp. 109–33.
Govindaraju, K. (1984). Compilation of working values and sample descriptions of 170 international reference samples of mainly silicate rocks and minerals. *Geostandards Newsletter*, **VIII**, 3–39.
Green, A. H. & Naldrett, A. J. (1981). The Langmuir volcanic peridotite-associated nickel deposits: Canadian equivalent of the Western Australian occurrences. *Econ. Geol.*, **76**, 1503–23.
Grønlie, A. (in press). Platinum-group minerals of the Lillefjellklumpen, nickel-copper deposit, Norway. *Norsk. Geol. Tidsskr.*
Gunn, A. G., Leake, R. C. & Styles, M. T. (1985). Platinum-group element mineralization in the Unst ophiolite, Shetland. Mineral Reconnaissance Programme Rep. British Geol. Surv., Vol. 73, 117 pp.
Hakli, T. A., Hanninen, E., Vuorelainen, Y. & Papunen, H. (1976). Platinum-group minerals in the Hitura nickel deposit, Finland. *Econ. Geol.*, **71**, 1206–13.
Hamlyn, P. R., Keays, R. R., Cameron, W. E., Warrington, E., Crawford, A. J. & Waldon, H. M. (1985). Precious metals in magnesian low-Ti lavas: Implications for metallogenesis and sulfur saturation in primary magmas. *Geochim. Cosmochim. Acta*, **49**, 1797–1811.
Hertogen, J., Janssen, M. J. & Palme, H. (1980). Trace elements in ocean ridge basalt glasses: implications for fractionation during mantle evolution and petrogenesis. *Geochim. Cosmochim. Acta*, **44**, 2125–43.
Hoffman, E. L., Naldrett, A. J., Van Loon, J. C. & Hancock, R. G. V. (1979). The noble-metal content of ore in the Levack West and Little Stobie mines, Ontario. *Can. Mineral.*, **17**, 437–51.
Hulbert, L. J. & von Gruenewaldt, G. (1982). Nickel, copper and platinum mineralization in the lower zone of the Bushveld Complex, south of Potgietererus. *Econ. Geol.*, **77**, 1296–1306.
Irivine, T. N. & Sharpe, M. (1982). Source rock compositions and depths of origin of Bushveld and Stillwater magmas. *Carnegie Inst. Washington Yrbk*, **81**, 294–303.
Jagoutz, E., Palme, H., Baddenhausen, H., Blum, K., Dreibus, G., Spettel, B., Lorenz, V. & Wanke, H. (1979). The abundance of major, minor and trace elements in the earth's mantle as derived from primitive ultramafic nodules. *Proc. 10th, Lunar Planet. Sci. Conf.*, NASA, Houston, pp. 2031–50.
Kaminskiy, F. V., Frantsesson, Ye. V. & Khvostova, P. (1975). First information on platinum metals (Pt, Pd, Rh, Ir, Ru, Os) in kimberlitic rocks. *Doklady Akad. Nauk. SSSR*, **219**, 190–3.
Keays, R. R. (1982). Palladium and iridium in komatiites and associated rocks: application to

petrogenetic problems. In *Komatiites*, ed. N. T. Arndt & E. G. Nisbet. Allen, London, pp. 435–57.
Keays, R. R. & Campbell, I. H. (1981). Precious metals in the Jimberlana Intrusion, Western Australia: Implications for genesis of platiniferous ores in layered intrusions. *Econ. Geol.*, **76**, 1118–41.
Keays, R. R., Ross, J. R. & Woolrich, P. (1981). Precious metals in volcanic peridotite-associated nickel sulphide deposits in western Australia II: Distribution within the ores and host rocks at Kambalda. *Econ. Geol.*, **76**, 1645–74.
Keays, R. R., Nickel, E. H., Groves, D. I. & McGoldrick, P. J. (1982). Iridium and palladium as discriminants of volcanic-exhalative hydrothermal and magmatic nickel sulfide mineralization. *Econ. Geol.*, **77**, 1535–47.
Khvostova, V. P., Golvnya, S. V., Chernysheva, N. V. & Bukhanova, A. I. (1976). Distribution of the platinum-group metals in chromite ores and ultramafic rocks of the Ray-Iz massif (Polar Urals). *Geochem. Int.*, **13**, 35–9.
Krill, A. G., Bergh, S., Mearns, E. W., Often, M., Olerud, S., Olesen, O., Sanstad, J. S., Siedlecka, A. & Solli, A. (1985). New isotopic dates from the Precambrian crystalline rocks of Finnmark. *Norges Geol. Unders. Bull.*, **403**, 37–54.
Lahtinen, J. (1985). PGE-bearing copper-nickel occurrences in the marginal series of the early Proterozoic Koillismaa Layered Intrusion, northern Finland. *Geol. Surv. Finland, Bull.*, **333**, 165–79.
Latysh, I. K. & Buturlinov, V. N. (1970). Platinum-group metals in igneous rocks of the border zone between Donbas and Azov Region. *Geochem. Int.*, **7**, 620–3.
Leblanc, M. & Johan, Z. (1986). Un nouveau type de mineralisation platinifere: exemple des filons a arseniures de nickel et chromite du massif lherzolitique des Beni-Bousera (Maroc). *C.R. Acad. Sci. Paris*, t303, Serie II, **2**, 163–6.
Lee, C. & Tredoux, M. (1986). Platinum-group element abundances in the lower and middle critical zones of the Eastern Bushveld Complex. *Econ. Geol.*, **81**, 1087–96.
Lesher, C. M. & Keays, R. R. (1984). Metamorphically and hydrothermally mobilized Fe–Ni–Cu sulphides at Kambalda, Western Australia. In *Sulphide Deposits in Mafic and Ultramafic rocks*, ed. D. L. Buchanan & M. J. Jones. Institute of Mining and Metallurgy, London, pp. 62–9.
Lightfoot, P. C., Naldrett, A. J. & Hawkesworth, C. J. (1984). The geology and geochemistry of the Waterfall Gorge section of the Insizwa Complex with particular reference to the origin of the nickel-sulfide deposits. *Econ. Geol.*, **79**, 1857–79.
McCallum, M. E., Lovacks, R. R., Carlson, R. R., Cooley, E. F. & Docrye, T. A. (1976). Platinum metals associated with hydrothermal copper ores of the New Rambler mine, Medicine Bow Mountains, Wyoming. *Econ. Geol.*, **71**, 1429–50.
McLaren, C. H. & De Villiers, J. P. R. (1982). The platinum-group chemistry and mineralogy of the UG-2 chromite layer of the Bushveld Complex. *Econ. Geol.*, **77**, 1348–66.
Massey, N. W. D., Crocket, J. H. & Kabir, A. (1983). Ir in Keweenawan basalts of the Mamainse Point Formation, Ontario. *Can. Mineral.*, **21**, 655–60.
Mitchell, R. H. & Keays, R. R. (1981). Abundance and distribution of gold, palladium and iridium in some spinel and garnet lherzolites, Implications for the nature and origin of precious metal-rich intergranular components in the upper mantle. *Geochim. Cosmochim. Acta*, **45**, 2425–42.
Morgan, J. (1986). Ultramafic xenoliths: Clues to earth's late accretionary history. *J. Geophys. Res.*, **91** (B12), 12375–87.
Morgan, J. W., Wanderless, G. A., Petrie, R. K. & Irving, A. J. (1981). Composition of the earth's upper mantle—I. Siderophile trace elements in ultramafic nodules. *Tectonophysics*, **75**, 47–67.
Naldrett, A. J. (1981). Platinum-group element deposits. *Can. Inst. Min. Metall., Spec. Iss.*, **23**, 197–232.
Naldrett, A. J. & Barnes, S.-J. (1986). The fractionation of the platinum-group elements with

special reference to the composition of sulphide ores. *Fortsch. Mineral. Petrol.*, **64**, 113–33.
Naldrett, A. J., Hoffman, E. L., Green, A. H., Chou, C-L. & Naldrett, S. R. (1979). The composition of Ni-sulfide ores, with particular reference to their content of PGE and Au. *Can. Mineral.*, **17**, 403–15.
Naldrett, A. J., Innes, D., Gorton, M. P. & Sowa, J. (1982). Compositional variations within and between five Sudbury ore deposits. *Econ. Geol.*, **77**, 1519–34.
Nilsson, L.-P. (1980). Undersøkelsel av ultramafiske bergarter og krommalm på strekeningen Råros-Feragen. Norges Geol. Unders. Rep. 1650/33A.
Oftedahl, C. (1980). The geology of Norway. *Norges Geol. Unders. Bull.*, **54**, 3–114.
Often, M. (1985). The early proterozoic Karasjok greenstone belt, Norway; a preliminary description of lithology, stratigraphy and mineralization. *Norges Geol. Unders. Bull.*, **403**, 75–88.
Ohnenstetter, D., Watkinson, D., Jones, P. C. & Talkington, R. (1986). Cryptic compositional variations in laurite and enclosing chromite from the Bird River Sill, Manitoba. *Econ. Geol.*, **81**, 1159–68.
Oshin, I. O. & Crocket, J. H. (1982). Noble metals in the Thetford mines ophiolite, Quebec, Canada. Part I Distribution of gold, iridium, platinum and palladium in the ultramafic and gabbroic rocks. *Econ. Geol.*, **77**, 1556–70.
Oshin, I. O. & Crocket, J. H. (1986). Noble metals in the Thetford mines ophiolite, Quebec, Canada. Part II Distribution of gold, silver, iridium, platinum and palladium in the Lac de l'Est volcano-sedimentary section. *Econ. Geol.*, **81**, 931–45.
Page, N. J & Talkington, R. W. (1984). Palladium, platinum, rhodium, ruthenium and iridium in peridotites and chromites from ophiolite complexes in Newfoundland. *Can. Mineral.*, **22**, 137–49.
Page, N. J, Rowe, J. J. & Haffty, J. (1972). Platinum metals lateral variations of platinum, palladium and rhodium in the Stillwater Complex, Montana. *Econ. Geol.*, **67**, 915–23.
Page, N. J, Myers, J. S. & Haffty, J. (1980). Platinum, palladium and rhodium in Fiskenaesset Complex, Southwest Greenland. *Econ. Geol.*, **75**, 907–15.
Page, N. J, Cassard, D. & Haffty, J. (1982*a*). Palladium, platinum, rhodium, ruthenium and iridium in chromitites from the Massif du Sud and Tiebaghi Massif, New Caledonia. *Econ. Geol.*, **77**, 1571–7.
Page, N. J, Pallister, J. S., Brown, M. A., Smewing, J. D. & Haffty, J. (1982*b*). Palladium, platinum, rhodium, iridium and ruthenium in chromite-rich rocks from the Samail ophiolite, Oman. *Can. Mineral.*, **20**, 537–48.
Page, N. J, Von Gruenewaldt, G., Haffty, J. & Aruscavage, P. J. (1982*c*). Comparison of platinum, palladium and rhodium distribution in some layered intrusions with special reference to the late differentiates (upper zone) of the Bushveld Complex, South Africa. *Econ Geol.*, **77**, 1405–18.
Page, N. J, Aruscavage, P. J. & Haffty, J. (1983). Platinum-group elements in rocks from the Voikar-Syninsky Ophiolite Complex, Polar Urals USSR. *Mineral. Deposita*, **18**, 444–55.
Page, N. J, Zientek, M. L., Czamanske, G. K. & Foose, M. P. (1985). Sulfide mineralization in the Stillwater complex and underlying rocks. Montana Bureau Mines and Geol. Spec. Pub. **92**, pp. 93–6.
Page, N. J, Singer, D., Moring, B., Carlson, A., McDade, J. & Wilson, S. A. (1986). Platinum-group element resources in podiform chromitites from California and Oregon. *Econ. Geol.*, **81**, 1261–71.
Papunen, H. (1986). Platinum-group elements in Svecokarelian nickel-copper deposits in Finland. *Econ. Geol.*, **81**, 1236–41.
Papunen, H. & Koskinen, J. (1985). Geology of the Kotalahti nickel-copper ore. *Geol. Surv. Finland Bull.*, **333**, 229–41.
Paul, D., Crocket, J. H. & Nixon, P. H. (1979). Abundances of palladium, iridium and gold in kimberlites and associated nodules. *Proc. 2nd Int. Kimberlite Conf.*, Vol. 1. American Geophysical Union. Washington, D.C., pp. 272–9.

Pedersen, R.-B. (in preparation) The Karmøy Ophiolite Complex.
Pedersen, R.-B., Furnes, H. & Dunning, G. (submitted). Norwegian ophiolite complexes reconsidered. *Geology*.
Prichard, H. M., Potts, P. J. & Neary, C. R. (1981). Platinum-group element minerals in the Unst chromite, Shetland Isles. *Inst. Mining Metall.*, **90**, 186–8.
Prichard, H. M., Potts, P. J. & Neary, C. R. (1984). Platinum and gold in the Shetland ophiolite. *Mining J.*, **303** (7772), 77.
Prichard, H. M., Neary, C. & Potts, P. J. (1986). Platinum-group minerals in the Shetland ophiolite. In *Metallogeny of Basic and Ultrabasic Rocks*, ed. M. J. Gallagher, R. A. Ixer, C. R. Neary & H. M. Prichard. Inst. Min. Metals, London, pp. 395–414.
Rajamani, V. & Naldrett, A. J. (1978). Partitioning of Fe, Co, Ni and Cu between sulfide liquid and basaltic melts and the composition of Ni-Cu sulfide deposits. *Econ. Geol.*, **73**, 82–93.
Razin, L. V. & Khomenko, G. A. (1969). Accumulation of osmium, ruthenium and other platinum group metals in chrome spinel in platinum bearing dunites. *Geochem. Int.*, **6**, 546–57.
Razin, L. V., Khvostov, V. J. & Noviko, V. A. (1965). Platinum metals in the essential and accessory minerals of ultramafic rocks. *Geochem. Int.*, **2**, 118–31.
Redman, B. A. & Keays, R. R. (1985). Archaean basic volcanism in the eastern goldfields province, Yilgarn Block, Western Australia. *Precambrian Res.*, **30**, 113–52.
Robins, B. & Gardner, P. M. (1975). The magmatic evolution of the Seiland province and Caledonian plate boundaries in northern Norway. *Earth Planet. Sci. Lett.*, **26**, 167–78.
Rowell, W. F. & Edgar, A. D. (1986). Platinum-group element mineralization in a hydrothermal Cu-Ni sulfide occurrence, Rathbun Lake, Northeastern Ontario. *Econ. Geol.*, **81**, 1272–7.
Sharpe, M. (1982). Noble metals in the marginal rocks of the Bushveld Complex. *Econ. Geol.*, **77**, 1286–95.
Smirnov, M. E. (1966). The structure of Noril'sk nickel-bearing intrusions and the genetic types of their sulfide ores. All-Union Sci. Res. Inst. Mineral. Raw Materials (VIMS) Moscow (in Russian).
Steele, T. W., Levin, J. & Copelowitz, I. (1975). The preparation and certification of a reference sample of a precious metal ore. Nat. Inst. Met. Rep. 1696.
Stockman, H. W. (1982). Noble metals in the Ronda and Josephine peridotites. Unpublished, Ph.D., thesis, Massachusetts Institute of Technology, Cambridge, MA.
Stockman, H. W. & Hlava, P. F. (1984). Platinum-group minerals in Alpine chromites from southwestern Oregon. *Econ. Geol.*, **79**, 491–508.
Sturt, B. & Roberts, D. (1978). Caledonides of northern Norway. In Caledonian-Appalachian orogen of the North Atlantic Region, ed. P. Scheuk. Geol. Surv. Can. Paper 78-13, pp. 17–24.
Sun, Shen-Su (1982). Chemical composition and origin of the earth's primitive mantle. *Geochim. Cosmochim. Acta*, **46**, 179–92.
Talkington, R. W. & Lipin, B. (1986). Platinum-group minerals in chromite seams of the Stillwater Complex, Montana. *Econ. Geol.*, **81**, 1179–86.
Talkingon, R. W. & Watkinson, D. H. (1984). Trends in the distribution of the precious metals in the Lac des Iles Complex, northwestern Ontario. *Can. Mineral.*, **22**, 125–36.
Talkington, R. W., Watkinson, D. H., Whittaker, P. J. & Jones, P. C. (1984). Platinum-group minerals and other solid inclusions in chromite of ophiolite complexes: Occurrence and petrological significance. *Tschermaks. Mineral. Petrol. Mitt.*, **32**, 285–301.
Thompson, J. F. H., Nixon, F. & Siversten, R. (1980). The geology of Vakkerlien nickel prospect Kvikne, Norway. *Geol. Surv. Finland Bull.*, **52**, 3–22.
Tolmachev, I. I., Kalinin, S. K., Terekhovich, S. I., Syromyatnikon, N. G. & Zaravnyayeva, V. K. (1971). Distribution of Pd, Pt and Au in the Riphean and Cambrian igneous rocks of the Boshchekulsh region, northeastern Kazakhstan. *Geochem. Int.*, **8**, 194–9.

Tredoux, M., Davies, G., Lindsay, N. M. & Sellschop, J. P. F. (1986). The influence of temperature on the geochemistry of the platinum-group elements and gold. Geocongress 86 extended abstracts, pp. 625–8. Geological Society of South Africa, Johannesburg.
White, R. W., Motta, J. & De Araujo, V. A. (1971). Platiniferous chromitite in the Trocantins Complex, Niquelandia, Goias, Brazil. US Geol. Surv. Prof. Pap., 750-D, pp. 26–33.
Wilson, A. H. & Prendergast, M. D. (1987). The Great Dyke of Zimbabwe—an Overview. Guidebook for the 5th Magmatic Sulphides Field Trip pp. 23–8. Geological Society of Zimbabwe, Harare.
Zientek, M. L., Foose, M. P. & Mei, L. (1986). Palladium, platinum and rhodium contents of rocks near the lower margin of the Stillwater Complex, Montana. *Econ. Geol.*, **81**, 1169–78.

APPENDIX: SOURCES OF DATA FOR FIGS 2, 3 AND 4

Mantle: 1, 2, 3, 4, 6, 7, 8, 9, 10, 18, 20, 21.
Komatiites: 31, 33, 38, 52, 54, 64, 65, 76.
High-MgO basalts: 32, 33, 38, 55.
Ocean floor basalts: 1, 9, 16, 22, 66.
Continental flood basalts: 3, 6, 37, 38, 41, 58, 59, 60.
Boninites and low-TiO_2 basalts: 24, 66.
Alkaline rocks: 2, 3, 5, 25, 27.
Ophiolites: 6, 7, 8, 9, 10, 11, 12, 14, 15, 16, 17, 18, 19, 21, 63.
Layered intrusions: 34, 36, 38, 39, 41, 42, 44, 45, 46, 49, 50, 51, 53, 61, 62, 76, 77, 78.
Platinum reefs: 34, 38, 39, 40, 43, 47, 48.
Cu-rich sulphide veins: 68, 69, 71, 72, 75.

Refs: 1. Morgan *et al.* (1981); 2. Mitchell and Keays (1981); 3. Paul *et al.* (1979); 4. Jagoutz *et al.* (1979); 5. Kaminskiy *et al.* (1975); 6. Stockman (1982); 7. Crocket and Chyi (1972); 8. Oshin and Crocket (1982); 9. Becker and Agiorgitis (1978); 10. Page and Talkington (1984); 11. Page *et al.* (1982*b*); 12. Economou and Naldrett (1984); 13. Page *et al.* (1982*a*); 14. Agiorgitis and Wolf (1977, 1978); 15. Gunn *et al.* (1985); 16. Crocket and Teruta (1977); 17. White *et al.* (1971); 18. Khvostova *et al.* (1976); 19. Chang *et al.* (1973); 20. Fominykh and Khvostova (1970); 21. Page *et al.* (1983); 22. Hertogen *et al.* (1980); 23. Crocket (1981); 24. Hamlyn *et al.* (1985); 25. Tolmachev *et al.* (1971); 27. Latysh and Buturlinov (1970); 29. Razin and Khomenko (1969); 30. Razin *et al.* (1965); 31. Keays *et al.* (1982); 32. Redman and Keays (1985); 33. Crocket and MacRae (1986); 34. Keays and Campbell (1981); 35. Page *et al.* (1986); 36. Talkington and Watkinson (1984); 37. Massey *et al.* (1983); 38. Naldrett (1981); 39. Page *et al.* (1985); 40. Barnes and Naldrett (1985); 41. Sharpe (1982); 42. Hulbert and von Gruenewaldt (1982); 43. McLaren and de Villiers (1982); 44. Gain and Mostert (1982); 45. Page *et al.* (1982*c*); 46. Davies and Tredoux (1985); 47. Gain (1985); 48. Steele *et al.* (1975); 49. Page *et al.* (1980); 50. Czamanske *et al.* (1981); 51. Lahtinen (1985); 52. Hakli *et al.* (1976); 53. Papunen and Koskinen (1985); 54. Green and Naldrett (1981); 55. Barnes *et al.* (1982); 58. Smirnov (1966); 59. Lightfoot *et al.* (1984); 61. Thompson *et al.* (1980); 62. Clark (1985); 63. Leblanc and Johan (1986); 64. Barnes and Naldrett (1987); 65. Cowden *et al.* (1985); 66. Oshin and Crocket (1986); 68. McCallum *et al.* (1976); 69. Rowell and Edgar (1986); 71. Hoffman *et al.* (1979); 72. Lesher and Keays (1984); 75. Dillon-Leitch *et al.* (1986); 76. Papunen (1986); 77. Talkington and Lipin (1986); 78. Zientek *et al.* (1986); 79. Govindaraju (1984).

Boyd, R., Barnes, S.-J. & Grønlie, A. 1988: Noble metal geochemistry of some Ni-Cu deposits in the Sveconorwegian and Caledonian Orogens in Norway. In: Prichard, H.M., Potts, P.J., Bowles, J.F.W. & Cribb, S.J. (eds.) Geo-Platinum 87, Elsevier, London, 145-158.

13

Noble Metal Geochemistry of some Ni-Cu Deposits in the Sveconorwegian and Caledonian Orogens in Norway

R. Boyd,[a] S.-J. Barnes[b] & A. Grønlie[a]

[a]*Geological Survey of Norway, PO Box 3006, N-7002 Trondheim, Norway*

[b]*Centre d'Etudes sur les Ressources Minérales, Université du Quebec, 555 Boulevard de l'Université, Chicoutimi, PQ, Canada G7H2B1*

ABSTRACT

New noble metal analyses are presented for five Ni-Cu deposits in Norway and are considered along with published data from a further four deposits. By far the richest deposits are: Fæøy averaging 1790 ppb Pt and 4760 ppb Pd, and Lillefjellklumpen averaging 1800 ppb Pt and 3070 ppb Pd. Both are small massive sulphide bodies, the former associated with late stage dykes within the Karmøy ophiolite while the latter is associated with MORB-type tholeiites within the Gjersvik island arc complex. The Vakkerlien and Espedalen deposits contain respectively 1380 and 1000 ppb (PGE – Au) in 100% sulphides. Other deposits have low contents of PGE (<300 ppb in 100% sulphides) but several are locally enriched in Au, particularly Ertelien, in which Cu-rich samples average 1430 ppb Au. Data from the Norwegian deposits and from elsewhere indicate that Ni-Cu deposits in intrusions in orogenic belts tend to have low noble metal contents.

INTRODUCTION

Norway has a long tradition in mining and prospecting for Ni-Cu ores, aspects of which are reviewed in a recent paper (Boyd & Nixon, 1985). The mineral pentlandite was first described, though not named, from the Espedalen deposit (Scheerer, 1845) and for a brief period before the discovery of the lateritic ores in New Caledonia, Norway was one of the world's leading Ni producers. The last mines to be active, Flåt and Hosanger, closed in 1944 and 1945 respectively. Prospecting in the 1970s revealed one new deposit of significance, Vakkerlien (Thompson *et al.*, 1980), and multiplied the reserves of another, Bruvann, tenfold (Boyd & Mathiesen, 1979). Pt and Pd analyses with detection levels of the order of 20–100 ppb were published for four Norwegian Ni-Cu deposits as long ago as 1932 Foslie & Johnson Høst, 1932) along with calculated grades for two deposits based on analyses of matte.

Knowledge of the platinum-group element (PGE) content of Norwegian orebodies did not advance, however, between 1932 and 1979 when the first modern PGE analyses, with detection levels of the order of 0·1–5 ppb, were published, for the Espedalen deposit, by Naldrett *et al.* (1979). Data have subsequently been published for the Vakkerlien deposit (Thompson *et al.*, 1980), for the Lillefjell-klumpen deposit (Grønlie, 1985, 1986, 1987) and for the Bruvann deposit (Boyd *et al.*, 1986, in press). This paper presents data from a further five deposits and will consider these with the results already published. These nine deposits include all the deposits in the country known to have (had) a tonnage of over 1000 metric tons Ni metal.

All the deposits except one, Fæøy, are Ni-dominated. Three, Hosanger, Flåt and Ertelien, while being completely dominated by Ni-Cu ore, also contain veins of Cu >> Ni mineralization which will be discussed separately.

GEOLOGICAL BACKGROUND

The location of the deposits is shown, on a simplified geological map of Norway (Fig. 1) and grades, tonnages, mineralogical and chemical data, are given in Table 1.

Two of the deposits considered in this paper are located in the Sveconorwegian (=Grenville) orogenic belt. The Flåt and Ertelien deposits occur in small plug-like intrusions (<5 km^2 in section) thought to immediately predate the Sveconorwegian orogeny. The other seven occur in the Caledonian orogenic belt, though Hosanger and Espedalen are pre-Sveconorwegian in age. Hosanger and Espedalen are associated with small intrusions, both of which probably originated within the Middle Proterozoic Jotun mafic intrusive complex, the largest preserved part of which is now exposed in the Jotun Nappe. The original dimensions of this intrusive complex must have been in excess of 300 km × 100 km implying a major magmatic event, probably associated with crustal extension. Of the deposits in the Caledonian belt, three, Bruvann, Skjækerdalen and Vakkerlien, can be described as synorogenic 'sensu lato' though at least for Bruvann and Vakkerlien, the term intra-orogenic, implying emplacement during a tensional episode, would be more precise while the remaining two, Lillefjellklumpen and Fæøy, are located in thrust slices of supra-subduction zone ophiolites (Dunning *et al.*, 1986; Grønlie, in press).

Flåt. This deposit occurs within the Evje-Iveland amphibolite complex (Barth, 1947; Bjørlykke, 1947; Pedersen, 1975). It includes disseminated and massive mineralization and is Norway's second largest deposit.

Ertelien. This deposit is associated with a small noritic plug (600 m × 450 m). Mineralization includes massive, breccia and disseminated types near the margin of the plug (Johanssen, 1974).

Hosanger. This deposit is located within a noritic sill in the Anorthosite Complex, part of the Bergen Arc System, and possibly an outlier of the Jotun Nappe (Kvale, 1960). It experienced granulite facies metamorphism during the Sveconorwegian Orogeny (Sturt *et al.*, 1975). The mineralization includes dis-

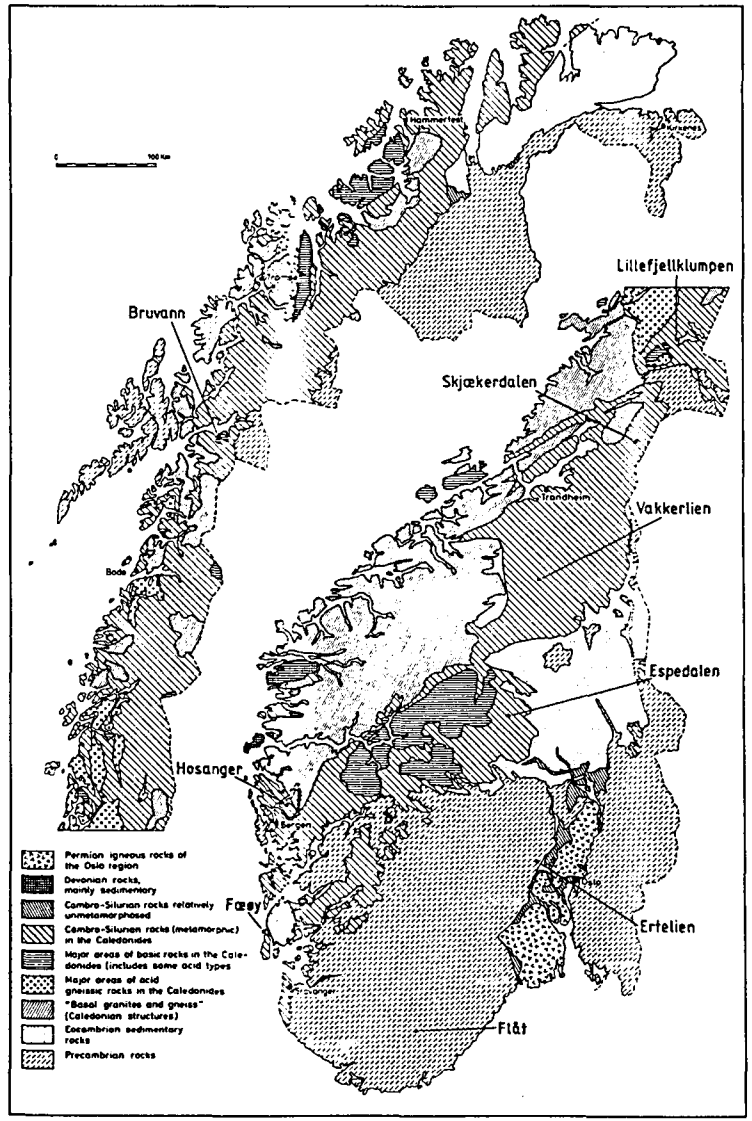

FIG. 1. Simplified geological map of Norway showing the location of the Ni-Cu deposits considered in this paper.

TABLE 1
Tonnage, mineralogy and geochemical data for samples analysed for PGE

	Metric tons metal × 10^3		Ave. grade %		Major sulphides	Trace minerals inc. known PGM	% Ni, Cu, ppb PGE + Au. Content in 100% sulphide (range of absolute concentrations in parentheses)	
	Ni	Cu	Ni	Cu			Ni	Cu
Bruvann (1)	142	34	0·32	0·08	po. pn. cp. py	Arsenopyrite gersdorffite niccolite molybdenite sphalerite No known PGM	9·0 (0·27–0·57)	2·1 (0·06–0·15)
Hosanger Ni-Cu	4·2	1·6	1·05	0·35	po. pn. cp. py	No data	3·2 (1·62–5·01)	0·4 (0·08–0·63)
Hosanger Cu-Ni	—	—	—	—		No data	0·6 (0·36–0·86)	7·7 (3·2–11·1)
Flåt Ni-Cu	19·5	12·2	0·75	0·47	py. po. pn. cp	Millerite violarite no known PGM	2·9 (0·27–6·06)	0·6 (0·06–2·71)
Flåt Cu-Ni	—	—	—	—		no data	0·8 (0·26–2·42)	7·2 (3·18–20·9)
Skjækerdalen	2·2	1·1	0·22	0·11	po. pn. cp	Bravoite linnaeite PGM not studied	3·1 (0·02–1·02)	2·7 (0·05–0·74)
Vakkerlien (2)	4	1·6	1·0	0·4	po. pn. cp. py	Gersdorffite violarite no known PGM	10·9 (n.a.)	2·2 (n.a.)
Espedalen (3)	1	0·4	1·0	0·4	po. pn. cp	Gersdorffite violarite no known PGM	6·6 (n.a.)	2·0 (n.a.)
Ertelien Ni-Cu	4·2	2·8	1·04	0·69	po. cp. py. pn	Gersdorffite violarite no known PGM	2·1 (0·5–3·47)	0·4 (0·09–1·44)
Ertelien Cu-Ni	—	—	—	—		Gersdorffite violarite no known PGM	0·7 (0·19–1·52)	11·8 (1·38–28·3)
Fædy	0·8	1	2·1	2·63	po. cp. pn. py	Kotulskite temagamite sperrylite	1·9 (0·19–2·35)	4·2 (0·87–16·3)
Lillefjell-klumpen (4)	<0·1	<0·1	4·0	1·2	po. py. pn. cp	Merenskyite sperrylite moncheite temagamite electrum Ag-pentlandite	3·6 (2·53–4·74)	1·2 (0·30–2·85)

Os	Ir	Ru	Rh	Pt	Pd	Au	Cu/Cu + Ni	Pd/Ir	n
—	6 (0·04–2·99)	—	—	52 (1·2–4·1)	70 (2–7)	1010 (1·0–55·5)	0·19	11·3	10
28 (10–37)	21 (6·6–28)	38 (<10–65)	7 (<2–18)	71 (29–120)	105 (36–185)	9 (3–14)	0·11	5·0	7
28 (17–47)	23 (<15–37)	59 (<20–110)	—[a]	—[a]	—[a]	342 (20–920)	0·93	—	3
23 (<2–38)	29 (0·6–54)	46 (<10–81)	11 (1–20)	68 (<10–150)	82 (21–174)	58 (7·3–290)	0·17	2·8	7
15 (<2–22)	19 (0·5–27)	53 (<10–68)	—[a]	—[a]	—[a]	650 (150–1 330)	0·90	—	4
—	—	—	—	100 (<3–7)	721 (<2–44)	536 (1–25)	0·47	—	7
39 (n.a.)	51 (n.a.)	62 (n.a.)	42 (n.a.)	788 (n.a.)	350 (n.a.)	49 (n.a.)	0·17	6·8	6
27 (n.a.)	26 (n.a.)	48 (n.a.)	36 (n.a.)	330 (n.a.)	250 (n.a.)	280 (n.a.)	0·23	9·6	6
7 (<3–32)	1·7 (0·3–4·1)	—	9 (<1–43)	273 (<10–2 400)	184 (75–400)	111 (2·2–430)	0·16	108	9
—	0·6 (<0·5–1·3)	—	10 (<2–33)	—[a]	—[a]	1 434 (78–4 000)	0·94	—	6
234 (31–490)	195 (6·4–410)	219 (72–480)	244 (23–440)	1 794 (640–5 400)	4 760 (2 600–8 000)	101 (6–310)	0·69	24	6
139 (23–250)	170 (14–290)	189 (<20–330)	214 (45–330)	1 799 (<100–5 900)	3 068 (410–4 700)	219 (8–1 910)	0·25	18	8

[a]Data unreliable because of analytical problems. n.a.: absolute values not available. Data taken from the following published sources: (1) Boyd *et al.* (1956); (2) Thompson *et al.* (1980); (3) Naldrett *et al.* (1979); (4) Grønlie (1985).

seminated to matrix sulphide near the base of the intrusion and veins of both Ni- and Cu-rich sulphide (Bjørlykke, 1949). The deposit was mined intermittently from 1883 to 1945. Modern PGE data are presented here for the first time.

Espedalen. The Espedalen deposit is located in an ultramafic-mafic intrusion, one of the second of three suites of mafic intrusives, in an outlier of the Jotun Nappe (Heim, 1981). It includes disseminated and breccia mineralization. PGE data were published by Naldrett *et al.* (1979).

Bruvann. This is Norway's largest Ni-Cu deposit and one of the largest Ni-Cu sulphide deposits in Europe, the Soviet Union excluded. It is a predominantly low-grade disseminated mineralization (Table 1), intercumulus to olivine and orthopyroxene in ultramafic cumulates in the northwestern part of the Råna intrusion (Fig. 1) (Boyd & Mathiesen, 1979).

Skjækerdalen. This deposit is associated with metagabbroic and ultramafic fragments in magmatic breccias in a small but complex polymagmatic intrusion, with maximum dimensions 4 km × 1 km in the Gula Group within the Caledonian Trondheim Nappe (Fig. 1). PGE data are reported for this deposit for the first time.

Vakkerlien. The Vakkerlien intrusion and its associated Ni-Cu mineralization have been described by Thompson *et al.* (1980) who also presented PGE data. The mineralization includes vein-, stringer- and disseminated types, all dominated by pyrrhotite, pentlandite and chalcopyrite, but with pyrite in most samples. The mineralization occurs in the core of an ultramafic-mafic sill in the Gula Group within the Caledonian Trondheim Nappe (Fig. 1).

Lilleffjellklumpen. This small mineralization (<100 t Ni metal) forms a massive sulphide lens lying concordantly between primitive MORB-type metabasalt and metagabbro in the allochthonous Gjersvik island arc complex in the Caledonides (Grønlie, 1985, 1986, in press). The mineralization shows variations in Cu/Cu + Ni ratio but without development of the Cu-rich veins with Cu/Cu + Ni averaging >0·9 found at Hosanger, Flåt and Ertelien. PGE data come from Grønlie (in press) though it has long been known that the body is rich in PGE (Foslie & Johnson Høst, 1932).

Fæøy. This mineralization is also from an oceanic environment in that it forms a massive mineralization within the dyke complex in the Karmøy ophiolite (Sturt *et al.*, 1980). Recent work (Dunning *et al.*, 1986) suggests that the Karmøy ophiolite is arc-related rather than 'normal' oceanic crust and gives a U/Pb age of 498 + 15/−5 Ma for plagiogranite in the complex. Analytical data from this deposit indicate a considerable range of Cu/Cu + Ni ratios, with values between 0·3 and 0·75 predominating. The data presented here are new though also this body was known to have high PGE levels (Foslie & Johnson Høst, 1932; Boyd & Nixon, 1985).

ANALYTICAL METHODS

The samples from Skjækerdalen, Hosanger, Ertelien, Flåt and Fæøy were analysed by Becquerel Laboratories of Toronto using INAA after preconcentration in a nickel-sulphide bead. Values obtained for three blind standards are shown by

Barnes *et al.* (this volume) who compare the results obtained using this method with accepted values. Interference effects inherent in the method give unreliable results for Pd and Rh in samples with >5% Cu and unreliable Pt results in samples with high Au contents: these effects are generally coincident.

Ni and Cu were analysed by atomic absorption and S by X-ray fluorescence by Caleb Brett Ltd of Manchester.

RESULTS

It is a well-established convention that PGE data for Ni-Cu sulphide deposits are presented recalculated to 100% sulphide and then, in diagrammatic form, normalized to chondrite values with the PGE and Au plotted in order of decreasing melting point from Os to Au (Naldrett *et al.*, 1979; Naldrett, 1981). The case for recalculation to 100% sulphides is based on the assumptions that the PGE are collected by sulphide droplets, and that major disturbance of the concentrations by later alteration has not taken place, and on the advantage in comparing data from different deposits given by the removal of effects caused by variable content of gangue in the samples analysed. The assumptions may not hold for sulphide-poor rocks.

The samples analysed from the five Ni-Cu deposits for which new data are presented here were, with the exception of Skjækerdalen, all matrix or massive sulphides with >50% sulphide. The data in this paper are presented as ranges of absolute values and as content in 100% sulphides (Table 1) and are shown diagrammatically (Figs 2(A–D)) according to the convention established by Naldrett *et al.* (1979).

The samples analysed for PGE show variable degrees of agreement with available reserve figures in terms of their Cu/Cu + Ni ratio. In three cases, Hosanger, Flåt and Ertelien, this is partly due to the combination of Ni-Cu and Cu>>Ni mineralizations in the bulk figures for the deposits. The closest correspondence is for Bruvann as the ten samples on which the averages shown in Table 1 are based, are bulk samples of drillcore representing complete ore-zone intersections. In several cases the deposits are worked out and/or only partially accessible and it is not possible to ensure representative ore sampling.

The deposits have been divided into three groups based on their content of Pt and Pd in 100% sulphides.

Group 1. Bruvann, Hosanger and Flåt, three of the four largest Ni-Cu sulphide deposits in the country, have concentrations of PGE in 100% sulphides an order of magnitude below chondrite for all PGE except Pd, which is just over 0·1 × chondrite (Fig. 2(A)). Concentrations of Pt and Pd are similar for all three and the concentrations of all PGE are similar for Hosanger and Flåt, while Bruvann has much lower concentrations (<c. 0·01 × chondrite) of Os, Ir, Ru and Rh. Few Ni-Cu deposits are recorded in the literature as having comparably low values of Pt and Pd: those known to the authors are Pipe (Naldrett *et al.*, 1979), Montcalm (Naldrett & Duke, 1980), Laukunkangas and Vammala (Papunen, 1986), St. Stephen, Lynn

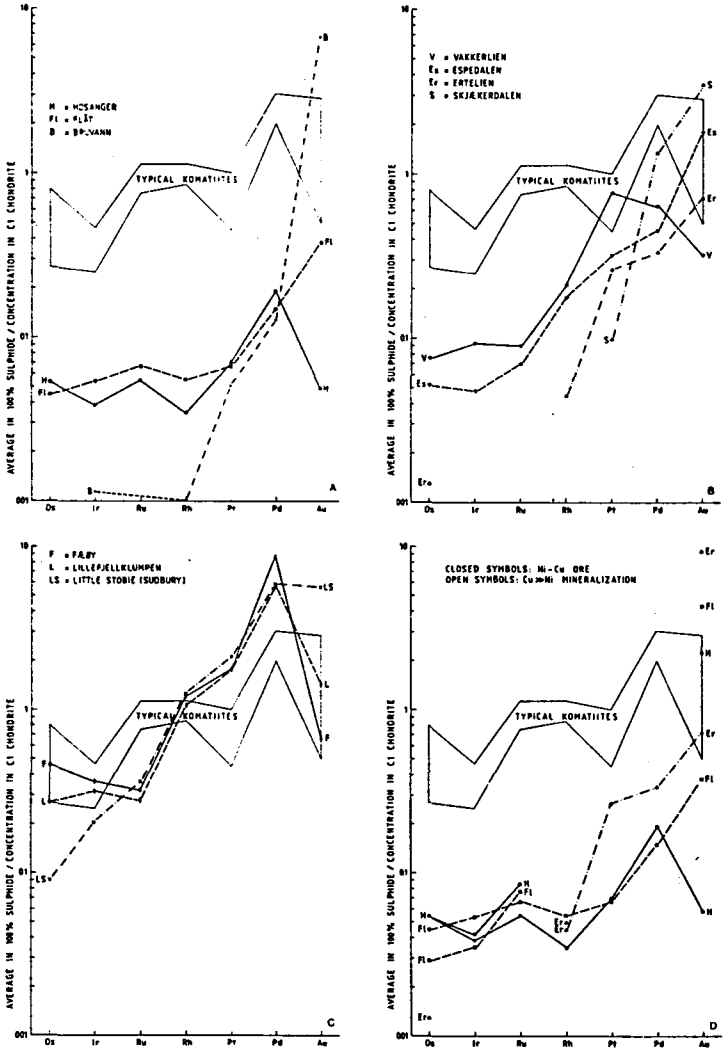

FIG. 2. Average chondrite-normalized noble metal contents in 100% sulphide in Norwegian Ni-Cu deposits. Published data are included from Naldrett *et al.* (1979) (Espedalen), Thompson *et al.* (1980) (Vakkerlien), Grønlie (1985) (Lillefjellklumpen), Boyd *et al.* (1986) (Bruvann). (A), (B), (C) show data from Ni-Cu mineralizations classified according to Pt- and Pd-levels with the field of komatiites and the average for Little Stobie (Naldrett, 1981) for reference. (D) shows data for Ni-Cu and Cu >> Ni mineralizations for Hosanger (solid line), Flåt (dashed line) and Ertelien (dashed-dot line).

Lake, Moak Lake and Renzy (Jonasson *et al.*, 1987). The Pd/Ir ratios are low for all three deposits and Hosanger and Flåt have, in general, patterns similar in form to the field shown by typical komatiites (Naldrett, 1981). The low PGE grades in these deposits are seemingly at variance with evidence of a relatively primitive magma from other indicators, for the case of Bruvann (Boyd *et al.*, 1987) and for mineralization in its host, the Råna intrusion in general (Barnes, 1987). Possible explanations are that the parental magmas were derived from an already depleted mantle or that PGE were removed in the crust but below presently accessible levels: both papers conclude that the evidence, particularly REE data (Barnes, 1986*a*), supports the second alternative.

The position of Au for Flåt and Hosanger refers to Au-poor Ni-Cu ore (Au is concentrated in Cu >> Ni mineralization in these deposits), while at Bruvann high Au values occur locally in disseminated Ni-Cu mineralization and no Cu-rich paragenesis is known to exist (based on a total of 28 500 m of drilling and several thousand assays).

Group 2 (Fig. 2(B)). Skjækerdalen, Vakkerlien, Espedalen and Ertelien contain Pt and Pd at higher levels than Group 1, but <chondrite, except for Pd at Skjækerdalen. The average Pd content at Skjækerdalen is however perhaps artificial, as one of the seven samples was unusually rich in Pd (4·7 ppm in 100% sulphide). Rh values from Espedalen and Vakkerlien are also markedly higher than those found in Group 1 deposits. For Espedalen, Ertelien and Skjækerdalen the contents of Os, Ir and Ru are similar to, or less than, those found in Group 1, with all deposits for which data was obtained showing flat patterns for these elements. Though the Pd/Ir ratios of Group 1 and Group 2 deposits overlap, they are generally higher in Group 2, especially for Ertelien, the Pd/Ir ratio from which is compatible with equilibration with a magma of composition between continental tholeiite and MORB (Naldrett & Barnes, 1986).

Group 3. Lillefjellklumpen and Fæøy (Fig. 2(C)) have Pt and Pd contents exceeding those of typical komatiites, while having concentrations similar to komatiites for Os, Ir, Rh and Au, and relatively low levels for Ru. The patterns for the two deposits are very similar. The concentrations of Pt and Pd are about half of those found in the ophiolite-hosted Illinois River massive sulphide deposit in Oregon (Foose, 1986) which includes both disseminated sulphides and pods of remobilized massive mineralization in deformed pyroxenitic and gabbroic cumulates. The levels for all PGE are about an order of magnitude lower than those found in the chromitite-associated Cliff mineralization in the Unst ophiolite, Shetland (Prichard *et al.*, 1986) which is located in a dunitic body in harzburgite tectonite. Chromitite-associated sulphide mineralization in the Eretria area of the Othris ophiolite has, however, much lower Pt and Pd levels (Economou & Naldrett, 1984) than those found at Lillefjellklumpen and Fæøy. The Ru, Rh, Pt and Pd concentrations at the two Norwegian deposits are close to those at Little Stobie, Sudbury (Naldrett, 1981).

Cu >> Ni mineralizations. Three of the deposits examined, Hosanger, Flåt and Ertelien, contain parageneses dominated by Cu (with Cu/(Cu + Ni) > 0·9) (Fig. 2(D)). No reliable data are available for Pt and Pd, and in two cases for Rh, in the

Cu-rich parageneses. The Ertelien Ni-Cu mineralization has exceedingly low contents of Os, Ir and Ru, with even lower contents of Os and Ir, and probably also of Ru, in the Cu >> Ni mineralization. At somewhat higher levels the same is true for Os and Ir at Flåt, while the Cu-Ni paragenesis at Hosanger has higher levels of Ir and Ru, and the same Os content as the Ni-Cu ore.

DISCUSSION

With the exception of the two deposits in Group 3, both from an 'ophiolitic' environment, there is no obvious relationship *within* the group of deposits discussed here between the apparent geotectonic environment or age of the deposits and their PGE or Ni-Cu grades. Group 1 contains three deposits, all with low Cu/(Cu + Ni) and Pd/Ir ratios (<19 and <11·3 respectively), but each from a different type of intrusion, only in the very broadest sense possibly, synorogenic. The Ni, Cu and PGE geochemistry, especially the ratios Cu/(Cu + Ni) and Pd/Ir, of these deposits indicate derivation from relatively primitive magmas. The Pd/Ir ratios are of the same order as those found in Ni-Cu deposits related to komatiites (Barnes *et al.*, 1985). One of the more apparent relationships in Group 1 is the inverse 'correlation' between the content of (Pt + Pd) and the size of the deposits. This might imply a low value of R, the ratio of silicate magma to the mass of sulphide melt equilibrating with it (Naldrett *et al.*, 1979), but the high content of Ni in 100% sulphides at Bruvann suggests that this is not the case for this deposit.

The deposits in Group 1 share their characteristics of low Pd/Ir ratio and very low PGE grade with several Ni-Cu deposits in other orogenic belts, e.g. in the Middle Proterozoic Svecokarelian belt in Finland (Papunen, 1986) and in the Appalachian Caledonides (Jonasson *et al.*, 1987). Even the more PGE-rich deposits located in orogenic belts have modest PGE grades, totalling <*c.* 2000 ppb in 100% sulphides, except for Hitura at which secondary processes have enriched the noble metals (Häkli *et al.*, 1976). This suggests that there may be a common mechanism leading to depletion of PGE in mafic bodies emplaced in the upper crust in orogenic belts. The examples of Bruvann (Boyd *et al.*, 1987) and mineralizations at Råna in general (Barnes, 1986*a*) indicate that this is due to depletion of PGE in the crust rather than melting of a depleted mantle.

Vakkerlien and Espedalen, in Group 2, have Cu/(Cu + Ni) and Pd/Ir ratios similar to the deposits in Group 1 while Ertelien, though it has a low Cu/(Cu + Ni) ratio has a Pd/Ir ratio >100 and Skjækerdalen has both a higher Cu/(Cu + Ni) ratio and a Pd/Ir ratio at least >100, implying a normal basaltic parent magma (Naldrett & Barnes, 1986).

The two deposits in Group 3 have higher Cu/(Cu + Ni) ratios than the other Ni-Cu mineralizations except for Skjækerdalen, but have relatively low Pd/Ir ratios (18 and 24), well below the values shown for MORB by Barnes *et al.* (1985). Mineralizations of this type could represent the 'missing' Cu-Ni-bearing sulphide melt which Czamanske & Moore (1977), concluded had been depleted from MORB-type basalt.

Cu-rich veins and/or ore bodies are known from many Ni-Cu deposits, including several at Sudbury (Naldrett, 1981) as well as Katiniq, Alexo and Insizwa. Alternative explanations for this Cu enrichment have been:

—Hydrothermal mobilization of Cu, Pt, Pd and Au (not affecting the other PGE) (McCallum *et al.*, 1976; Keays *et al.*, 1981, 1982).
—Subsolidus diffusion (Naldrett & Kullerud, 1967; Hoffman *et al.*, 1979).
—Fractionation of PGE from the sulphide melt into monosulphide solid solution (MSS) (Distler *et al.*, 1977; Malevskiy *et al.*, 1977; Naldrett *et al.*, 1982).
—Preferential partition of Pt, Pd and Au into a high-temperature Cu-rich sulphide liquid. That such a liquid can exist was suggested by Hawley (1962) and demonstrated by Craig & Kullerud (1969).

The data for the three deposits shown on Fig. 2(D) are inconsistent with the first of these explanations being the sole reason for the Cu >> Ni parageneses in that the process resulting in this type of mineralization has not only a marked effect on the Au content but has also a systematic effect at the other end of the spectrum because the ratio (PGE)Cu >> Ni/(PGE)Ni-Cu shows an almost consistent increase from Os to Ir, Ir to Ru and Ru to Au for Flåt and Hosanger. The data available from Ertelien are also consistent with this pattern. The conclusion must be that the process causing formation of the Cu >> Ni mineralization has affected all the PGE + Au in a systematic manner and that any additional effect due to hydrothermal alteration has not disturbed the resulting pattern. A more detailed study of the mineralogy and field relationships of these ores than has been possible in this project would be required before drawing any further conclusions on which process caused the formation of the Cu >> Ni mineralization but we feel that the last explanation is the most probable.

ACKNOWLEDGEMENTS

This work has been supported by the European Economic Community Raw Materials Program (Contract no. MSN-2-0215-N(B)), by the Royal Norwegian Council for Scientific and Industrial Research (NTNF) and by the Geological Survey of Norway (NGU). We would like to thank Astri Hemming and the late Lars Holiløkk for help in preparing the figures and Gunn Sandvik Nielsen for typing the manuscript.

REFERENCES

Barnes, S.-J. (1986*a*). Investigation of the potential of the Tverrfjell portion of the Råna intrusion for platinum-group element mineralization. NGU-rapport nr. 86.021 (Geological Survey of Norway report no. 86.021), 169 pp.
Barnes, S.-J. (1986*b*). Platinum-group elements in the Tverrfjell portion of the Råna layered intrusion, Nordland, Norway. *Terra Cognita*, 6, 559 (abs.).

Barnes, S.-J. (1987). Unusual base- to noble-metal ratios from the Råna layered intrusion, Nordland, Norway. *Norsk geol. tidsskr.*, **67**, 215–32.

Barnes, S.-J., Naldrett, A. J. & Gorton, M. P. (1985). The origin of the fractionation of platinum-group elements in terrestrial magmas. *Chem. Geol.*, **53**, 303–23.

Barnes, S.-J., Boyd, R., Korneliussen, A., Nilsson, L.-P., Often, M., Pedersen, R. B. & Robins, B. (1988). The use of mantle normalization and metal ratios in discriminating the effects of partial melting, crystal fractionation and sulphide segregation on platinum-group elements, gold, nickel and copper: examples from Norway. In *Geo-Platinum 87*, 113–43. Elsevier Applied Science Publishers, London.

Barth, T. F. P. (1947). The nickeliferous Iveland-Evje amphibolite and its relation. *Nor. geol. unders.*, **168a**, 71 pp.

Bjørlykke, H. (1947). Flåt nickel mine. *Nor. geol. unders. Bull.*, **168b**, 39 pp.

Bjørlykke, H. (1949). Hosanger nikkelgruve. *Nor. geol. unders. Bull.*, **172**, 38 pp.

Boyd, R. & Mathiesen, C. O. (1979). The nickel mineralization of the Råna mafic intrusion, Nordland, Norway. *Can. Mineral.*, **17**, 287–98.

Boyd, R. & Nixon, F. (1985). Norwegian nickel deposits: a review. In *Nickel-copper Deposits of the Baltic Shield and Scandinavian Caledonides*, ed. H. Papunen & G. I. Gorbunov, Geol. Surv. Finland. Bull., Vol. 333, pp. 363–94.

Boyd, R., McDade, J. M., Millard, H. T. & Page, N. J. (1988). Platinum and palladium geochemistry of the Bruvann nickel-copper deposit, Råna, North Norway. *Terra Cognita*, 6, 559–60 (abs.).

Boyd, R., McDade, J. M., Millard, H. T. & Page, N. J. (1987). Platinum and metal geochemistry of the Bruvann nickel-copper deposit, Råna, North Norway. *Norsk geol. tidsskr.*, **67**, 205–14.

Craig, J. R. & Kullerud, G. (1969). Phase relations in the Cu–Fe–Ni–S system and their application to magmatic ore deposits. In *Magmatic Ore Deposits*, ed. H. D. B. Wilson. Economic Geology Monograph, Vol. 4, Economic Geology Publishing Company, pp. 344–58.

Crocket, J. H. (1974). Gold. In *Handbook of Geochemistry*, ed. K. H. Wedepohl, II-4. Springer-Verlag, Berlin.

Czamanske, G. K. & Moore, J. G. (1977). Composition and phase chemistry of sulphide globules in basalt from the Mid Atlantic ridge valley near 37°N latitude. *Geol. Soc. Amer. Bull.*, **88**, 587–99.

Distler, V. V., Malevskiy, A. Yu. & Laputina, I. P. (1977). Distribution of platinoids between pyrrhotite and pentlandite in crystallization of a sulphide melt. *Geochem. Int.*, **14**, 30–40.

Dunning, G. R., Krogh, T. E. & Pedersen, R. B. (1986). U/Pb zircon ages of Appalachian-Caledonian ophiolites. *Terra Cognita*, 6, 155 (abs.).

Economou, M. I. & Naldrett, A. J. (1984). Sulfides associated with podiform bodies of chromite at Tsangli, Eretria, Greece. *Mineral. Deposita*, **19**, 289–97.

Foose, M. P. (1986). Setting of a magmatic sulfide occurrence in a dismembered ophiolite, southwestern Oregon. *US Geol. Survey. Bull.*, **1626-A**, 21 pp.

Foslie, S. & Johnson Høst, M. (1932). Platina i sulfidisk nikkelmalm. *Nor. geol. unders. Bull.*, **137**, 71 pp.

Grønlie, A. (1985). PGM-mineraliseringen ved Lillefjellklumpen nikkel-magnetkis forekomst, Nord-Trøndelag. In *Nye malmtyper i Norge*, ed. F. M. Vokes. BVLI, Trondheim, pp. 82–98.

Grønlie, A. (1986). Platinum-group minerals in the Lillefjellklumpen nickel-copper deposit, Norway. *Terra Cognita*, **5**, 560 (abs.).

Grønlie, A. (in press). Platinum-group minerals in the Lillefjellklumpen nickel-copper deposit, Norway. *Norsk geol. tidsskr.*

Gunn, A. G., Leake, R. C. & Styles, M. T. (1985). Platinum-group element mineralization in the Unst ophiolite, Shetland. Mineral Reconnaissance Programme Rep. Br. geol. Surv., No. 73, 117 pp.

Häkli, T. A., Hänninen, E., Vuorelainen, Y. & Papunen, H. (1976). Platinum-group minerals in the Hitura nickel desposit, Finland. *Econ. Geol.*, **71**, 1206–13.

Hawley, J. E. (1962). The Sudbury ores: their mineralogy and origin. *Can. Mineral.*, **7**, 1–207.

Heim, M. (1981). Basement/cover relations in the allochthon at Espedalen (Jotun-Valdres Nappe complex, S. Norway). *Terra Cognita*, 1, 51 (abs).

Hoffman, E. L., Naldrett, A. J., Alcock, R. A. & Hancock, R. G. V. (1979). The noble metal content of ore in the Levack West and Little Stobie mines, Ontario. *Can. Mineral.*, **17**, 437–52.

Johanssen, G. A. (1974). Nikkel-, kobbermalmforekomster og bergarter i Tyristrand og Holleia. Cand. real. thesis. University of Oslo, 126 pp. (unpublished).

Jonasson, I. R., Eckstrand, O. R. & Watkinson, D. H. (1987). Preliminary investigations of the abundance of platinum, palladium and gold in some samples of Canadian nickel-copper ores: in Current Research, Part A, Geological Survey of Canada, Paper 87-1A, pp. 835–46.

Keays, R. R., Ross, J. R. & Woolrich, P. (1981). Precious metals in volcanic peridotite-associated nickel sulphide deposits in Western Australia. II. Distribution within the ores and host rocks at Kambalda. *Econ. Geol.*, **76**, 1645–74.

Keays, R. R., Nickel, E. H., Groves, D. I. & McGoldrick, P. J. (1982). Iridium and palladium as discriminants of volcanic-exhalative and hydrothermal and magmatic nickel sulfide mineralization. *Econ. Geol.*, **77**, 1535–47.

Kvale, A. (1960). The nappe area of the Caledonides in western Norway. *Nor. geol. unders. Bull.*, **212e**, 43 pp.

Malevskiy, A. Yu., Laputina, I. P. & Distler, K. V. (1977). Behaviour of the platinum-group metals during crystallization of a sulfide melt. *Geochem. Inst.*, **14**, 177–84.

McBryde, W. A. E. (1972). Platinum metals. In *Encyclopedia of Geochemical and Environmental Sciences*, ed. R. W. Fairbridge. Van Nostrand Reinhold, New York.

McCallum, M. E., Lovacks, R. R., Carlson, R. R., Cooley, E. F. & Doerye, T. A. (1976). Platinum metals associated with hydrothermal copper ores of the New Rambler mine, Medicine Bow Mountains, Wyoming. *Econ. Geol.*, **71**, 1429–50.

Naldrett, A. J. (1981). Platinum-group element deposits. In *Platinum-group Elements: Mineralogy, Geology, Recovery*, ed. L. J. Cabri. Canadian Institute of Mining and Metallurgy Special Volume 23, pp. 197–232.

Naldrett, A. J. & Barnes, S.-J. (1986). The behaviour of platinum-group elements during fractional crystallization and partial melting with special reference to the composition of magmatic sulphide ores. *Fortschr. Mineral.*, **64**, 113–33.

Naldrett, A. J. & Duke, J. M. (1980). Pt metals in magmatic sulfide ores. *Science*, **208**, 1417–24.

Naldrett, A. J. & Kullerud, G. (1967). A study of the Strathcona Mine and its bearing on the origin of the nickel-copper ores of the Sudbury district, Ontario. *J. Petrol.*, **8**, 453–531.

Naldrett, A. J., Hoffman, E. L., Green, A. H., Chen-Lin Chou & Naldrett, S. R. (1979). The composition of Ni-sulfide ores with particular reference to their content of PGE and Au. *Can. Mineral.*, **17**, 403–15.

Naldrett, A. J., Innes, D., Gorton, M. J. & Sowa, J. (1982). Compositional variations within and between five Sudbury ore deposits. *Econ. Geol.*, **77**, 1519–34.

Oshin, I. O. & Crocket, J. H. (1982). Noble metals in the Thetford mine ophiolite, Quebec, Canada, Part I. Distribution of gold, iridium, platinum and palladium in the ultramafic and gabbroic rocks. *Econ. Geol.*, **77**, 1556–70.

Papunen, H. (1986). Platinum-group elements in Svecokarelian nickel-copper deposits, Finland. *Econ. Geol.*, **81**, 1236–41.

Pedersen, S. (1975). Intrusive rocks of the northern Iveland-Evje area, Aust-Agder. *Nor. geol. unders. Bull.*, **322**, 1–11.

Prichard, H. M., Potts, P. J. & Neary, C. R. (1981). Platinum-group element minerals in the Unst Chromite, Shetland Isles. *I.M.M. Trans.*, **90**, B186–B188.

Prichard, H. M., Neary, C. R. & Potts, P. J. (1986). Platinum-group minerals in the Shetland Ophiolite complex. In *Metallogenesis of Basic and Ultrabasic Rocks*, ed. M. J. Gallagher, R. A. Ixer, C. R. Neary & H. M. Prichard. Institution of Mining and Metallurgy Symposium Volume, pp. 395–414.

Scheerer, T. (1845). Om nikkelens forekomst i Norge. *Nyt Mag. For Naturvitenskaperne*, **4**, 91–6.

Sturt, B. A., Skarpenes, O., Ohanian, A. T. & Pringle, I. R. (1975). Reconnaissance Rb/Sr isochron study in the Bergen Arc System and regional implications. *Nature*, **253**, 595–9.

Sturt, B. A., Thon, A. & Furnes, H. (1980). The geology and preliminary geochemistry of the Karmøy ophiolite, S.W. Norway. *Proc. Int. Ophiolite Symposium Cyprus*, 1979. Ministry of Agriculture and Natural Resources, Geological Survey Department, Cyprus, pp. 538–44.

Thompson, J. F. H., Nixon, F. & Sivertsen, R. (1980). The geology of the Vakkerlien nickel prospect, Kvikne, Norway. *Bull. Geol. Soc. Finland*, **52**, 3–22.

2.2 Platinum-group mineral inclusions in chromitite from the Osthammeren ultramafic tectonite body; south central Norway by L.P.Nilsson summary version in press in the journal Mineralogy & Petrology, this, complete version submitted to Norsk Geologisk Tidsskrift.

PLATINUM-GROUP-MINERAL INCLUSIONS IN CHROMITITE FROM THE OSTHAMMEREN ULTRAMAFIC TECTONITE BODY; SOUTH CENTRAL NORWAY

L.P. Nilsson

Geological Survey of Norway, P.O. Box 3006-Lade, N-7002 Trondheim, Norway

Abstract

A variety of platinum-group minerals (PGMs) has been found in one single sample of massive chromitite from the Osthammeren ultramafic tectonite (serpentinite) body, Norway. The PGM-inclusions occur in two distinctly different ways:

1. Os, Ir, Ru and minor Pt occur in primary magmatic, euhedral-subhedral, small (<5-20 µm), mainly single-phase inclusions of Os-free laurite, Os-laurite, osmiridium and Pt_2 (Ir, Os)$Fe_{0,65}$. They are totally enclosed in fresh unaltered chromite. A few PGM-inclusions are however associated with small blebs of Na-bearing hornblende or phlogopite indicating that the presence of volatiles at an early stage may have influenced the formation of these PGMs.

2. Purely secondary PGMs occur as anhedral - (subhedral), texturally often very complex grains or grain-aggregates with varying size (5-70 µm) and consisting of from one to eight PGM-phases plus Ni-sulphide and Ni-arsenide. These PGMs always occur within, or in contact with, late formed cataclastic (metamorphic) cracks or very fine fissures, in the primary magmatic chromite grains. The finer fissures are generally tightened by ferrite-chromite, a hydrothermal alteration product of chromite. The wider cracks are usually serpentine- and chlorite-filled and are rimmed by

ferrite-chromite against the chromite. Os, Ir, Ru, Rh, Pt and minor Pd are represented in grains of this group, and the secondary PGM-association found consists of Os-free laurite, Os-laurite, erlichmanite, Ir-rich erlichmanite, native Os, iridosmine (in lamellae), osarsite, irarsite, hollingworthite, Rh-rich platarsite, Ru-rich platarsite, sperrylite, (Ir, Rh)SbS, IrSbS, (Ir, Pt, Pb)S_2 (new?), Pd-antimonide (probably stibiopalladinite) plus the associated phases pentlandite, heazlewoodite and niccolite.

Follow-up analyses of new chromitite samples showed that these resemble the Harold's Grave chromitites in the Shetland ophiolite complex with regard both to PGE-pattern and PGE-level.

Introduction

Platinum analyses of Norwegian chromium ore were first carried out by Lunde (1927), Lunde & Johnson (1928), Noddack & Noddack (1931a, b) and Goldschmidt & Peters (1932). Since that time however little has been published about platinum or platinum-group elements (PGE) in Norwegian chromium ore until recently (Barnes et al. 1987a, b, 1988).

The following account is based on results obtained as a part of a pilot study of platinum-grup elements in rocks and ore mineralizations in Norway (Barnes et al. 1987a), and a succeeding study of platinum-group minerals (PGM) in the PGE-anomalous chromitites found.

Seventy chromitite samples from nineteen ultramafic tectonite bodies in central Norway were analysed for Au, Pt and Pd by atomic absorption

spectrometry (AAS). Only four of the samples showed clearly anomalous Pt and/or Pd-values (Table 1); two of these contained PGM inclusions. The first comes from the tiny Osthammeren serpentinite lens in the eastern Trondheim region in the Caledonides of South-Central Norway and the other from the Ørnstolen ultramafic body in North-Central Norway. PGM inclusions in the Ørnstolen body will be treated in a separate paper.

DISTRIBUTION, SETTING AND CONSTITUTION OF THE CHROMITITE DEPOSITS AND THEIR HOST ROCKS

Figure 1 shows the distribution of ultramafic tectonites in South-Central Norway. These bodies are distributed mainly in one single nappe unit of the Caledonian tectonostratigraphy in this part of the country. The nappe has been given different local names in different areas; from east to west across central Norway it has been called the Essandsjø Nappe, Bottheim Group and Blåhø Nappe. These nappes are thought to correlate with the Seve Nappes in Sweden; all of them are regarded as part of the lowermost unit in the Upper Allochton (Gee et al. 1985a). Osthammeren and most of the other partly or totally metamorphosed ultramafic tectonites shown in Fig. 1 represent mantle material (harzburgite and dunite with or without chromitite) possibly intruded along faults or weakened zones in a transitional continental - oceanic terrain in an early extensional phase of the Caledonian orogeny (opening of the Iapetus ocean) (Stephens & Gee 1985). Parts of the strongly deformed and recrystallized amphibolites of the Essandsjø Nappe and correlated nappes which host a number of the ultramfic bodies represent volcanic units of tholeiitic, low-K character with affinity to MORB (Stephens et al. 1985, Solyom et al. 1979). Results

of age determinations of the metabasites however, have not given well-constrained ages. A possible age range from upper Proterozoic to middle Ordovician is given by Stephens et al. (op. cit.).

The distribution, setting, composition, origin and emplacement of the ultramfic tectonites and cumulate bodies (i.e. "alpine-type" ultramafites) within the Scandinavian Caledonides are dealt with in detail by Moore & Qvale (1977), Stigh (1979), Qvale & Stigh (1985) and Bucher-Nurminen (1988).

Figure 2 shows the Osthammeren body and its neighbouring tectonite bodies. The Osthammeren body is very small (about 0.05 sq km), and magmatic features are totally obliterated. It consists of almost massive to moderately sheared serpentinite crosscut by a few minor magnesite-serpentine veins. Its larger neighbouring tectonite body, the ca. 15 sq km Feragen body provides a better illustration of the setting of the chromitite ores. This body, the central parts of which are only moderately serpentinized, consists of roughly equal amounts of harzburgite and chrome ore bearing dunite. This body has contributed about 80 % of Norway's total chromite production or about 32550 metric tons (Poulsen 1960, Engzelius 1940).

In the tiny Osthammeren body a sample later shown to be PGM-bearing was collected from massive chromitite-ore, with very little gangue, in one of eleven small claims distributed roughly along two lines, one running SW-NE, the other SSE-NNW across the top plateau of the knoll-shaped ultramafic body, Figure 3. Petrographic inspection of nine polished sections of the ore sample revealed that the chromite is deformed by a weak cataclastic fabric, and that it has a slight to moderate ferrite-chromite alteration along cracks and grain boundaries. There are also numerous pale yellow awaruite grains, often grouped in relatively large irregular clots in the

serpentine and chlorite gangue between the chromite grains. Pentlandite and heazlewoodite also occur, often in the same textural form as awaruite. The appearance of awaruite is characteristic of the Osthammeren, Feragen and neighbouring almost sulphur-free ultramafic bodies. Awaruite and heazlewoodite are derived from the alteration of primary silicate and sulphide phases.

Analytical techniques

Fifteen grains and grain-aggregates occurring as high reflectance inclusions in chromite grains were found by systematic inspection of the nine polished sections of the PGE-anomalous chromitite sample by use of reflected light microscope with a magnification of 200x. The inclusions observed were distributed in eight of the nine sections with one to three grains in each section. Further studies with a scanning-electron microscope (SEM) and quantitative analyses (mainly WDS) with a Jeol 733 microprobe performed at the Continental Shelf and Petroleum Technology Research Institute (IKU), Trondheim, Norway confirmed that the inclusions were PGM. The operating conditions for the microprobe were: accelerating voltage 25 kV, beam current 15 nA, beam diameter approx. 1 µm, counting time 10 or 40 s. The following X-ray lines were used: K_{α} - S, Ni, Fe and Cr; L_{α} - Os, Ir, Ru, Rh, Pt, Pd, Au, As, Sb and Te. Metal standards were used for all elements except S (chalcopyrite), Fe and Cr (chromite). A minor interference exists between several of the X-ray lines of the elements concerned. The metallic standards for Os, Ir, Ru, Rh, Pt, Pd, As and Sb were therefore analysed for these same eight elements plus S, Au, Te, Ni, Cr and Fe to obtain a quantitative measure of the interference. The Rh standard yielded as much as 18.1 wt% Pd, but not more than 0.42 wt% of any of the other elements

concerned. The Ru standard yielded 1.5 wt% Pd and 1.0 % Rh, the Ir-standard 1.4 % Au and the Pt-standard 1.0 % Au. Interference between other elements was quantified to be less than 1.0 wt %.

Seventy-four quantitative analyses were carried out on the PGM-inclusions and a selection of these is listed in Table 2. Analyses are tabulated following Auge (1985) and Legendre & Auge (1986); raw analytical data from the probe are first corrected only for interference. Thereafter analyses are recalculated to 100 % after subtraction of Cr and Fe from chromite enclosing the PGM, and thirdly atomic concentrations are calculated from the corrected analyses. Some of the PGM-grain-aggregates show very complex compositions and textures. To illustrate this, a variety of photomicrographs, mineral location maps, back-scattered electron images (BEI) and X-ray images of several elements present in the PGMs accompany the description.

PGM description and results of analyses

The fifteen PGM inclusions investigated range in size from ca. 5 to 70 µm and vary in habit from anhedral clots or clusters to nearly perfect idiomorphic crystals. The inclusions contain fourteen PGM phases and three associated Ni-sulphide and -arsenide phases. A synthesis of the PGM association found is given in Table 3. The PGM-nomenclature used in this table and in the text is based on that of Cabri (1981).

There are two distinct groups of inclusions.

Group one consists of subhedral - euhedral rather small (5-20 µm), single-phase or two-phase crystals that are always trapped within fresh

undisturbed parts of the chromite grains (grains no. 2, 9, 10 and 12 to 15 in Table 3). Two of these PGM-inclusions (grains no. 9 and 12 in Table 3) are observed in contact with silicate blebs interpreted from quantitative analyses as phlogopite and Na-bearing hornblende.

Group two consists of anhedral -(subhedral) grains or grain-aggregates with size varying from ca. 5 to 70 µm and consisting of up to eight different PGM-phases and in some cases associated Ni-sulphides and Ni-arsenide (grains no. 1, 3 to 8 and 11 in Table 3). Group two inclusions are always associated with very fine cataclastic cracks in the primary chromite grains. These cracks are filled with silicates (serpentine or chlorite) and/or with ferrite-chromite, i.e. ferrite-chromite has developed (grown) from the chromite nearest to the crack and filled or tightened the cracks partially or totally.

The diversity of PGM-phases present in eight of the nine sections studied is notable, especially when bearing in mind that all the sections are from one single hand-size specimen. The complete PGM-association of the Osthammeren body with its eleven chromitite showings is therefore probably at least a little larger than shown in Table 3. Several ophiolitic chromitite deposits from around the world have been investigated in recent years and show PGM associations similar to that found in the Osthammeren body e.g. the Aetorache deposit in the Vourinos ophiolite complex (Auge 1985), and even more closely chromitite occurrences in the Hochgrössen ultramafic massif in Austria (Thalhammer and Stumpfl 1988), the Harold's Grave and Cliff deposits in the Shetland ophiolite complex (Prichard, Neary and Potts 1986, Tarkian and Prichard 1987, Prichard, Potts and Neary 1987), and a chromitite deposit in N.W. China (Chang et al. 1973).

LAURITE - ERLICHMANITE SOLID SOLUTION SERIES

Laurite is by far the most common PGM in the sections analysed. Os-free or Os-poor laurite appears in 6 of the 15 PGM grains found, and Os-enriched laurite in 10 of these. Together this mineral appears in 13 of the 15 PGM grains found and in 7 of the 8 PGM-bearing sections (Table 3).

The microprobe analyses, 31 in number, together show an almost complete solid-solution between $Ru_{0.997}Os_{0.003}S_2$ and $Ru_{0.48}Os_{0.52}S_2$. 12 of these analyses are listed in Table 2 (analyses 1 to 12). Grain-aggregate no. 3 inside which 10 of the 31 analyses were performed, shows a remarkable Ru-Os solid solution (compare the X-ray images of Os and Ru in Fig. 6). The results of the quantitative analyses are plotted in the triangular Os-Ir-Ru diagram, Fig. 4a. In addition to the extensive Ru-Os solid solution this diagram also shows a low Ir content in the secondary and somewhat Os-enriched laurites, resembling laurites from Shetland (Tarkian & Prichard 1987), but lower than in most laurite compositions reported, e.g. Legendre & Auge (1986), Tarkian (1987) and Auge (1988). The few primary and Os-enriched laurites plotted are somewhat richer in Ir and resemble the laurites in the cited references more closely. There is otherwise generally no significant difference in chemical composition between primary laurite inclusions and laurite in the secondary PGM-grain-aggregates. Erlichmanite which is much less common than laurite appears in the two grain-aggregates which are most complex, both with regard to texture and composition (grains no. 1 and 3 shown in Fig. 5 and 6 respectively). Analysis 11 in Table 2 gives the composition of erlichmanite in grain no. 3. It is a normal Irpoor variety which closely resembles the erlichmanite-analyses quoted by Cabri (1981) in his Table 8.49.

On the other hand analysis 12 in Table 2 shows an erlichmanite (in grain

no. 1) with an unusually high Ir-content. Only Begizow et al. (1976) referred to in Tarkian (1987) and recently Auge (1988) have reported erlichmanite with a similarly high Ir-content.

The range of Ru-Os solid solution revealed from the microprobe analyses fits well with laurite and erlichmanite analyses from different sources (Auge 1988, Tarkian 1987, Cabri 1981 and Constantinides et al. 1980). It exceeds the compositional ranges reported e.g. by Legendre & Auge (1986), Talkington & Watkinson (1986), Auge (1985), Tarkian & Prichard (1987) and Thalhammer & Stumpfl (1988) somewhat towards the Os end member.

SULPHARSENIDES

Sulpharsenides of Os, Ir, Ru, Rh and Pt occur in grains nr. 1, 3, 4, 6 and 11 (Table 3). The sulpharsenides occur exclusively in secondary grains, never as inclusions in unaltered chromite. Both osarsite (?), irarsite, hollingworthite and platarsite were detected (analyses 13 - 26 in Table 2) all of them showing intermediate compositions. Pure end-member composition seems to be rare. Together the analyses show extensive solid solution (SS) between several of PGE present in the sulpharsenides. The atomic proportions of the elements are plotted in the ternary systems IrAsS - RhAsS - PtAsS (Fig. 4B) and RuAsS - RhAsS - PtAsS (Fig. 4D). In addition the triangular (Os + Ir)AsS - RuAsS - PtAsS diagram (Fig. 4C) is used to demonstrate SS within Rh-poor and Rh-free members. The ternary system IrAsS - RhAsS - PtAsS (Fig. 4B) shows extensive SS between Ir and Rh by plotting Ru-Pt poor and Rh-enriched irarsites and a wide range of compositions plotting within the hollingworthite field. This extensive Ir - Rh SS is consistent with results recently obtained by e.g. Tarkian & Prichard (1987) and Thalhammer & Stumpfl (1988).

In the present case the RuAsS - RhAsS - PtAsS diagram (Fig. 4D) does not give satsifactorily discriminating information. This diagram is usually based on including Ir-content with Pt and minor Os-content with Ru (Tarkian 1987). The present hollingworthites (anal. 19-23) which are both Ir- and Pt-bearing and in 3 out of 5 instances are richer in Ir than Pt are therefore spread from the Rh-corner towards the platarsite-field and even into this field (analysis 19).

There is definitely no SS between hollingworthite (anal. 19-23) and Rh-poor/Rh-free and Ru-Os-Ir-enriched platarsite (anal. 24-26) in Fig. 4D. Two of these platarsites (anal. 24 and 25) closely resemble the platarsite (?) reported by Thalhammer & Stumpfl (1988) in their analyses nr. (8).

The zoning irarsite (inner phase) - hollingworthite is found in complex sulpharsenides from several places e.g. Häkli et al. (1976) from Hitura, Finland, Tarkian & Prichard (1987) and Thalhammer & Stumpfl (1988). A further zoning hollingworthite - Pt rich hollingworthite/Rh-rich platarsite is found in the present study, and a RhAsS - PtAsS SS is indicated by Thalhammer & Stumpfl (1988) based on their analyses. This Ir-Rh-Pt zoning and SS will not be reflected in the Ru-Rh-Pt diagram as it is normally used. The problem with discriminating between PGE-sulpharsenides in the Ru-Rh-Pt diagram in the present study can be compensated for by use of a (Os+Ir) - Ru - Pt diagram (Fig. 4C). This diagram shows that there is a SS between the mentioned Ru-Os-Ir enriched Rh-poor/Rh-free platarsites (anal. 24-26) on the one hand and Os-Pt-Ru-enriched and Rh-poor/Rh-free irarsites (anal. 15-17) and even a Pt-Ru-Ir-enriched osarsite (anal. 13) on the other hand. At the same time this diagram shows the Ru-content which is considerable in most of the analyses (except the ones closest to the (Os+Ir)-corner).

This (Os+Ir) - Pt solid solution between Rh-poor/Rh-free sulpharsenides

is clearly distinct from the Ir - Rh - Pt solid-solution series. Ir-Rh SS is well established by the work of Prichard & Tarkian (1987) and a further Rh-Pt SS is proposed by Thalhammer & Stumpfl (1988). Even the irarsites can be divided in two compositionally distinct groups belonging to two SS series: the one enriched in Os-Pt-Ru (anal. 15-17) and the other enriched in Rh (anal. 14 and 18). Towards the Ir- or (Ir+Os)-corner these two groups of course overlap with each other (anal. 18).

Osarsite (?). One of the analyses performed inside the area marked as platarsite in Fig. 6 (analysis 13 in Table 2) proved to be unusually rich in Os (at % Os > at % Pt). Further, the contents of Ir, Ru and Rh are less than those of Os and Pt. Together this gives a somewhat hybrid intermediate osarsite composition, far from the composition of normal Pt-free osarsites reported e.g. by Auge (1985) and Cabri (1981) Table 8.48.

Due to the poor stoichiometry with considerable S excess in analysis 13, it is natural to assume that S-radiation from the neighbouring Os-laurite and/or erlichmanite has contributed to the S-content in the analysis and thereby disturbed the stoichiometry severely. From this it follows that the Os-content in analysis 13 then seems to be somewhat doubtful. However Os is definitely enriched at the analysis spot and in the platarsite area around the spot (Fig. 6). Platarsite is further enriched in Os compared with neighbouring irarsite in grain no. 3, though rather irregularly.

Other analyses of sulpharsenides in Table 2 show As excess relative to S. These are in sulpharsenide not bordering more As-rich phases such as sperrylite but the same sulphides, etc. as in the case of analysis 13. Analysis 26 in Table 2 e.g. which is also from platarsite in grain no. 3 shows a considerable As excess. This may indicate a certain amount of solid

solution between As and S in the sulpharsenides present. The high Os-content in analysis 13 should therefore not be discounted in spite of the poor stoichiometry.

Irarsite is the most common sulpharsenide and is reported from a variety of locations (see e.g. Cabri 1981). Irarsite is also the most common sulpharsenide in the present study, occurring in five PGM grains/ grain-aggregates. A compositional division of irarsites into two different solid solution series as described in the present study is not emphasized in the literature with the exception of the work of Chang et al. (1973) from China [paper in Chinese but several analyses of different sulpharsenides are presented]. They report (page 79 and 81) both a Rh-free Ru-rich irarsite, and a Rh-enriched Ru-free variety. Both varieties are however Os- and Pt-poor/free. The ten irarsites quoted by Cabri (1981, Table 8.55) do not support a Rh/Ru-Pt-Os division with perhaps the exception of two analyses (3(i) and 3(ii)) from Driekop, Transvaal quoted by Tarkian & Stumpfl (1975). Auge (1985) in his Table 1 presents Rh-poor irarsites somewhat enriched in Os and Ru but not in Pt. Perhaps the strongest support for a Rh/Ru-Pt-Os division of irarsites can be drawn from the works of Tarkian & Prichard (1987) and Harris (1974). Tarkian & Prichard's irarsite analyses are without exception Rh-enriched and free of, or almost free of Ru, Pt and Os. The eleven irarsite analyses presented by Harris in his Table 2, contrast strongly to these. Harris's analyses are tabulated with Ir content decreasing from 60.3 to 40.9 wt %. The corresponding Ru and Pt values increase from 0.4 to 7.4 wt % and from 3.0 to 10.7 wt % respectively. Rh however shows only a slight increase in corresponding values from 0.1 to 3.1 wt %. Os is low in all these analyses. From the analyses Harris emphasizes the negative correlation between Ir and (Ru + Pt).

Hollingworthite was detected in only one grain (no. 1) in the present study. Fig. 5 shows that the (bulk) sulpharsenides constitute the second outermost phase in the complexly zoned PGM-aggregate. The sulpharsenides are themselves zoned in the succession irarsite (innermost) - hollingworthite - Pt-rich hollingworthite/Rh-rich platarsite (see X-ray intensities of Ir, Rh, Pt and As in the lower right tongue in Fig. 5). Furthermore through each portion of this tongue the chemical composition gradually changes.

This is exemplified by the compositional change through the middle (hollingworthite) portion of the tongue: analysis 20 (innermost) - 21 - 19, see Fig. 4B. Analysis 22 is from the central part of the hollingworthite area, but not directly comparable with the other analyses (from two different batches of analyses). Analysis 23 is from a small patch outside the main aggregate. The line connecting analysis 20 - 21 - 19 in Fig. 4B indicates a continuation towards the area around the irarsite - hollingworthite - platarsite triple junction. The zoning described here has clearly occurred in a secondary (hydrothermal) environment in metamorphic cracks radiating away from the main part of the grain-aggregate (see photomicrograph in Fig. 5).

On the basis of data from various deposits Tarkian (1987) reports that there are apparently two varieties of hollingworthite: one with Ru > Ir at % and the other with Ir > Ru at %. The present five analyses indicate broadly that these belong to the group with Ir > Ru at %.

Hollingworthite has been reported from several locations. Tarkian (1987) has given a synthesis of reported analyses by plotting them in the ternary Ir - Rh - Pt and Ru - Rh - Pt diagrams. In addition Thalhammer & Stumpfl (1988) present hollingworthite analyses from the Hochgrössen massif in Styria, Austria, and Auge (1988) has detected the mineral in chromite in dunite from Tiebaghi, New Caledonia.

Platarsite is probably the least abundant PGE-sulpharsenide. It is reported from the Bushveld Complex in the Driekop (Stumpfl 1972, Tarkian & Stumpfl 1975) and Onverwacht (Cabri et al. 1977) dunite pipes and from the Merensky reef (Kingston & El Dosuky 1982, Tarkian 1987). Recently Thalhammer & Stumpfl (1988) have reported a Ru-rich Pt arsenide similar to the platarsite reported by Cabri et al. Further Chang et al. (1973, page 85) have reported an analysis of a Pt-rich sulpharsenide from N.W. China that plots in the platarsite compositional field close to the triple junction in the IrAsS - RhAsS - PtAsS triangular diagram.

In the present study Pt-rich sulpharsenides are encountered in grains no. 1, 3 and 6. In grain no. 1 Pt-enriched sulpharsenide occurs in the outer part of the lower right tongue in Fig. 5 (partly discussed above under hollingworthite). Unfortunately this part of the grain was lost during clearing of the polished section. From comparison of the X-ray images in Fig. 5 and the hollingworthite analyses (no. 19 - 23 in Table 2 and Fig. 4B) the Pt-rich area can only be described safely as Pt-rich hollingworthite or Rh-rich platarsite, probably plotting close to the triple junction in Fig. 4B as indicated above. The composition would then resemble the one reported by Chang et al. (1973) from China and intermediate compositions plotted in the Ir-Rh-Pt diagram in Thalhammer & Stumpfl (1988).

In grain no. 3, Fig. 6, the sulpharsenide is zoned in parallel stripes of irarsite and platarsite, the latter also here as an outer (latest) phase. This platarsite (analyses 24-26 in Table 2 and Fig. 4C and 4D) differs markedly in composition from the Pt-Rh-rich sulpharsenide in grain no. 1. Analyses 24-26 show a Rh-poor to Rh-free but Os-Ir-Ru enriched platarsite corresponding to the Rh-poor or Rh-free but Os-Pt-Ru enriched irarsites

just described (anal. 15 - 17 and Fig. 4C). These platarsite analyses closely resemble analysis no. (8) in Thalhammer & Stumpfl (1988) and to some extent the analyses from the Merensky reef (Kingston & El Dosuky 1982, Tarkian 1987), but they do not resemble the platarsite-analyses from the Driekop (Stumpfl 1972, Tarkian & Stumpfl 1975) and Onverwacht (Cabri et al. 1977) dunite pipes which show both Ru- and Rh-enrichment.

Pt-ARSENIDE (SPERRYLITE)

Sperrylite ($PtAs_2$) has been found at three locations in one polished section, see Table 3. In all three cases the mineral is part of complex anhedral secondary grains. Two quantitative sperrylite analyses are listed in Table 2 (analyses 27 and 28). In addition to Pt small amounts of other PGE appear in these analyses, probably mostly due to radiation from neighbouring PGM-phases. In analysis 28 there seem to be clear Ru and S contributions from the adjoining Os-free laurite (Fig. 7B and analysis 2).

The sperrylite in grain no. 6 (analysis 27) is also intergrown with other PGMs, see Fig. 8, and the Os, Ir, Ru and S-values are mainly caused by contributions from these phases (compare the X-ray images). The Sb value in this analysis which is in agreement with Sb-values reported by Prichard et al (1987) in sperrylite from Cliff, Shetland, is noteworthy. The sperrylite in grain no. 4, Fig. 7A, , occupies an area considered too little for a meaningful quantitative analysis.

Prichard et al. (op.cit.) have also reported small amounts of Fe (max 0.46 wt%) in their sperrylite-analyses. In the present study however, Fe is omitted in the corrected and recalculated analysis due to the Fe and Cr contamination from the enclosing chromite grains which consist of both Cr-rich chromite and Fe-rich ferrite-chromite (see raw analyses in Table 2).

ALLOYS AND NATIVE Os

Alloys of Os and Ir occur as exsolution lamellae of iridosmine (Os, Ir) in grains no. 1 (Fig. 5) and no. 4 (Fig. 7A) and as a primary, single-phase subhedral inclusion of osmiridium (Ir, Os) (grain no. 13, Table 3 and Fig. 7C). The iridosmine lamellae have very high reflectance (Tarkian & Bernhard 1984) and therefore contrast sharply in the reflected-light microscope with the enclosing irarsite, erlichmanite, IrSbS and (Ir, Pt, Pb)S_2 which have clearly lower reflectance (Tarkian & Bernhard, op cit; in the case of irarsite and erlichmanite and Tarkian & Prichard 1987 in the case of IrSbS). These lamellae also stand out clearly on back-scattered electron images (BEI) due to the alloy's high average atomic mass (60-70 wt % Os) compared with PGE-sulphides and -sulpharsenides with markedly lower average atomic mass, see Fig. 5 and Fig. 7A. Two quantitative analyses, one of iridosmine and one of osmiridium are listed in Table 2 (analysis 29 and 30) and plotted in the triangular Ru-Os-Ir-diagram of Harris and Cabri (1973), see Fig. 4E. Analysis 29, performed on an Os-Ir-lamella in grain no. 1 (Fig. 5) shows a relatively limited contribution from the adjoining phases. Analysis 30, performed on the single-phase grain, contains minor amounts of Ru, Rh, Pt and Pd. The relatively high Pt content, 8.57 wt %, resembles that in an analysis reported by Legendre (1982), p. 25, from Güleman, Eastern Turkey with 10,08 wt % Pt, and far exceeds the Pt-values reported by Augé (1985), p. 166 and 168, who points out the Pt-enrichment in his osmiridium analyses (max. 2.5 wt % Pt).

Grain no. 10 in Table 3 is also a primary, single-phase subhedral inclusion in chromite, Fig. 7D. The quantitative analysis, no. 31 in Table 2, gives a very special composition, Pt_2 (Ir, Os) $Fe_{0,65}$ which resembles

most closely the unnamed PGM, Pt_2Ir Fe reported by Chang et al. (1973) from N.W. China (UN 1973-2 in Cabri, 1981). The Fe-content of the recalculated analysis (Table 2) was based on microprobe-analyses of the host chromite. Iron was subtracted in an amount making the same Cr/Fe-ratio as for the host, chromite grains. The average of eight analyses of fresh, unaltered chromite gave the following composition: MgO 12.95 wt %, Al_2O_3 9.29 %, Cr_2O_3 61.38 % and $FeO_{tot.}$ 16.70 %.

The only native metal phase observed is Os which appears as small, irregular patches, max 0.8 µm large, disseminated in the 70 µm large no. 3 grain aggregate, both in the Ru-Os sulphide phase and in the Ir-Pt sulpharsenide phase, see Fig. 6 and 7E. The occurrence of native Os resembles precisely that reported by Tarkian and Prichard (1987) and Prichard et al. (1987) from Harold's Grave, Shetland. In addition Prichard et al. (op.cit.) report dissemination of native Os in NiSb which is intergrown with RuS_2 and IrAsS. NiSb has not been found in the present study. The largest patch of native Os in grain no. 3 (Fig. 7E) was the target for a quantitative analysis (no. 32 in Table 2), but it was impossible to prevent a very significant amount of Os, Ru and S from the host Os-rich laurite, and somewhat smaller amounts of Ir, Pt and As from the closely adjoining platarsite, as contributions to the more or less pure Os-phase. For this reason "true" Ir and/or Ru in the analysis cannot be serparated from the "false" contributions, and the analysis can therefore not be plotted in the Ru - Os - Ir - diagram in Fig. 4E. For the same reason the analysis is not recalculated to 100 wt % by eliminating the obvious errors from the sulphide and sulpharsenide (in the case of analysis no. 34 such a recalculation is done presuming a "pure" Pd-Sb-phase, with only a little Pb added, see next section).

Several of the Os-analyses reported in Cabri (1981) table 8.51, from six localities around the world have some Ir, up to 11 wt %, and minor Ru, Pt, Pd and Rh in their totals.

Tarkian and Prichard (op. cit.) point to primary crystallization of native Os and to an exsolution texture as two possible modes of origin of the dispersed blebs of native Os. If native Os is exsolved from Os-rich laurite it would leave an Os-depleted (Os-poor) laurite the phase in which they have observed blebs of native Os. They argue further that if, e.g. arsenic is present this can cause exsolution of native Os from Os-rich laurites. In the present study (grain no. 3) Os-rich laurite contains dispersed blebs of native Os. Erlichmanite and the sulpharsenides may also contain inclusions of native Os, but this was not clearly ascertained from the back-scattered images made. The only phase that definitely does not contain native Os blebs in grain no. 3 is the outermost, latest crystallized, Os-free laurite. The sulpharsenides therefore have probably reacted with their intergrown Os-bearing phases and caused the formation of native Os blebs before Os-free laurite nucleated as a latest, outermost phase at a stage when Os-availability had decreased dramatically.
As with the case in Shetland the totally chromite-engulfed (primary) inclusions of Os-rich laurite show no blebs of native Os, neither does Os-free laurite belonging to the same type of inclusion. It is therefore most likely that the blebs of native Os are formed in a reaction between sulpharsenides and Os-rich laurite as also suggested by Tarkian and Prichard, and that the blebs therefore represent an exolution texture.

Pd-ANTIMONIDE

A minute patch of a Pd-Sb-rich phase was located in grain no. 6, Fig. 8. A quantitative EDS-estimate was first performed giving ca. 45 wt % Pd and ca. 15 % Sb (analysis 33 in Table 2). Thereafter a quantitative WDS-analysis was carried out (analysis 34) giving a total of only about 54 wt%. The Pd/Sb-ratio was however roughly similar to the first analysis. Much Cr and Fe from adjoining chromite and Ni and S from pentlandite and heazlewoodite appear in the total. Further, minor Os, Ir, Pt and As from the other PGMs in grain no. 6 occur in the total too. This suggests that Pd and Sb are the main components of the phase (see X-ray images). According to Cabri (1981), Table 8.34 and Tarkian & Prichard (1987) Table 11, small amounts of Cu and/or Te may also be present in similar Pd-Sb minerals, but these elements were not analyzed in this case. These authors further report minor Pt and/or As in their analyses, but the X-ray images show that neither of these elements are enriched in the actual tiny patch. Otherwise the corrected and recalculated analysis 34 does not fit quite well with the stibiopalladinites/mertieites reported by the authors cited (some Pd-excess in anal. 34) possibly due to the very low total.

Ir-Rh SULPHANTIMONIDE

In grain no. 1 a zoned Ir-Rh sulphantimonide was detected. An outer phase (Ir, Rh)SbS coincides with the distribution of overlapping areas of Sb and Rh (see X-ray images of these elements in Fig. 5) whereas the inner phase, IrSbS, coincides with the Sb-bearing but Rh-free areas. Quantitative analyses of IrSbS and (Ir, Rh)SbS are listed in Table 2 (analysis 35 and

36). Analysis 36 closely resembles analysis UN 1976-11 (Cabri 1981; p. 190), where the sulphantimonide appears as inclusions in Pt-Fe alloy grains. Ir-Sb-S and Rh-Sb-S, both rather pure, are recently reported in two small neighbouring grains within a large composite PGM-inclusion in chromite from Cliff, Shetland (Prichard et al. 1987, Tarkian & Prichard 1987). Those phases have only been analysed qualitatively, but optical properties are given.

Ir-Pt-Pb SULPHIDE

In the central part of grain no. 1, Fig. 5, a sulphide of Ir-Pt-Pb occurs. The areal extent of this sulphide coincides with the area of Pb- and Pt-enrichment in the central part of the X-ray images of these elements. The chemical composition of the sulphide, analysis 38 in Table 2, leads to the structural formula (Ir, Pt, Pb)S_2 or more precisely $(Ir_{0,64}\ Pt_{0,22}\ Pb_{0,18})_{1,04}\ S_{1,95}$. This composition has not been reported earlier, but it bears some compositional and structural similarities e.g. to malanite (Cu, Pt, Ir)S_2 which is reported from China (Peng et al. 1978).

Discussion

PGM-ASSEMBLAGE AND PGE-LEVEL: COMPARISON WITH OTHER OPHIOLITE-HOSTED CHROMITITES

The number and diversity of PGM-phases so far determined from only one hand-size sample representing the Osthammeren chromitites is notable (see Table 3). However the total of PGE in a follow-up analysis of the anomalous

sample was shown to be only 2.1 ppm. A further twelve PGE analyses of new chromitite samples from the same claim and from other claims in the Osthammeren body averaged only 1.5 ppm total PGE. The average of ten samples from the host serpentinite showed only 40 ppb total PGE (Table 4). By comparison, PGM-rich samples from the Cliff chromitite occurrence in Shetland are generally much richer in total PGE (an order of magnitude or more), and samples with as much as 80 ppm PGE are recorded (Prichard et al. 1987, Table 15). However, compared with other ophiolitic chromitites which also show some diversity in PGMs the Osthammeren sample is not strikingly low in PGE content. From Harold's Grave, Shetland, which shows the same diversity in PGMs as the high-grade Cliff chromitites (Prichard et al. 1986, 1987) PGE values of 7.7 and 1.3 ppm have been reported. This chromitite occurrence also bears strong similarities in PGM-assemblage (laurite, irarsite, native osmium, Pt-arsenide, Pd-antimonide and Rh-Ni antimonide) to the Osthammeren sample. From the Tiebaghi and Massif du Sud ophiolites in New Caledonia, Legendre (1982) and Legendre & Auge (1986) report four PGMs in chromitites from each complex and PGE-contents in the range ca. 0.4 - 0.9 ppm (3 analyses, table 15 in Legendre 1982). Legendre (op. cit.) further reports three PGMs and two PGE-values, ca. 0,3 and 0.5 ppm from the Al-Ays ophiolite complex in Saudi-Arabia. Auge (1988) describes six PGMs in chromitite and five in chromite grains in dunite from Tiebaghi, but no PGE-values. The present comparison suffers however somewhat because there are no PGE-data available from the PGM-rich locality reported from N.W. China (Chang et al. 1973) which bears strong similarities in PGM-association to the Osthammeren sample. This is also the case with regard to the recently reported PGM-rich chromitite occurrences in the Hochgrössen massif, Austria (Thalhammer & Stumpfl 1988).

No PGE-analyses have been found in the literature from the PGM-rich

Aetorache deposit in the Vourinos complex of Greece (Augé 1985) which bears some similarities in PGM-association to the Osthammeren sample (with the exception of e.g. the Pt- and Pd-bearing phases in the latter).

A PGE-analysis from Skyros, Greece (Economou 1986, p. 446-447) resembles the chromitite analysis in Table 4 with regard both to level and trend (Fig. 9), but there are no data on PGMs from Skyros. The same is the case with some of the PGE-analyses of chromitite from the Ray-Iz complex, Polar Urals (Khvostova et al. 1976).

It may be concluded that the chromitite occurrences from the Hochgrössen massif, Austria, the Harold's Grave chromitite occurrence in the Shetland ophiolite complex and the chromitite deposit in N.W. China are the ones that resemble most closely the chromitite sample treated in this study. The PGM-assemblage of these chromitites are compared with the Osthammeren assemblage in Table 5. Analysis "G" in Prichard et al. (1986, p. 409) from Harold's Grave also resembles the two analyses of the PGM-anomalous Osthammeren sample (sample 138/2), compare Table 4 and Fig. 9. The Pt-content in the Osthammeren sample is however, at least three times higher than in analysis "G", and causes appearance of sperrylite and/or platarsite in 5 of the 15 investigated grains. Sperrylite is very rare at Harold's Grave and platarsite is not reported (Prichard et al. 1986, p. 404). The abundant laurite - irarsite (plus eventual native Os) assemblage at Harold's Grave is however also found in five of the Osthammeren PGM-grains.

PARAGENESIS

The distinctly bimodal occurrence of the PGM inclusions in the Osthammeren chromitite is striking: 1) The primary, magmatic, small (<5 - 20 µm), euhedral - subhedral, mainly single-phase inclusions of laurite, Os-laurite, osmiridium and $Pt_2(Ir, Os)Fe_{0,65}$ associated with or without silicate inclusions enclosed in chromite grains. 2) The secondary anhedral - (subhedral), often very complex grains or grain-aggregates with varying size (<5 - 70 µm) and composed of up to eight PGM-phases plus Ni-sulphides and/or Ni-arsenide.

Primary inclusions

The first group is considered to be magmatic, or "magmatic - hydrothermal", in origin for several reasons. Firstly the PGM-inclusions are always totally enclosed within the chromite grains, either in the central part of these or closer to the rims. The inclusions are never situated in ferritechromite-altered parts of the chromite grains nor associated with cataclastic cracks through these. There are no systematic differences, in composition or otherwise, between PGM-inclusions within the central parts of chromite grains and those situated closer to the rim of the chromite grains. Such differences are reported from Shetland by Prichard et al. (1987). Both Os-free, Os-poor and Os-enriched laurites belong to this group of inclusions. In one grain (no. 2) Os-free laurite hosts patches of Os-enriched laurite. The PGM-inclusions in this group are often euhedral indicating that the PGMs have crystallized before they were entrapped within the chromite grains. The association of two of the PGM-inclusions (grain no. 9 and 12) with inclusions of phlogopite and Na-

bearing hornblende respectively (anhedral droplets) is notable. It indicates that the formation of this group of PGM-inclusions may have an association with hydrous silicates, i.e. that the PGMs may have nucleated in the presence of, or in contact with, volatile-bearing silicates. The significance of volatiles in the formation of PGMs in layered intrusions has been widely demonstrated e.g. by the works of Stumpfl and coworkers (e.g. Stumpfl & Tarkian 1976, Ballhaus & Stumpfl 1986 and Stumpfl 1986). Recently McElduff and Stumpfl (1987) and Stumpfl (1987) have also described the association of PGM-inclusions with hydrous, and frequently sodic, inclusions in chromite from Hji Pavlou chromitite mine, Troodos ophiolite, Cyprus and from other ophiolite complexes. The association of PGM- and silicate-inclusions in ophiolitic chromitites is further treated in detail by e.g. Talkington et al. (1984, 1986) from several Canadian and other complexes and by Stockman & Hlava (1984) from Oregon.

From several ophiolite complexes alloys of Ru - Os - Ir are reported as primary magmatic phases occurring either alone or coexisting with sulphides (laurite) in the form of euhedral-subhedral inclusions (Augé 1985, Legendre & Auge 1986). In the present study osmiridium (Ir, Os) occurs as a primary inclusion (in one instance only), while iridosmine (Os, Ir) is only found as exsolution lamellae in the core-region of two secondary and complex grains, see Fig. 5 and 7. The occurrence of a Pt-rich alloy with the composition $Pt_2(Ir, Os)Fe_{0,65}$ as a primary magmatic inclusion shows that Pt has been available early in the formation of the PGMs. Usually Pt (and Rh and Pd) are more strongly fractionated and available so late that they appear only in PGMs situated in the altered rim of chromite grains or in the altered silicate gangue interstitial to the chromite grains, if present at all.

Secondary inclusions

The secondary PGM-inclusions are considered to have a hydrothermal origin, generated during the serpentinization of the host ultramafic tectonite. There is clear evidence for this in the fact that these grains or grain-aggregates are, without exception, situated within or associated with (in contact with) cataclastic cracks in the chromite grains, i.e. cracks generated during regional metamorphism. The finest fissures are generally visible only as thin strings of ferritechromite. This means that ferrite-chromite has developed from chromite and tightened these very fine fissures. Somewhat wider cracks cutting into or through the chromite grains are usually filled with serpentine and/or chlorite. The chromite is normally altered to ferrite-chromite, which appears as narrow rims along these cracks.

The inclusions of this group contain from one to eight PGM-phases plus Ni-phases (Table 3). They are anhedral or weakly subhedral in a few cases (i.e. grain no. 8). They may be concentrically zoned (grain 1 and 3), show exsolution lamellae of Os - Ir alloy (grain 1 and 4), or show more irregular (cluster) development with a weaker tendency to zonal arrangement of the PGMs (grain 6 and 7). Grains no. 1 and 3 are perhaps the best representatives of this group of inclusions. In grain no. 1 (Fig. 5) a core of (Ir, Pt, Pb)S_2 crystallized simultaneously with the formation of exsolution-lamellae of iridosmine (Os, Ir) along a few structurally preferred directions. Surrounding the sulphide erlichmanite (OsS_2) and IrSbS crystallized, with some overlap. In the upper part of the grain OsS_2 crystallized before IrSbS whereas the opposite was the case in the lower part of the grain. In both phases exsolution of Os,Ir-lamellae still continued. At a certain line, which makes up the shape of a six-sided crystal

(se Os- and Rh- X-ray images) Os is exhausted and Rh starts to be available in the outer phases. The IrSbS is changed to (Ir, Rh)SbS. Thereafter As becomes available and a zoned sulpharsenide crystallizes in the succession irarsite-hollingworthite - Pt-rich hollingworthite / Rh-rich platarsite (lower right tongue on Fig. 5). As an outermost phase Os-free laurite crystallized. The crystallization of the two outermost phases took place even in the ferrite-chromite-filled fissures radiating from the main part of the grain as small patches (Fig. 5).

In the case of grain no. 3 (Fig. 6) the sulpharsenide and sulphide phases which occur side by side, are developed independently in solid solution series of laurite-erlichmanite and Rh-poor/free irarsite-platarsite. Both Os-poor and Os-rich laurite occur in irregular patches, the latter rimmed by erlichmanite, and the Os-poor laurite by a more Os-rich intermediate member. Irarsite and platarsite are arranged in irregular stripes, but here too, platarsite occurs as an outer phase as in the case of grain no. 1. An outermost phase of Os-free laurite rims both the sulpharsenides and the Os-laurite - erlichmanite. Small patches or droplets of exsolved native Os occur scattered within the Os-enriched laurite.

In grain no. 6 the supposed inner phases Os-laurite and irarsite are rimmed by Os-free laurite and platarsite followed by sperrylite (Fig. 8). Pentlandite and heazlewoodite then surround the complex PGM-aggregate, and a droplet of Pd-antimonide crystallized independantly of the other PGM-phases.

In grain no. 4 (Fig. 7A) exolution lamellae of iridosmine are hosted by irarsite which neighbours Os-laurite. A small patch of sperrylite makes up an outermost phase.

Conclusions

Chromitite hosted PGMs from the Osthammeren ultramafic tectonite (serpentinite) body occur in two distinctly different ways:

1. Os, Ir, Ru and minor Pt occur in primary magmatic, euhedral-subhedral, small (<5 - 20 µm), mainly single-phase inclusions of Os-free laurite, Os-laurite, osmiridium and Pt_2 (Ir, Os)$Fe_{0,65}$. They are totally enclosed in fresh unaltered chromite. Two PGM-inclusions were however found associated with small blebs of Na-bearing hornblende or phlogopite. This means that the presence of volatiles in an early stage may have influenced the formation of these PGMs.

2. Purely secondary PGMs occur as anhedral - (subhedral), texturally often very complex grains or grain-aggregates with varying size (5 - 70 µm) and consisting of from one to eight PGM-phases plus Ni-sulphide and Ni-arsenide. These PGMs always occur within, or in contact with, late formed cataclastic (metamorphic) cracks or very fine fissures, in the primary magmatic chromite grains. The finer fissures are generally tightened by ferrite-chromite, a hydrothermal alteration-product of chromite. The wider cracks are usually serpentine- and chlorite-filled and are rimmed by ferrite-chromite against the chromite. Os, Ir, Ru, Rh, Pt and minor Pd are represented in grains of this group, and the secondary PGM-association found consists of Os-free laurite, Os-laurite, erlichmanite, Ir-rich erlichmanite, native Os, iridosmine (in lamellae), (?) osarsite, irarsite, hollingworthite, Pt-rich hollingworthite/ Rh-rich platarsite, Ru-rich platarsite, sperrylite, (Ir, Rh)SbS, IrSbS, (Ir, Pt, Pb)S_2 (new?), Pd-antimonide (probably stibiopalladinite) plus the associated phases pentlandite, heazlewoodite and niccolite.

From the literature it seems that there are few examples where primary magmatic or "magmatic-hydrothermal" PGM-inclusions on the one hand, and secondary, hydrothermal, late stage PGMs on the other, appear side by side and show such distinct differences in occurrence as in the present case.

ACKNOWLEDGEMENTS

S.-J. Barnes and R. Boyd took the initiative to have the chromitite samples analyzed for PGE. R. Boyd further critically read drafts of the manuscript, suggested many improvements and corrected the language. T. Boassen (IKU) assisted in performing the SEM- and microprobe analyses, A. Hemming drew the figures, I. Aamo made the photographic plates, T. Jacobsen made polished sections and G. Sandvik typed the manuscript. To all these persons I offer my sincere thanks. The project has been supported by the Royal Norwegian Council for Scientific and Industrial Research (NTNF).

References

Askvik, H. & Rokoengen, K. (1985): Geologisk kart over Norge, berggrunnskart KRISTIANSUND - M 1:250 000, Nor. geol. unders.

Augé, T. (1985): Platinum-group-mineral inclusions in ophiolitic chromitite from the Vourinos Complex, Greece. Canadian Mineralogist 23, 163-171.

Augé, T. (1988): Platinum-group minerals in the Tiebaghi and Vuorinos ophiolitic complexes: genetic implications. Canadian Mineralogist 26, 177 - 192.

Barnes, S.-J., Boyd, R., Korneliussen, A., Nilsson, L.P., Often, M., Pedersen, R.-B. & Robins, B. (1987a): Geochemistry of platinum metals in rocks and ores in Norway: Pilot project. Draft report. Norges geologiske undersøkelse, rapport 87.021, 50 pp.

Barnes, S.-J., Boyd, R., Korneliussen, A., Nilsson, L.P., Often, M., Pedersen, R.B. & Robins, B (1987b): The use of noble and base metal ratios in the interpretation of ultramafic and mafic rocks; examples from Norway. Abstract, Geo-Platinum 87 Symposium. The Open University, U.K.

Barnes, S.-J., Boyd, R., Korneliussen, A., Nilsson, L.P., Often, M., Pedersen, R.B. & Robins, B. (1988): The use of mantle normalization and metal ratios in discriminating the effects of partial melting, crystal fractionation and sulphide segregation on platinum group elements, gold, nickel and copper: examples from Norway. In: Prichard,

H.M., Potts, P.J., Bowles, J.F.W. & Cribb, S.J. (eds.) Geo-Platinum 87, Elsevier Applied Science Publishers, London, 113-143.

Begizov, V.D., Zav'yalov, E.N. & Khvostova, V.P. (1976): [The minerals of the erlichmanite-laurite and hollingworthite-irarsite series from Ural placers]. Zapiski Vsesoyuznogo Mineralogicheskogo Obschchestva 105, 213-218. [in Russian].

Bucher-Nurminen, K. (1988): Metamorphism of ultramafic rocks in the Central Scandinavian Caledonides. Nor. geol. unders. Special Publ. 3, 86-95.

Cabri, L.J. (ed.) (1981): Platinum-group elements: mineralogy, geology, Can. Inst. Min. Metall., Spec. vol. 23, 267 pp.

Cabri, L.J., Laflamme, J.H.G. & Stewart, J.M. (1977): Platinum-group minerals from Onverwacht. II Platarsite, a new sulfarsenide of platinum. Canadian Mineralogist, 15, 385-388.

Chang, P.K., Yu, C.M. and Chiang, C.U. (1973): [Mineralogy and occurrence of the platinum-group elements in a chromite deposit in northwestern China]. Geochimica 2, 76-85. [in Chinese].

Constantinides, C.C., Kingston, G.A. & Fisher, P.C. (1980): The occurrence of platinum group minerals in the chromitites of the Kokkinorotsos chrome mine, Cyprus. In: Panayiotou, A. (ed.) Proceedings of the International Ophiolite Symposium Cyprus. Ministry of Agriculture and Natural Resources, Geological Survey Department, Cyprus, 93-101.

Economou, M.I. (1986): Platinum-group elements (PGE) in chromite and sulphide ore within the ultramafic zone of some Greek ophiolite complexes. In: Gallagher, M.J., Ixer, R.A., Neary, C.R. & Prichard, H.M. (eds.) Metallogeny of basic and ultrabasic rocks. IMM, London, 441-453.

Engzelius, J.G. (1940): En undersøkelse av Feragen kromittfelt med særlig vekt på Skargruben. Unpublished siv. ing. thesis, Tech. Univ. Norway, Trondheim, 102 pp.

Falck-Muus, R. (1957): Krommalmforekomstene øst for Røros. Tidsskr. f. Kjemi, Bergvesen og Metallurgi, No. 5, 6, 7 and 8.

Gee, D.G., Guezou, J.-C., Roberts, D. & Wolff, F.C. (1985a): The central-southern part of the Scandinavian Caledonides. In: Gee, D.G. & Sturt, B.A. (eds.), The Caledonide Orogen: Scandinavia and Related Areas. John Wiley and Sons, New York, 109-133.

Gee, D.G., Kumpulainen, R., Roberts, D., Stephens, M., Thon, A. & Zachrisson, E. (1985b): Scandinavian Caledonides: Tectonostratigraphic Map, 1:2 mill. Sveriges geol. unders., serie Ba 35.

Goldschmidt, V.M. & Peters, C. (1932): Zur Geochemie der Edelmetalle. Nachr. Akad. Wiss. Göttingen, Math.-Phys. Kl. IV, 377-401.

Guezou, J.C (1981): RØROS, 1:250 000, preliminary bedrock map. Nor. geol. unders.

Gunn, A.G. (1989): Drainage and overburden geochemistry in exploration for platinum-group element mineralization in the Unst ophiolite, Shetland, U.K. Journ. of Geochem. Explor., 31, 209-236.

Häkli, T.A., Hänninen, E., Vuorelainen, Y. & Papunen, H. (1976): Platinum-group minerals in the Hitura nickel deposit, Finland. Econ. Geol. 71, 1206-1213.

Harris, D.C. (1974): Ruthenarsenite and iridarsenite, two new minerals from the Territory of Papua and New Guinea and associated irarsite, laurite and cubic iron-bearing platinum. Canadian Mineralogist 12, 280-284.

Harris, D.G. & Cabri, L.J. (1973): The nomenclature of the natural alloys of osmium, iridium and ruthenium based on new compositional data of alloys from world-wide occurrences. Canadian Mineralogist 12, 104-112.

Khvostova, V.P., Golvnya, S.V., Chernysheva, N.V. & Bukhanova, A.I. (1976): Distribution of the platinum group metals in chromite ores and ultramafic rocks of the Ray-Iz massif (Polar Urals). Geochem. Int. 13, 35-39.

Kingston, G.A. & El-Dosuky, B.T. (1982): A contribution of the platinum-group mineralogy of the Merensky Reef at the Rustenburg Platinum Mine. Econ. Geol. 77, 1367-1384.

Krill, A. (1986): Eidsvoll quarry, Oppdal, South Norway: a one-outcrop model for some aspects of Trollheimen-Dovrefjell tectonics. Nor. geol. unders. Bull. 404, 23-32.

Krill, A.G. & Sigmond, E.M.O. (1986): Surnadalens dekkelagfølge og dens fortsettelse mot vest. Abstract, Geolognytt 21.

Krill, A. (1987): STANGVIK, Berggrunnskart 1420-4, 1:50 000, foreløpig utgave, Nor. geol. unders.

Legendre, O. (1982): Minéralogie et Géochimie des Platinoides dans les Chromitites Ophiolitiques. Comparison avec d'autres Types de Concentrations en Platinoides. Thése de troisième cycle, Université de Paris, France, 171 pp.

Legendre, O. & Augé, T. (1986): Mineralogy of platinum-group mineral inclusions in chromitites from different ophiolite complexes. In: Gallagher, M.J., Ixer, R.A., Neary, C.R. & Prichard, H.M. (eds.) Metallogeny of basic and ultrabasic rocks. IMM, London, 361-372.

Lunde, G. (1927): Über das Vorkommen des Platins in norwegischen Gesteinen und Mineralien. Beitrag zur Geochemie der Platinmetalle. Z. anorg. u. allg. Chem. 161, 1-20.

Lunde, G. & Johnson, M. (1928): Vorkommen und Nachweis der Platinmetalle in norwegischen Gesteinen II. Z. anorg. u. allg. Chem. 172, 167-195.

McElduff, B. & Stumpfl, E.F. (1987): Platinum in the ultramafic sequence, Troodos: mineralogical and geochemical evidence. Abstract. Symposium Troodos 87 Ophiolites and oceanic lithosphere. Nicosia, Cyprus 4-10 Oct., 1987.

Moore, A.C. & Qvale, H. (1977): Three varieties of alpine type ultramafic rocks in the Norwegian Caledonides and Basal Gneiss Complex. Lithos, 10, 149-161.

Nilsen, O. & Wolff, F.C. (1988): Geologisk kart over Norge, berggrunnskart RØROS & SVEG - 1:250 000, Nor. geol. unders.

Nilsson, L.P. (1978): En malmgeologisk undersøkelse av kromittforekomstene i Feragenfeltet med henblikk på å bestemme eventuelle økonomiske produkter. Unpublished siv. ing. thesis, Tech. Univ. Norway, Trondheim, 125 pp.

Noddack, I. & Noddack, W. (1931a): Die Geochemie des Rheniums. Z. Physik. Chem. 154, 207-244.

Noddack, I. & Noddack, W. (1931b): Die Häufigkeit der Platinmetalle in der Erdrinde. Z. Physik. Chem., Bodenstein-Festband, 890-894.

Peng, Z., Chang, C. and Ximen, L. (1978): [Discussion on published articles in the research of new minerals of the platinum-group discovered in China in recent years]. Acta Geologica Sinica No. 4, 326-336. [in Chinese with English abstract].

Poulsen, A.O. (1960): Exploitation of mineral raw materials in Norway. In: Holtedahl, O. (Ed.) Geology of Norway. Nor. geol. unders. 208, 532-540.

Prichard, H.M., Neary, C.R. & Potts, P.J. (1986): Platinum group minerals in the Shetland Ophiolite. In: Gallagher, M.J., Ixer, R.A., Neary, C.R. & Prichard, H.M. (eds.) Metallogeny of basic and ultrabasic rocks. IMM, London, 395-414.

Prichard, H.M., Potts, P.J., Neary, C.R., Lord, R.A. & Ward, G.R. (1987): Development of techniques for the determination of the platinum-group elements in ultramafic rock complexes of potential economic significance: mineralogical studies. Report commissioned by the EEC Raw Materials Programme, 162 pp.

Qvale, H. & Stigh, J. (1985): Ultramfic rocks in the Scandinavian Caledonides. In: Gee, D.G. & Sturt, B.A. (eds.) The Caledonide Orogen - Scandinavia and Related Areas, Wiley, Chichester, 694-715.

Roberts, D. (1988): Grong, 1:250 000, utkast til foreløpig berggrunnskart. Nor. geol. unders.

Roberts, D. & Wolff, F.C. (1981): Tectonostratigraphic development of the Trondheim region Caledonides, Central Norway. Journ. of Struct. Geol. 3, 487-494.

Rui, I.J. (1981): BREKKEN, berggrunnsgeologisk kart 1720-II, 1:50 000. Nor. geol. unders.

Rui, I.J. (1981b): RØROS, berggrunnsgeologisk kart 1720-III, 1:50 000. Nor. geol. unders.

Siedlecka, A., Nystuen, J.P., Englund, J.O. & Hossack, J. (1987): LILLEHAMMER - berggrunnskart M 1:250 000. Nor. geol. unders.

Sigmond, E.M.O., Gustavson, M. & Roberts, D. 81984): Berggrunnskart over NORGE - M 1:1 mill., Nor. geol. unders.

Solli, A. (1989): Geology within the area of 1:250 000 map sheet NAMSOS, Central Norway, extended abstract, Geol. Fören. Stockh. Förh., 111, (in press).

Solyom, S., Andreasson, P.G. & Johansson, I. (1979): Geochemistry of amphibolites from Mt. Sylarna, Central Scandinavian Caledonides. Geol. Fören. Stockh. Förh., 101, 17-27.

Stephens, M. & Gee, D.G. (1985): A tectonic model for the evolution of the eugeoclinal terraines in the central Scandinavian Caledonides. In: Gee, D.G. & Sturt, B.A. (eds.) The Caledonide Orogen - Scandinavia and Related Areas, Wiley, Chichester, 953-978.

Stephens, M., Furnes, H., Robins, B. & Sturt, B.A. (1985): Igneous activity within the Scandinavian Caledonides. In: Gee, D.G. & Sturt, B.A. (eds.) The Caledonide Orogen - Scandinavia and Related Areas, Wiley, Chichester, 623-656.

Stigh, J. (1979): Ultramfites and Detrital Serpentinites in the Central and Southern Parts of the Caledonian Allochthon in Scandinavia, Dept. of Geol., Chalmers Univ. of Technology, Göteborg, Publ. A27, 222 pp.

Stockman, H.W. & Hlava, P.F. (1984): Platinum-group minerals in alpine chromitites from southwestern Oregon. Econ. Geol. 79, 491-508.

Stumpfl, E.F. (1972): Compositional variations in the hollingworthite-irarsite group. N. Jb. Miner. Mh., 9, 406-415.

Stumpfl, E.F. (1986): Distribution, transport and concentration of platinum group elements. In: Gallagher, M.J., Ixer, R.A., Neary, C.R. & Prichard, H.M. (eds.) Metallogeny of basic and ultrabasic rocks. IMM, London, 379-394.

Stumpfl, E.F. (1987): Platinum metallogeny: a hydrothermal process. Abstract. Symposium Troodos 87 Ophiolites and oceanic lithosphere. Nicosia, Cyprus 4 - 10 Oct., 1987.

Stumpfl, E.F. & Tarkian, M. (1976): Platinum Genesis: New Mineralogical Evidence. Econ. Geol. 71, 1451-1460.

Stumpfl, E.F. & Rucklidge, J.C. (1982): The platiniferous dunite pipes of the eastern Bushveld. Econ. Geol. 77, 1419-1431.

Talkington, R.W., Watkinson, D.H., Whittaker, P.J. & Jones, P.C. (1984): Platinum-group minerals and other solid inclusions in chromite of ophiolitic complexes: occurrence and petrological significance. TMPM 32, 285-301.

Talkington, R.W., Watkinson, D.H., Whittaker, P.J. & Jones, P.C. (1986): Platinum group element-bearing minerals and other solid inclusions in chromite of mafic and ultramafic complexes: chemical compositions and comparisons, In: Carter, B. et al. (eds.) Metallogeny of basic and ultrabasic rocks (regional presentations). Theophrastus publications S.A., Athens, 223-249.

Tarkian, M. (1987): Compositional variations and reflectance of the common platinum-group minerals. Mineralogy and Petrology 36, 169-190.

Tarkian, M. & Stumpfl, E.F. (1975): Platinum Mineralogy of the Driekorp Mine, South Africa. Mineral. Deposita 10, 71-85.

Tarkian, M. & Bernhardt, H.J. (1984): A key-diagram for the optical determination of platinum group minerals. TMPM 33, 121-129.

Tarkian, M. & Prichard, H.M. (1987): Irarsite-hollingworthite solid-solution series and other associated Ru-, Os-, Ir-, and Rh-bearing PGM's from the Shetland ophiolite complex. Mineral. Deposita 22, 178-184.

Thalhammer, O.A.R. & Stumpfl, E.F. (1988): Platinum-group minerals from Hoch grössen ultramafic massif, Styria: first reported occurrence of PGM in Austria. Trans. Inst. Min. Metall. 97, B77-B82.

Tucker, R. (1986): Geology of the Hemnefjord - Orkanger area South-central Norway. Nor. geol. unders. Bull. 404, 1-21.

Wolff, F.C. (1977): Geologisk kart over Norge, berggrunnskart ØSTERSUND 1:250 000, Nor. geol. unders.

Wolff, F.C. (1976): Geologisk kart over Norge, berggrunnskart TRONDHEIM 1:250 000, Nor. geol. unders.

Zachrisson, E. (1986): Scandinavian Caledonides - stratabound sulphide deposits, M. 1:1.5 mill. Sveriges geol. unders., serie Ba 42.

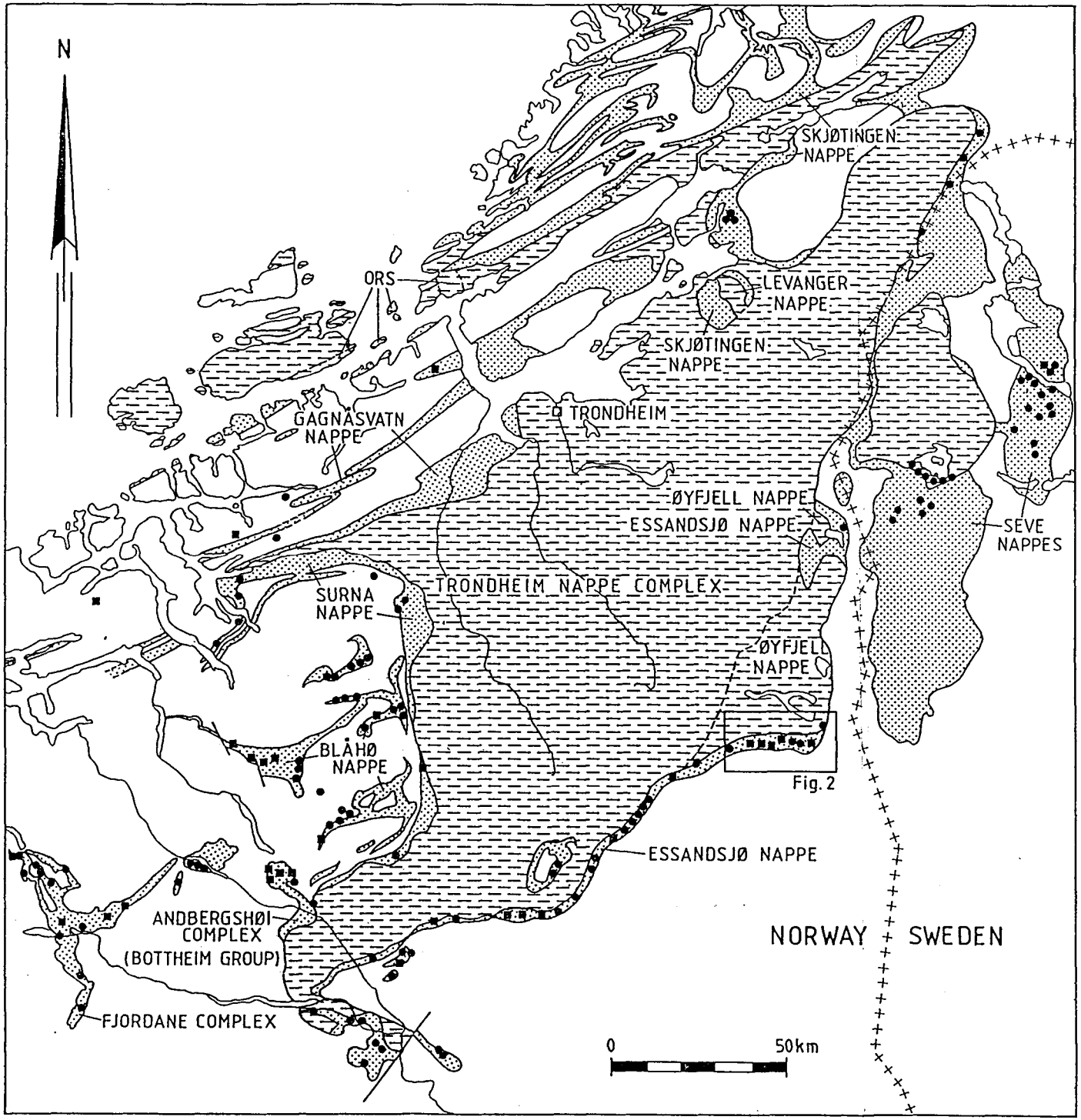
N
ORS
SKJØTINGEN NAPPE
LEVANGER NAPPE
SKJØTINGEN NAPPE
GAGNÅSVATN NAPPE
TRONDHEIM
ØYFJELL NAPPE
ESSANDSJØ NAPPE
SEVE NAPPES
TRONDHEIM NAPPE COMPLEX
SURNA NAPPE
ØYFJELL NAPPE
BLÅHØ NAPPE
Fig. 2
ESSANDSJØ NAPPE
ANDBERGSHØI COMPLEX (BOTTHEIM GROUP)
FJORDANE COMPLEX
NORWAY SWEDEN
0
50km

Fig. 1

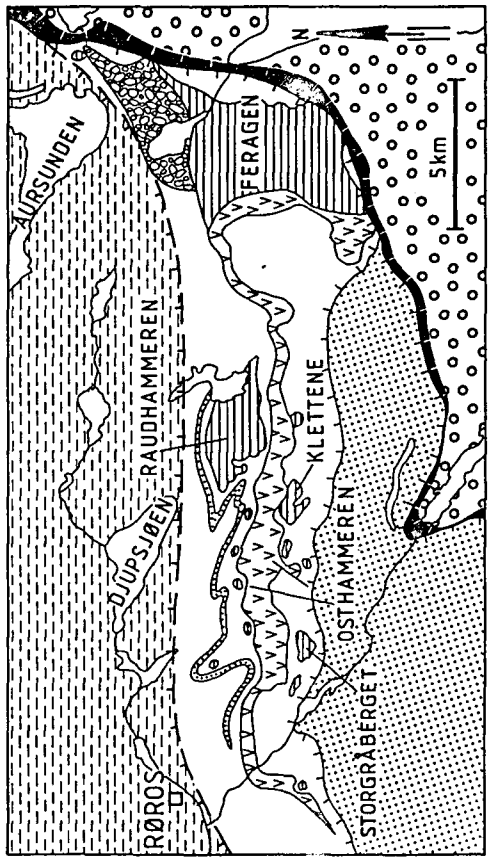

Fig. 2 Nilsson

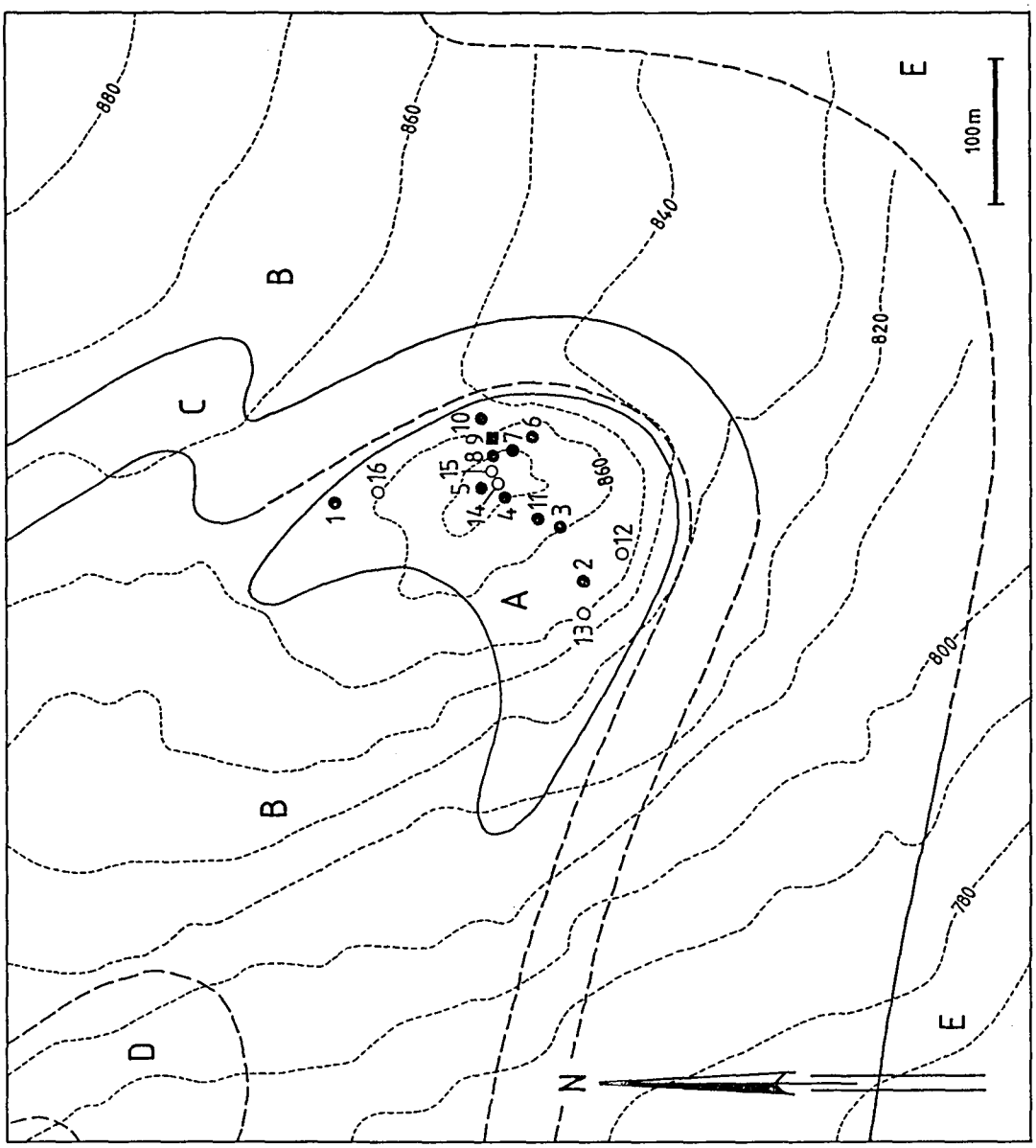

Fig. 3 Nilsson

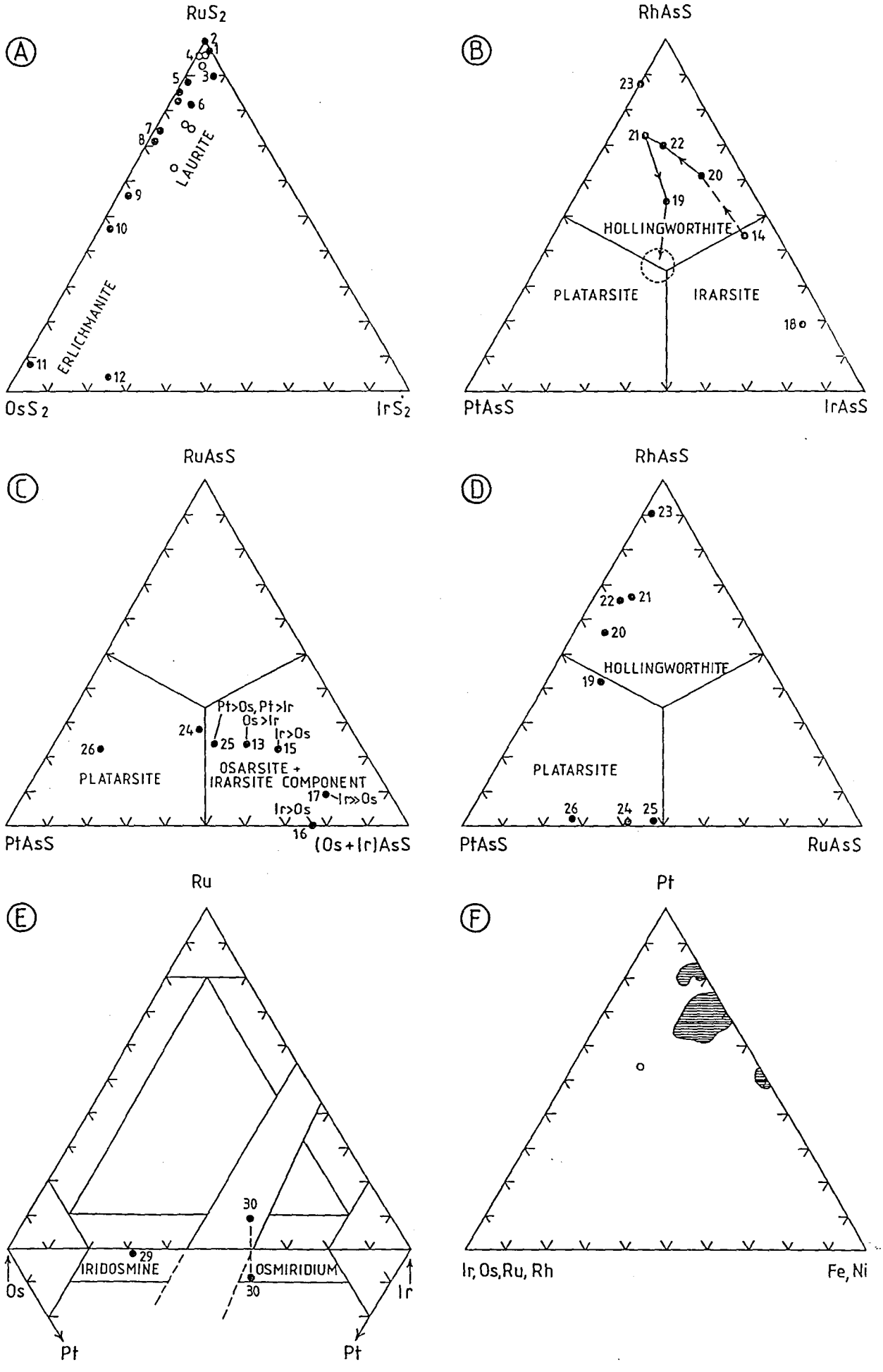

Fig. 4 Nilsson

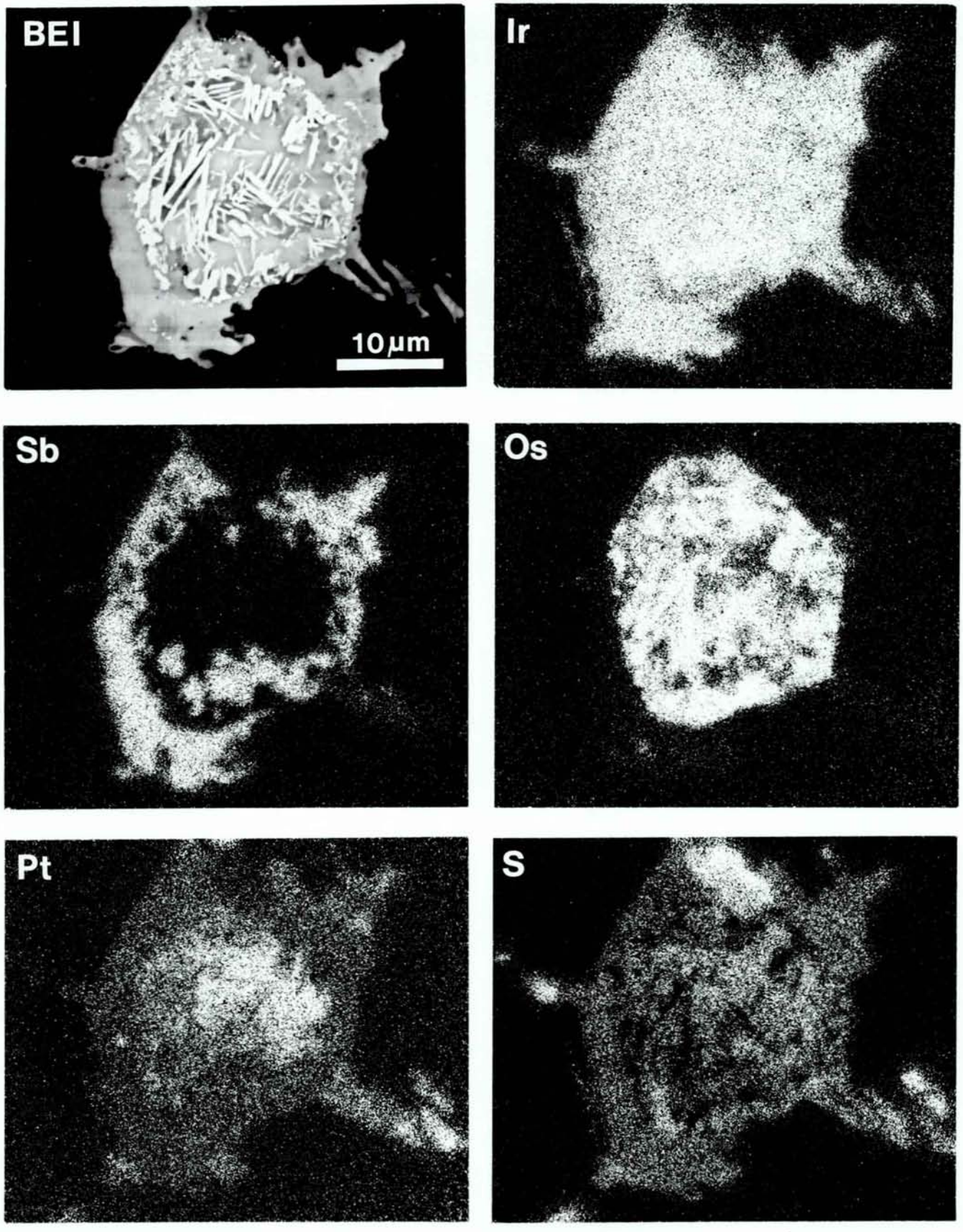

Fig. 5

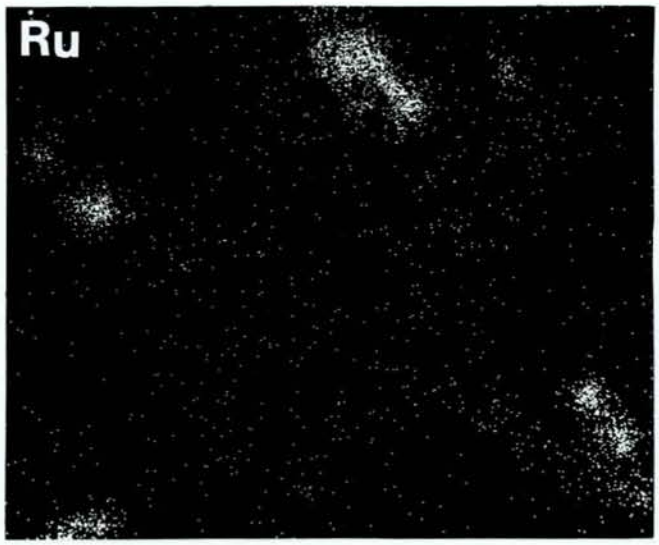

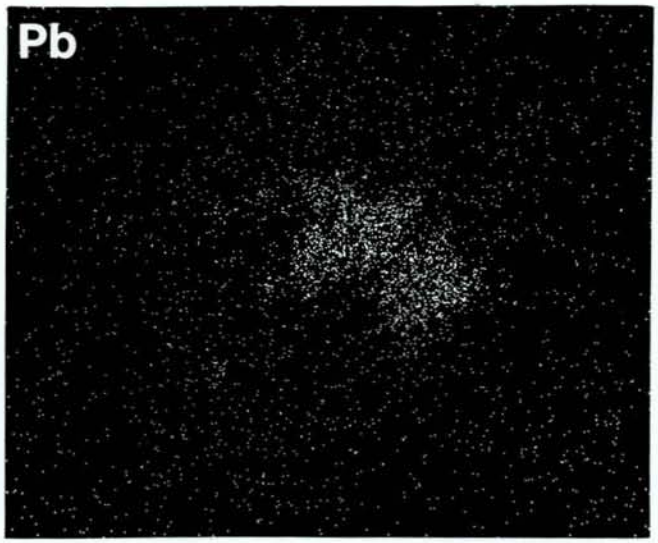

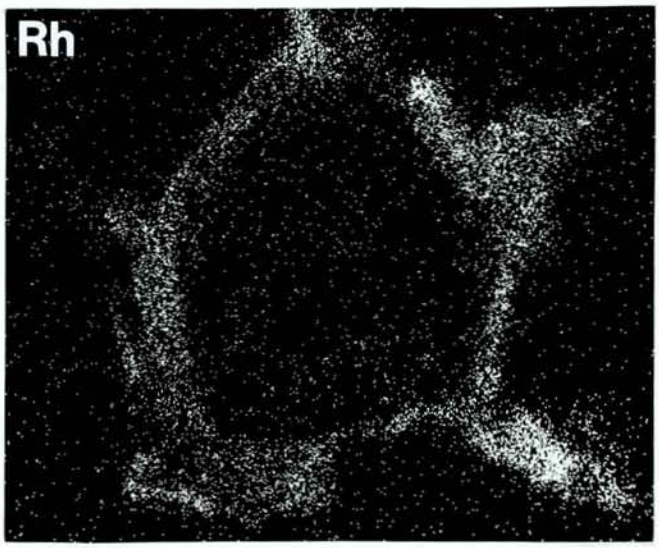

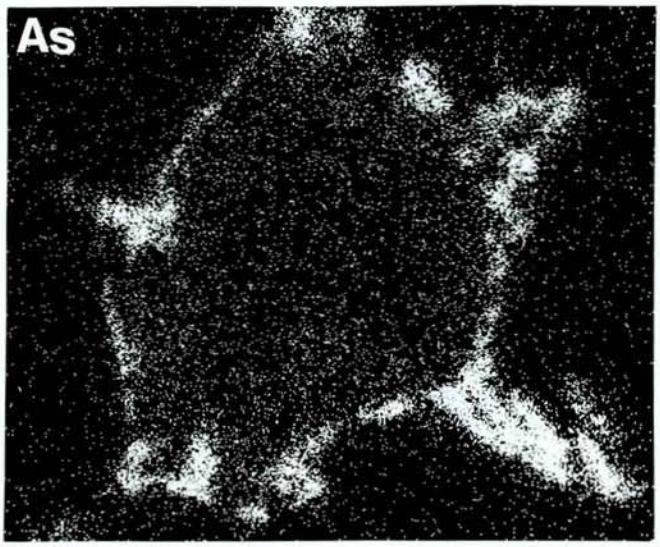

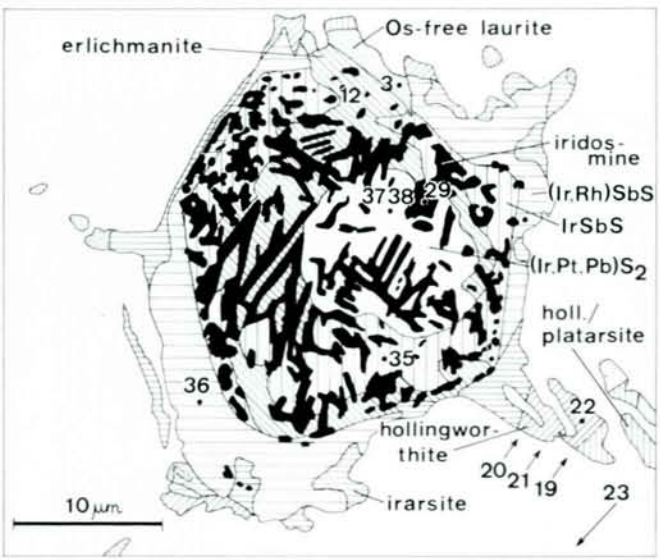

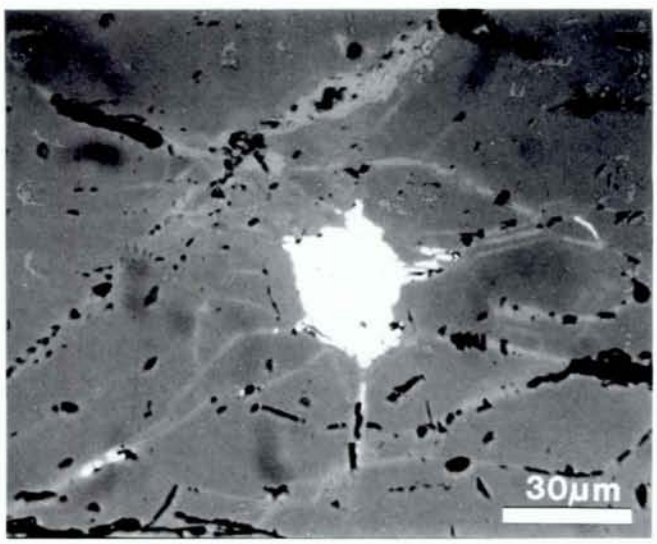

Fig. 5 (continued)

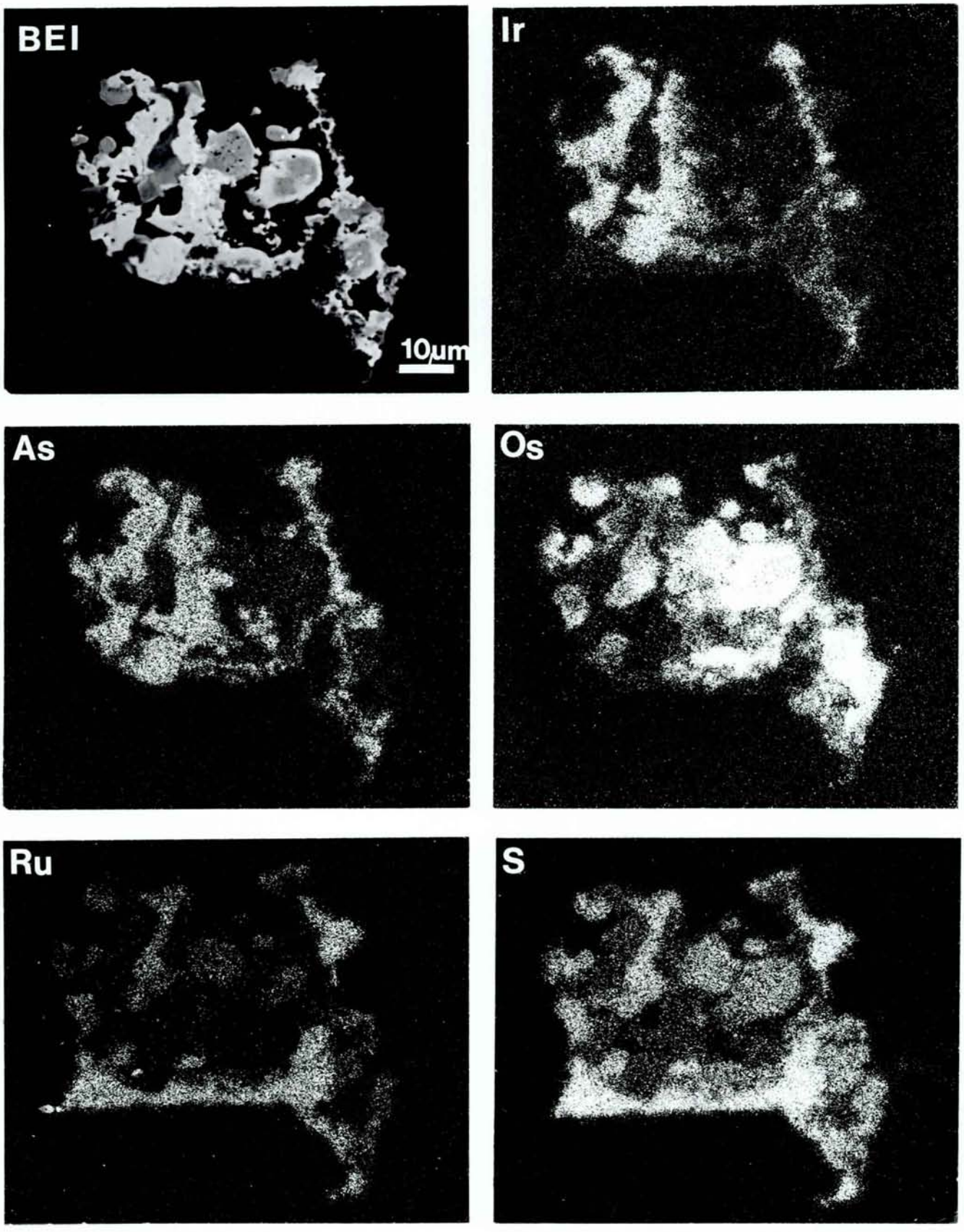

Fig. 6

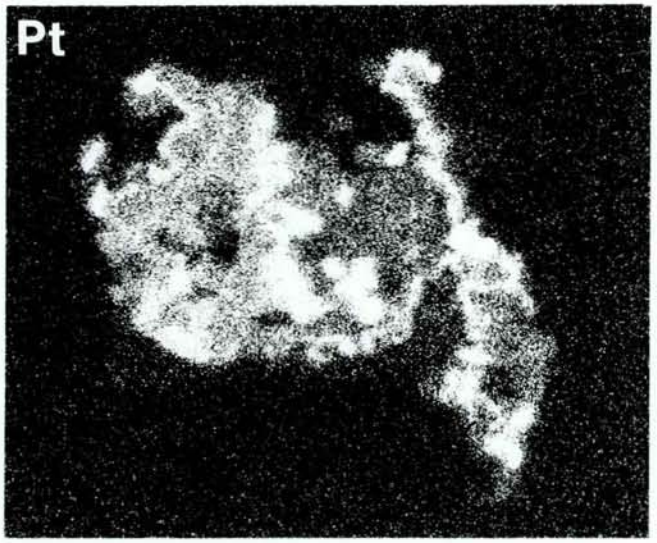

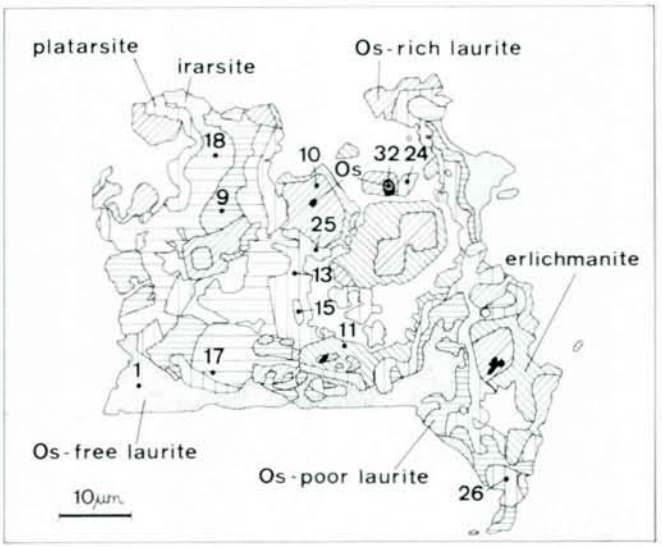

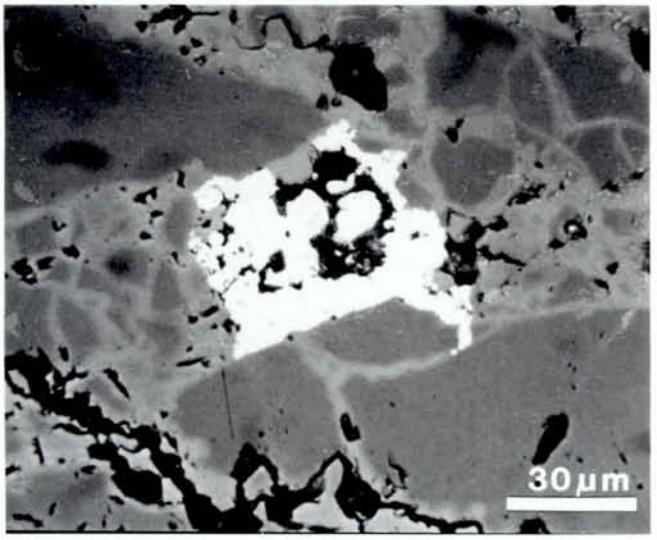

Fig. 6 (continued)

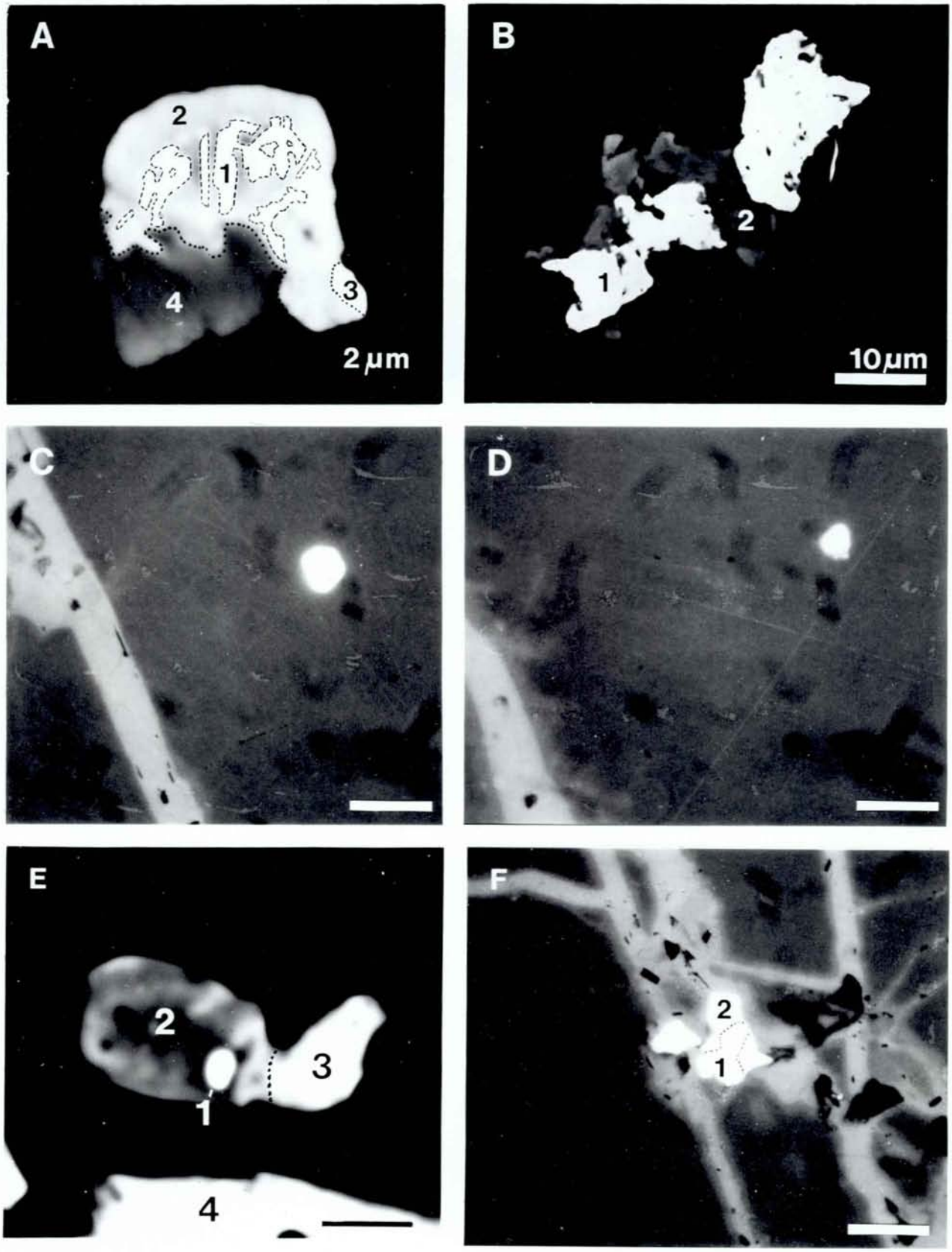

Fig. 7.

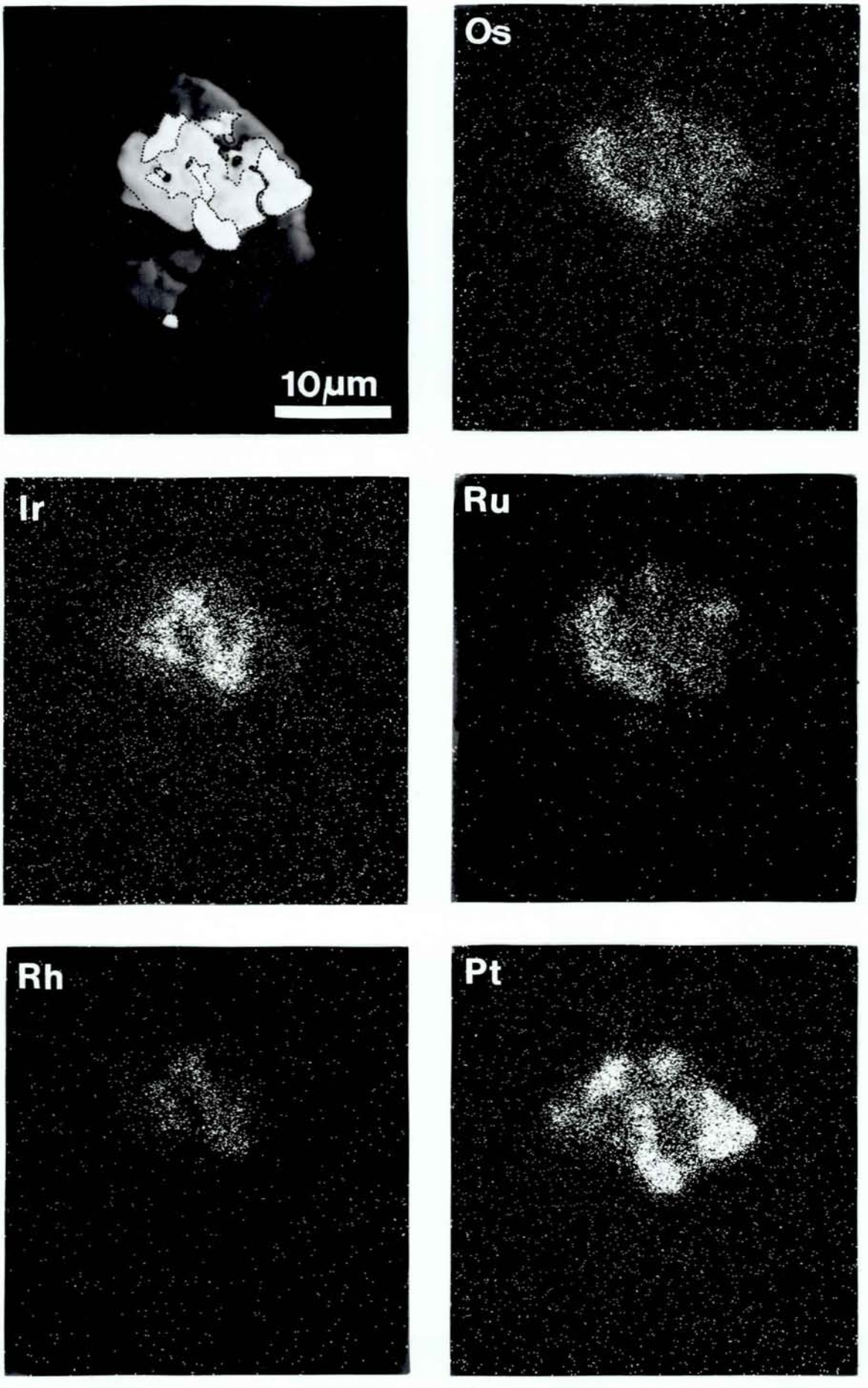

Fig. 8

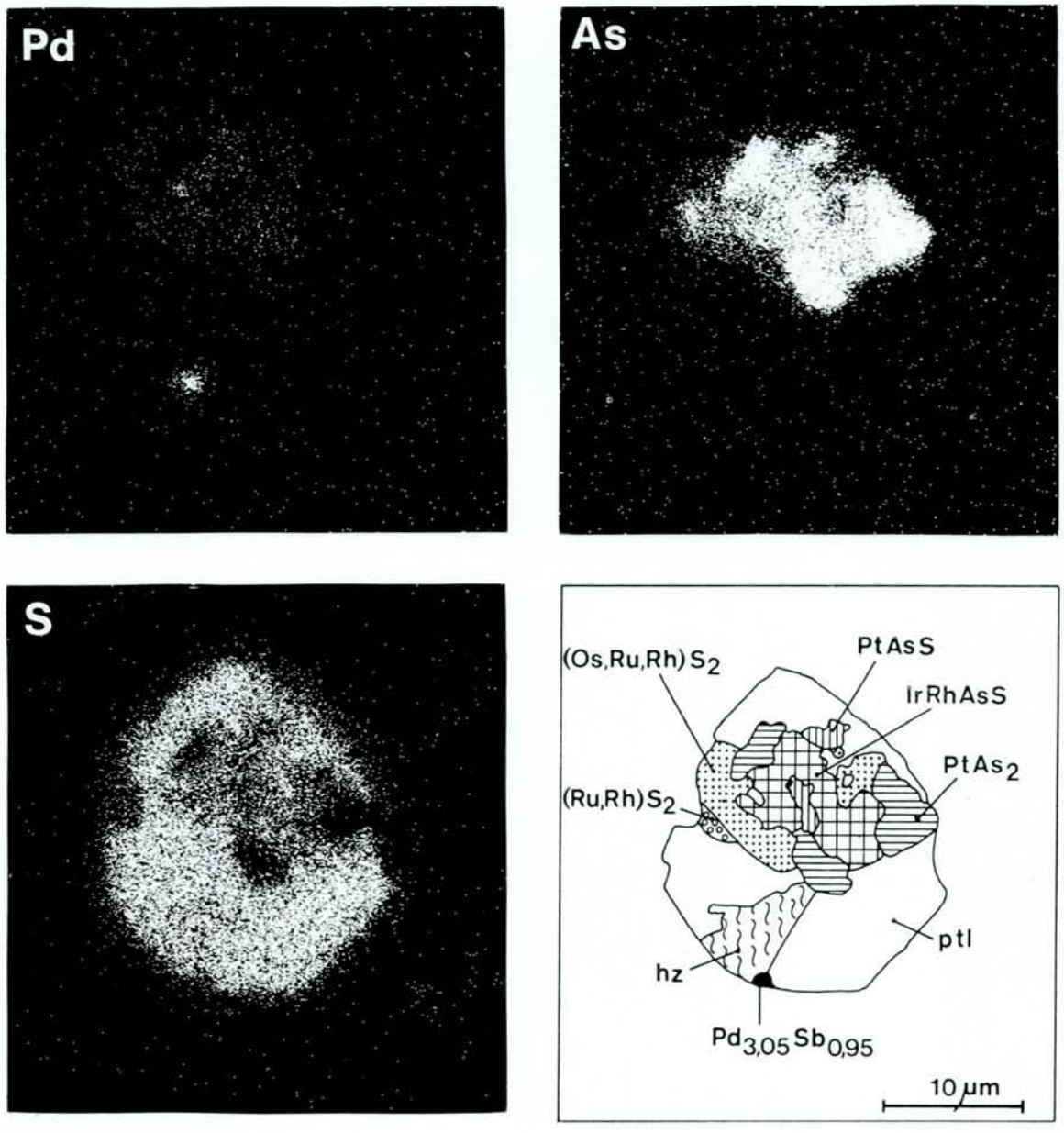

Fig. 8 (continued)

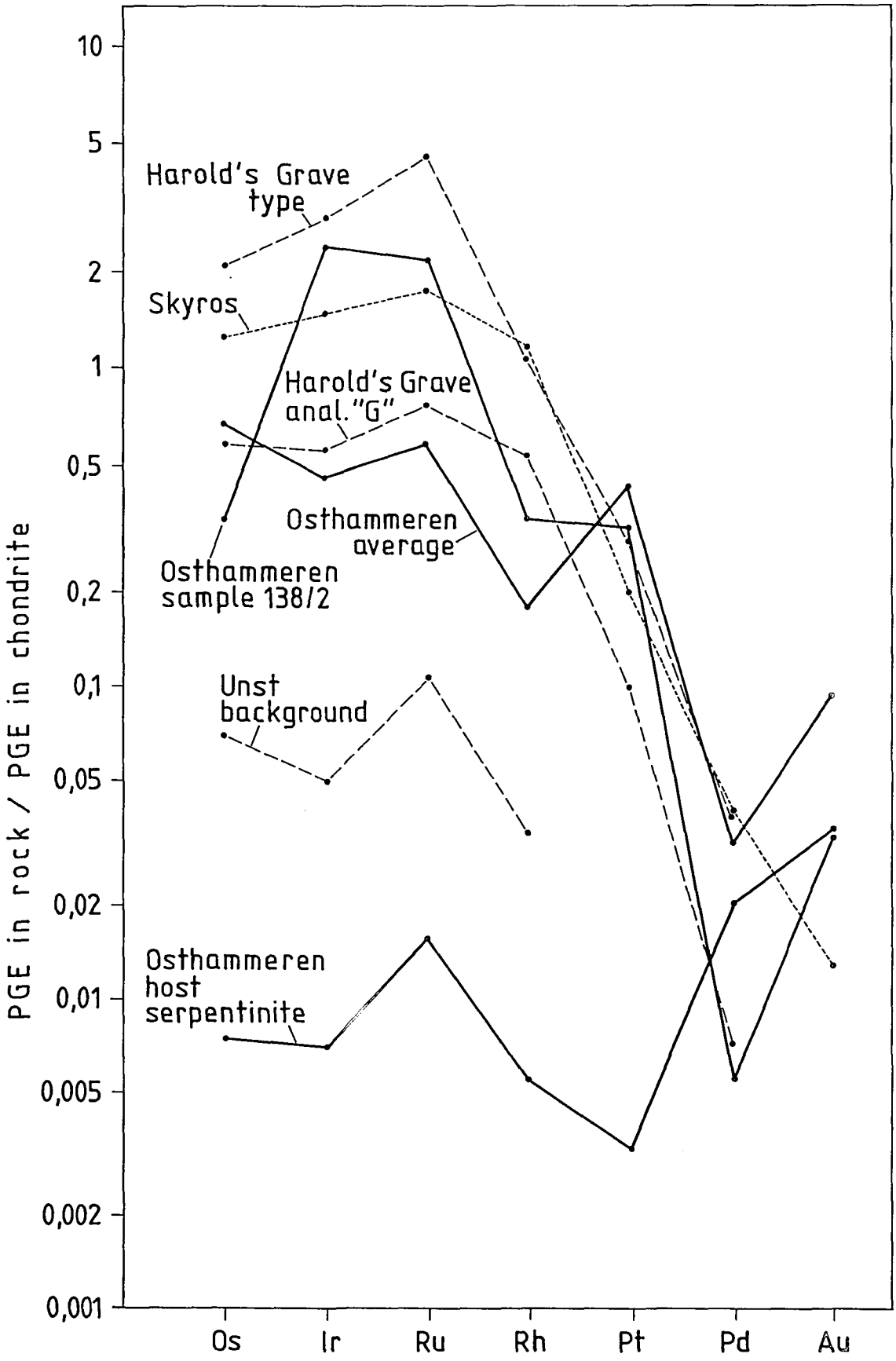

Fig. 9 Nilsson

Fig. 1. Location of ultramafic tectonites with chromitite occurrences recorded (squares) and bodies with no known chromitite enrichments (coarse dots) in the Caledonides of South Central Norway.
Non-patterned areas: Parautochthonous gneissic basement, basal clastic rocks and lower Caledonian nappes (Lower- and Middle Allochthon) [undifferentiated].
Dotted areas: Skjøtingen-Essandsjø-Blåhø Nappe unit and nappe units of similar or assumed similar tectonostratigraphic position.
Dashed line areas: Levanger-Øyfjell Nappe unit, Trondheim Nappe Complex and Old Red Sandstone molasse deposits (ORS).

The Osthammeren - Feragen area of Fig. 2 is shown by frame.

Data for map compilation from NGU-archives, Wolff (1976, 1977), Stigh (1979), Guezou (1981), Roberts & Wolff (1981), Sigmond et al. (1984), Askvik og Rokoengen (1985), Gee et al. (1985a, b), Krill & Sigmond (1986), Krill (1986, 1987), Tucker (1986), Zachrisson (1986), Siedlecka et al. (1987), Nilsen & Wolff (1988), Roberts (1988) and Solli (1989). Data on chromitite occurrences from NGU-archives, Tucker (1986) and author's own observations.

Fig. 2. The Osthammeren body and neighbouring ultramfic tectonite bodies in the Essandsjø Nappe, ESE of Røros. Key to map symbols: area with circles: Røa Nappe, arkose and feldspatic quartzite; horisontal lines: Dalvolsjø Nappe, Augen-gneiss; coarse dots: Hummelfjell Nappe, feldspathic quartzite, etc. with dolerite dikes;

non-patterned; Essansjø Nappe, calcite bearing phyllite, etc. with subordinate quartzite (fine dots), gabbro (hooks) and ultramafic tectonites (lined areas); dashed line: Øyfjell Nappe, calcareous gray and graygreen phyllite; gravel pattern: Devonian clastic sedimentary rocks.

Map compiled from Roberts & Wolff (1981), Rui (1981a, b) and Nilsen & Wolff (1988).

Fig. 3. The Osthammeren serpentinite Lens (A) situated in the middle of the hinge of an overturned fold with gently NNE-dipping axial plane. The lens itself is clearly streched along both fold limbs and thickened in the hinge.
B on map is calcareous phyllite with horizons of greenschist (C) and quartzite (D) belonging to the Essandsjø Nappe. E is a long and narrow gabbroic body. The chromitite showing (claims) are marked with filled circles and the location (claim) of the PGM-anomalous sample with a filled square. Location of serpentinite samples outside the claims marked with open circles.
Contour invervals of 10 m are dotted to give an impression of the knoll-shape of the lens.
Lithological boundaries from Rui (1981b).

Fig. 4. Microprobe analyses (at %) of PGM sulphides (A), sulpharsenides (B, C and D) and alloys (E and F). In diagram B contents of Os, Ru and Pd have been included for Ir, Rh and Pt, respectively. In diagram D Ir and Os are included with Pt and Ru respectively.

Symbols: o primary inclusions, ● secondary inclusions. Analysis numbers refer to those in Table 2. Shaded areas in diagram F where most Pt-Fe alloys plot according to compilation by Tarkian (1987).

Fig. 5. Back-scattered electron image (BEI), X-ray images for Ir, Sb, Os, Pt, S, Ru, Pb, Rh and As, mineral location map and photomicrograph of a complex secondary PGM-inclusion (grain-aggregate no. 1). For description see section on paragenesis.

Fig. 6. Back-scattered electron image (BEI), X-ray images for Ir, As, Os, Ru, S and Pt, mineral location map and photomicrograph of a complex secondary PGM-inclusion (grain-aggregate no. 3). For description see section on paragenesis.

Fig. 7. Back-scattered electron images (A, B, E) and photomicrographs (C, D and F) of PGM-inclusions. A: Secondary composite inclusion of iridosmine-lamellae (1) hosted in irarsite (2). (3) is sperrylite and (4) Os-laurite (grain no. 4). B: secondary inclusion of sperrylite (1) and Os-free laurite (2) (grain no. 5). C: primary osmiridium inclusion hosted in chromite. Ferrite-chromite string at left (grain no. 13). D: primary inclusion of $Pt_2(Ir,Os)Fe_{0.65}$ (grain no. 10). E: patch of native osmium (1) in Os-rich laurite (2), (3) is platarsite and (4) erlichmanite (part of grain-aggregate no. 3). F: Secondary inclusion of Os-laurite (1) and pentlandite (2) situated in ferrite-chromite (light strings).

The darker areas between the strings are unaltered chromite (grain no. 8). Scale bar is 10 μm on C, D and F and 2 μm on E.

Fig. 8. Back-scattered electron image (BEI), X-ray images for Os, Ir, Ru, Rh, Pt, Pd, As and S, and mineral location map of a complex secondary PGM-inclusion (grain-aggregate no. 6). For description see section on paragenesis.

Fig. 9. Chondrite-normalized PGE patterns of Osthammeren chromitites and host serpentinite; data for Harold's Grave from Prichard et al. (1986) and Gunn (1989); for Skyros, Greece from Economou (1986).

TABLE 1

Content of Pt, Pd and Au in ppb in PGE-enriched chromitites compared with normal chromitites from ultramafic tectonites (serpentinites) in central Norway.

Location		n	Pt	Pd	Au
Osthammeren		1	760	<2	8
Ørnstolen		1	299	1391	718
Skamsdalen		1	178	156	120
Aurtand		1	427	104	5
normal chromitites (=non anomalous to weakly anomalous samples)	a	66	12.0	6.2	10.0
	g	66	6.7	1.8	3.8

a = arithmetic mean, g = geometric mean.
Values below detection limits (<x) calculated as $\frac{x}{2}$.
Detection limits were 3,2 and 1 ppb for Pt, Pd and Au respectively.
Analyst: Caleb Brett Laboratories Ltd., St. Helens, UK
Method: Fire assay and atomic absorption spectrometry

TABLE 2. Representative analyses of various platinum-group minerals in one single hand-size chromitite sample from the Osthammeren ultramafic tectonite body, Norway.

Analysis no.		1	2	3	4	5	6	7	8	9	10	11	12	13
Grain/gr.-aggr.no.		3	5	1	2	11	2	8	6	3	3	3	1	3
(1)	Os	0.33	0.33	2.90	3.60	12.36	15.83	20.90	23.44	34.98	42.25	66.22	55.37	23.44
	Ir	3.63	0.09	6.91	1.57	0.39	6.85	1.12	1.55	2.07	2.49	1.72	17.99	14.02
	Ru	57.02	56.81	43.03	58.64	38.45	50.08	33.73	32.46	24.91	20.66	2.68	1.29	8.92
	Rh	0.10	0.54	2.64	-	0.20	1.02	0.07	0.63	-	0.12	1.37	0.05	0.41
	Pt	0.35	3.31	1.16	0.22	0.29	0.18	0.30	5.35	4.60	4.29	2.94	0.56	21.30
	Pd	0.61	0.57	0.88	-	0.67	0.19	0.45		0.31			0.02	0.20
	As	0.25	2.90	6.66	0.03	2.21	0.12	1.63	4.51	3.88	3.78	3.02	0.48	21.40
	S	37.72	34.02	29.15	37.66	32.14	25.20	36.00	29.34	32.63	31.21	28.06	26.81	15.61
	Sb	-	-	0.13	-		-			-			-	
	Pb			-									0.09	
	Ni	0.05	0.08	0.03	0.02	0.36	0.32			0.26			0.02	
	Au	0.44	0.54		0.37		0.31			0.15				
	Te	-	-		-		-			-				
	Bi			-									0.02	
	Cr	0.61	1.04	2.96	0.01	5.32	1.40	2.89	0.97	0.28		0.40	1.49	0.21
	Fe	0.36	0.81	2.20	-	7.51	0.56	3.59		0.68			0.84	0.22
	TOT.	101.47	101.04	98.65	102.12	99.90	102.06	100.68	98.25	104.75	104.80	106.41	104.98	105.73
(2)	Os	0.33	0.33	3.10	3.53	14.19	15.81	22.19	24.10	33.70	40.31	62.47	53.89	22.26
	Ir	3.61	0.09	7.39	1.54	0.45	6.84	1.19	1.59	1.99	2.38	1.62	17.53	13.31
	Ru	56.74	57.27	46.03	57.43	44.15	50.03	35.81	33.37	24.00	19.71	2.53	1.26	8.47
	Rh	0.10	0.54	2.82	-	0.23	1.02	0.07	0.65	-	0.11	1.29	0.05	0.39
	Pt	0.35	3.34	1.24	0.22	0.33	0.18	0.32	5.50	4.43	4.09	2.77	0.55	20.23
	Pd	0.61	0.57	0.94	-	0.77	0.19	0.48		0.30			0.02	0.19
	As	0.25	2.92	7.12	0.03	2.54	0.12	1.73	4.64	3.74	3.61	2.85	0.47	20.32
	S	37.53	34.30	31.18	36.88	36.90	25.17	38.22	30.16	31.44	29.78	26.47	26.12	14.82
	Sb	-	-	0.14	-					-			-	
	Pb			-									0.09	
	Ni	0.05	0.08	0.03	0.02	0.41	0.32			0.25			0.02	
	Au	0.44	0.54		0.36		0.31			0.14				
	Bi			-									0.02	
(3)	Os	0.10	0.10	1.00	1.06	4.35	5.85	6.87	8.43	11.92	14.94	26.23	23.37	10.52
	Ir	1.06	0.03	2.37	0.46	0.14	2.51	0.36	0.55	0.70	0.87	0.67	7.52	6.22
	Ru	31.76	33.15	28.08	32.49	25.44	34.86	20.85	21.98	15.98	13.75	2.00	1.03	7.53
	Rh	0.05	0.31	1.69	-	0.13	0.70	0.04	0.42	-	0.08	1.00	0.04	0.34
	Pt	0.10	1.00	0.39	0.06	0.10	0.06	0.10	1.88	1.53	1.48	1.13	0.23	9.32
	Pd	0.32	0.31	0.54	-	0.42	0.13	0.27		0.19			0.02	0.16
	As	0.19	2.28	5.86	0.02	1.97	0.11	1.36	4.12	3.36	3.40	3.04	0.52	24.37
	S	66.23	62.58	59.96	65.78	67.04	55.29	70.16	62.62	65.99	65.49	65.93	67.20	41.54
	Sb	-		0.07	-		-			-			-	
	Pb			-									0.04	
	Ni	0.05	0.08	0.03	0.02	0.41	0.38			0.29			0.03	
	Au	0.13	0.16		0.10		0.11			0.05				
	Bi			-									0.01	

- element not detected.
analysis 1 - 4: laurite; 5 - 10: (Os-laurite); 11: erlichmanite; 12: (Ir-rich erlichmanite); 13: osarsite.
Mineral names in brackets are not used in Cabri (1981), but are used in this subscript to specify the composition of the PGM-phases.
(1): raw analyses in weight percent of the element (after corrections due to element interference).
(2): analyses recalculated after subtraction of Fe and Cr. (3): atomic concentration calculated from the corrected analyses.

Table 2 (continued)

Analysis no.		14	15	16	17	18	19	20	21	22	23	24	25	26
Grain/gr.-aggr.no.		6	3	4	3	3	1	1	1	1	1	3	3	3
(1)	Os	7.97	14.67	8.75	2.15	2.26	0.38	0.22	0.14	0.09	-	9.46	17.94	4.26
	Ir	26.34	26.69	34.01	44.88	47.61	11.20	13.15	4.94	9.17	0.05	14.52	11.81	3.80
	Ru	4.78	5.92		2.11	2.93	3.52	1.87	2.69	2.47	1.05	9.55	8.83	6.70
	Rh	12.17	2.45		0.88	3.98	10.51	13.63	19.36	21.76	36.51	-	0.11	0.29
	Pt	6.15	14.61	13.25	9.03	5.20	10.15	3.46	8.77	8.11	5.64	25.35	26.70	41.37
	Pd		-		0.28	-	0.72	0.76	1.34	1.31	2.51	0.24	0.19	0.07
	As	20.03	25.48	23.37	24.69	22.73	21.20	21.42	23.70	31.71	29.65	25.91	23.74	28.36
	S	14.81	14.05	9.16	13.65	14.02	7.49	8.25	8.87	12.07	11.96	12.62	12.80	8.00
	Sb	2.99					0.20	1.81	0.90	1.27	2.95			
	Pb						-		0.01	-	-			
	Ni						0.04	0.03	0.05	-	0.03			
	Bi									-				
	Cr	1.24	0.26		0.63	0.62	14.09	12.50	10.92	4.40	2.91	0.77	0.27	3.20
	Fe		0.21		0.52	0.51	6.69	8.32	5.08	1.79	1.52	0.83	0.26	2.53
	TOT.	96.48	104.81	88.54 *	98.82	99.86	86.19	85.42	86.77	94.15	94.78	99.25	102.65	98.58
(2)	Os	8.37	14.12	9.88	2.20	2.29	0.58	0.34	0.20	0.10	-	9.69	17.57	4.59
	Ir	27.66	25.70	38.41	45.95	48.22	17.12	20.36	6.98	10.43	0.06	14.87	11.56	4.09
	Ru	5.02	5.70		2.16	2.97	5.38	2.89	3.80	2.81	1.16	9.78	8.65	7.22
	Rh	12.78	2.36		0.90	4.03	16.07	21.10	27.36	24.74	40.41	-	0.11	0.31
	Pt	6.46	14.07	14.96	9.25	5.27	15.52	5.36	12.39	9.22	6.24	25.96	26.15	44.56
	Pd		-		0.29	-	1.10	1.18	1.89	1.49	2.78	0.25	0.19	0.08
	As	21.03	24.53	26.39	25.28	23.02	32.41	33.16	33.49	36.05	32.82	26.53	23.25	30.54
	S	15.55	13.53	10.35	13.98	14.20	11.45	12.77	12.53	13.72	13.24	12.92	12.53	8.62
	Sb	3.14					0.31	2.80	1.27	1.44	3.27			
	Pb						-		0.01	-	-			
	Ni						0.06	0.05	0.07	-	0.03			
(3)	Os	3.71	6.70	5.18	1.05	1.09	0.26	0.14	0.08	0.04	-	4.56	8.58	2.35
	Ir	12.13	12.06	19.91	21.65	22.63	7.52	8.51	2.86	4.16	0.02	6.92	5.59	2.08
	Ru	4.19	5.09		1.94	2.65	4.49	2.30	2.96	2.13	0.86	8.66	7.95	6.97
	Rh	10.47	2.07		0.79	3.53	13.18	16.47	20.91	18.42	29.28	-	0.10	0.29
	Pt	2.79	6.50	7.64	4.29	2.44	6.71	2.21	4.99	3.62	2.39	11.91	12.46	22.27
	Pd		-		0.25	-	0.87	0.89	1.40	1.07	1.95	0.21	0.17	0.07
	As	23.66	29.53	35.10	30.55	27.71	36.51	35.56	35.15	36.86	32.67	31.68	28.84	39.75
	S	40.88	38.06	32.17	39.48	39.95	30.15	32.00	30.73	32.79	30.80	36.06	36.32	26.22
	Sb						0.22	1.85	0.82	0.91	2.00			
	Pb						-		-	-	-			
	Ni						0.09	0.07	0.09	-	0.04			

analysis 14 - 18: irarsite; 19 - 23: hollingworthite; 24 - 26: platarsite.

* = much Cr and Fe present in analysis according to EDS spectrum, but no Ru or Rh according to X-ray images.

Table 2 (continued)

Analysis no.		27	28	29	30	31	32	33	34	35	36	37	38
Grain/gr.-aggr.no.		6	5	1	13	10	3	6	6	1	1	1	1
(1)	Os	2.47	0.07	64.48	31.57	9.81	70.66		0.43	4.67	0.15	4.72	4.71
	Ir	0.53	0.17	28.89	51.55	17.79	1.43		0.18	49.74	43.23	44.50	43.87
	Ru	2.03	2.00	-	4.45	1.66	7.56		-	-	0.18	-	-
	Rh	-	0.39	-	2.11	0.85	0.08		-	0.94	6.32	0.35	0.31
	Pt	48.82	52.41	1.28	8.42	59.78	2.37		1.48	1.49	1.19	15.52	15.41
	Pd		-	0.08	-	0.11	0.40	45	16.30	0.01	-	0.06	-
	As	35.97	42.81	0.06	0.03	0.08	2.40		0.64	0.49	0.37	0.01	0.12
	S	3.13	1.52	0.38	-		16.02		6.15	9.10	10.07	24.67	22.19
	Sb	1.63	-	-	-			15	5.83	30.09	32.37	-	-
	Pb								0.03	-		6	13.60
	Ni		0.05	0.08	0.11	0.16			6.77	-	0.02	0.40	0.42
	Au		0.17	0.04	0.01						0.03	0.11	
	Te		-	-							-	-	
	Bi								-	-			-
	Cr	1.53	1.93	0.87		2.56	0.63		11.34	0.89	1.80	0.84	0.74
	Fe		0.86	0.66	0.75	6.10	0.84		4.75	0.35	0.67	0.37	0.37
	TOT.	96.11 *	102.38	96.82	99.00	98.90	102.39	60 **	53.90	97.77	96.40	97.55 ***	101.74
(2)	Os	2.61	0.07	67.67	32.11	10.27	70.02			4.84	0.16	4.90	4.68
	Ir	0.56	0.17	30.32	52.47	18.62	1.42			51.53	46.02	46.19	43.60
	Ru	2.15	2.01	-	4.53	1.74	7.49			-	0.19	-	-
	Rh	-	0.39	-	2.15	0.89	0.08			0.97	6.73	0.36	0.31
	Pt	51.62	52.63	1.34	8.57	62.56	2.35			1.54	1.27	16.11	15.31
	Pd		-	0.08	-		0.40	75	73.56	0.01	-	0.06	-
	As	38.03	42.99	0.06	0.03	0.12	2.38			0.51	0.39	0.01	0.12
	S	3.31	1.53	0.40	-	0.08	15.87			9.43	10.72	25.61	22.05
	Sb	1.72	-	-	-			25	26.31	31.17	34.46	-	-
	Pb								0.14	-		6.23	13.51
	Ni		0.05	0.08	0.11	0.17				-	0.02	0.42	0.42
	Au		0.17	0.04	0.01							0.11	
	Fe					5.56							
(3)	Os	1.48	0.04	66.38	30.49	8.94	37.07			2.93	0.09	2.17	2.25
	Ir	0.31	0.10	29.43	49.30	16.04	0.74			30.89	25.55	20.20	20.72
	Ru	2.29	2.17	-	8.09	2.85	7.46			-	0.20	-	-
	Rh	-	0.40	-	3.77	1.43	0.08			1.09	6.98	0.29	0.27
	Pt	28.53	29.39	1.28	7.93	53.09	1.21			0.91	0.69	6.94	7.17
	Pd			0.14	-	-	0.38	77.44	76.13	0.01	-	0.05	-
	As	54.73	62.52	0.15	0.07	0.26	3.20			0.78	0.56	0.01	0.15
	S	11.13	5.20	2.33	-	0.41	49.85			33.89	35.68	67.16	62.83
	Sb	1.52		-	-			22.56	23.80	29.50	30.20	-	-
	Pb								0.07			2.53	5.96
	Ni		0.09	0.25	0.34	0.48					0.04	0.60	0.65
	Au		0.09	0.04	0.01						0.02	0.05	
	Fe					16.48							

analysis 27 - 28: sperrylite; 29: iridosmine; 30: osmiridium; 31: $Pt_2(Ir,Os)Fe_{0.65}$; 32: native Os; 33 - 34: Pd-antimonide, probably stibiopalladinite; 35: IrSbS; 36: (Ir,Rh)SbS; 37 - 38: $(Ir,Pt,Pb)S_2$ (not earlier reported?).

* = some Ni and Fe present in analysis

** = semiquantitative (EDS) analysis only

*** = Pb analyzed semiquantitatively

Table **3**

Paragenesis of platinum-group-mineral (PGM) inclusions in one single hand-size sample of massive chromitite from the Osthammeren ultramafic tectonite body, South central Norway, based on analyses of nine polished sections.

polished section no.	2A			2B			2C	2D				2E	2F	2G	2I	Quantitative analyses of the investigated phases. Numbers refer to analysis-numbering in Table 2.
grain/grain-aggregate no.	1	2	3	4	5	6	7	8	9	10	11	12	13	14	15	
PGM-phases laurite RuS_2	●	○	●		●	●								○		1 - 4
[Os-laurite] $(Ru,Os)S_2$		○	●	●		●	●	●	○		●	○			○	5 - 10
erlichmanite OsS_2			●													11
[Ir-rich erlichmanite] $(Os,Ir)S_2$	●															12
? osarsite OsAsS			●													13
irarsite IrAsS	●		●	●		●					●					14 - 18
hollingworthite RhAsS	●															19 - 23
platarsite PtAsS	●		●			●										24 - 26
sperrylite $PtAs_2$				●	●	●										27 - 28
iridosmine Os,Ir	●			●												29
osmiridium Ir,Os													○			30
$Pt_2(Ir,Os)Fe_{0.65}$										○						31
native Os			●													32
? stibiopalladinite ($\approx Pd_3Sb$)						●										33 - 34
IrSbS	●															35
(Ir,Rh)SbS	●															36
NEW? $(Ir,Pt,Pb)S_2$	●															37 - 38
associated phases pentlandite $(Fe, Ni)_9S_8$						●	●	●								
niccolite NiAs							●									
heazlewoodite Ni_3S_2						●										

○ = primary euhedral/subhedral inclusion ● = secondary and/or modified anhedral grain/grain-aggregate

Mineral names in brackets are not used in Cabri (1981), but are used in this table to specify the composition and the distribution of the PGM-phases.

TABLE 4

Content of PGE and Au in ppb in chromitites and host serpentinite from the Osthammeren ultramafic tectonite body.

Sample no.	Location (claim no./ loc. no. ref. to Fig. 3)		Os	Ir	Ru	Rh	Pt	Pd	Au	TOT	Ore-type/ host rock	Analyst/ analytical method
LPN78-138/2	9						760	<2	8		massive ore (PGM-anomalous sample)	1
-138/2	9		174.2	674.4	841.0	65.2	323.4	2.9	4.9		massive ore (PGM-anomalous sample)	2
		DUP	166.3	659.2	835.8	64.9	316.1	3.0	5.2			
										2068.5	Average of two analyses	
-139			5.5	5.2	6.2	0.9	1.7	1.7	11.8		serpentinite	
LPN87-1/1	1		62	41	100	8.0	25	9.0	10		transition dissemination/-	3
		DUP	54	39	100	9.0	7.5	30	10		massive ore	
-2	2		130	160	160	130	9300	79	200		massive ore	
		REP	380	73	150	22	39	6.5	8			
		REP	86	79	170	28	49	8.5	12			
-3	3		62	58	140	31	83	11	2		massive ore	
-4/1	4		140	130	230	19	79	28	6		massive ore in veins	
		DUP	130	110	190	28	120	6.0	6		and schlieren	
-4/3	4		120	110	180	17	84	5.0	2		massive ore	
-5	5		530	510	640	63	470	7.0	6		massive ore in vein	
		DUP	130	110	750	78	480	11	10			
-6/1	6		50	54	100	21	1000	19	20		massive ore in vein	
		REP	270	43	97	11	22	10	2			
		REP	44	44	130	13	24	40	2			
-8/1	8		92	90	170	18	72	28	4		transition dissemination -	
		DUP	70	73	150	26	68	27	4		massive ore in fine veins	
-9/1	9		550	420	590	34	160	22	12		massive ore in veins	
		REP	560	290	610	32	120	9.0	6			
		REP	560	430	550	35	190	34	8			
-9/2	9		670	490	640	50	430	20	2		massive ore in veins	
-10/1	10		570	470	520	27	210	8.5	10		massive ore in veins	
-10/2	10		1400	810	1400	73	350	6.0	30		massive ore	
		DUP	1100	610	1100	54	230	8.0	32			
			346	243	396	35	449	17	14	1500	Average of samples 1/1 to 10/2 n = 12	
-1/2	1		6	5.0	4.0	<0.5	2.0	6.0	<2		serpentinite	3
-4/2	4		6	6.5	8.0	1.0	<0.5	8.5	4		"	
-6/2	6		4	3.5	14	1.0	2.5	21	6		"	
-8/2	8		2	4.0	5.5	1.0	7.0	5.5	4		"	
-9/3	9		4	1.5	8.0	2.0	4.5	19	<2		"	
-12	12		2	2.0	5.5	1.0	1.5	4.5	2		"	
-13	13		2	6.0	12	1.5	3.0	15	2		"	
-14	14		2	2.5	35	1.5	7.5	6.0	<2		"	
-15	15		6	4.0	7.0	1.0	3.0	14	24		"	
-16	16		4	3.0	11	1.0	3.0	12	8		"	
			3.8	3.8	11.0	1.1	3.4	11.2	5.3	39.6	Average of samples -1/2 to 16 n = 10	

Analyst:
1 Caleb Brett Laboratories Ltd., St. Helens, UK

2 Memorial University, St. John's, Newfoundland, Canada
3 Analytical Services (W.A.) PTY.LTD, Perth, Western Australia

Method:
Fire Assay and atomic absorption spectrometry
Fire Assay and ICP-Mass Spec'
Fire Assay and ICP-Mass Spec'

TABLE 5

PGM-assemblage detected in sample no. 138/2 of compact chromitite from the Osthammeren ultramfic tectonite body, Norway, compared with PGM-assemblage in chromitites from different PGE/PGM-rich ophiolite (alpine-type) complexes.

	Osthammeren	Harold's Grave chromitite occurence, Shetland ophiolite (Prichard et al. 1986)	chromitite deposit in N.W. China (Chang et al. 1973)	chromitite occurrences in the Hochgrössen ultramafic massif Styria, Austria (Thalhammer & Stumpfl 1988)	Aetorache chromitite deposit, Vourinos ophiolite complex, Greece (Auge 1985)
laurite	●	●	●	●	●
erlichmanite	○				
osarsite	○				○
irarsite	●	●	●	●	○
hollingworthite	○			○	
platarsite	○		○	○	
sperrylite	●	○	●	●	
sperrylite-iridarsenite				○	
iridosmine	○				●
ruthenirridosmine					○
osmiridium	○		○		○
$Pt_2(Ir,Os)Fe_{0.65}$	○				
native Os	○	○			
Pd-antimonide	○	○	○		
IrSbS	○	○			
(Ir,Rh)SbS	○				
RhSbS		○			
$(Ir,Pt,Pb)S_2$	○				
$(Pt,Ir,Rh,Os)_{2.7}Cu_{1.3}S_6$				○	
Rh-Ni antimonide		○			
cooperite				○	

● = Major PGMs ○ = Minor PGMs

2.3 Inclusions of platinum group minerals (PGM), base-metal sulphides (BMS) and sulpharsenide in chromitite and host rocks from the Ørnstolen ultramafic tectonite body, north central Norway by L.P.Nilsson.

INCLUSIONS OF PLATINUM-GROUP-MINERALS (PGM), BASE-METAL SULPHIDES (BMS) AND SULPHARSENIDE IN CHROMITITE AND HOST ROCKS FROM THE ØRNSTOLEN ULTRAMAFIC TECTONITE BODY, NORTH CENTRAL NORWAY

Introduction

A pilot-study of platinum-group-elements (PGE) in different geological environments was carried out in 1986 by the Geological Survey of Norway, NGU (Barnes et al. 1987a,b). The pilot study included Ni-Cu sulphide deposits, large layered intrusions, komatiites, ophiolites and related rocks and Alaska-type "concentric" intrusions. This account will deal only with results from the group "ophiolites and related rocks" and more specifically with chromitites and their host rocks from the Ørnstolen ultramafic tectonite lens situated on a small island, Selsøy, in North Central Norway, Fig. 1 and 2.

In the pilot study seventy chromitite samples from seventeen different ultramafic tectonite lenses and two ophiolite fragments, Velfjord and Rødøy, in central Norway were analysed for Pt, Pd and Au by atomic absorption spectrometry (AAS). Only four of the samples showed clearly anomalous values (Table 1), and two of these proved to contain inclusions of platinum-gruop minerals (PGM), namely a sample from the Ørnstolen ultramafic lens and one from the Osthammeren serpentinite lens, the latter situated in South Central Norway. PGM in the Osthammeren lens are treated in a separate paper (Nilsson, in press).

Results of follow-up studies, present status of work and suggestions for further studies

In the pilot study one of the five chromitite samples from the Ørnstolen body to be analyzed showed anomalous Pd-, Au- and Pt-values (Table 2). Follow-up sampling was conducted in 1986 and 1987. The 1986 samples were not analyzed for PGE, but polished sections were made, and in these, three inclusions containing PGM were detected (see later). The 1987 samples were analysed for all six PGE plus Au (Table 3), but the results were disappointing. Four polished sections of the most anomalous sample (no. 3-

1) with 375 ppb PGE_{TOT} were systematically studied in reflected light using 100 x and 500 x magnification. Altogether 15 inclusions, mostly however minute in size, were detected in chromite and tentatively determined as PGM and BMS/sulfarsenide. Most of the smaller euhedral-subhedral inclusions are probably PGM (laurite, etc.), whereas larger, subhedral-anhedral ones are probably mostly single-phase or composite BMS/sulfarsenide-inclusions. Microprobe-analyses should be carried out on these inclusions i order to complete the Ørnstolen study, though the bulk PGE-analyses (Table 3) show clearly that the Ørnstolen chromitites and their host rocks are not of economic interest.

Distribution, setting and constitution of the chromitites and their host rocks

The Ørnstolen ultramafic tectonite body and similar small ultramafic lenses which occur are numerous in this region, are all hosted in metasedimentary and metavolcanic sequences overlying Proterozoic basement mainly consisting of gneissic granites which crop out in several tectonic windows in the region (Gustavson & Gjelle 1987, Bucher-Nurminen 1988). The metasupracrustal assemblage belongs to the Helgeland Nappe Complex which is part of the Uppermost Allochthon (Gee et al. 1985). The ultramafic bodies and their chromitite occurrences are described by Vogt (1984), Carstens (1918), Sørensen (1955 a,b, 1979), Korneliussen (1976), Bakke & Korneliussen (1986) and Bucher-Nurminen (1988) most of whom considered them to be metaperidotites, partly carbonate-bearing (sagvandites). Recent investigations of the Ørnstolen body have revealed that most or all magmatic minerals and textures are totally obliterated, with the exception of chromite which locally shows primary magmatic relics in the form of alternating bands of chromite and silicate/carbonate in dismembered clusters or pods of chromitite (Fig. 4A,B). A preliminary lithological map of the Ørnstolen body is shown in Fig. 3.

The main rock type is a medium- to coarse-grained rock with variable proportions of the prograde metamorphic minerals forsterite (Fo), enstatite (En), tremolite (smaragdite) (Tr) and chlorite (Chl) variably altered to retrograde assemblages of talc (Tlc) and Magnesite (Mgs). The Fo-En-Tr-Chl

assemblage corresponds to the maximum P-T assemblage found in the ultramafites in the region (Bucher-Nurminen 1988). Several of the lithological varieties occurring within the body are not distinguished on the map while other more easily mappable assemblages are shown. Within a limited area in the NE (Fig. 3) up to ca. 10 cm long En-prisms and splinters occur without preferential orientation but evenly distributed in a Fo-Tr-(Mgs)-(Tlc) groundmass. Large jack-straw-textured olivines which are abundant in the metaperidotites in the Nord-Helgeland region (Bakke & Korneliussen 1986) were however not found in the Ørnstolen lens. Other varieties include, at loc. 2, (Fig. 3) an En-Fo assemblage only slightly altered to Tlc, Chl and Mgs; at loc. 3, a Fo-Tr-Mgs rock with subordinate En-relics and with some Tlc and Chl, and a coarse grained En-Fo rock in which En is partly altered to talc (also at loc. 3). At loc. 6 there is a Fo-Tr-(En) rock with very strong chloritization of the Fo. In the southern part of the Ørnstolen body a pyroxene and amphibole-rich assemblage can be distinguished from the other rock-types. A sample from loc. 17 shows a coarse-grained Ca-rich pyroxene (augite?) partly altered to amphibole (Tr) with some Fo and Mgs developed. The cpx may be a primary magmatic mineral only partly altered to a secondary assemblage. The magmatic precursor has probably been a clinopyroxenite or websterite. In a 2-3 m wide border-zone against the enclosing garnet-micaschist there is a black, plagioclase-bearing hornblendite (outermost) followed inward by a green, plagioclase-free variety.

Six small, medium-grained, granular pale yellowish presumably pure forsterite pods were located within the more coarse-grained and fibrous lithologies, see Fig. 3. Five very small chromitite occurrences were located, four in the Fo-En-Tr- bearing rocks, and one in one of the pale yellowish forsterite pods. At three of these five occurrences prospecting work was carried out in the 1860's by the chemical factory Leren Chromfabrik which based its production of chromium salts on domestic chromite supplies.

Most of the chromitite remaining in the deposits is low-grade dissemination ore occurring in short parallel bands or more irregular clusters. Small quantities of massive ore remain (e.g. sample KØ4-86). The high-grade ore was usually carefully hand-sorted before it was shiped to the chromium

factory which based its production (mainly) on the best quality ore. Small pods (< 0,5 m across) and thin stringers of in-situ massive or strong dissemination ore outside the claims were also located within the ultramafic body.

Geochemistry and mineralogy of selected samples of chromitites and host rocks

The great variety of the Ørnstolen rocks is reflected in chemical analyses of selected specimens from the body. Chemical analyses of chromitites and different silicate-carbonate lithologies are given in Table 4. The table also includes macroscopic and microscopic descriptions of the analysed samples. The samples in which PGM were determined by microprobe-analyses were not analysed chemically, but a mineralogical description of these is given in Table 5.

Analytical techniques

Polished sections of three chromitite samples and one sample of silicate-carbonate host rock were systematically examined by both transmitted- and reflected light microscopy, in the latter case using 200 x magnification. High-reflectance inclusions were located both in the chromitite and in the host rocks. Further studies of these inclusions with a scanning electron microscope (SEM) and quantitative analyses (mainly WDS) with a Jeol 733 microprobe carried out at the Continental Shelf and Petroluem Technology Research Institute (IKU), Trondheim, Norway confirmed that the inclusions were PGM, base-metal sulphides (BMS) and a sulpharsenide.

Description of the inclusions and results of analyses

Eight microprobe-analyses were performed on the inclusions found, and the results are listed in Table 6. More of these inclusions were composite: both a two-phase PGM-inclusion, a BMS/PGM-inclusion and two BMS/sulph-arsenide-inclusions were determined in addition to single-phase inclusions.

A synthesis of the mineral assemblage found is given in Table 7.

Laurite

A 7 μm large, euhedral (prism-shaped) inclusion of Os-free laurite was located in chromite clearly removed from the nearest cataclastic fracture (Fig. 5A, B). A somewhat darker shade in this part of the host chromite grain which becomes gradually lighter in other areas of the grain indicates that the PGM is situated in the least altered or unaltered part of the chromite grain.

Very few examples of the otherwise common and distinct edge-sharp chromite/ferritechromite boundary were found in the Ørnstolen chromitites.

A 16 μm large, subhedral two-phase inclusion composed of Os-bearing laurite and irarsite was also located in the darkest, apparently unaltered part of a chromite grain (Fig. 5 C,D), but in the latter case only 5 μm from the boundary of the host grain.

The chemical composition of both laurites fits well with laurite analyses from the literature (e.g. Cabri 1981, Legendre & Auge 1986).

Irarsite

The irarsite mentioned in the former section makes up the smaller part of the two-phase PGM-inclusion. The occurrence of an As-bearing PGM in apparently primary (fresh) chromite is noteworthy. It indicates that As was available in PGM-formation also prior to chromite formation. Usually As is abundant in secondary (hydrothermal) PGM, but it is rare in primary PGM. Though the texture indicates a primary inclusion, a secondary (hydrothermal origin should not be completely ruled out. The microprobe analysis (No. 3 in Table 6) shows a normal irarsite composition, in this case weakly Rh-enriched, but low in Os, Ru and Pt.

Pd-Bi phase (? sobolevskite PdBi)

A minute anhedral PGM-grain (≈ 2 µm) associated with gersdorffite, pentlandite and pyrrhotite was detected in a polished section of the host silicate rock (Fig. 5 I,J). The PGM-grain is situated in the silicates close to a composite grain of base-metal sulphides. Due to its size the quantitative analysis of the PGM (analysis 4 in Table 6) naturally shows a poor total with a substantial contribution from the adjoining silicates. The recalculated analysis gives a good approximation to stoichiometry, and the structural formula $(Pd_{0,98}\ Pt_{0,02})_{\leq 1.00}\ (Bi_{0,64}\ Au_{0,28}\ Te_{0,08})_{\leq 1.00}$ seems to indicate the rare PGM sobolevskite (Cabri 1981, p. 157).

Base-metal sulphides (BMS) and Ni-sulpharsenide

A 20 µm large anhedral-subhedral composite inclusion of millerite, gersdorffite and secondary sulphides was detected in ferritechromite (?) close to a grain boundary possibly separating primary chromite from secondary ferritechromite, suggesting a secondary origin for the inclusion (Fig. 5 G,H). The difference in reflectance between the two oxide phases is however very small.

In polished section no. AK-3B of the host silicate-carbonate rock a minute Pd-Bi grain (earlier described) was detected in association with gersdorffite, pentlandite and pyrrhotite (Fig. 5 I,J). The main grain in the (grain-) aggregate consists of pentlandite hosting pyrrhotite-lamellae. NiAsS occupies a small part of the main grain. The small grain close to the PGM also consists of pyrrhotite and ?pentlandite. The whole assemblage is anhedral and measures 140 µm across.

Four individual euhedral-subhedral inclusions of pentlandite were detected as primary inclusions in fresh (unaltered) chromite (Fig. 5 E,F). The composition of one of these pentlandites, measuring 4 x 3 µm, is given in analysis 8 in Table 6. This analysis shows a PGE-free pentlandite with a considerable Ni-excess relative to Fe, typical of ptl-inclusions hosted in

ophiolite chromitite (Auge 1989).

Discussion

The anomalous Pd, Au and Pt-values detected in one of five chromitite samples from Ørnstolen during the pilot study (Table 1 and 2) were not confirmed by the subsequent PGE follow-up analyses (Table 3) nor by a search for PGM in sections of other follow-up samples (Table 6 and 7). On the contrary the follow-up analyses of chromitites and host rocks all gave low or very low PGE-contents (Table 3). Further only "normal" Os-Ir-Ru-enriched, primary PGM-inclusions were detected in other follow-up samples of chromitite, no Pd-, Au- or Pt-bearing phases of significance. Only a single, minute Pd-Bi inclusion in a host silicate-carbonate rock points to the presence of a Pd-Au-Pt rich PGM-assemblage (Table 6 and 7). Eventual Pd-Au-Pt rich phases are assumed to belong to a secondary PGM-assemblage. The occurrence of the Pd-Bi phase within a completely altered silicate-carbonate rock supports this viewpoint. Unfortunately there were no reference materials available for PGM-studies of the Pd-Au-Pt rich sample (no AK4) after a follow-up analysis of this one which included all six PGE + Au (see Table 2).

In ultramafic tectonite bodies and ophiolites the PGE except for Pd are generally enriched in chromitite relative to the host rocks. The samples in Table 3 shows on average a 3.5 x enrichment of PGE_{TOT} in chromitite relative to the host silicate-carbonate rocks. The Pd-values have however about the same level in chromitites and host rocks. From several places both domestic (e.g. Osthammeren) and foreign (e.g. Oregon, Stockman & Hlava 1984) it has been documented that Os, Ir, Ru, and somestimes Pt, are enriched in massive chromitite compared to different types of impregnation ore such as schlieren-ore, fine-banded impregnation, leopard-ore and fine-grained dissemination ore. One should therefore expect to find the highest grades of these elements in the richest chromium-ore. Unfortunately there was not much rich, massive ore left at Ørnstolen, and the best chromitite-samples analysed must be characterized as belonging to a strong impregnation-/massive ore transition type. The SiO_2-values which directly reflect the gangue-content in the chromitite are as high as 8.02, 9.00,

10.21 and 19.33 wt % in the four analysed chromitites in Table 3, whereas the four best (i.e. lowest) values from the PGE-rich Osthammeren chromitites are only 1.73, 2.94, 3.27 and 3.44 wt % SiO_2.

The chondrite-normalized PGE-pattern for the Pd-Au-Pt anomalous Ørnstolen sample is peculiar. It resembles the pattern given by samples from the Cliff chromitite occurrence in the Unst ophiolite complex (Prichard et al. 1986, 1987) with a marked Pd-top and enrichment in Pt and Au (see Fig. 6). The Cliff pattern lies however about one order of magnitude above the Ørnstolen-pattern.

The Pd-(Pt)-(Au) enrichment has not yet been explained mineralogically (only the minute (≈ 2 μm) Pd-Bi-rich inclusion gives a weak indication of its presence). With regard to the Cliff occurrence Prichard & Lord (1989) and Ixer & Prichard (1989) have demonstrated the occurrence of PGM-inclusions not only in chromitites, but e.g. in the form of rows of minute Pd-enriched PGM inclusions along cleavage planes and cracks in primary clinopyroxene crystals in the host silicate rock.

The following preliminary conclusions can be made:

1) Pd, Au and Pt seem to be very locally strongly enriched in chromitite.
2) There are no anomalous Os, Ir, Ru or Rh-enrichments in any one of the analysed chromitites. Only a few small Os-Ir-Ru rich PGM inclusions in chromite are identified.
3) There are no clearly anomalous values of PGE or Au in the host silicate-carbonate rocks though weak enrichments of Pt and/or Pd occur in these samples. One single, minute sulfide-associated Pd-Au rich inclusion in a silicate-carbonate rock however testifies to the presence of a Pd-Au-Pt rich assemblage in these rocks, and indicates that the Pd-Au-Pt anomaly found in a chromitite may be a hydrothermal enrichment situated in the gangue or in late metamorphic (cataclastic) cracks in the chromite grains.

A geochemical and mineralogical explanation of the unusual Pd-Au-Pt anomaly should be further sought for scientific reasons: there is definitely no economic potential in the Ørnstolen body.

References

Auge, T. 1988: Platinum-group minerals in the Tiebaghi and Vourinos ophiolitic complexes: genetic implications. Can. Mineral. 26, 177-192.

Bakke, S. & Korneliussen, A. 1986: Jack-straw-textured olivines in some Norwegian metaperidotites. Nor. geol. tidsskr. 66, 271-276.

Barnes, S.-J., Boyd, R., Korneliussen, A., Nilsson, L.P., Often, M., Pedersen, R.-B. & Robins, B. 1987a: Geochemistry of platinum metals in rocks and ores in Norway: Pilot project. Draft report. Nor. geol. unders., rapport 87.021, 50 pp.

Barnes, S.-J., Boyd, R., Korneliussen, A., Nilsson, L.P., Often, M., Pedersen, R.B. & Robins, B. 1987b: The use of noble and base metal ratios in the interpretation of ultramafic and mafic rocks; examples from Norway. Abstract, Geo-Platinum 87 Symposium. The Open University, U.K.

Bucher-Nurminen, K. 1988: Metamorphism of ultramafic rocks in the Central Scandinavian Caledonides. Nor. geol. unders. Special Publ. 3, 86-95.

Cabri, L.J. (ed.) 1981: Platinum-group elements: mineralogy, geology, recovery. Can. Inst. Min. Metall., Spec. vol. 23, 267 pp.

Carstens, C.W. 1918: Norske peridotitter I. Nor. geol. tidsskr. 5, 1-42.

Gee, D.G., Kumpulainen, R., Roberts, D., Stephens, M., Thon, A. & Zachrisson, E. 1985: Scandinavian Caledonides: Tectonostratigraphic Map 1:2 mill. Sveriges geol. unders., seie Ba 35.

Gunn, A.G. 1989: Drainage and overburden geochemistry in exploration for platinum-group element mineralization in the Unst ophiolite, Sheland, U.K. Journ. of Geochem. Explor., 31, 209-236.

Gustavson, M. & Gjelle, S. 1987: Geologisk kart over Norge. Berggrunnskart MO I RANA, M 1:250 000, foreløpig utgave, Nor. geol. unders.

Ixer, R.A. & Prichard, H.M. 1989: The mineralogy and paragenesis of Pt, Pd, Au and Ag-bearing assemblages at Cliff, Shetland. Abstract, 5th Int. Platinum Symp., Helsinki. Geol. Surv. Finl. Bull. 61, p. 40.

Korneliussen, A. 1976: "Malmgeologisk undersøkelse med henblikk på økonomisk utnyttelse av kromittforekomstene på kartbladene Rødøy og Lurøy i Nordland. Unpubl. siv.ing. thesis. Geol. Inst. NTH, 172 pp.

Legendre, O. & Augé, T. 1986: Mineralogy of platinum-group mineral inclusions in chromitites from different ophiolite complexes. In: Gallagher, M.J., Ixer, R.A., Neary, C.R. & Prichard, H.M. (eds.) Metallogeny of basic and ultrabasic rocks. IMM, London, 361-372.

Prichard, H.M. & Lord, R.A. 1989: Magmatic and seconardy PGM in the Shetland ophiolite complex. Abstract, 5th Int. Platinum Symp., Helsinki. Geol. Surv. Finl. Bull. 61, p. 39.

Prichard, H.M., Neary, C.R. & Potts, P.J. 1986: Platinum group minerals in the Shetland Ophiolite. In: Gallagher, M.J., Ixer, R.A., Neary, C.R. & Prichard, H.M. (eds.) Metallogeny of basic and ultrabasic rocks. IMM, London, 395-414.

Prichard, H.M., Potts, P.J., Neary, C.R., Lord, R.A. & Ward, G.R. 1987: Dev elopment of techniques for the determination of the platinum-group elements in ultramafic rock complexes of potential economic significance: mineralogical studies. Report commissioned by the EEC Raw Materials Programme, 162 pp.

Rekstad, J.B. 1925: Geologisk generalkart, blad Træna, M 1:250 000, Nor. geol. unders.

Stockman, H.W. & Hlava, P.F. 1984: Platinum-grup minerals in alpine chromitites from southwestern Oregon. Econ. Geol. 79, 491-508.

Sørensen, H. 1955a: A petrographical and structural study of the rocks around the peridotite at Engenbræ, Holandsfjord, Northern Norway. Nor.

geol. unders. 191, 71-102.

Sørensen, H. 1955b: A preliminary note on some peridotites from Northern Norway. Nor. geol. tidsskr. 35, 93-104.

Sørensen, H. 1979: Metamorphic and metasomatic processes in the formation of ultramafic rocks. In: Wyllie, P.J. (ed.) Ultramafic and related rocks. R.E. Krieger publishing company, Huntington, New York, 204-212.

Vogt, J.H.L. 1894: Beiträge zur genetischen Classification der durch magmatische Differentiationsprocesse und der durch Pneumatolyse entstandenen Erzvorkommen. Zeitschr. für prakt. Geol., 381-399.

TABLE 1

Content of Pt, Pd and Au in ppb in PGE-enriched chromitites compared with normal chromitites from ultramafites in central Norway.

Location		n	Pt	Pd	Au
Osthammeren		1	760	<2	8
Ørnstolen		1	299	1391	718
Skamsdalen		1	178	156	120
Aurtand		1	427	104	5
normal chromitites (=non anomalous to weakly anomalous samples)	a	66	12.0	6.2	10.0
	g	66	6.7	1.8	3.8

a = arithmetic mean, g = geometric mean.
Values below detection limits (<x) calculated as $\frac{x}{2}$.
Detection limits were 3,2 and 1 ppb for Pt, Pd and Au respectively.
Analyst: Caleb Brett Laboratories Ltd., St. Helens, UK
Method: Fire assay and atomic absorption spectrometry

Table 2.
Content of PGE and Au in ppb in chromitite samples from the Ørnstolen ultramafic tectonite body, North central Norway. (Extract of PGE pilot-project results).

Sample no.	Pt	Pd	Au	Os	Ir	Ru	Rh
AK 1	22	74	32				
AK 2	6	<2	138				
AK 3	56	63	11				
AK 4	299	1391	718				
AK 4*	398	1621	832	11	25	41	10
AK 5	7	10	10				

Analyst: Caleb Brett Laboratories Ltd., St. Helens, UK
Method: Fire assay and AAS
* = ICP-MS follow up analysis performed at Memorial University, St. Johns, Newfoundland.

Table 3.
Content of PGE and Au in ppb in chromitite and host ultramafic silicate-carbonate rocks from the Ørnstolen ultramafic tectonite body, North central Norway.

Sample no.	Os	Ir	Ru	Rh	Pt	Pd	Au	
Chromitites								
1 - 1	12	12	42	5.5	4.0	7.0	12	
3 - 1	38	36	54	8.5	160	77	10	
3 - 4	32	27	73	12	5.0	13	4	
9 - 1	62	31	68	9.0	72	32	10	
average	36	26.5	59.3	8.8	60.3	32.3	9	223.2 ppb PGE_{TOT}
Ultramafic rocks								
3 - 2	10	5.5	25	3.5	16	14	8	
3 - 3	4	<0.5	6.5	0.5	2.0	12	10	
6 - 1	2	<0.5	2.5	<0.5	3.5	32	2	
14 - 1	4	<0.5	7.5	1.0	72	32	10	
17 - 1	<2	<0.5	4.0	2.5	15	37	4	
average	4.2	1.3	9.1	1.6	21.7	25.4	6.8	63.3 ppb PGE_{TOT}

Analyst: Analytical Services (W.A.) PTY.LTD., Perth, Western Australia (24-05-88)
Method: Fire assay and ICP-Mass spec'
A detailed mineralogical description of the analysed samples is given in Table 4.

Table 4. Chemical analyses of chromitite-ore and ultramafic host silicate-carbonate rocks from the Ørnstolen ultramafite tectonite lens, North central Norway.

Location/Sample. Element	Main-element values in wt %, trace elements in ppm. chromitites 1-1	3-1	3-4	9-1	ultramafic silicate-carbonate rocks 3-2	3-3	6-1	14-1	17-1
SiO_2	19.33	8.02	10.21	9.00	37.17	47.99	40.17	40.60	50.42
Al_2O_3	3.51	6.61	6.24	12.32	1.44	1.40	2.17	0.43	1.95
Cr_2O_3	21.31	(43.86)	28.23	24.76	1.62	1.07	1.01	0.89	1.03
FeO					4.49	4.80	4.04	8.41	3.66
Fe_2O_3					0.95	1.65	2.37	1.10	0.78
Fe_2O_{3TOT}	20.32	26.77	22.09	21.41					
TiO_2	0.04	0.06	0.13	0.09	0.03	0.01	0.04	0.01	0.04
MgO	28.52	16.61	18.87	14.16	38.78	40.75	34.67	42.96	19.82
CaO	0.12	0.04	0.13	0.05	3.27	0.15	4.52	3.47	19.36
Na_2O	0.19	<0.10	0.13	0.17	0.35	0.33	0.41	0.37	0.42
K_2O	<0.01	<0.01	<0.01	<0.01	0.02	<0.01	0.05	<0.01	<0.01
MnO	0.55	0.36	0.36	0.23	0.14	0.12	0.11	0.17	0.10
P_2O_5	<0.01	<0.01	<0.01	<0.01	<0.01	<0.01	<0.01	<0.01	0.02
H_2O^+	0.41	0.86	1.11	2.69		1.79	7.10	1.34	1.51
H_2O^-	0.02	-	0.05	0.07		0.03	0.40	0.05	0.06
CO_2							0.12	1.45	1.56
LOI					11.37				
TOTAL	101.38	99.18	94.34	103.91	87.57	84.97	99.67	100.23	98.52
Nb	<5	<5	<5	<5	<5	<5	5	<5	<5
Zr	13	14	16	13	14	14	16	12	14
Y	<5	<5	<5	<5	<5	<5	<5	<5	<5
Sr	<5	<5	<5	<5	7	<5	11	11	8
Rb	<5	<5	<5	<5	<5	<5	<5	<5	<5
Zn	513	831	600	809	40	37	22	22	16
Cu	31	6	9	491	6	<5	<5	28	14
Ni	0.31%	0.16%	0.19%	0.16%	0.17%	0.18%	0.17%	0.11%	203
V	168	639	696	702	52	40	35	36	118
Ba	18	16	24	19	<10	10	12	<10	15
Pb	<10	<10	<10	<10	<10	<10	<10	<10	<10
Co	321	345	314	323	82	101	91	138	42

Table 4 (continued)

Description of samples (description of hand-specimens (all samples) plus thin sections (silicate-carbonate rocks only)

CHROMITITES

Location/Sample no. (First number is location number refering to Fig. 3. Second number is sample no. from the actual locality).

1-1: Fine-grained, weak dissemination ore with (?) forsterite gangue.

3-1: Fine-grained ore, transition between strong dissemination and massive ore.

3-4: Strong dissemination/massive ore.

9-1: Strong dissemination ore / massive ore in thin strings and small clusters.

ULTRAMAFIC SILICATE - CARBONATE ROCKS

3-2: Medium- to coarse grained greenish-glassy rock with bright green tremolite-prisms (smaragdite). Forsterite (Fo) - tremolite (Tr) - magnesite (Mgs) assemblage with subordinate remnants of enstatite (En). Some alteration to talc (Tlc) and chlorite (Chl). Estimated composition: ≈ 30 vol.% Fo, ≈ 30% Tr, ≈ 20% Mgs, < 10% En, < 5% Tlc and < 5 % Chl. Observed mineral transitions: Tr → Mgs + Tlc; Fo → Mgs; En → Tlc

3-3: Light yellowish green - pale brown, medium to coarse-grained En-Fo rock with cm-long pale enstatite-sheaves. Estimated composition: ≈ 30% Fo, ≈ 50% En, ≈ 20% Tlc derived from En. Chl rims altered chromite (Chr) grains. Fo developed as a corona between Chr with surrounding Chl and enclosing En.

6-1: Red dark grayish green, medium-coarse grained Fo - (Tr) - (En) rock with some alteration. Estimated composition: ≈ 35% Fo, ≈ 15 % Chl derived from alteration of Fo, ≈ 20% Tr, ≈ 20 % Mgs and ≈ 10% En. Observed mineral transitions: Fo → Chl; Fo → Mgs; Tr → Mgs.

14-1: Medium grained, glassy grayish to bright green Fo -(Tr) - (En) rock with some alteration. Estimated composition: ≈ 70% Fo, ≈ 15% Tr, ≈ 10% Mgs, < 5% Tlc and < 5% (?) En. Observed transitions: Tr → Tlc + Mgs; three intergrown/partly dissolved Tr-crystals, i.e. three generations of unstable Tr.

17-1: Medium grained, patchy dark grayish black to light green Cpx-Tr rock. Estimated composition: ≈ 50% secondary Ca-rich, fine-grained medium-grained amphibole, ≈ 30% primary (?) rel. coarse grained Cpx (augite or diopside), ≈ 10% Fo, ≈ 5% Mgs and < 5 % (?) En. Observed transitions: Cpx → Tr.

Table 5: Mineralogical description of samples investigated by microprobe (see Table 6 and 7).

Sample no.

KØ 1B: Chromitite. Fine-grained, low-grade chromite dissemination in parallel bands. Chromite (Chr) is strongly/totally altered to ferrite-chromite (Fe-Chr). Gangue composed totally of forsterite (Fo).

KØ 2A: Chromitite. Fine-grained, rel. weak chromitite dissemination. Chr strongly altered to F-Chr. Gangue composed of Fo which is partly retrograded. Estimated gangue-composition: ≈ 60 vol-% Fo, ≈ 20% magnesite (Mgs), ≈ 10% talc (Tlc) and ≈ 10% secondary, fine-grained amphibole (? Tremolite (Tr)).

KØ 3B: Medium-grained patchy yellowish - light green Fo -(Tr) rock. Estimated composition: ≈ 70% Fo, ≈ 20% Tr, < 5% Chr, Fe-Chr and Mt and ≈ 5% Mgs.

KØ 4: Chromitite. Transition very strong impregnation/massive ore. Chr is partly fresh and partly altered to Fe-Chr. Estimated gangue-composition: ≈70% Fo and ≈ 30% chlorite (Chl) and a secondary fibrous amphibole.

Table 6
Composition of platinum-group mineral (PGM), sulfide and sulfarsenide inclusions in chromitite and host-rocks from Ørnstolen ultramfic tectonite body, North central Norway.

Analysis no.		1	2	3	4	5	6	7	8
Grain/gr.-aggr.no		4	3	3	10	7	7	7	2
(1)	Os	1.98	18.24	3.05		0.10	0.10		0.12
	Ir	0.36	8.01	53.12		0.13	0.20		0.23
	Ru	57.26	38.38	1.32		-	-		-
	Rh	0.81	1.53	3.61		-	-		-
	Pt	0.38	0.29	0.58	1.16	0.27	0.35		0.28
	Pd				26.45				-
	Au				14.34				
	As	2.80	1.47	24.87		-	40.06		-
	Sb								-
	Bi				34.38				0.12
	Te				2.65				
	S	37.03	39.63	15.21	0.04	34.03	17.47	36.14	33.44
	Pb								0.06
	Ni					52.20	28.74	28.28	40.82
	Co*					1	1.5	2	1
	Cr	2.12	0.97	1.40		2.18	2.56	5.21	0.02
	Fe	0.67	0.53	0.63	1.46	2.54	1.23	17.55	21.16
	TOT	103.41	109.05	103.79	80.48 **	92.45	92.21	89.18	97.24

Analysis no.		1	2	3	4	5	6	7	8
(2)	Os	1.98	18.24	3.05					
	Ir	0.36	8.01	53.12					
	Ru	57.26	38.38	1.32					
	Rh	0.81	1.53	3.61					
	Pt	0.38	0.29	0.58	1.16				
	Pd				26.45				
	Au				14.34				
	As	2.80	1.47	24.87		-	40.06		-
	Bi				34.38				0.12
	Te				2.65				
	S	37.03	39.63	15.21	0.04	34.03	17.47	36.14	33.44
	Pb								0.06
	Ni					52.20	28.74	28.28	40.82
	Co					1	1.5	2	1
	Cr	2.12	0.97	1.40		2.18	2.56	5.21	0.02
	Fe	0.67	0.53	0.63	1.46	2.54	1.23	17.55	21.16
	TOT	103.41	109.05	103.79	80.48	91.95 ***	91.56	89.18 ****	96.62

- element not detected
analysis 1: laurite RuS_2; 2: Os-laurite $(Ru,Os)S_2$; 3: irarsite IrAsS; 4: Pd-bismuthide, possibly sobolevskite PdBi; 5: millerite $Ni_{1-x}S$; 6: gersdorffite NiAsS; 7: violarite or bravoite; 8: pentlandite $(Ni,Fe)_9S_8$
* = EDS-estimate only. ** = low total due to significant contribution from adjoining phases.
*** = estimate 1 % Fe in chromite
****= estimate 2.5 % Fe in chromite
(1): raw analyses in weight percent of the element
(2): corrected analyses due to element interference
(3): analyses recalculated after subtraction of Cr and Fe from host chromite (anal. 1-3 and 5-8) and Fe from host silicate (anal. 4)
(4): atomic concentration calculated from the corrected analyses.

Table 6 (continued)

Analysis no.		1	2	3	4	5	6	7	8
Grain/gr.-aggr.no									
(3)	Os	1.97	16.96	3.00					
	Ir	0.36	7.45	52.20					
	Ru	56.91	35.69	1.30					
	Rh	0.81	1.42	3.55					
	Pt	0.38	0.27	0.57	1.47				
	Pd				33.47				
	Au				18.15				
	As	2.78	1.37	24.44		-	45.64		-
	Bi				43.51				0.12
	Te				3.35				
	S	36.80	36.85	14.95	0.05	38.34	19.90	44.36	34.62
	Pb								0.06
	Ni					58.80	32.74	34.71	42.26
	Co					1.13	1.71	2.45	1.04
	Fe					1.73		18.47	21.90

Analysis no.		1	2	3	4	5	6	7	8
(4)	Os	0.59	5.36	1.40					
	Ir	0.11	2.33	24.03					
	Ru	31.81	21.22	1.14					
	Rh	0.44	0.83	3.05					
	Pt	0.11	0.08	0.26	1.16				
	Pd				48.38				
	Au				14.17				
	As	2.10	1.10	28.86		-	33.53		-
	Bi				32.07				0.03
	Te				4.04				
	S	64.85	69.08	41.26	0.24	53.21	34.17	58.95	48.86
	Pb								0.01
	Ni					44.56	30.17	25.19	32.57
	Co					0.85	1.60	1.77	0.80
	Fe					1.38		14.09	17.74

Table 7

Paragenesis of platinum-group-mineral (PGM), base metal sulfide (BMS) and sulfarsenide inclusions in chromitites, and a host ultramafic silicate rock, Ørnstolen ophiolitic tectonite body, north central Norway.

	polished section no.	KØ-1B		KØ-2A	KØ-4					KØ-3B	
	grain/grain-aggregate no.	1	2	3	4	5	6	7	8	9	10
PGM-phases	laurite RuS_2				O						
	Os-laurite $(Ru, Os)S_2$			O							
	irarsite IrAsS			O							
	$(Pd_{0.98}Pt_{0.02})_{\leq 1.00}$ $(Bi_{0.64}Au_{0.28}Te_{0.08})_{\leq 1.00}$? sobolevskite										?●
BMS and sulfarsenide	pentlandite $(Ni, Fe)_9S_8$		?O			O	O		O	?O	O
	bravoite $(Ni, Fe)S_2$ and/or violarite $FeNi_2S_4$							●			
	heazlewoodite Ni_3S_2	●									
	pyrrhotite $Fe_{1-X}S$										O
	gersdorffite NiAsS							O			O
	Millerite $Ni_{1-X}S$							O			

O = primary euhedral/subhedral inclusion
● = secondary and/or altered anhedral grain/grain-aggregate

section 1B, 2A and 4 are chromitites
section 3B is a host ultramafic silicate rock to the chromitites

CAPTIONS FOR FIGURES

Fig. 1. Location of the Ørnstolen ultramafic body within the Scandinavian Caledonides. The location of the PGE/PGM-rich Osthammeren serpentinite lens referred to in the text is also shown.

Fig. 2. Simplified geological sketch map of the Hestmona-Rødøy district, North-Helgeland region showing the location of the Ørnstolen body (arrow) and neighbouring ultramafic tectonite bodies (black) hosted in Caledonian metasedimentary rocks (micaschists and micagneiss) (inclined line). Precambrian to Cambro-Silurian granitic gneisses, etc. (non-patterned areas). Map compilation based on Gustavson & Gjelle (1987) with some ultramafic bodies from Korneliussen (1976) and Rekstad (1925).

Fig. 3. Simplified litological map of the Ørnstolen body showing chromitite occurrences and sample locations described in the text. Key to map symbols: non-patterned areas in ultramafite: Forsterite (Fo) - Tremolite (Tr) - Enstatite (En) rock; horizontal line: isolated Fo-pods/lenses; fine-dotted area: Fo-Tr-magnesite (Mgs) rock with disseminated large En-needles; vertical line: Tr-altered clinopyroxenite/olivine websterite; inclined line: transition area; dashed line: host micaschist/micagneiss; brick pattern: calcite marble horizon.
✖ = worked chromitite (Chr) occurrence; ● = unworked Chr-occurrence;
◉ = main hand-sorting place; o = sample location in silicate-carbonate rock. Numbering refer to samples tabulated or described in the text.

Fig. 4. A: Dismembered schlieren and pods of chromitite (Chr); B: alternating Chr and silicate-carbonate layers; C: remaining low-grade Chr-mineralization at loc 1 in Fig. 3; D: En-prisms and splinters in a Fo-Tr-(Mgs)-(Tlc) groundmass; E: sample of fine-grained Chr-dissemination; F: sample of strong dissemination/ massive ore (transition type).

Fig. 5. Photomicrographs (A - I) and back-scattered electron images (BEI) (J-L) of PGM, BMS and sulfarsenide inclusions in chromite (Chr) and host rock. Grain numbering refer to Table 6 and 7. A, B: Os-free laurite prism in Chr (grain no. 4); C, D: composite inclusion of Os-laurite and irarsite in Chr (3); E, F: pentlandite inclusion in Chr (6); G,H: composite BMS/sulfarsenide inclusion in Chr (7); I: composite PGM, BMS, sulfarsenide grain-aggregate hosted in silicate-carbonate rock (10); J: Pd-Bi phase (1), pentlandite (2), pyrrhotite (3) and gersdorffite (4), in grain-aggr. no. 10; K: irarsite (1), Os-laurite (2), not identified (3) in grain no. 3. L: millerite (1), gersdorfite (2) and bravoite/violarite (3) in grain no. 7.

Fig. 6. Chondrite-normalized PGE-patterns of Ørnstolen chromitites and ultramafic rocks; data for Cliff, Shetland from Prichard et al. (1987) and Gunn (1989).

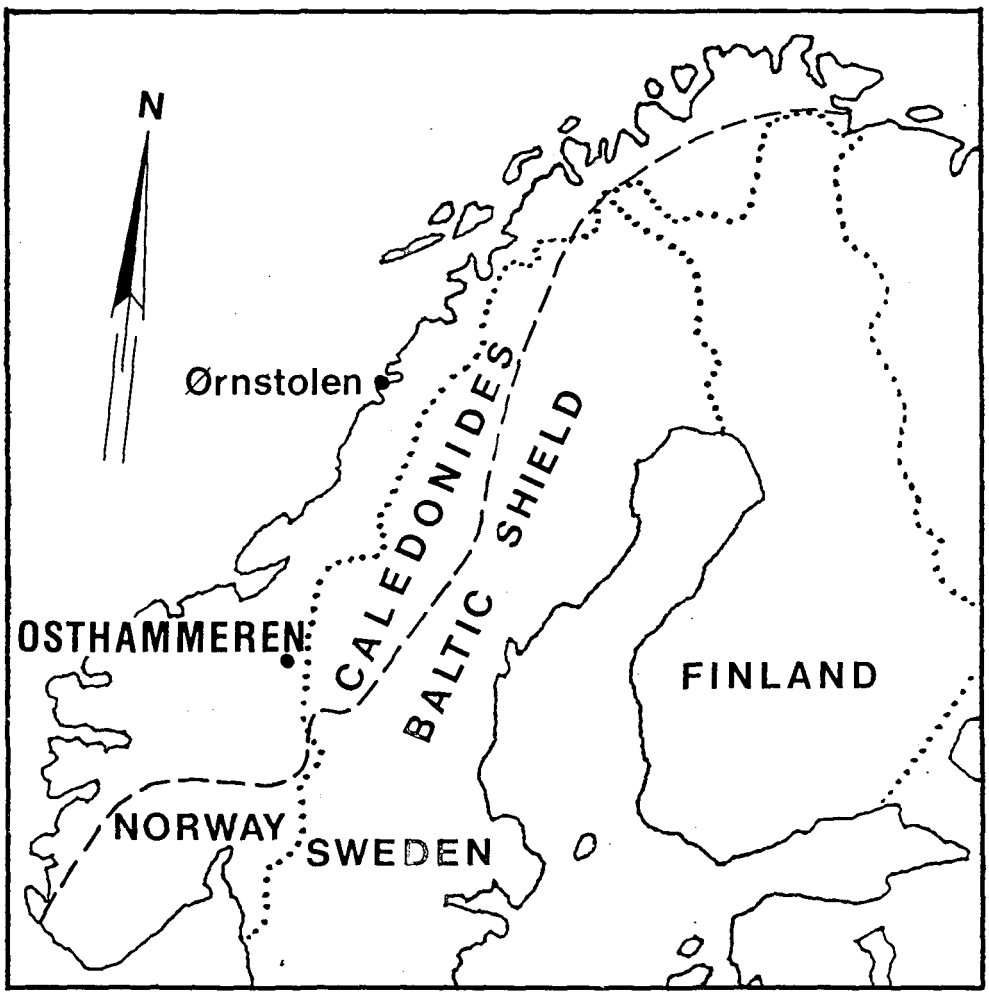

Fig. 1

Fig. (1) Nilsson

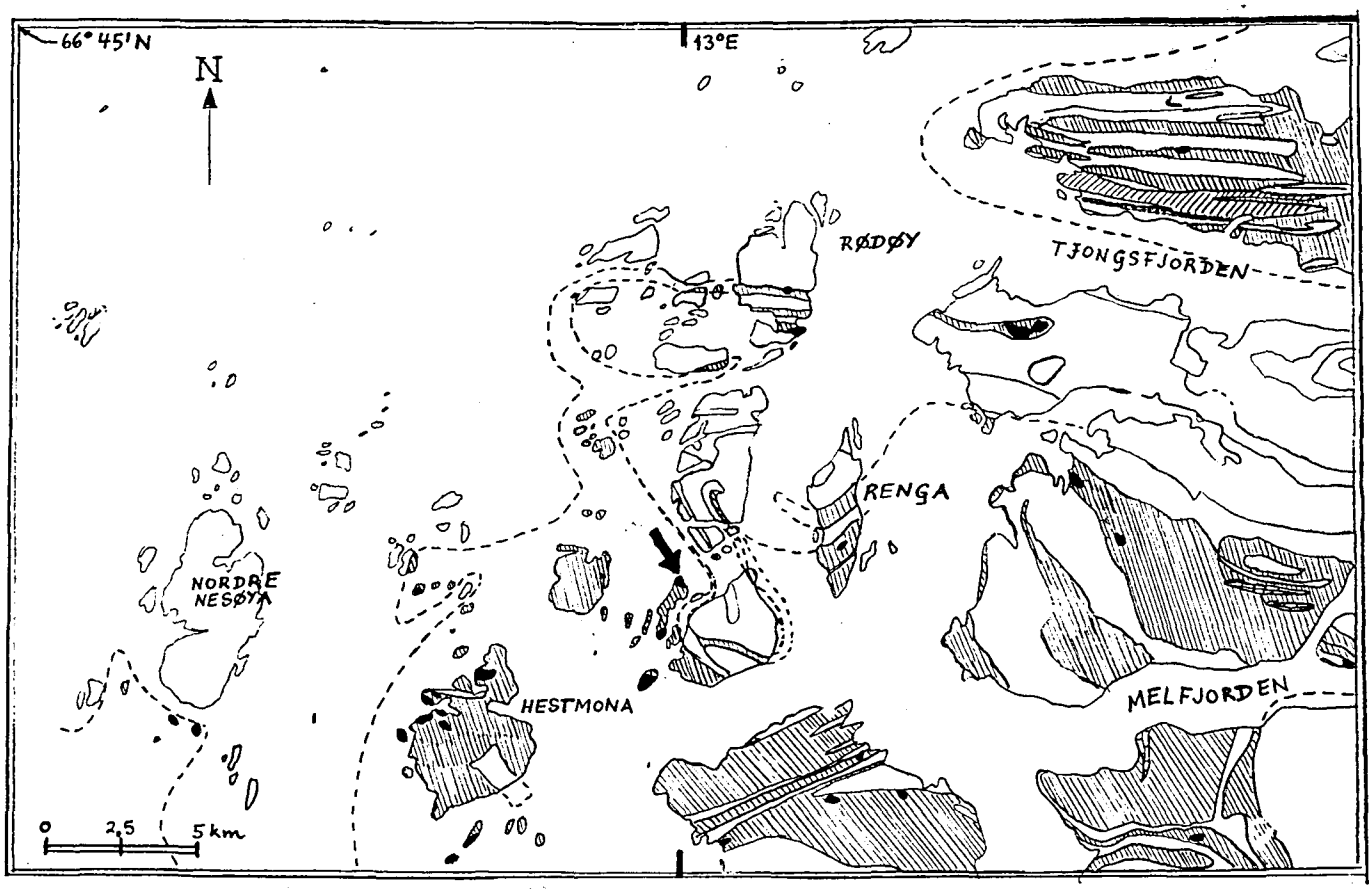
66°45'N
13°E
N
RØDØY
TJONGSFJORDEN
RENGA
NORDRE
NESØYA
HESTMONA
MELFJORDEN
0 2,5 5 km

Fig. 2.

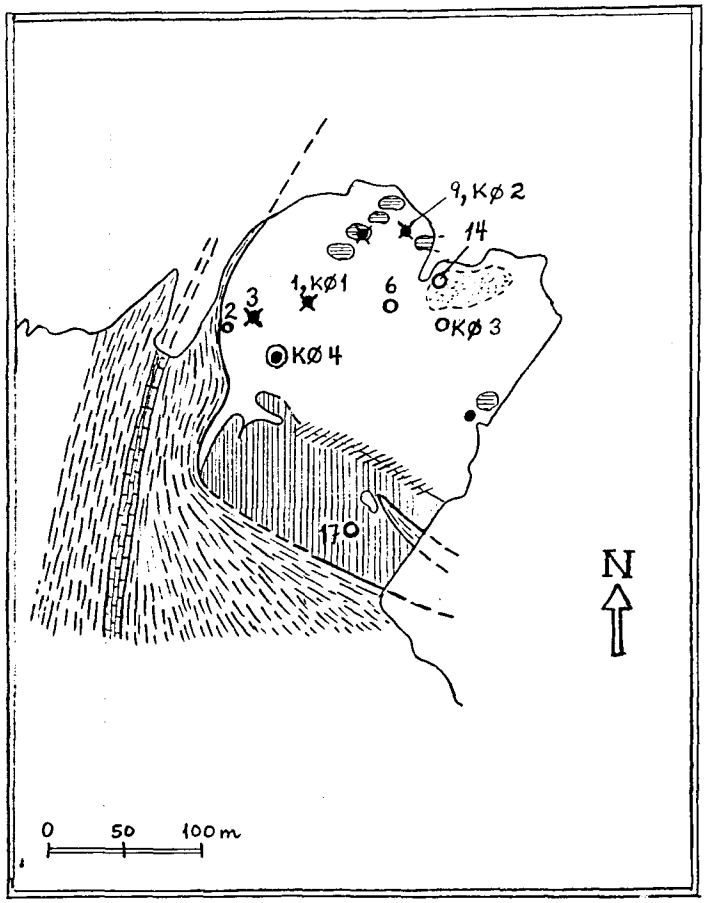

Fig. 3

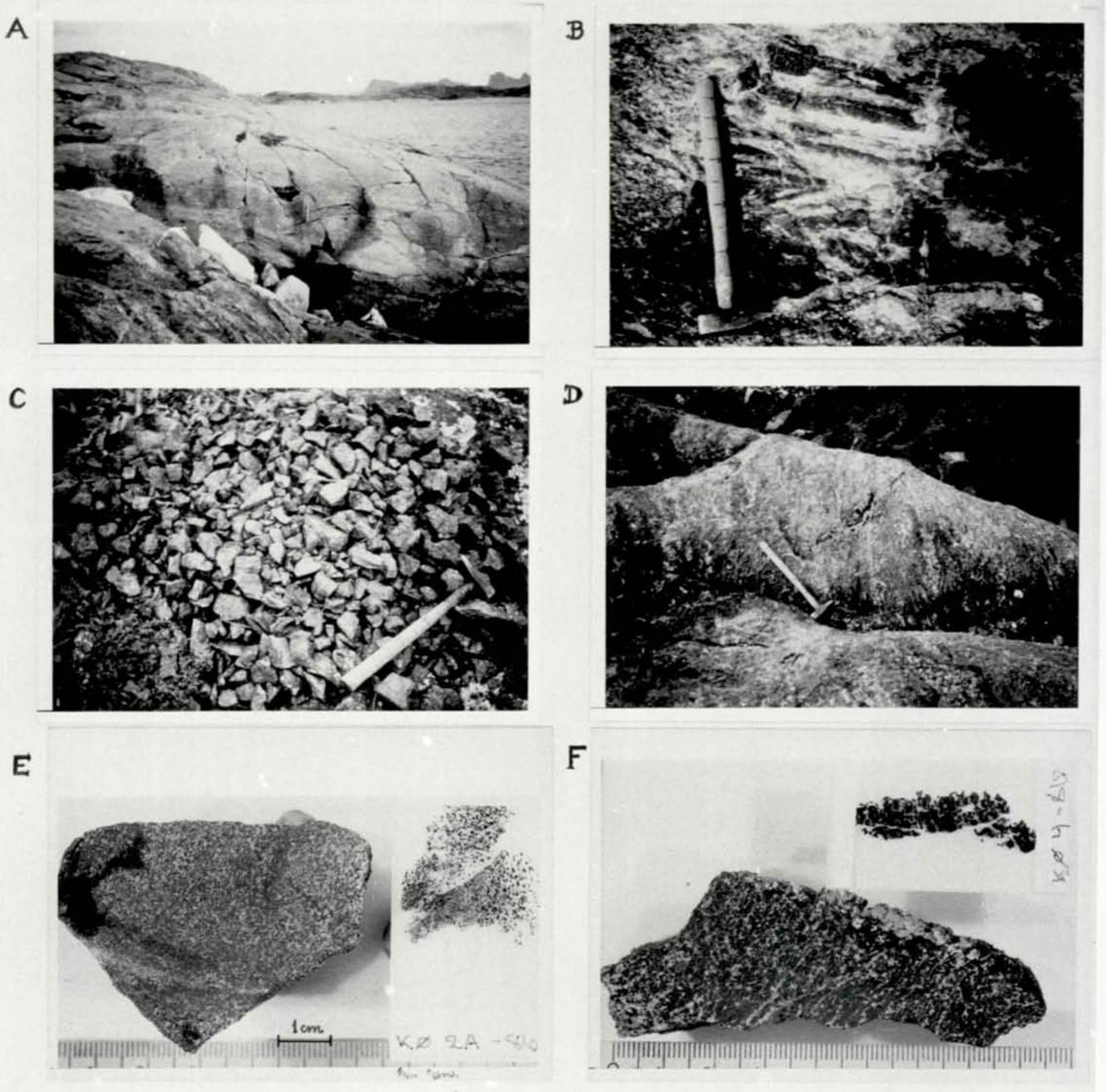

Fig. 4

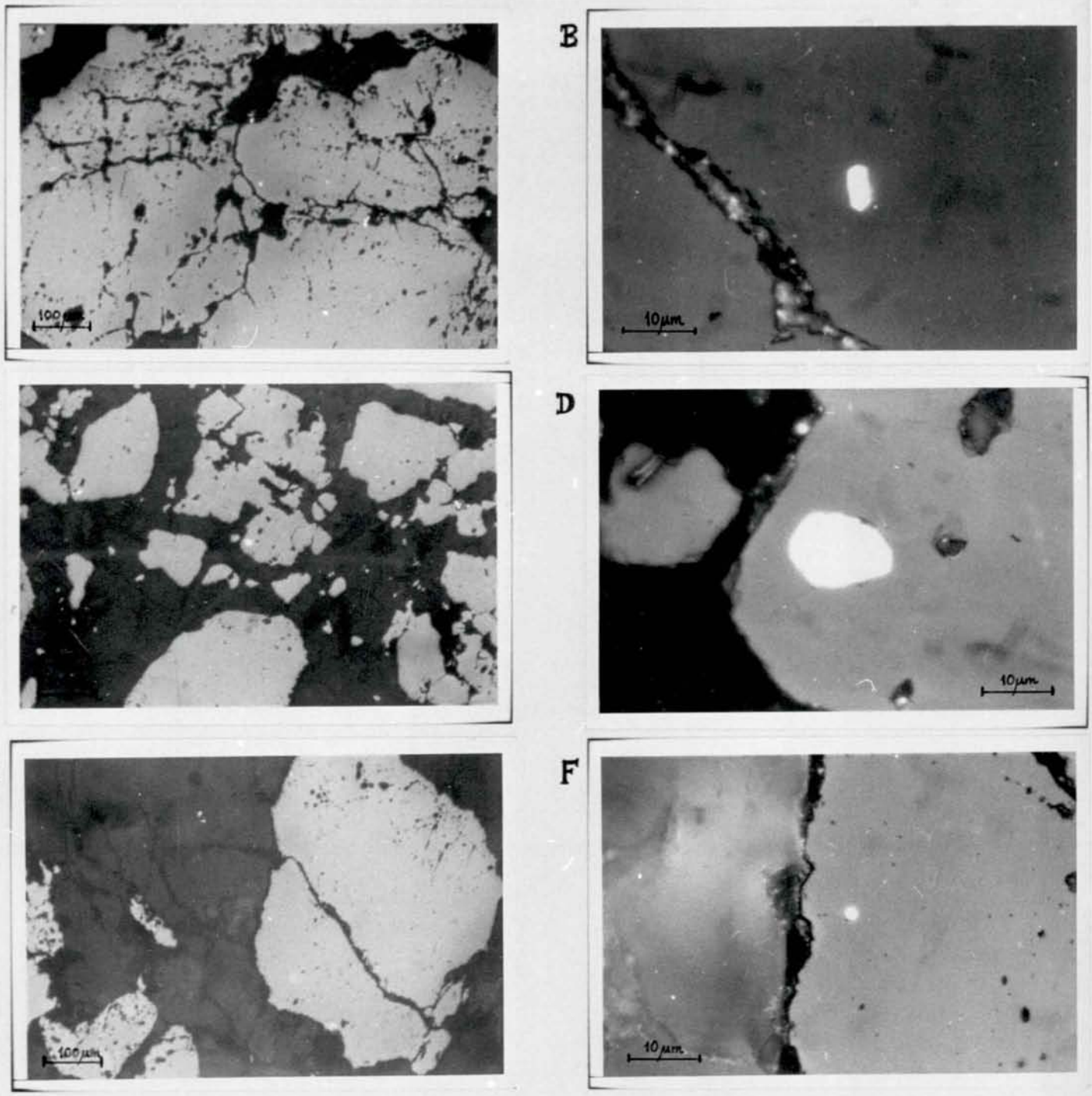

Fig. 5

G

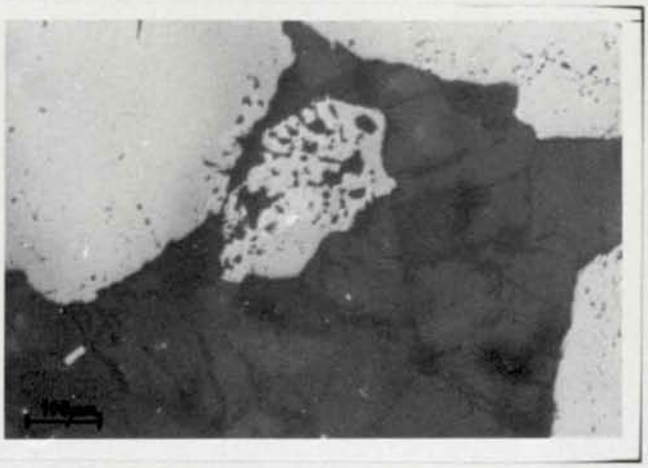

H

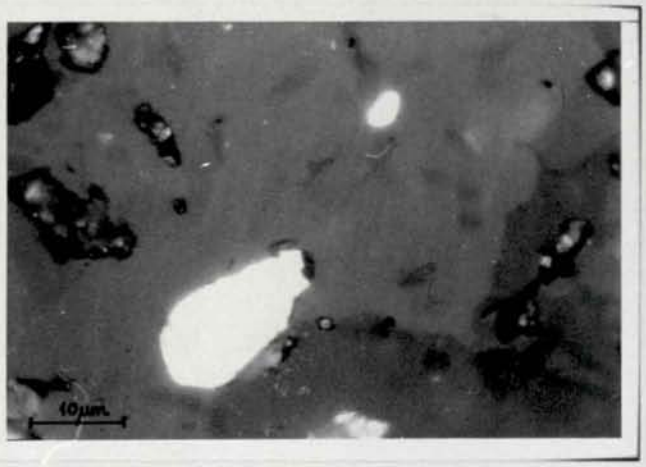

I

J

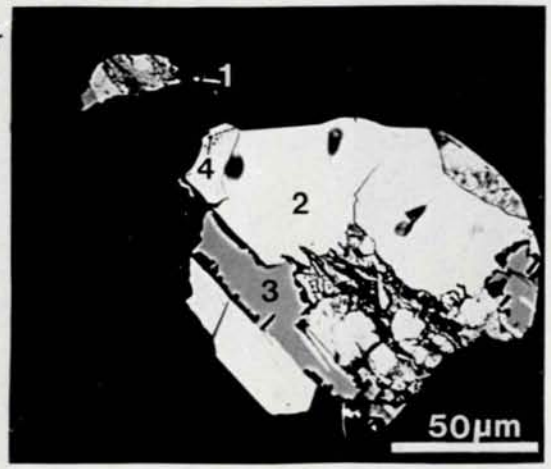

K

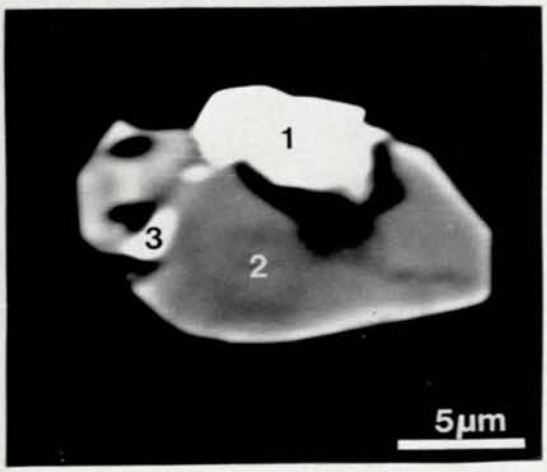

L

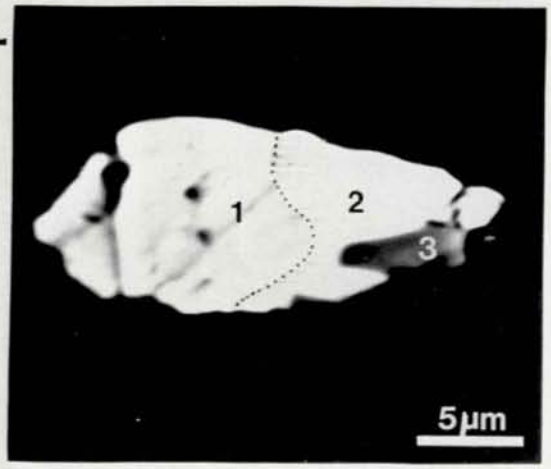

Fig. 5 (cont.)

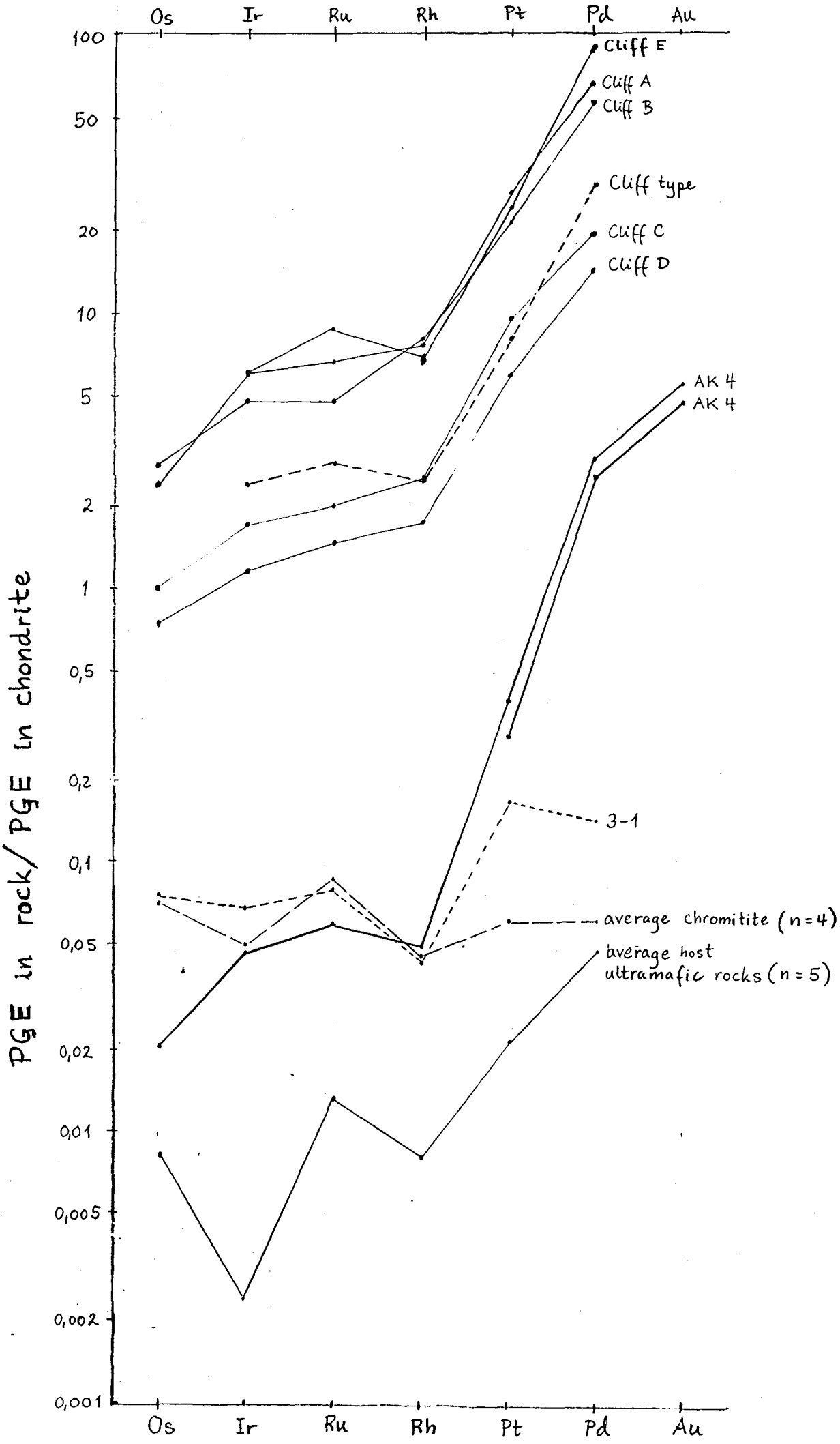
Os
Ir
Ru
Rh
Pt
Pd
Au
100
50
20
10
5
2
1
0,5
0,2
0,1
0,05
0,02
0,01
0,005
0,002
0,001
PGE in rock/ PGE in chondrite
Cliff E
Cliff A
Cliff B
Cliff type
Cliff C
Cliff D
AK 4
AK 4
3-1
average chromitite (n=4)
average host ultramafic rocks (n=5)

Fig. 6

2.4 Hydrothermal gold-enriched iron and iron-copper occurrences in the Hatten ultramafic tectonite lens, Hattfjelldal by L.P.Nilsson

HYDROTHERMAL GOLD-ENRICHED IRON AND IRON-COPPER OCCURRENCES IN THE HATTEN ULTRAMAFIC TECTONITE LENS, HATTFJELLDAL, NORWAY: A PRELIMINARY REPORT

Introduction

Mineral occurrences composed of magnetite, copper-sulphides and/or iron-sulphides hosted (directly) by serpentinite or by lenses of hydrothermal quartz in serpentinite represent a very rare ore type in the solitary ultramafic tectonite (= serpentinite) lenses in the Scandinavian Caledonides. However in the Hattfjelldal-Krutådal area in the central part of the Caledonides minor mineralizations of these assemblages occur abundantly in ultramafic bodies.

The aim of this account is to give a short field description based on a reconnaissance of the Hatten ultramafic body in 1987 and a presentation of analytical results obtained from the samples collected.

Brief review of earlier work

O.A. Corneliussen (1891) was the first to give a detailed description of the minor iron- and copper-bearing occurrences situated on the top plateau of the very steep-sided ca. 0,7 km^2 large "Hatten" (= the hat) ultramafic tectonite body. Corneliussen mentions pyrrhotite in hydrothermal quartz and chromite ore from the neighbouring ultramafic bodies.

J.H.L. Vogt (1894) treats these occurrences in one of his larger works dealing with classification of ore deposits. He states that they resemble the "Monte Catini type" of Cu mineralization in serpentinite or ophiolitic rocks known from Tuscany, Italy and several other occurrences in the Mediterranean countries. In accordance with his view of ore deposit formation in general Vogt keeps the possibility open for a magmatic differentiation process also in this case.

G. Holmsen (1913) was the first to undertake a regional geological mapping of the whole Hattfjelldal area. He discovered most of the ultramafic bodies in the area and mapped the outline of these. Holmsen further recognized what he interpreted as

several generations of intrusions of ultramafic magma, namely (serpentinite) dykes surrounded by schistose serpentinite within the ultramafites.

The files of the NGU-Bergarkivet (archives) show that 15 showings of iron-copper mineralization and 3 chromite showings in the Hatten body were reported to the mine superintendant in the years 1860 and 1874. Corneliussen (l.c.) reports work done at two of the iron-copper showings only. In addition six pyrite showings are reported from the Gryttined body on north side of the Krutvassdalen. Several of the ultramafic bodies are indicated on the geological map-sheet Hattfjelldal, scale 1:50 000 (Dallmann 1986), based on mapping by W.K.Dallmann and L.K. Stølen. Stølen, who treated the ultramafic bodies in a cand. scient. thesis (Stølen 1985), has found cumulate chromite enrichments in the Røddiken ultramafic body close to the Røssvatnet lake, and further chromite mineralization in a serpentinite body south of Grensetjern close to the Swedish border. In this same area (Krutådal) several Pb-occurrences are reported in the phyllites hosting the serpentinite bodies, and this whole region (of the Caledonides) hosts a number of significant Zn-Pb, Pb-Zn and Pb-Ag-(barite) deposits.

A platinum analysis of chromium ore from "Hatfjeld" (=Hatten) giving 0.83 ppm Pt has been reported (Lunde & Johnson 1928). There are, however, no precise locality descriptions of the 3 chromite showings on the Hatten body or of any of the other ultramafic bodies in the area. None of the 3 chromite showings on the Hatten body were therefore found during the present author's reconnaissance.

Distribution, setting and constitution of the ultramafic tectonite (serpentinite) bodies

All the ultramafic bodies in the Hattfjelldal area are situated in the eastern part of the area, within the Joesjö Nappe (Dallmann 1986). This nappe is a part of the Lower Köli Nappe Complex which in turn represents the upper part of the Upper Allochthon (Gee et al. 1985).
The ultramafic bodies are hosted in phyllites, greenstones and greenschists (Gustavson 1981, Dallmann 1986). The Lower Köli Nappes are thought to represent a single, possibly composite terrane (the Virisen terrane of Stephens & Gee (1985)) comprising bimodal volcanic rocks related to an ensimatic rifted-arc development. These are associated with various phylites and both solitary ultramafic complexes and detrital ultramafites (Stephens et al. 1985, Stephens & Gee 1989).

The Hattfjelldal ultramafites and host rocks are metamorphosed under greenschist facies conditions producing a partial or total serpentinization of the primary olivine and olivine-pyroxene rocks. The smaller bodies generally show stronger alteration than the larger ones, the inner parts of which show primary minerals.

The Hatten body seems to represent a fragment of harzburgite. A single 50-100 m wide and ca. 700 m long dunite body transects the harzburgite on the top plateau of Hatten in an E-W direction. Towards the west this body divides in two major branches one of which crops out in the ca. 200 m high vertical southern cliff of Hatten. The outcrop of the Hatten ultramafite with its 330 m difference in altitude between the lowest and highest points provides an excellent three-dimensional view of the lens-shaped body which measures ca. 600 x 1200 m in horizontal section.

The dunite body interfingers with the harzburgite on a local scale producing what locally resembles magmatic layering. Generally, however, the border is quite irregular, leaving no doubt that the dunite is "intrusive" into or crosscuts the harzburgite.

The harzburgite and dunite both, of which are strongly or totally serpentinized are easily distinguishable even at a considerable distance. The former weathers with a greyish-brown colour, the latter brownish-red (almost brick-red).

Shear-zones on the Hatten plateau and their associated iron- and iron-copper mineralizations

On the Hatten plateau several parallel, very fine stipes or fissures to coarser joints, etc. (probably) representing shear zones run approximately WNW-ESE, parallel to a more or less well-developed cracking of the serpentinized rocks. Of the earlier workers dealing with the geology of Hatten only Suhrland (1861, page 232) has emphasized these structures.

Several quite small occurrences of magnetite and magnetite plus copper-sulphides are associated with the shear zones which seem to postdate the sepentinization of the ultramafite. Newly formed serpentine has individual crystals oriented along the smaller and larger lineaments making up the shear zones. Due to heavy overburden on the neighbouring phyllites the writer was not able to acertain whether the shear zones could be traced from the ultramafite into its host rocks.

Six of a total of 15 reported showings on the Hatten body were visited, and five were sampled for chemical analysis (loc. 1 - loc. 5). The dunite and harzburgite were also sampled (see Table 1). A small collection of samples were first analyzed for Au and PGE at Analytical Services (W.A.) PTY.LTD in May 1988, see Table 2.

Table 1. Mineralized and unmineralized locations sampled on the Hatten solitary ultramafite, Hattfjelldal, Norway.

Loc.	1	mt - (Cu-sulphide mineralization)	
	2	mt - (Cu-sulphide ")	Cu-richest
	3	mt	
	4	mt - (Cu)	
	5	mt - (Cu)	
	(6)	mt	not sampled
	7	serpentinized dunite	
	8	serpentinized harzburgite	

Table 2. Content of Au and PGE in ppb in samples from the Hatten solitary ultramafite, Hattfjelldal, Norway

Loc./sample	Os	Ir	Ru	Rh	Pt	Pd	Au
1	2	2.0	<0.5	1.5	160	11	250
DUP	110	10	2.0	2.5	120	6.5	240
2	2	1.0	<0.5	1.5	<0.5	17	550
DUP	100	9.0	4.5	4.0	7.5	12	530
5	<2	0.5	4.0	1.5	2.0	12	200
DUP	80	8.5	4.5	3.5	4.5	11	190
7	4	2.0	15	1.0	7.0	7.0	6
8	4	2.0	10	2.0	4.5	7.0	<2

Table 2 shows that the mineralized samples are enriched in Au, though the values are only qualitative, and to a lesser degree in Pt (sample 1 only). The duplicate values for Os and Ir are not reliable.

Table 3. Analyses of magnetite and Cu-sulphide mineralized samples from the Hatten solitary ultramafite, Hattfjelldal, Norway.

ACME ANALYTICAL LABORATORIES LTD. 852 E. HASTINGS ST. VANCOUVER B.C. V6A 1R6 PHONE(604)253-3158 FAX(604)253-1716

GEOCHEMICAL ANALYSIS CERTIFICATE

ICP - .500 GRAM SAMPLE IS DIGESTED WITH 3ML 3-1-2 HCL-HNO3-H2O AT 95 DEG. C FOR ONE HOUR AND IS DILUTED TO 10 ML WITH WATER. THIS LEACH IS PARTIAL FOR MN FE SR CA P LA CR MG BA TI B W AND LIMITED FOR NA K AND AL. AU DETECTION LIMIT BY ICP IS 3 PPM.
- SAMPLE TYPE: P1-P7 CRUSHED ROCK P8 ROCK P9 ROCK PULP AU* ANALYSIS BY ACID LEACH/AA FROM 30 GM SAMPLE.

Geological Survey of Norway FILE # 89-4750.

SAMPLE#	Mo PPM	Cu PPM	Pb PPM	Zn PPM	Ag PPM	Ni PPM	Co PPM	Mn PPM	Fe %	As PPM	U PPM	Au PPM	Th PPM	Sr PPM	Cd PPM	Sb PPM	Bi PPM	V PPM	Ca %	P %	La PPM	Cr PPM	Mg %	Ba PPM	Ti %	B PPM	Al %	Na %	K %	W PPM	Au* PPB
89362 1A	16	99999	70	292	.1	92	1	109	10.86	2	5	ND	1	1	1	5	87	17	.01	.001	2	76	4.09	1	.01	2	2.14	.01	.01	1	11
89363 1B	4	98684	46	243	3.6	285	30	285	28.46	2	5	4	2	1	1	11	2	6	.01	.002	2	2	.89	1	.02	5	.45	.01	.01	1	3260
89364 1C	2	11739	8	65	1.2	800	69	164	6.82	8	5	ND	1	1	1	2	2	9	.01	.001	2	274	9.28	1	.01	22	.41	.01	.01	1	60
89365 2A	1	77945	35	198	16.6	2422	166	545	18.39	5	5	ND	1	1	11	7	5	6	.01	.003	2	177	7.21	1	.01	42	.05	.01	.01	1	390
89366 2B	1	66232	72	168	14.7	1069	87	547	28.49	2	5	3	2	1	2	10	2	9	.01	.001	2	202	2.23	1	.01	14	.04	.01	.01	1	1700
89367 2C	1	99999	49	431	30.8	1052	81	420	10.41	7	5	ND	1	1	65	5	14	1	.02	.015	2	192	6.07	1	.01	30	.11	.01	.01	5	280
89368 2D	1	53911	26	132	9.3	927	51	496	16.28	2	5	ND	1	1	9	8	2	8	.01	.001	2	96	7.27	1	.01	44	.03	.01	.01	1	280
89369 2E	1	35258	16	109	6.6	1388	79	571	18.29	3	5	ND	1	1	3	7	2	8	.01	.001	2	639	8.13	1	.01	43	.04	.01	.01	1	290
89370 3	2	61287	28	193	6.0	1618	190	582	34.44	2	5	ND	2	1	1	10	11	2	.01	.001	2	101	.79	1	.01	6	.15	.01	.01	1	50
89371 5A	1	54366	14	144	4.0	1256	115	490	28.51	5	5	ND	2	1	1	12	2	10	.01	.001	2	81	2.72	1	.01	18	.27	.01	.01	1	350
89372 5B	2	22705	21	95	2.5	2940	135	494	22.19	8	5	ND	2	1	1	3	2	16	.01	.001	2	128	6.23	1	.01	24	.13	.01	.01	1	135
89373 5C	1	43726	17	115	4.1	1705	95	491	18.18	4	5	ND	1	1	5	7	2	13	.01	.002	2	304	8.84	1	.01	48	.42	.01	.01	1	108

Sample 1A: mostly cp in silicate (same as sample 1 in Table 2)

Sample 1B: compact Cu-sulphide + mt ore

Sample 1C: weak mt and Cu-sulphide impregnation in serpentinite

Sample 2A: mt-ore with rich Cu-sulphide impregnation (same as sample 2 in Table 2)

Sample 2B: compact mt-ore with rich Cu-sulphide impregnation

Sample 2C: small fragments rich in silicates, Cu-sulphides and malachite with some mt

Sample 2D: rich in silicates, some mt, Cu-sulphides and malachite

Sample 2E: silicates, magnetite, minor malachite and Cu-sulphides

Sample 3 : compact mt, minor silicate and malachite

Sample 5A: compact mt, minor silicate and malachite (same as sample 5 in Table 2)

Sample 5B: silicate, mt, minor malachite

Sample 5C: silicate, mt

Due to the anomalously high Au-content shown by the mineralized samples in the reconnaissance analyses (Table 2) it was decided to analyse a broader collection of the mineralized material sampled from Hatten.

The material was sent to ACME Analytical Laboratores Ltd., Vancouver, Canada in the middle of November 1989 and results reported back Nov. 22nd 1989, see Table 3.

The results in Table 3 confirm the earlier results in a broad sense. Gold is enriched in the iron-copper mineralized material, though irregularly. This may be due to a nugget-effect in the Au enrichment. Table 3 shows that there are no unambigous positive Au-Cu and/or Au-Fe correlations, though the two most Au-rich samples are also rich in both Cu and Fe.

A study of the ore mineralogy is in progress. Table 3 indicates that no minerals are specific accompaniments to Au. Ag, As, Sb and Bi do not occur at anomalous levels and show no positive correlation with Au. Te contents are however not available.

References

Corneliussen, O.A. 1891: Bidrag til kundskaben om Nordlands amts geologi. In: Reusch, H. (ed.) Det nordlige Norges geologi. Nor. geol. unders. 4, 149-189.

Dallmann, W. 1986: Hattfjelldal. Berggrunnskart 1926.2, foreløpig utgave 1:50 000. Nor. geol. unders.

Gee, D.G., Kumpulainen, R., Roberts, D., Stephens, M., Thon, A. & Zachrisson, E. 1985: Scandinavian Caledonides: Tectonostratigraphic Map, 1:2 mill. Sveriges geol. unders., serie Ba 35.

Gustavson, M. 1981: Geologisk kart over Norge, berggrunnskart Mosjøen - M 1:250 000. Nor. geol. unders.

Holmsen, G. 1913: Oversikt over Hatfjelddalens geologi. Nor. geol. unders. 61, 34 pp.

Lunde, G. & Johnsen, M. 1928: Vorkommen und Nachweis der Platinmetalle in norwegischen Gesteinen II. Z. anorg. u. allg. Chem. 172, 167-195.

Stephens, M. & Gee, D.G. 1985: A tectonic model for the evolution of the eugeoclinal terranes in the central Scandinavian Caledonides: In: Gee, D.G. & Sturt, B.A. (eds.) The Caledonide Orogen - Scandinavia and Related Areas, Wiley, Chichester, 953-978.

Stephens, M., Furnes, H., Robins, B. & Sturt, B.A. 1985: Igneous activity within the Scandinavian Caledonides. In: Gee, D.G. & Sturt, B.A. (eds.) The Caledonide Orogen - Scandinavia and Related Areas, Wiley, Chichester, 623-656

Stephens, M. & Gee, D.G. 1989: Terranes and polyphase accretionary history in the Scandinavian Caledonides. Geol. Soc. Am. Spec. Papåer 230, 17-30.

Stølen, L.K. 1985: En geologisk studie av solitære ultramafiske bergarter og omkringliggende metavulkanitter/metasedimenter i Krutådalsområdet, Hattfjelldal, Nordland. Unpubl. cand.scient.thesis, Univ. of Oslo.

Suhrland, R. 1861: Geognostiske og geografiske Bemærkninger samlede paa en Reise til Helgeland 1843. Nyt Mag. f. Nat. vid. 11, 226-240.

Vogt, J.H.L. 1894: Beiträge zur genetischen Classification der durch magmatische Differentiationsprocesse und der durch Pneumatolyse entstanderen Erzvorkommen. Zeitschr. für prakt. Geol., 381-399.

2.5 Platinum group minerals (PGM), gold and associated minerals in the Raudberg field ultramafic tectonites, Vik, Sogn og Fjordane, western Norway by S.Bakke, T.Boassen and L.P.Nilsson.

3. draft

Date 28/03 1990.

PLATINUM GROUP MINERALS (PGM), GOLD AND ASSOCIATED MINERALS IN THE RAUDBERG FIELD ULTRAMAFIC TECTONITES, VIK, SOGN OG FJORDANE, WESTERN NORWAY

Stig Bakke, Tony Boassen and Lars Petter Nilsson.

Bakke, S., Boassen, T. and Nilsson, L.P.: Platinum group minerals (PGM), gold and associated sulphides in the Raudberg field ultramafic complex, Vik, Sogn og Fjordane, Western Norway.

S. Bakke and T. Boassen, Continental Shelf and Petroleum Technology Research Institute, 7034 Trondheim, Norway.
L.P.Nilsson, Norwegian Geological Survey, P.O.Box 3006-Lade, 7002 Trondheim, Norway.

INTRODUCTION

The subsurface size of the Raudberg field ultramafic tectonite complex was discovered as a result of a semi-regional soapstone prospecting program which was started in 1981. The field is situated around the mountain Raudberg 900 to 1100 m above sea level and 8 km south of Framfjord, Sogn og Fjordane, Western Norway (Fig. 1).

Three large and several minor strongly tectonized ultramafic bodies covering about 3.2 km^2 i horizontal section consisting mainly of metadunite, serpentinite and soapstone from the core outwards, were discovered during the program (Fig.2). The economic feasibility of exploiting the very large amounts of soapstone is under assessment at present. In addition the almost pure forsterite dunite and the contents of Ni/Co-sulphides, and -arsenides have been studied with aims to evaluate whether they could contribute to the economy of an eventual mining operation. Moreover, a preliminary study of the contents of PGM in core samples has been carried out.

This paper will document the main results of this preliminary study based on SEM/microprobe investigations of PGM, Au, sulpharsenides, sulphides, arsenides and oxides in heavy mineral concentrates, derived from samples from one of the diamond drill cores from the Raudberg field ultramafic tectonite complex.

GEOLOGICAL SETTING AND CONSTITUTION OF THE ULTRAMAFIC BODIES

The Raudberg field is situated at the western margin of the Caledonides in South Norway, in the Lower Allochthon (Sigmond et al. 1984, Gee et al.

1985), between the Precambrian gneiss basement to the NW and Middle Allochthon Jotun Nappe Complex (Sigmond et al. 1984, Gee et al. 1985) to the SE (Fig. 1). The lower Allochthon consists mainly of different phyllonitic rocks and mica schists with tectonized lenses of amphibolite, gneiss, quartz-shist, trondhjemite(), calcite marble and different types of ultramafic rocks (Lyse 1982). A few hundred meters east of the field the Bulko Nappe (Lyse 1982), the lower sheet of the upper Bergsdalen Nappe (Kvale 1960, Sigmond et al. 1984) wedges out northwards.

Two main and several minor deformation phases have affected the field. The oldest main phase is characterized by tight, almost isoclinal folds with amplitudes of 5 to 10 m and wavelengths of 2 to 5 m and axes extending SW-NE, corresponding to Ingdahl's (1986) F2 with age late Silurian to early Devonian. The youngest main phase is characterized by open folds with axes perpendicular to F2 with amplitudes of 1 to 5 m and wavelengths of 5 to 20 m, corresponding to Ingdahl's (1986) F3. The rocks have suffered retrograde metamorphism after a maximum of approximately lower amphibolite facies metamorphism.

The ultramafic bodies show a common zonation with a dunite core grading into serpentinite and soapstone outwards. The volume fractions of these rocks are dependent on the size of the ultramafic bodies. In general the soapstone mantle is about 8 m and the serpentinite zone 10 to 20 m thick. The rest of the body's core is mainly dunite. This means that bodies with the shortest axis less than about 16 m consist solely of soapstone. The contacts between the ultramafic tectonite bodies and the their country rocks show classical examples of metasomatism as described by e.g. Sanford (1982).

The dunite is mainly white to light grey with Fo 97-98 equigranular olivine grains with magnetite inclusions probably caused by early progressive metamorphism of serpentinite as described by Pactunc (1984). The magnetite pigment causes high magnetic susceptibility in the dunite and partly in the serpentinite. The serpentinite surrounding the dunite is derived from it and consists mainly of antigorite with varying amounts of chlorite, magnesite and/or breunnerite. The serpentinite grades outwards into the soapstone mantle which consists mainly of 60/40 talc/breunnerite. The polyphase metamorphism has destroyed almost all primary structures, only faulted and folded chromitite layers and a few 10 cm thick possible metapyroxenite (?) layers in the serpentinite zone being preserved.

The Caledonian deformation phases have controlled the shape of the ultramafic bodies. The two main phases have forced the extremely incompetent soapstone to flow in a ductile state into low pressure areas and have changed the original about 8 m thick soapstone mantle into a few cm thick zone in high pressure areas and commonly over fifty meters thick concentrations in low pressure areas. Pressure differences are caused by the competence contast between the incompetent phyllonitic rocks and soapstone, and the competent serpentinitic and dunitic parts of the ultramafic tectonites.

Varying amounts of Ni/Co-sulphides and arsenides of different types are found in all the ultramafic rock types. In general the forsteritic dunite core contains mainly heazlewoodite and cobaltite as Ni/Co bearing minerals, the serpentinite mainly gersdorffite and some heazlewoodite, cobaltite and pentlandite occurs, and in the soapstone pentlandite is the main Ni(/Co)-

bearing mineral with minor gersdorffite. The general trend in the ultramafic bodies is that in Ni/Co-bearing sulphides/arsenides As and Ni decreases from the core outwards and S increases. Other Ni/Co sulphides/arsenides observed as accessories are maucherite and millerite in dunite and serpentinite, and linnaeite group minerals in soapstone (Aarflot 1984).

ANALYTICAL TECHNIQUES

Sample descriptions

Four investigated samples were taken from one single drillhole in the SE part of Raudberg ultramafic body (Fig. 2), penetrating sections of dunite, serpentinite and soapstone. Table 1 summarizes the composition of the samples.

Table 1. Composition of drill-core samples selected for noble-metal studies.

Sample no.	Length	Lithology	Mineralogy
1	21.0 m	Dunite	
2	21.9 m	Upper serpentinite	
3	9.2 m	Lower serpentinite	
4	14.1 m	Lower soapstone	

Sample preparation

Sample preparation was performed at NGU's mineralogical lab. Each sample was first crushed in a jaw-crusher, then ground in a disc-mill and sieved. The sieve-fraction < 250 μm was used in the subsequent waterboard separation. The heavy mineral concentrates from the waterboard were treated on a free fall weak-magnetic-field separator for removal of magnetite, followed by separation in three stages using heavy liquids (spec. gravity 2.96, 3.3 and 4.0). The concentrates from the last heavy liquid (Clerici) separation were further treated on a "Gold-hound" automatic rotating washing pan designed especially for panning gold and other very heavy minerals like the PGM. In this particular case the pan was tilted to recover also a small fraction of the more aboundant oxide- and sulphide minerals in order to get a heavy mineral concentrate at all. Both the heavy mineral concentrates and the "tailings", which later on proved to consist of the same minerals, from the "Gold-hound" panning were collected. The "tailings" were treated further by Frantz magnetic separation in several steps.

The concentrates obtained by this procedure, 13 in number, were then studied in a binocular lens, and selected mineral grains were identified using a Debye-Scherrer camera. A summary of microscopic and Debye-Scherrer mineral identifications and the laboratory treatment is given in Table 2.

Table 2. Preparation of the concentrates and minerals identified by

binocular lens and Debye-Scherrer camera.

Concentrate no.	derived from sample no.	treatment	minerals identified
1A	1	G.h	chr, hz
2A	2	G.h	chr, ger, nic, ptl
3A	3	G.h	chr, py, ger, ptl
4A	4	G.h	py, ger, ptl
1B	1	mag. 0.7 A	chr, hz, tre(?)
1C	1	unmag. 1.6 A	py, hz
2B	2	mag. 0.1 A	chr, pol, ptl, hem
2C	2	unmag. 1.6 A	chr, ger, ptl
3B	3	mag. 0.5 A	chr, ptl
3C	3	mag. 0.7 A	chr, py, ptl
3D	3	unmag. 1.6 A	chr, ptl
4B	4	mag. 0.3 A	chr, py, ptl
4C	4	unmag. 1.6 A	chr, py, ptl

Treatment: The "A" concentrates are heavy mineral concentrates from "Gold hound" (G.h) panning. The "B", "C" and "D" concentrates are tailings from the "Gold hound" panning, further separated on Frantz separator. Identified minerals: chromite (chr), heazlewoodite (hz), gersdorffite (ger), niccolite (nic), pentlandite (ptl), pyrite (py), trevorite (tre), polydymite (pol) and hematite (hem).

The concentrates were then mounted in epoxy and polished. Further studies were done with an EDS system on a Jeol 733 Superprobe Scanning Electron Microscope (SEM), quantitative analyses were done with the WDS equipment on the same SEM. The EDS/WDS investigation revealed a number of platinum group minerals (PGM), gold, sulpharsenides, and associated sulphides and arsenides as listed in Table 3.

Twenty-seven quantitative analyses were carried out on the PGM and associated phases, and a selection of these is listed in Table 4. Analyses are first corrected only for interference. Thereafter analyses are recalculated to 100 % after subtraction of "contaminating" elements from the host phases, and thirdly atomic concentrations are calculated from the corrected analyses. Subtraction of elements due to "contamination" from the host phases is difficult and the results are therefore tentative. The PGM grain-aggregates show rather complex compositions and textures. To illustrate this, back-scattered electron images (BEI), a mineral location map and X-ray images of several elements present in the PGM, accompany the description.

Table 3. Summary of PGM, associating minerals (hosting or bordering PGM) and non-associated minerals (not in direct contact with PGM) found by EDS and WDS analyses.

Consentrate no.	1A	2A	3A	4A	1B	1C	2B	2C	3B	3C	3D	4B	4C
PGM-phases													
irarsite (Ir,Rh,Pt)AsS							▲	▲					▲
iridosmine Os,Ir,(Pt)		△?						▲					
ruthenian osmium Os,Ir,Ru			▲										
geversite $PtSb_2$								▲					
isoferroplatinum Pt_3Fe								▲					
Pt-Fe- alloy							▲						
Cu-Au-Os-Pt- alloy			▲										
michenerite PdBiTe									▲				
Phases associated with or non-associated with PGM.													
native Au			○?		●								
breithauptite NiSb		○					○/▲						
niccolite NiAs		○?	○	○	●	○	○						
heazlewoodite Ni_3S_2			▲				▲	▲					▲
pentlandite $(Ni,Fe)_9S_8$	○	○/△	△	○	○				△	○	○		
gersdorffite (Ni,Co)AsS		○?				○		○		○?		○?	
cobaltite CoAsS	○	●											
chalcopyrite $CuFeS_2$	○												
galena PbS		○					○					○	
barite $BaSO_4$			○	○							○		
Te-Bi-Se-phase					●								
Te-Bi-phase									○				
Te-bearing phase		●											
chromite	○	○											
Fe-Mg-Ca-(Mn)ox					○								
uraninite								○					
monazite										○			

▲ = PGM and associated minerals (microprobe analysis)
△ = PGM and associated minerals (EDS-determination only)
● = minerals non-associated with PGM (microprobe analysis)
○ = minerals non-associated with PGM (EDS-determination only)

Table 4. Microprobe analyses (WDS) of noble-metal minerals, associated minerals and non-associated minerals in heavy-mineral concentrates from the Raudberg area solitary ultramafites, Vik, Sogn og Fjordane, Western Norway

Analysis no.		1	2	3	4	5	6	7	8	9	10	11	12	13	14	15	16	17	18	19	20
Concentrate no.		2B	2C	4C	3A	2C	2C	2B	3A	2C	3B	1B	2B	4A	2A	1B	3A	2B	2C	4C	ptl-STD
(1)	Os	2.63	1.15	3.41	34.04	35.13	0.75	0.93	15.37	0.74		0.10	0.98			0.08	-	0.07	-	-	0.02
	Ir	30.79	33.13	32.35	9.43	8.66	1.63	0.94	0.08	1.49		0.39	0.28			0.14	0.23	0.05	0.23	0.03	0.13
	Ru	3.72	4.40	0.11	12.08	0.70	-	-	-	-		-	-			-	-	-	-	-	-
	Rh	2.51	4.16	8.68	-	-	-	-	-	-		0.02	0.88			-	-	-	-	-	-
	Pt	7.84	9.37	8.69	1.98	13.11	51.59	31.43	9.81	23.24	1.49	0.64	3.69	2.18	0.36	0.40	0.20	0.31	0.39	0.29	0.29
	Pd	0.77	1.27	1.84	0.59	0.46	0.09	0.12	0.52	0.33	26.61	0.14	0.62	-	0.24	0.07	-	-	-	-	-
	Au			1.54	5.95				29.26	0.67	0.71	98.07		0.72	0.32	0.40	0.43	0.57		0.39	0.34
	Ag										1.29			-	-						
	As	22.98	24.72	24.42	0.33	0.99	0.20	0.12	-	1.36	0.04	0.12	0.69	-	0.05	52.81	0.07	0.01	0.05	0.07	-
	Sb	0.04	0.22		2.05	2.96	0.16	0.04	-	33.79	0.78	-	53.48	-	0.10	0.05	-	-	-	-	-
	Bi										44.19			72.60	1.76						
	Te										31.72			3.46	24.11						
	Se										-			8.17	-						
	Hg													*	*						
	S	17.23	14.25	9.91	7.36	14.52	8.87	15.28	3.14	4.14	0.94	0.01	2.58	5.19	15.19	0.24	24.36	24.01	23.57	22.45	32.92
	Pb	0.17				0.08	0.35	-					-						0.19		
	Cu			7.28	4.91				37.13	0.46	0.02	0.10		0.06	0.05	0.02	0.06	0.04		0.02	0.07
	Ni	16.58	12.26	13.38	21.85	25.69	32.52	46.65	8.73	29.24	3.67	2.38	37.06	2.54	20.86	46.23	73.99	74.55	73.25	74.81	35.90
	Co			0.18	0.39				0.52	0.52	0.30	0.27		0.04	0.60	0.03	0.04	0.06		0.03	0.11
	Fe	1.21	-	0.04	0.43	1.76	5.63	4.35	0.23	1.64	1.81	0.48	0.82	1.91	14.42	0.34	0.05	1.11	0.02	0.02	29.86
	Cr	0.04	0.06			0.01	0.05	0.03					0.03						0.03		
	TOT	106.50	104.97	112.92	101.37	104.07	101.85	99.88	104.78	97.60	113.56	102.62	101.11	96.88	78.06	100.81	99.71	100.77	97.72	98.10	99.62

- element not detected.
analysis 1-3: irarsite (IrAsS); 4: ruthenian osmium (Os,Ru,Ir); 5: iridosmine (OsIr); 6: isoferroplatinum Pt_3Fe, 7: Pt-Fe-alloy; 8: $Cu_2(Au,Os,Pt)$, 9: geversite $PtSb_{2-}$; 10: michenerite PdBiTe; 11: native Au; 12: breithauptite NiSb; 13: Bi-Se-(Te)-phase; 14: Te-(Bi)-phase; 15: niccolite NiAs; 16-19: heazlewoodite $Ni_{3\pm x}S_2$; 20: pentlandite-standard
* = Hg not detected on EDS spectrum
(1): raw analyses in weight percent of the element (2): raw analyses after corrections due to element interference (3): analyses recalculated after subtraction of/correction for Ni, S and Fe from host heazlewoodite and pentlandite and subtraction/correction of element contributions from adjoining PGE-phases, etc. (4): atomic concentration calculated from the corrected analyses.

Table 4. (continued)

Analysis no.	1	2	3	4	5	6	7	8	9	10	11	12	13	14	15	16	17	18	19	20
Concentrate no.	2B	2C	4C	3A	2C	2C	2B	3A	2C	3B	1B	2B	4A	2A	1B	3A	2B	2C	4C	ptl-STD
(2) Os	2.63	1.15	3.41	34.04	35.13	0.75	0.93	15.37	0.74		0.10	0.98								
Ir	30.79	33.13	32.35	9.43	8.66	1.63	0.94	0.08	1.49		0.39	0.28								
Ru	3.72	4.40	0.11	12.08	0.70	-	-	-	-		-	-								
Rh	2.51	4.16	8.68	-	-	-	-	-	-		0.02	0.88								
Pt	7.61	9.37	8.69	1.98	13.11	51.59	31.43	9.81	23.24	1.49	0.64	3.69	2.18	0.36						
Pd	0.31	0.51	0.26	0.59	0.46	0.09	0.12	0.52	0.33	26.61	0.14	0.46	-	0.24						
Au			1.10	5.95				29.26	0.67	0.71	98.07		0.72	0.32						
Ag										0.49			-	-						
As	22.98	24.72	24.42	0.33	0.99	0.20	0.12	-	1.36	0.04	0.12	0.69	-	0.05	52.81	0.07	0.01	0.05	0.07	-
Sb	0.04	0.22		2.05	2.96	0.16	0.04	-	33.79	0.78	-	53.48	-	0.10	0.05	-	-	-	-	-
Bi										44.19			72.60	1.76						
Te										31.72			3.46	24.11						
Se										-			8.17	-						
S	17.23	14.25	9.91	7.36	14.52	8.87	15.28	3.14	4.14	0.94	0.01	2.58	5.19	15.19	0.24	24.63	24.01	23.57	22.45	32.92
Pb	0.17				0.08	0.35	-					-						0.19		
Cu			7.28	4.91				37.13	0.46	0.02	0.10		0.06	0.05	0.02	0.06	0.04		0.02	0.07
Ni	16.58	12.26	13.38	21.85	25.69	32.52	46.65	8.73	29.24	3.67	2.28	37.06	2.54	20.86	46.23	73.99	74.55	73.25	74.81	35.90
Co			0.18	0.39				0.52	0.52	0.30	0.27		0.04	0.60	0.03	0.04	0.06		0.03	0.11
Fe	1.21	-	0.04	0.43	1.76	5.63	4.35	0.23	1.64	1.81	0.48	0.82	1.91	14.42	0.34	0.05	1.11	0.02	0.02	29.86
Cr	0.04	0.06			0.01	0.05	0.03					0.03						0.03		
TOT	105.81	104.21	110.90	101.37	104.07	101.85	99.88	104.78	97.60	112.76	102.62	100.95	96.88	78.06	99.72	98.84	99.78	97.11	97.40	98.86

Table 4. (continued)

Analysis no.		1	2	3	4	5	6	7	8	9	10	11	12	13	14	15	16	17	18	19	20
Concentrate no.		2B	2C	4C	3A	2C	2C	2B	3A	2C	3B	1B	2B	4A	2A	1B	3A	2B	2C	4C	ptl-STD
(3)	Os	3.19	1.31	3.83	57.36	78.15	1.25	2.46	16.58			0.10	1.14								
	Ir	37.38	37.75	36.29	15.89	19.27	2.71	2.49	0.09			0.39	0.33								
	Ru	4.52	5.01	0.12	20.36	1.56	-	-	-	-		-	-								
	Rh	3.05	4.74	9.74	-	-	-	-	-	-		0.02	1.03								
	Pt	9.24	10.68	9.75			85.93	83.21	10.58	39.38	1.41	0.64		2.50	1.33						
	Pd	0.38	0.58	0.29	0.99	1.02	0.15	0.32	0.56	0.56	25.10	0.14	0.54	-	0.89						
	Au			1.23					31.57	1.14	0.67	97.86		0.83	1.19						
	Ag										0.46			-	-						
	As	27.90	28.17	27.39	0.56				-		0.04		0.80	-	0.19	52.97	0.07	0.01	0.05	0.07	-
	Sb				3.45				-	57.26	0.74	-	62.32	-	0.37	0.05	-	-	-	-	-
	Bi										41.68			83.27	6.52						
	Te										29.92			3.97	89.33						
	Se										-			9.37	-						
	S	14.34	11.75	11.12												0.24	24.93	24.07	24.27	23.05	33.32
	Pb						0.58	-					-						0.20		
	Cu								40.06	0.78		0.10		0.07	0.19						
	Ni												33.85			46.37	74.90	74.74	75.43	76.82	36.34
	Co			0.20	0.66				0.56	0.88		0.27				0.03	0.04	0.06		0.03	0.11
	Fe			0.04	0.72		9.38	11.52				0.48				0.34	0.05	1.11	0.02	0.02	30.23
	Cr																		0.03		

Table 4. (continued)

Analysis no.	1	2	3	4	5	6	7	8	9	10	11	12	13	14	15	16	17	18	19	20
Concentrate no.	2B	2C	4C	3A	2C	2C	2B	3A	2C	3B	1B	2B	4A	2A	1B	3A	2B	2C	4C	ptl-STD
(4) Os	1.45	0.63	1.86	70.07	76.63	1.04	1.95	9.20			0.10	0.53								
Ir	16.82	17.83	17.48	7.00	18.70	2.23	1.96	0.05			0.39	0.15								
Ru	3.87	4.50	0.11	17.06	2.88	-	-	-	-		-	-								
Rh	2.56	4.18	8.76	-	-	-	-	-	-		0.04	0.89								
Pt	4.10	4.97	4.63			69.55	64.46	5.72	28.41	1.05	0.63		2.26	0.90						
Pd	0.31	0.49	0.25	0.79	1.79	0.22	0.45	0.56	0.74	34.12	0.25	0.45	-	1.10						
Au			0.58					16.92	0.81	0.49	95.74		0.74	0.79						
Ag										0.62			-	-						
As	32.21	34.13	33.84	0.63				-		0.08		0.95	-	0.33	46.78	0.05	0.01	0.03	0.05	-
Sb				2.40				-	66.20	0.88	-	45.62	-	0.40	0.03	-	-	-	-	-
Bi										28.85			70.35	4.10						
Te										33.92			5.49	91.99						
Se										-			20.95	-						
S	38.69	33.27	32.11												0.50	37.82	36.72	37.03	35.43	47.21
Pb						0.44	-					-						0.05		
Cu								66.55	1.73		0.30		0.19	0.39						
Ni												51.39			52.26	62.05	62.26	62.84	64.48	28.12
Co			0.31	0.95				1.00	2.10		0.88				0.03	0.03	0.05		0.03	0.08
Fe			0.07	1.09		26.52	31.17				1.66				0.40	0.04	0.97	0.02	0.02	24.59
Cr																		0.03		

DESCRIPTION OF PGM, NATIVE Au AND ASSOCIATED MINERALS, - AND ANALYTICAL RESULTS

Sulpharsenides

Irarsite is the only PGE sulpharsenide detected in the present study. The mineral occurs in three of the thirteen concentrates examined, in each case as anhedral inclusions hosted in heazlewoodite, see Figures 3, 4 and 8D The grain-sizes range from 3 to 8 μm. In concentrate no. 2C irarsite is intergrown with other PGM, in concentrate no. 2B the mineral is closely associated with gersdorffite, whereas in concentrate no. 4C irarsite occurs as an isolated single-phase inclusion in heazlewoodite. The composition of the irarsites detected is given in in Table 4, analyses 1, 2 and 3. Analyses 1 and 2 show a Pt-enriched and Rh- and Ru-bearing intermediate member, whereas analysis 3 reveals an almost Ru-free, Rh-enriched composition.

The atomic proportions of the elements are plotted in the ternary system IrAsS - RhAsS - PtAsS, Figure 9. The composition of the irarsites fits well with irarsite compositions given in the literature, summarized e.g. in Cabri (1981) and Tarkian (1987).

Osmium-rich alloys

Os-rich alloys were identified in concentrates no. 2C and 3A. In concentrate no. 3A the lower part of an only 3 μm large two-phase inclusion in heazlewoodite and ?pentlandite is occupied by ruthenian osmium Os,Ru,Ir, (Figure 5). In concentrate no. 2C the central part of the 16 μm large four-phase PGM-inclusion is occupied by what is interpreted as iridosmine Os,Ir or native Os. The compositions of the two Os-rich alloys found are given in Table 4, analyses 4 and 5.

Analysis 4 in Table 4 is interpreted as an alloy of Os with some Ir, but with only minor amounts of Ru present. The relatively high amount of Pt in the raw analysis is probably largely due to Pt-radiation from the neighbouring Pt-rich PGM, see the complex intergrowths of the PGM-phases and the small size of the total PGM aggregate in Figure 4. Due to the intergrowth and size even the X-ray image(s), which is often informative about the presence of an element, does not give any significant information in handling this particular problem. Cabri (1981) in his Tables 8.50 and 8.51 does not report iridosmine or "osmium" with more than 2.6 wt% Pt. In the this case it is impossible to state or even estimate how much Pt is present (if present at all) in the alloy, but 13.11 wt% as the raw analysis shows is definitely a value several times too high. To avoid poorly based speculations Pt is therefore eliminated together with As, S, Sb etc. in the corrected and recalculated analysis 5 in Table 4. According to Harris and Cabri (1973) this composition plots in the field of "iridosmine". Both the ruthenian osmium found in concentrate 3A and this last one are plotted in the triangular Os-Ir-Ru diagram of Harris and Cabri (1973), see Fig. 9.

Platinum-rich alloys

Alloys containing essentially Pt and Fe were detected in concentrates 2B and 2C (analyses 7 and 6 in Table 4). In cons. 2B the Pt-Fe-alloy occurs as two small patches, one at each end of an anhedral inclusion of breithauptite (NiSb) hosted in heazlewoodite (Figure 3). Due to the size of these patches (the largest is approximately 3.5 μm) the raw analysis (no. 7 in Table 4)is naturally severely disturbed by Ni- and S-radiation from the host heazlewoodite. However, the analysis is astonishingly little affected by the neighbouring breithauptite (only 0.04 wt% Sb in the analysis). After correction for Ni, S and elements present in small amounts, there remains some Fe which can best be ascribed to the Pt-rich phase. After this correction the recalculated analysis no. 7 reveals a Pt-Fe alloy with minor Os and Ir probably substituting for Pt. It is impossible from the analysis to interpret the alloy as isoferroplatinum (ideal Pt_3Fe) or tetraferroplatinum (ideal PtFe), it can only be labelled "Pt-Fe alloy".

Also in the case of analysis 6 in Table 2 the raw analysis is severely disturbed by Ni- and S-contamination from the host heazlewoodite. However, after identical corrections and recalculation, analysis 6 fits very well with isoferroplatinum Pt_3Fe reported from a variety of locations (Cabri 1981, Table 8.75).

Cu-Au-Os-Pt-alloy

The upper part of the PGM bearing inclusion in concentrate no 3A (Fig. 5) consists of a Cu-rich Cu-Au-Os-Pt alloy, the composition of which is shown in analysis 8, Table 4. The atomic proportions of the elements presented in analysis 8 after recalculation give an unusual alloy with composition $Cu_{0.68}Au_{0.17}Os_{0.09}Pt_{0.06}$, or ca. $Cu_2(Au,Os,Pt)$ which has not been reported earlier(?). In this case the X-ray images in Figure 5. support the analysis. The X-ray image of Os for instance shows that Os is clearly present in this Cu-rich phase and not only a result of radiation from the lower Os-rich part of the inclusion.

Platinum-Antimonide

In concentrate 2C (Fig. 4) a Pt-antimonide is intergrown with other PGM and hosted in heazlewoodite. The raw-analysis no. 9 in Table 4 of this phase is, like several of the other analyses, severely disturbed by Ni- and S-contamination from the host heazlewoodite. After subtraction and recalculation, however, the atomic proportions of the elements present show that the Pt-antimonide is geversite (ideal $PtSb_2$), in the this case with some Sb-excess in the structural formula.

Pd-Bi-telluride

In concentrate no. 3B a 17 μm large inclusion of a Pd-Bi-telluride was located in pentlandite, Figure 8c. Analysis no. 10 in Table 4 revealed after recalculation (subtraction of Ni, Fe and S from the host pentlandite) a michenerite composition $(Pd_{1.04}Pt_{0.03})_{\Sigma 1.07}$ $(Bi_{0.88}Sb_{0.03})_{\Sigma 0.91}$ $Te_{1.03}$ with some Pd-excess compared with michenerite compositions quoted by Cabri (1981) p. 155. The Pd-excess is not in agreement with experimental studies

carried out by Hoffman and MacLean (1976) who demonstrated a narrow Pd-range from 31.5 to 33.2 at% compared with 34.7 at% in the present case. The reason for this deviation from the experimental results may be due to the poor total sum of the analysis (113.56 wt%) which in its turn may be caused by a weakly tilted surface of the PGM-inclusion (indicated by the back-scattered electron image, Fig. 8c) and hence uneven radiation of the X-rays.

Native Gold, associated minerals and non-associated minerals

Native Au was detected in concentrate 1B, and possibly in concentrate 3A (EDS-scan with Au included in the element association found). In concentrate 1B, Fig. 6, Au is associated with niccolite and a Fe-Mg-Ca-(Mn) oxide(?) grain. A quantitative analysis of the Au-grain revealed pure Au without significant Ag or other elements present, analysis 11 in Table 4. An analysis of the associated niccolite (no. 15 in Table 4) contained small and apparently significant amounts of Os, Ir, Pt, Pd and S (the significance criterion is: peak radiation is higher than three times the square-root of background radiation). However similar trace amounts of PGE and Au also occur in all the analysed heazlewoodites and in an analysis of the pentlandite-standard used. The small amounts of PGE and Au in these minerals are not real but caused by element interference, see Table 4.

Minerals associated with PGM and Gold

From Table 3 we can see that the only phases found hosting PGM are hz and ptl of which hz seems to be the more important. In concentrate 2B, Fig. 3, a Ni-antimonide is associated with the PGM. When Ni and S from the host hz and Pt and Fe from the neighbouring PGM are removed from the raw-analysis (no. 12 in Table 4), there remains a relatively pure Ni-antimonide close to stoichiometric NiSb (breithauptite) in composition. Niccolite and an oxide (probably a spinel) are the only phases found associated with native Au.

The present mineral investigation is still at an early stage, and therefore a discussion with conclusions will not be included in this report.

The sulfides and sulfarsenides occur only scarcely disseminated within the ultramafic silicate-carbonate rocks and the noble-metal minerals even more scarcely within the sulfides and sulfarsenides. It is therefore almost impossible to find PGM or Au in situ (in thin polished sections, etc.) in the actual rocks. We are forced to use laboratory preconcentration. However in polished sections of heavy-mineral concentrates we loose the possibility of a direct study of the textural relationships between the PGM-bearing sulfides, etc. and their host silicate-carbonate assemblages and hence important information about the genesis of the noble-metal minerals.

To quote the famous ore mineralogist, Professor Paul Ramdohr (1967, p. 245): "Small amount of platinoid elements are, no doubts, present even in "platinum-free" ophiolitic peridotites. Hahn-Weinheimer (1961) mentions values in the range of 0.1 ppm. It is, however, unlikely that these would ever be observed microscopically".

REFERENCES

Aarflot, G., 1984: En geologisk og mineralogisk undersøkelse av talkforekomster i Raudbergfeltet i Stølsheimen. Unpubl. thesis Norw. Inst. of Tech.

Bakke, S., 1986: Talk i Raudbergfeltet, Vik i Sogn, Unpubl. NGU report 86.018.

Cabri, L.J. (ed.) 1981: Platinum-group elements: mineralogy, geology, recovery. Can. Inst. Min. Metall., Spec. vol. 23, 267 pp.

Gee, D.G., Kumpulainen, R., Roberts, D., Stephens, M.B.,Thon, A. and Zachrisson, E., 1985: Scandinavian Caledonides Techtonostratigraphic map. In Gee,D.G: and Sturt, B.A. (eds.) The Caledonian Orogen - Scandinavia and Related Areas. John Wiley & Sons Chichester.

Hahn-Weinheimer, P. and Rost, F. 1961: Akzessorische Mineralien und Elemente in Serpentinit von LeupoldsgrÜn (MÜnchberger Gneismasse). Geochem. Acta 21, 165.

Harris, D.G. and Cabri, L.J. 1973: The nomenclature of the natural alloys of osmium, iridium and ruthenium based on new compositional data of world-wide occurrences. Canadian Mineralogist 12, 104-112.

Hoffman, E. and MacLean, W.H. 1976: Phase relations of michenerite and merenskyite in the Pd-Bi-Te system. Econ. Geol. 71, 1461-1468.

Ingdahl, S.E., 1986: Strukturell-metamorf utviking i det klassiske Os området og betydningen dette har for forståelsen av de Skandinaviske Kaledonider. NGT no. 21 p 30.

Kvale, A. 1960: The nappe area of the Caledonides in Western Norway. Nor. geol. unders. 212 e.

Lyse, K., 1982: Geologisk kartlegging av fyllittsonen i Vik i Sogn. Unpubl.NGU report.

Pactunc, A.D., 1984: Metamorphism of the ultramafic rocks of the Thompson mine, Thompson Nickel belt, northern Manitoba. Can. Mineral. 22 pp 77-91.

Ramdohr, P. 1967: A widespread mineral association, connected with serpentinization - with notes on some new or insufficiently defined minerals. N. Jb. Miner. Abh. 107, 241-265.

Sanford, R.F., 1982: Growth of ultramafic reaction zones in greenshist to amphibolite facies metamorphism. Am. Jour. Sci. 282 5, 543-616

Sigmond, E.M.O., Gustavson, M. and Roberts, D., 1984: Berggrunnskart over Norge 1:1000000. Nor. Geol. Unders.

Tarkian, 1987: Compositional variations and reflectance of the common platinum-group minerals. Mineralogy and Petrology 36, 169-190.

CAPTIONS FOR FIGURES

Fig. 1. Location of the Raudberg field ultramafic tectonite complex (R) in phyllonitic rocks of the Lower Allochthon situated between the Jotun Nappe Complex and autochthonous basement of the Western Gneiss Region. F = Framfjord. Compiled from Sigmond et al. (1984).

Fig. 2. The Raudberg field ultramafic tectonite complex consisting of three large and several minor ultramafic bodies. Outcroping ultramafic rocks shown by inclined line pattern and horisontal projection of subsurface ultramafic rocks shown by thick line. Data from Bakke (1986).

Fig. 3. Back-scattered electron image (BEI) and X-ray images for Ni, Ir, As, Pt and Sb. A heazlewoodite-grain (1) are hosting breithauptite (2), A Pt-Fe alloy (3), irarsite (4) and gersdorffite (5). Concentrate no. 2B. Scale bar is 10 μm.

Fig. 4. Back scattered electron image (BEI 1) and X-ray images for Os, Ir, Pt, As and Sb of a complex PGM-aggregate hosted in heazlewoodite. BEI 1 only shows the total PGM-aggregate (white) in the heazlewoodite (light grey). Strong and overlapping Ir- and As-radiation shows areas of irarsite, strong Os-radiation is due to iridosmine and strong Sb-radiation is caused by geversite. Isoferroplatinum is shown by strong Pt-radiation, while irarsite shows a weaker Pt-radiation. Concetrate no. 2C. Scale bar is 1 μm.

Fig. 4. (continued) Back-scattered electron image (BEI 2), mineral location map (based on interpretation of BEI 1 and 2, X-ray images and the quantitative analyses in Table 4) and X-ray images for Ni and S of the same PGM-aggregate as in Fig. 2A.
On BEI 2 the contrast is set to emphasize more detailes of the PGM-aggregate itself and the complex intergrowths of the PGM-aggregate with heazlewoodite (black). Concentrate no. 2C. Scale bar is 1 μm.

Fig. 5. Back-scattered electron image (BEI) and X-ray images for Cu, Au, Pt, Os and Ru of a two-phase inclusion of $Cu_2(Au,Os,Pt)$ (1) and ruthenian osmium (2) in pentlandite (3) and heazlewoodite (4). Concentrate no. 3A. Scale bar is 1 μm.

Fig. 6. Back-scattered electron image (a and b) and X-ray image for Au. A small grain of native Au (1) intergrown with niccolite (2) and an oxide-phase (3).
Concentrate no. 1B. Scale bar is 30 μm on (a) and 3 μm on (b).

Fig. 7. Back-scattered electron image (BEI) and X-ray images for Bi, Te and Se of a Bi-rich grain bordering pentlandite on one side (not shown on BEI). Patchy enrichments of Te and Se which only partly overlap each other (analysis 13 in Table 4). Concentrate no. 4A. Scale bar is 10 μm.

Fig. 8. Back-scattered electron images of PGM-inclusions (A,C,D) and a Te-rich phase (B). A: Os,Ir,Pt-bearing PGM-inclusion (1) quantitatively not successfully determined hosted in pentlandite (2) and secondary sulphides derived from pentlandite (3). Note well developed hexagonal parting in pentlandite, concentrate no. 2A. B: Minute inclusion of Te-rich phase (1) in pentlandite (2), concentrate no. 3B. C: Michenerite (1) hosted in pentlandite (2), concentrate no. 3B. D: Rh-enriched irarsite (1) hosted in heazlewoodite (2), concentrate no. 4C. Scale bar is 10 μm in all figures.

Fig. 9. Microprobe analyses (at %) of PGM sulfarsenides (irarsite) (A) and alloys (B). In diagram A contents of Os, Ru and Pd have been included for Ir, Rh and Pt, respectively. Analysis numbers refer to those in Table 4.

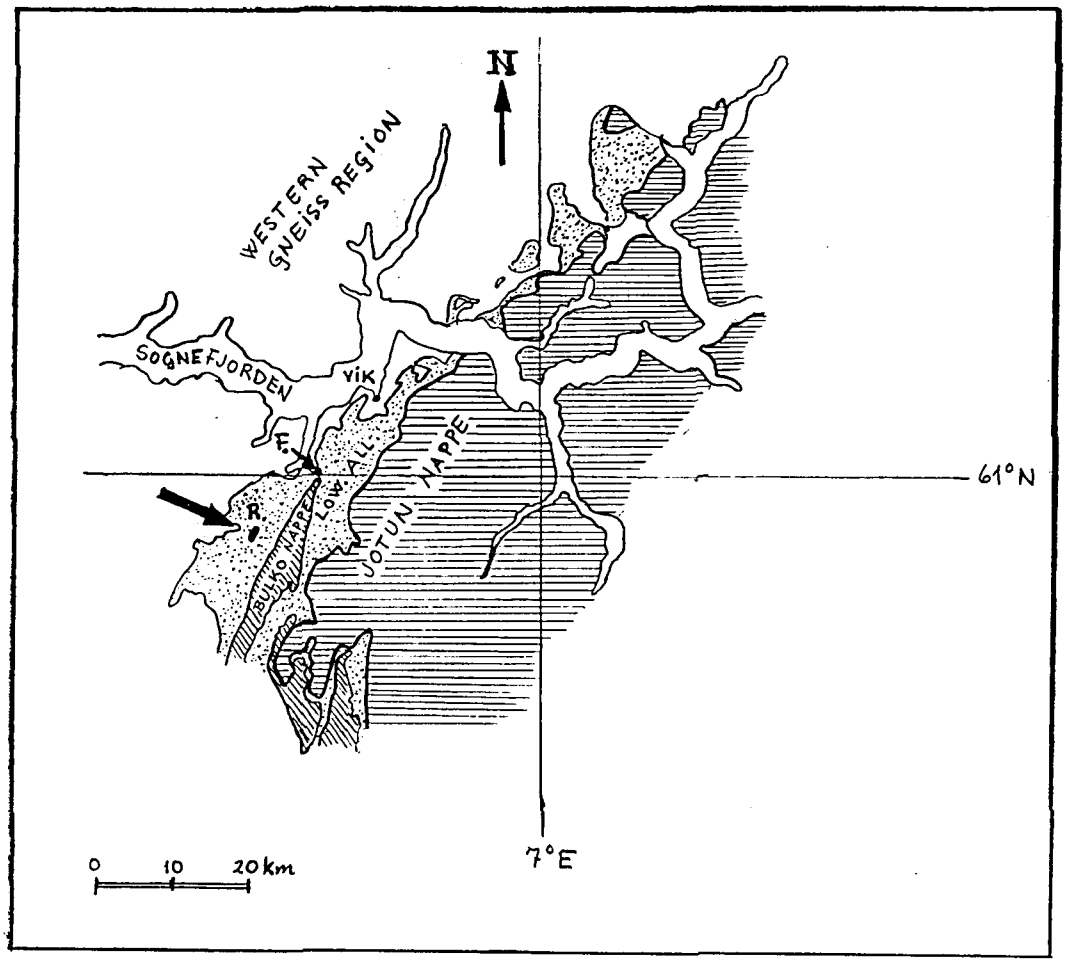
N
WESTERN GNEISS REGION
SOGNEFJORDEN
VIK
F.
R.
LOW ALL.
JOTUN NAPPE
61°N
7°E
0 10 20 km

Fig. 1

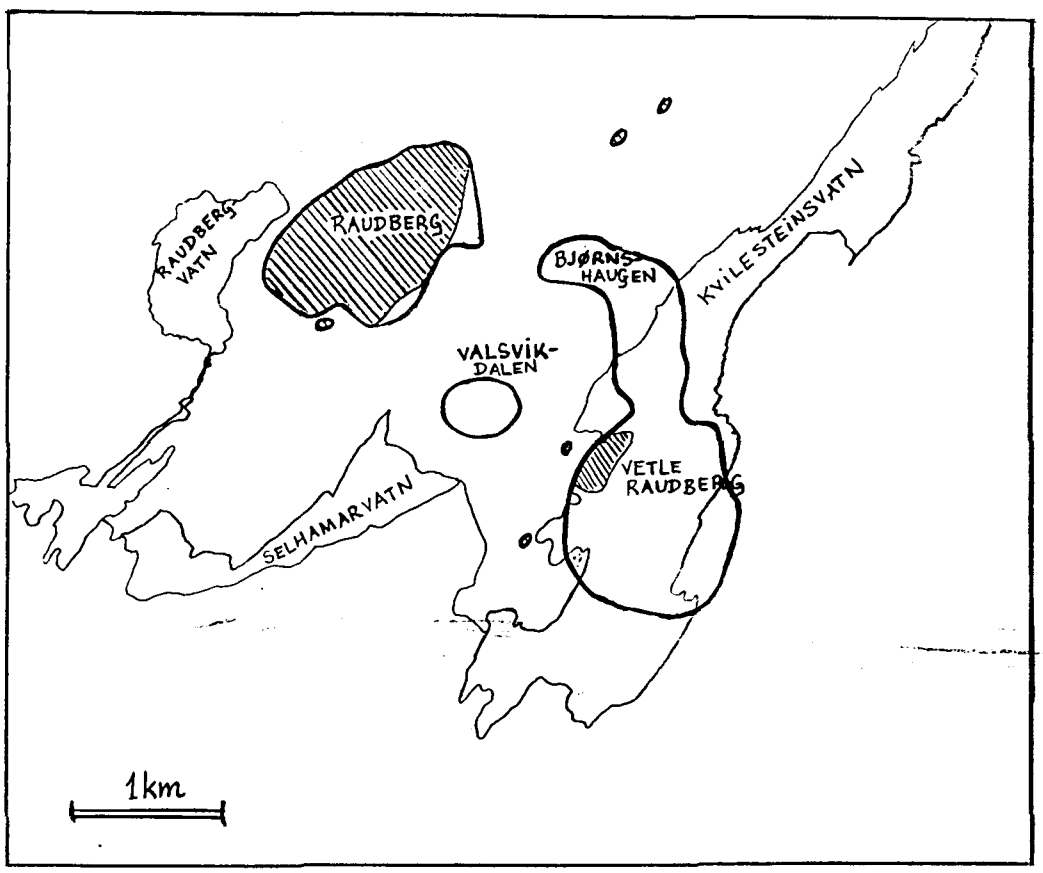
RAUDBERG VATN
RAUDBERG
BJØRNS-HAUGEN
KVILESTEINSVATN
VALSVIK-DALEN
VETLE RAUDBERG
SELHAMARVATN
1km

Fig. 2

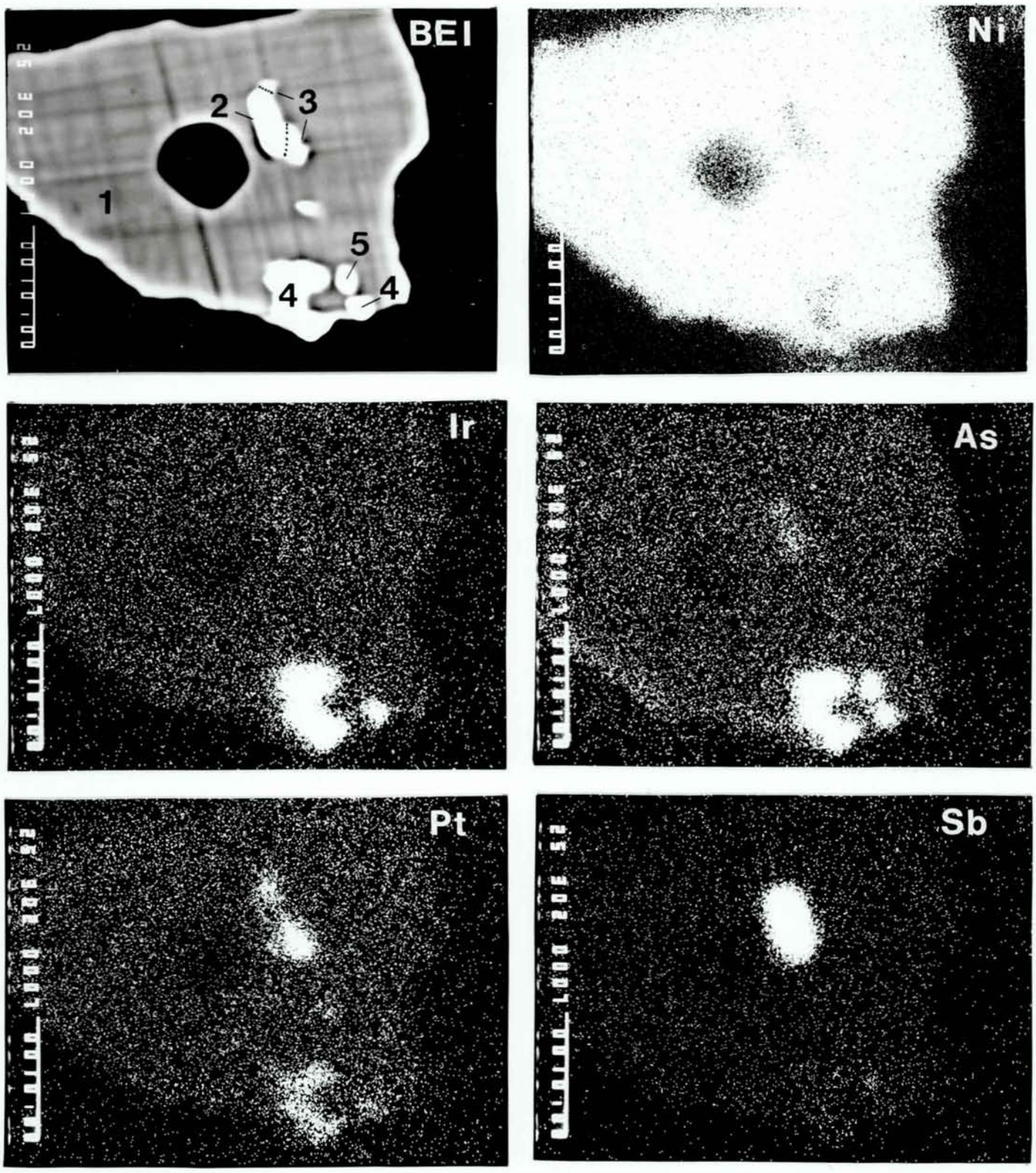

Fig. 3

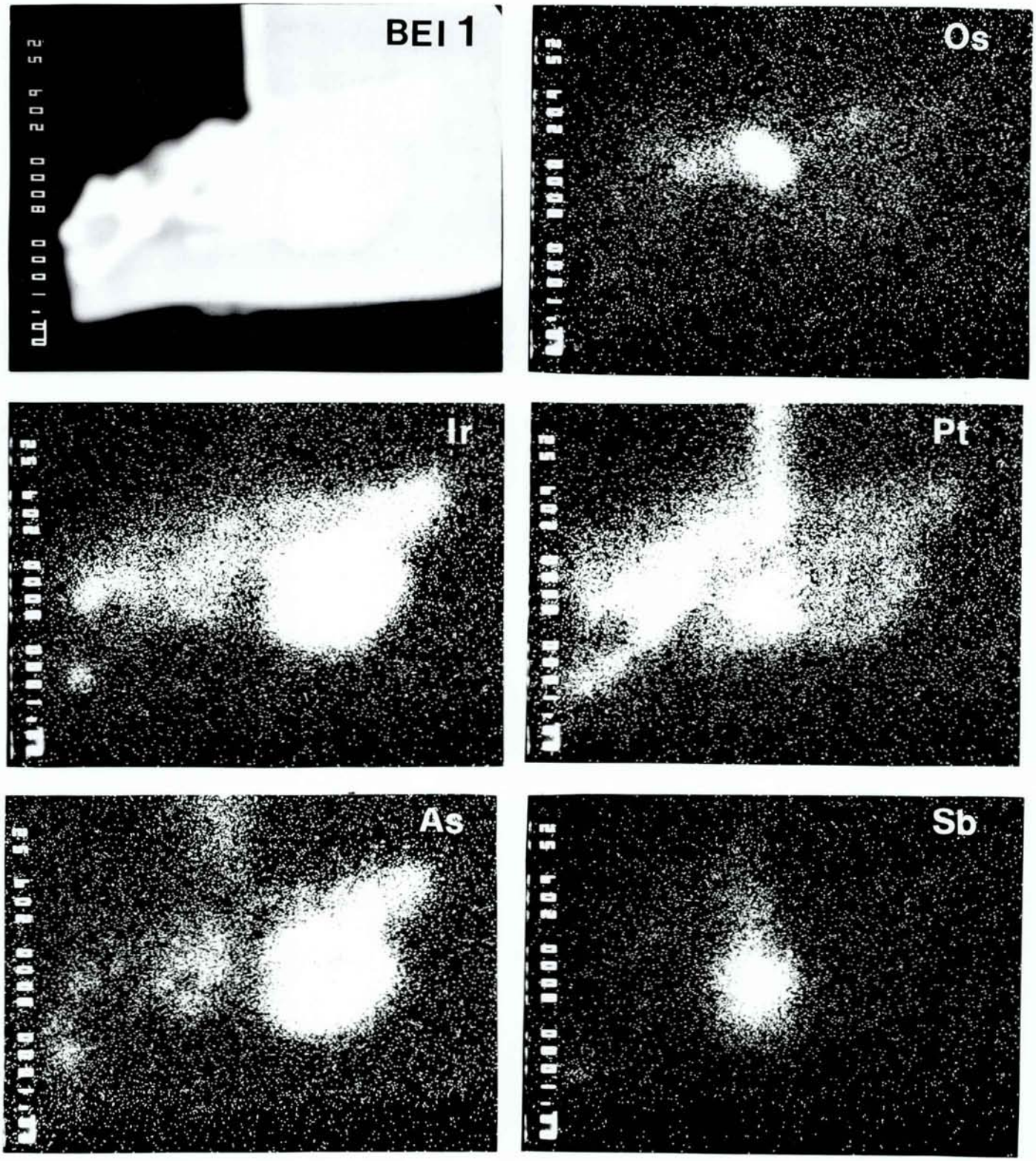

Fig. 4


BEI 2

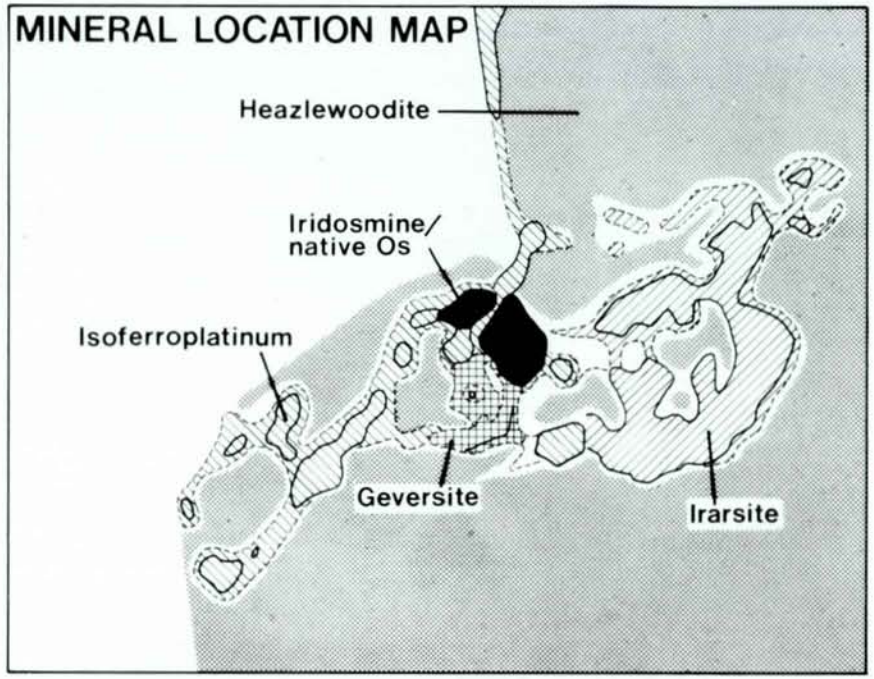
MINERAL LOCATION MAP
Heazlewoodite
Iridosmine/
native Os
Isoferroplatinum
Geversite
Irarsite

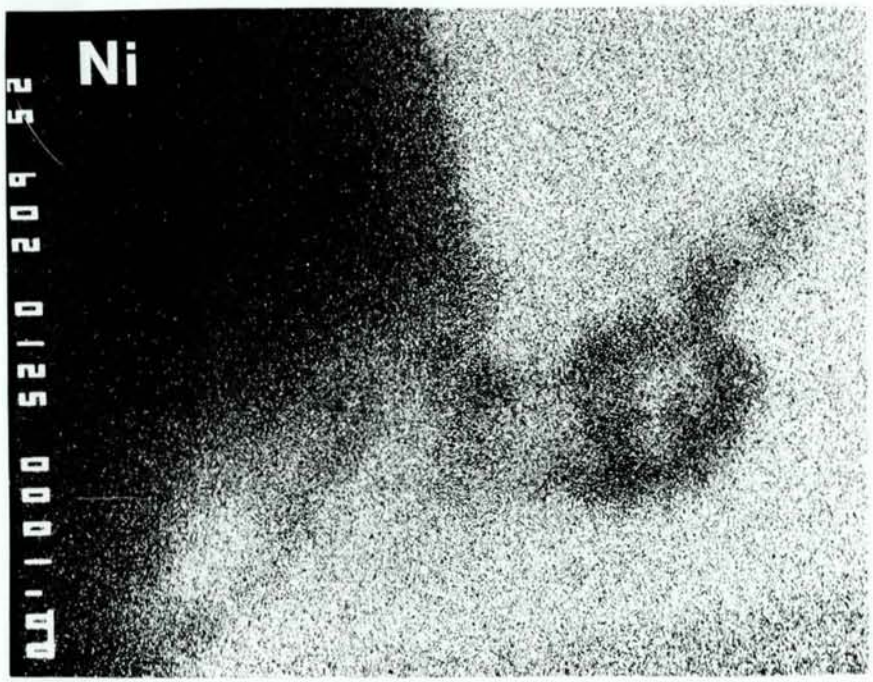
Ni

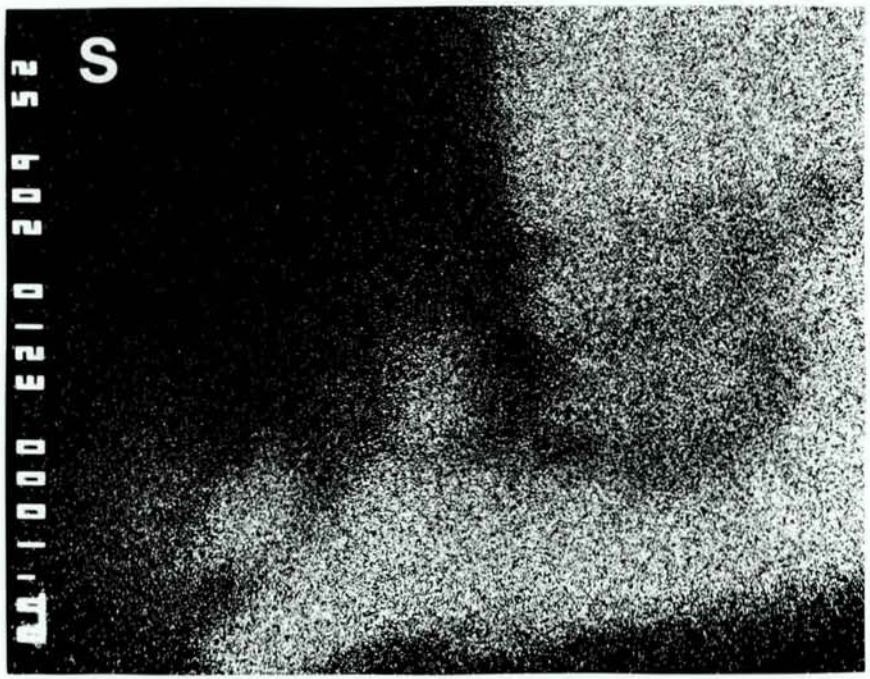
S

Fig. 4 (cont.)

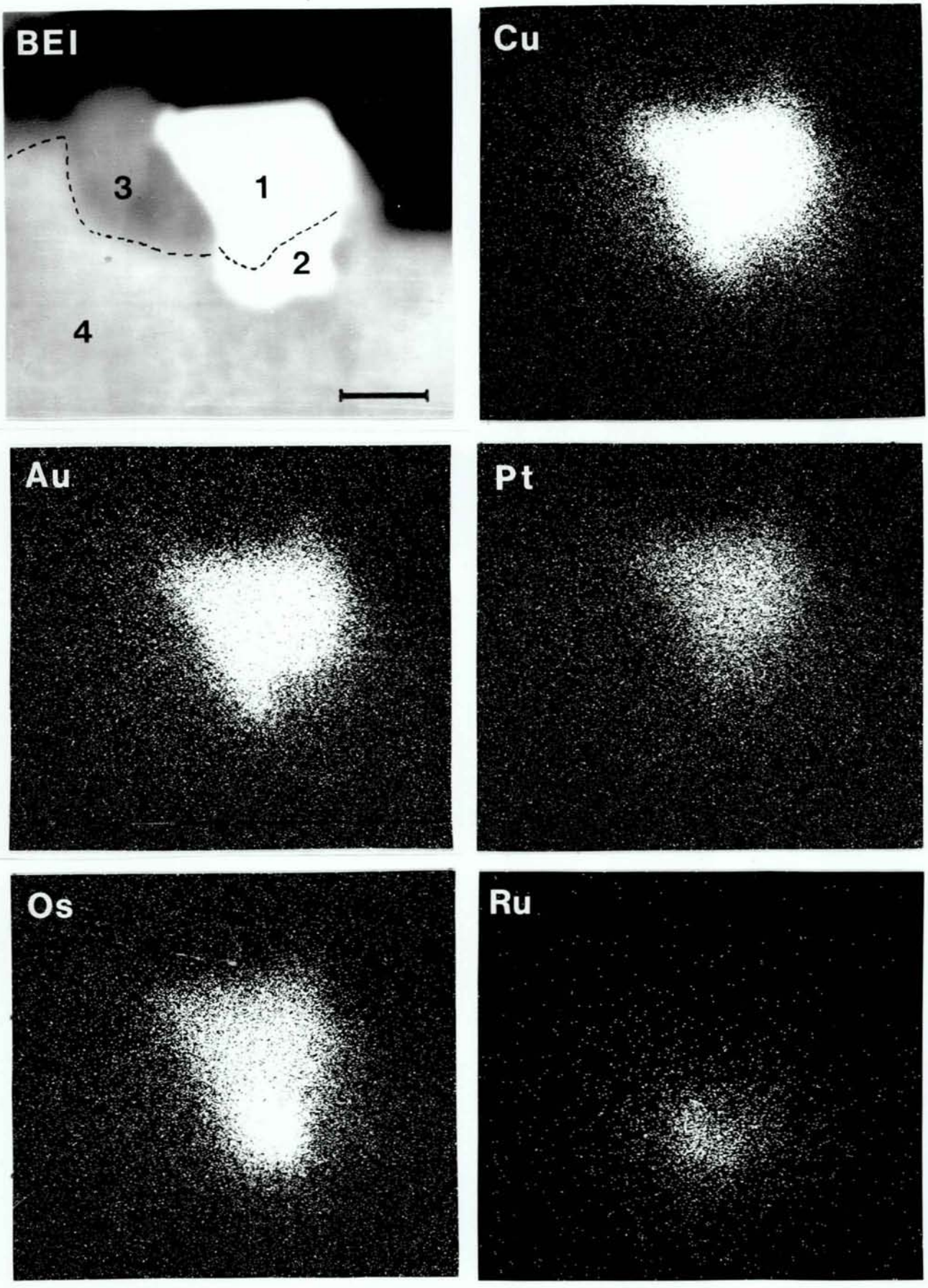

Fig. 5

Kons. 3A
Raudberget, Vik i Sogn

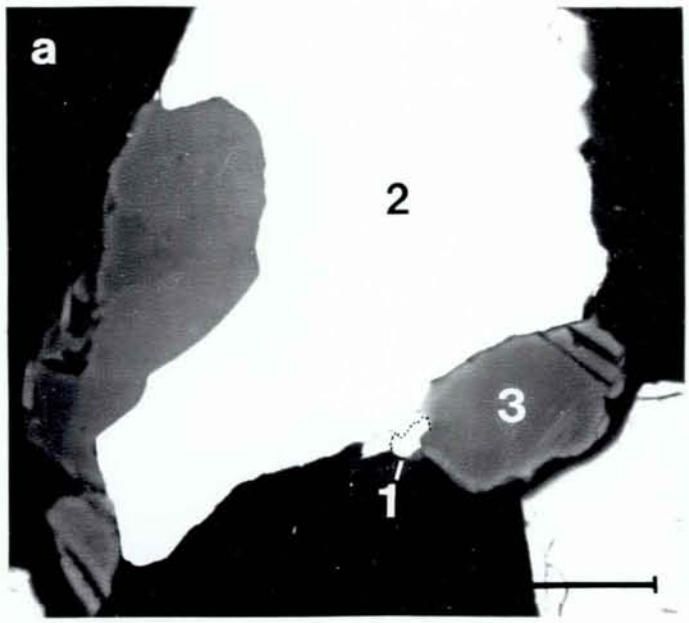

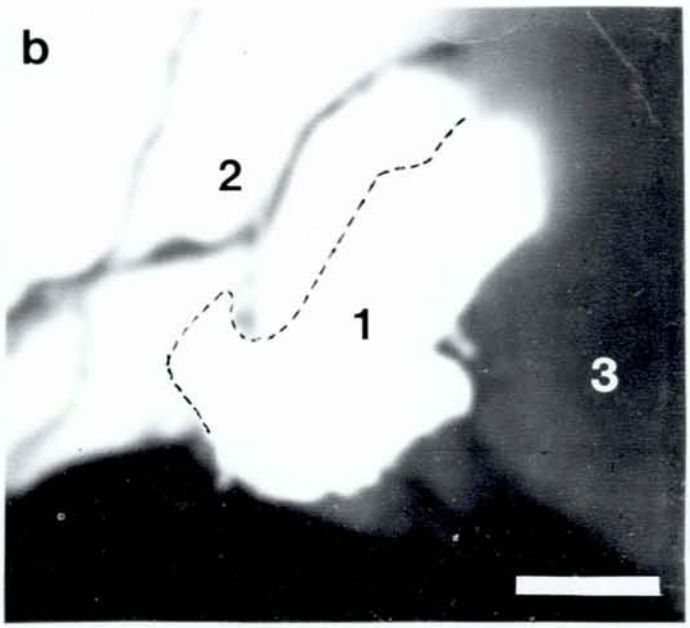

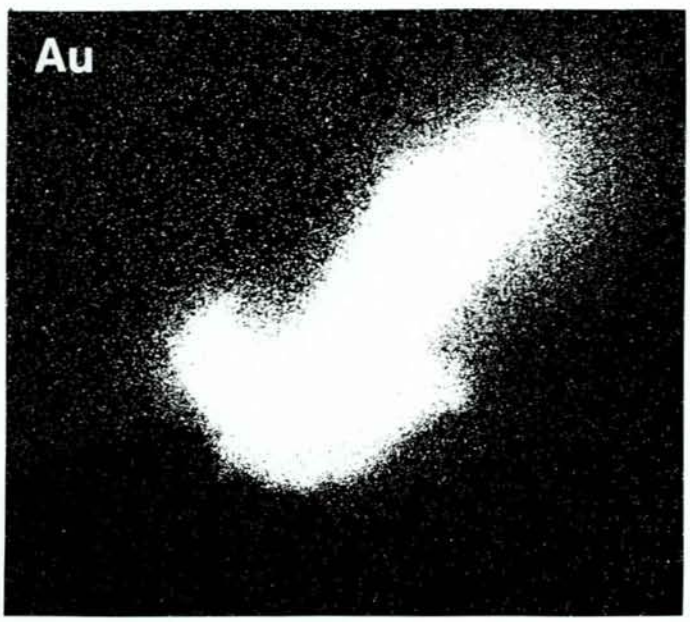

Fig. 6

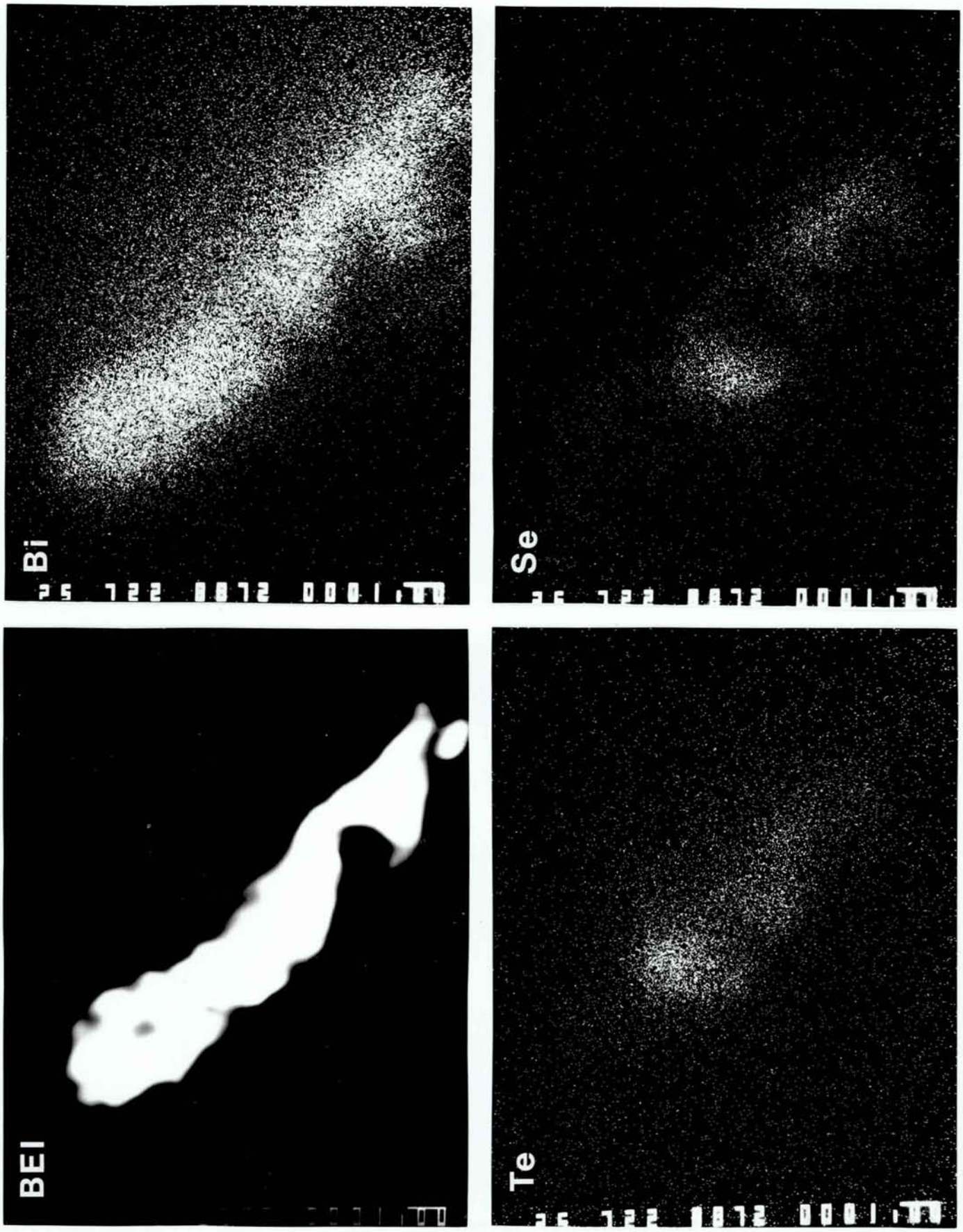

Fig. 7

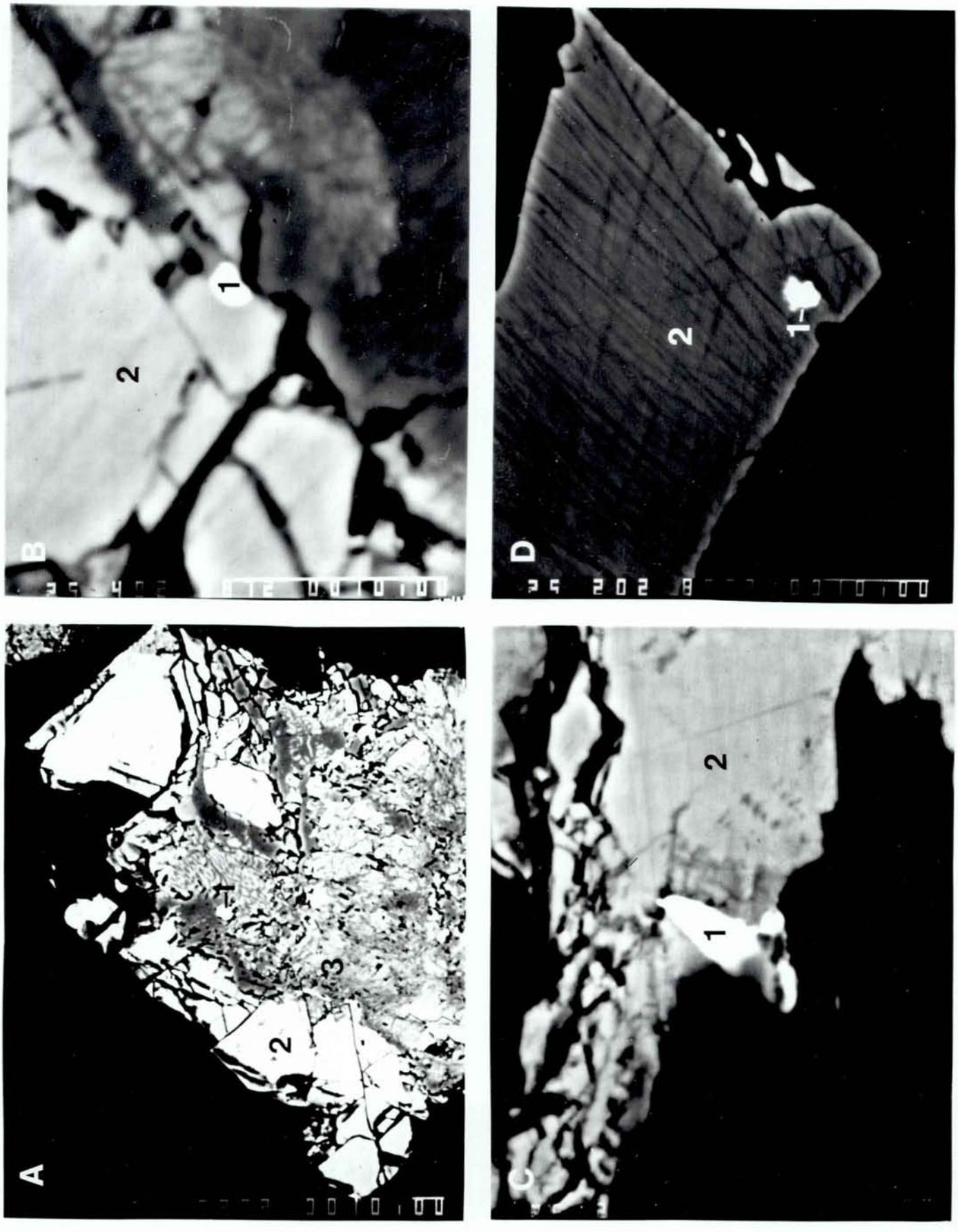

Fig. 8

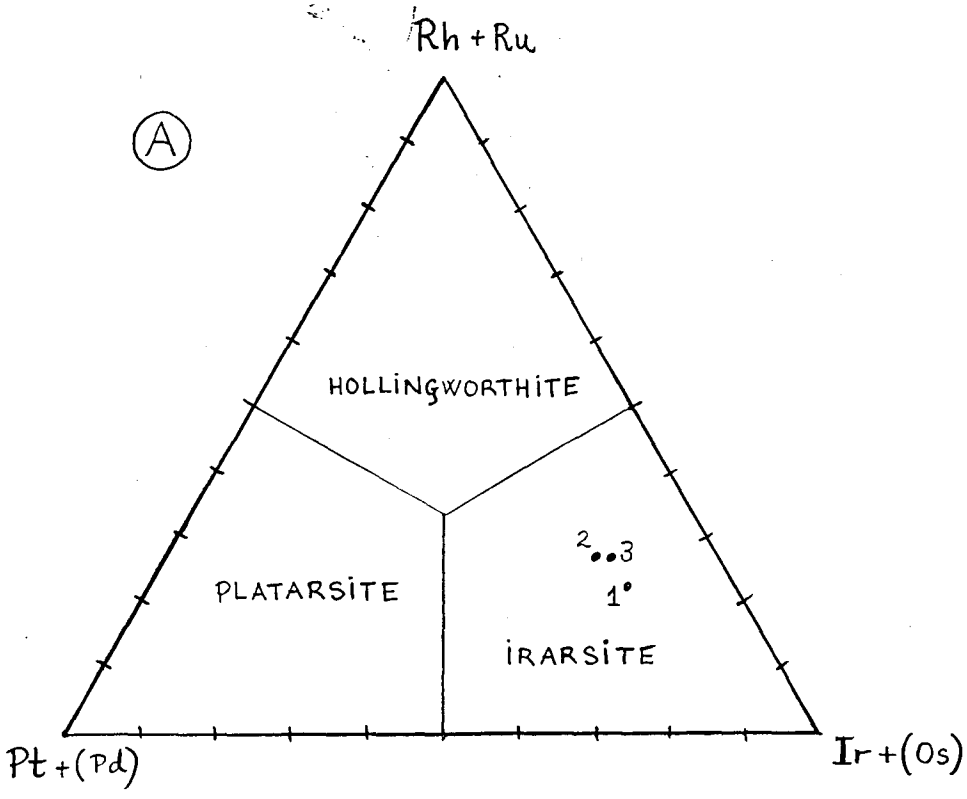
Rh + Ru
A
HOLLINGWORTHITE
PLATARSITE
IRARSITE
2
3
1
Pt + (Pd)
Ir + (Os)

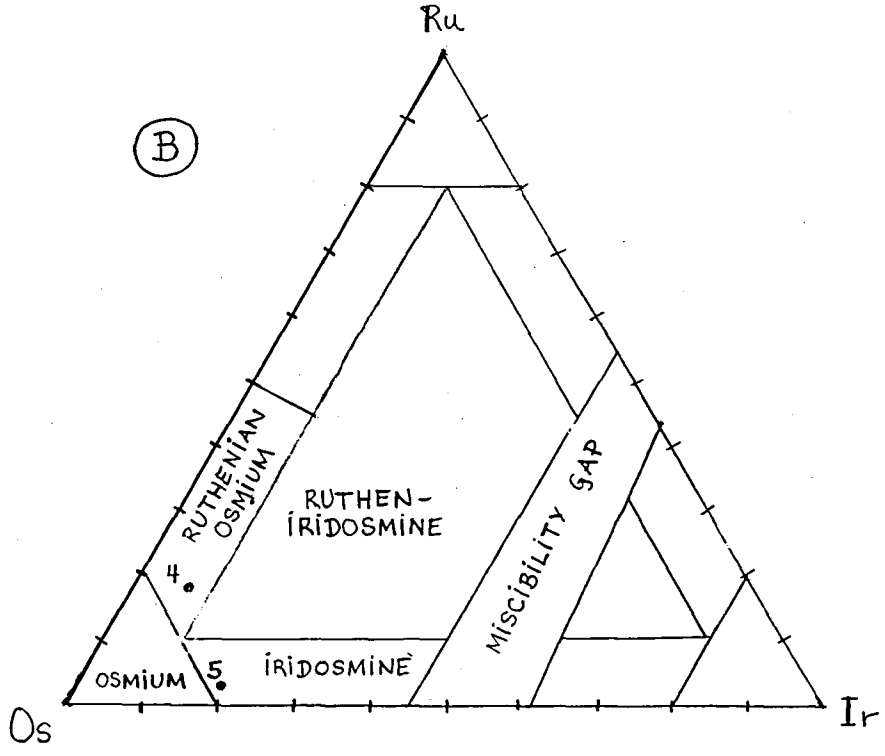
Ru
B
RUTHENIAN OSMIUM
RUTHEN-IRIDOSMINE
MISCIBILITY GAP
4
OSMIUM
5
IRIDOSMINE
Os
Ir

Fig. 9.

4.2 Platinum group element abundances in the ultramafic rocks of the Leka Ophiolite Complex, Norway - evidence for the presence of Pt-Pd-enriched stratabound horizons in an ophiolite by R.B.Pedersen and G.M.Johannesen.

Platinum Group Element abundances in the ultramafic rocks of the Leka Ophiolite Complex, Norway - evidence for the presence of Pt-Pd enriched stratabound horizons in an ophiolite

By

Rolf-Birger Pedersen and Geir Mossige Johannesen

Abstract

Three types of stratabound platinum group element (PGE) enrichments are documented within ol-cumulates of the layered series on Leka: 1) Os,Ir,Ru enrichments associated with chromitites, 2) Pt-dominated enrichments, and 3) Pd-dominated enrichments that are associated with discrete 10-50 cm thick sulphide-rich horizons. Drill-cores across the Pt- and Pd-enriched horizon have yielded half- and meter-averages of ca. 1ppm (total PGE + Au), and one of the horizons gave above 3ppm PGE in hand-samples. The horizons can be traced laterally for more than 1,5 km. B-autoradiography of one of the enriched core-samples show that the Pt/Pd-enrichments may only be a few centimetres thick, and that they are caused by well defined horizons that are rich in discrete PGE-bearing minerals (mainly tellurides, antimonides, arsenides and alloys of Pd and Pt).

The PGE enrichments are associated with the base of cyclic units and they seem therefore to have been formed during, or shortly after, influx of primitive magma into the chamber. The Pt/Pd-enriched horizons are displaced relatively to chromitites, and this fact explain why ophiolitic chromitites, in contrast to chromitites of intracratonic layered intrusions, are depleted in Pt-Pd relative to Os,Ir,Ru. The study demonstrate that ophiolites should not be excluded as potential sources for Pt, and the various processes that may control the enrichment of PGE in such complexes are discussed.

Introduction

During the last decade several studies have shown that ophiolite hosted chromitites may be enriched in platinum-group elements (PGE)(Page et al.1982; Page et al.1983,; Page and Talkington,1984; Page et al. 1986; Talkington and Watson, 1986). These are typically enriched in Os,Ir and Ru (IPGE), and contrast with the Pt,Pd (PPGE) enriched chromitites of layered intrusions such as the Bushveld Complex (Gain,1985; von Gruenewaldt et al.,1986). However, within the Caledonian Unst ophiolite (Shetland) PPGE-enriched chromitites with extraordinary high total PGE contents have been reported (Pritchard et al. 1986), and show that podiform chromiti-

tes can not be excluded as hosts for PPGE-enriched deposits.

Podiform chromitites are generally assumed to represent disrupted remnants of masses crystallized from mantle-derived magma en route to the magma chamber (Dickey, 1975; Greenbaum,1977; Lago et al. 1982). Due to uncertainties regarding the genesis of the podiform chromitites, ie. the exact petrogenetic process, their depth of formation, the amount of magma such a deposit may collect PGE from etc, considerable PGE enrichments in these bodies should not induce too much optimisms for the PGE-potential of the ophiolitic layered series (and visa versa for barren podiform chromitites).

Detailed studies of the PGE potential of the ophiolitic layered series have been given little attention. This may have many reasons, but the fact that ophiolitic chromitites in general are PPGE-depleted has clearly established the impression that ophiolites not are potential Pt-sources. However, a series of platinum group minerals have been reported from the ultramafic cumulates of the Zambales ophiolite, were Pt also has been extracted as a by-product from the mining of Ni-sulphides that are located within strongly serpentines "black dunites" (Hulin, 1959; Abrajano and Bacuta, 1982; Orberger et al. 1987). Orberger et al. (1987) conclude that the Pt and Pd have been redistributed in the rocks and that the formation of the PGM is related to syn- or post serpentinization processes.

Orthomagmatic stratabound Pt-Pd deposits had at the initiation of this study not been documented from ophiolite complexes. We considered the reason for this either to be due to a lack of systematic prospecting , or to fundamental limitations such as Pt-Pd-depleted parental magma, or magma chamber processes particular to ophiolitic magma chambers that prohibit the formations of significant PGE-enrichments.

The scope of this study has therefore been to establish the distribution of PGE within the ultramafic rocks of the Leka ophiolite, and to evaluate if parental magma compositions and the magma chamber processes operating in ophiolitic magma chambers may allow strong enough enrichment of the PGE to form economic deposits.

Geology of the Leka ophiolite

The Leka Ophiolite Complex (LOC) (Prestvik 1980; Furnes et al. 1988) is one of several ophiolite complexes exposed within the Norwegian Caledonides. The complex is exposed on the island of Leka in Mid-Norway, and exhibits all the components of an ophiolite complex, ie. tectonized harzburgites, ultramafic and mafic cumulates, sheeted dykes and pillow lavas (Fig. 1). Acid differentiates within the complex yielded a U/Pb zircon age of 497 +/-3 Ma (Dunning and Pedersen 1988) and the Leka ophiolite is therefore presently the northernmost of a series of Lower Ordovician Caledonian ophiolite complexes which includes the following complexes: Thetford Mines (New Brunswick), Bay of Islands (Newfoundland), Bett's Cove (Newfoundland), Ballantrae (Scotland), Karmøy(Southwest Norway). Meta-basalts within the LOC show a range of trace element compositions that are comparable to N-MORB, island arc

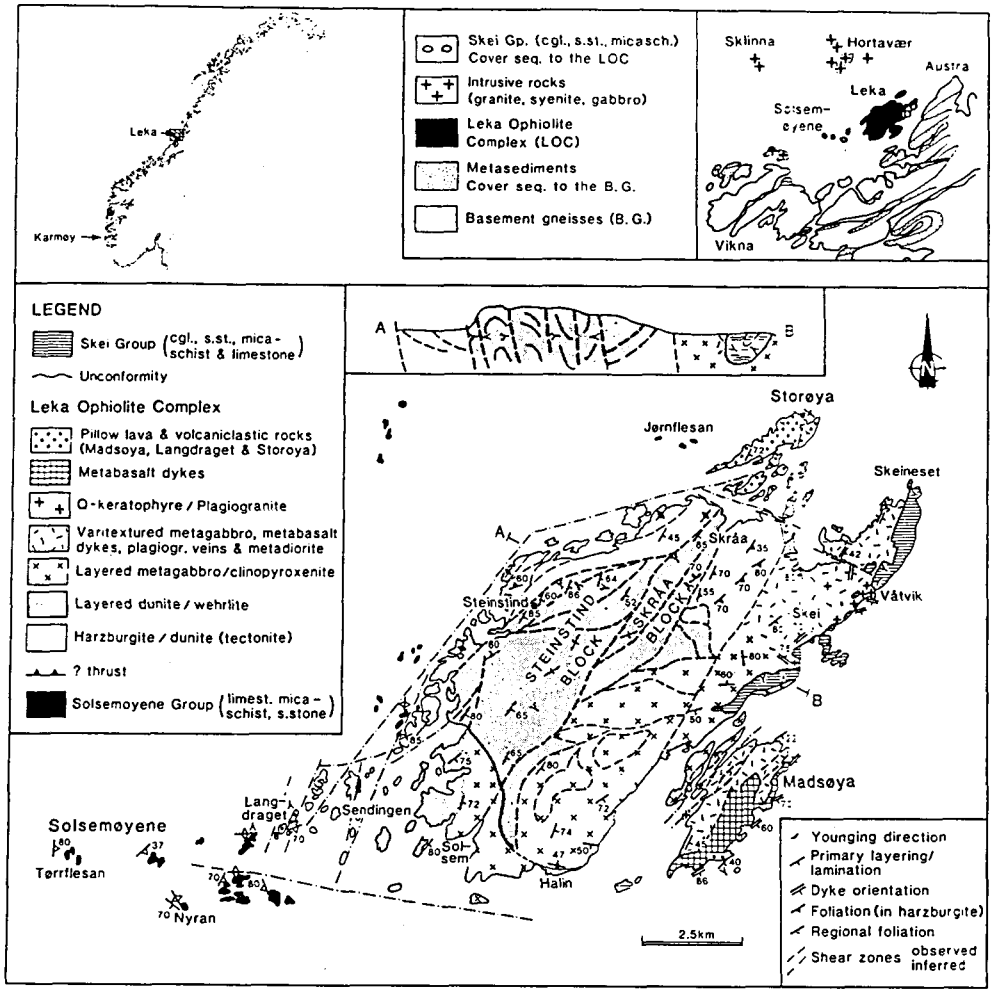

FIG. 1. Simplified geological map of the Leka Ophiolite Complex (From Furnes et al. 1988)

tholeiites(IAT), boninites as well as alkaline basalts (Furnes et al. 1988), which together with the geology of these complexes suggest that the LOC together with the other Lower Ordovician ophiolite complexes within the orogen formed within an extensive Lower-Ordovician island-arc/arc-basin system (Dunning and Pedersen 1988; Pedersen et al. 1988; Pedersen & Hertogen 1990).

Ultramafic Tectonites

The ultramafic rocks of the LOC have been subdivided into non-layered and layered ultramafic rocks (Prestvik 1980), which were interpreted to represent residual upper mantle and ultramafic cumulates respectively. A recent investigation of the non-layered rocks (Albrektsen et al. in press) shows that these rocks have many of the characteristics of mantle tectonites, i.e.: they consist mainly of harzburgites with a strong compositional banding, and of dunite bodies variable size, which are particularly frequent at the assumed uppermost part of the tectonites, below the ultramafic zone of the layered series. Dykes and veins of dunite and pyroxenite cut the compositional banding, and have themselves also been exposed to ductile deformation. Tabular dunite bodies as well as some dunite and pyroxenite veins contain in many cases a central zone that is enriched in chromite. The zone is generally composed of disseminated chromitite, but in a few cases ten to twenty centimetre thick zones of massive chromitite are developed.

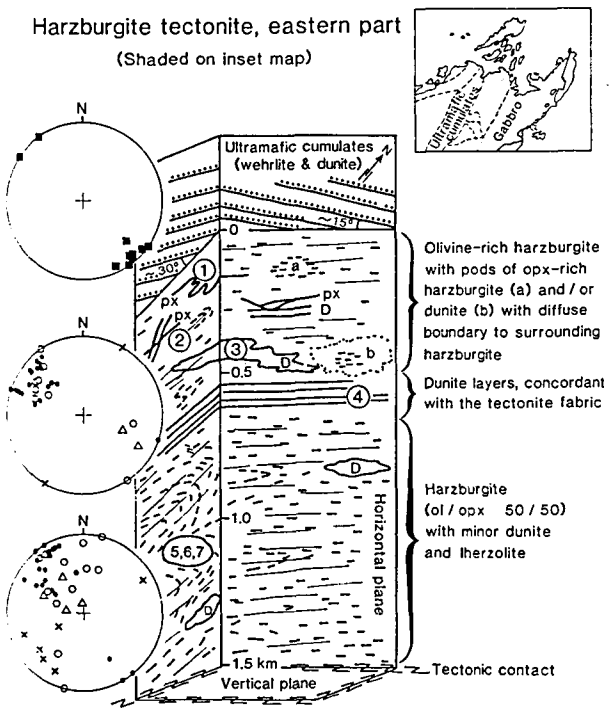

FIG. 2. Schematic illustration of internal lithological and structural relationship within the mantle tectonites and its relation to the ultramafic cumulate rocks (after Furnes et al. 1988).

The Ultramafic zone of the Layered Series

The lower part of the layered series is dominated by thick sub-zones (up to several hundred metres) of ol-cumulates interlayered with similarly thick sub-zones of ol-pyroxene cumulates (Fig. 3). Some of the sub-zones of ol-cumulates can be subdivided into several cyclic units. These cyclic units start with extreme ol-adcumulates at the base. The contact with the unit below may be gradual over a few tens of centimetres, but in many cases the boundary is very sharp. Horizons of chromitite occur frequently some distance above the base of the units (generally within 2-3 metres). The chromitite-enriched horizons vary in thickness from 5 metres down to horizons that are only a few centimetres thick, and some cyclic units exhibit no such enrichment at all along their base. Sulphide-enriched horizons that vary in thickness from ten centimetres to half a metre occur also along the base of many cyclic units. Where both a chromitite horizon and a sulphide-rich horizon are developed the first is developed some distance below the latter.

Clinopyroxene (cpx) and locally orthopyroxene (opx) appear upwards first as sporadic grains, and increase then in amount until cotectic proportions with olivine are reached. In the ol-cumulate sub-zones the cyclic units are less complete and a new unit may start before cotectic proportions are established, or even before cpx appear in the rock so that the units can only be defined by cryptic variations.

The cyclic units have been mapped laterally for nearly 3 km (Fig.3), until the lack of exposure makes it impossible to trace them further. Cyclic units that can easely be defined in the field may fade laterally, towards central parts of the intrusion, so that they can only be detected by cryptic variations.

Vertical and lateral variations in mineral composition

Cryptic vertical and lateral variations in olivine composition have been studied within parts of an ol-cumulate sub-zone (Fig 4). Although ca 90% of this unit is composed of extreme ol-adcumulates, the exposed parts of the sub-zone can be subdivided in the field into five cyclic units denoted cyclic units I,II,III,IV and V, where only units II,III and IV are fully exposed. A several metre thick chromitite horizon is exposed ca 15 metres above the base of unit III and serves toget-

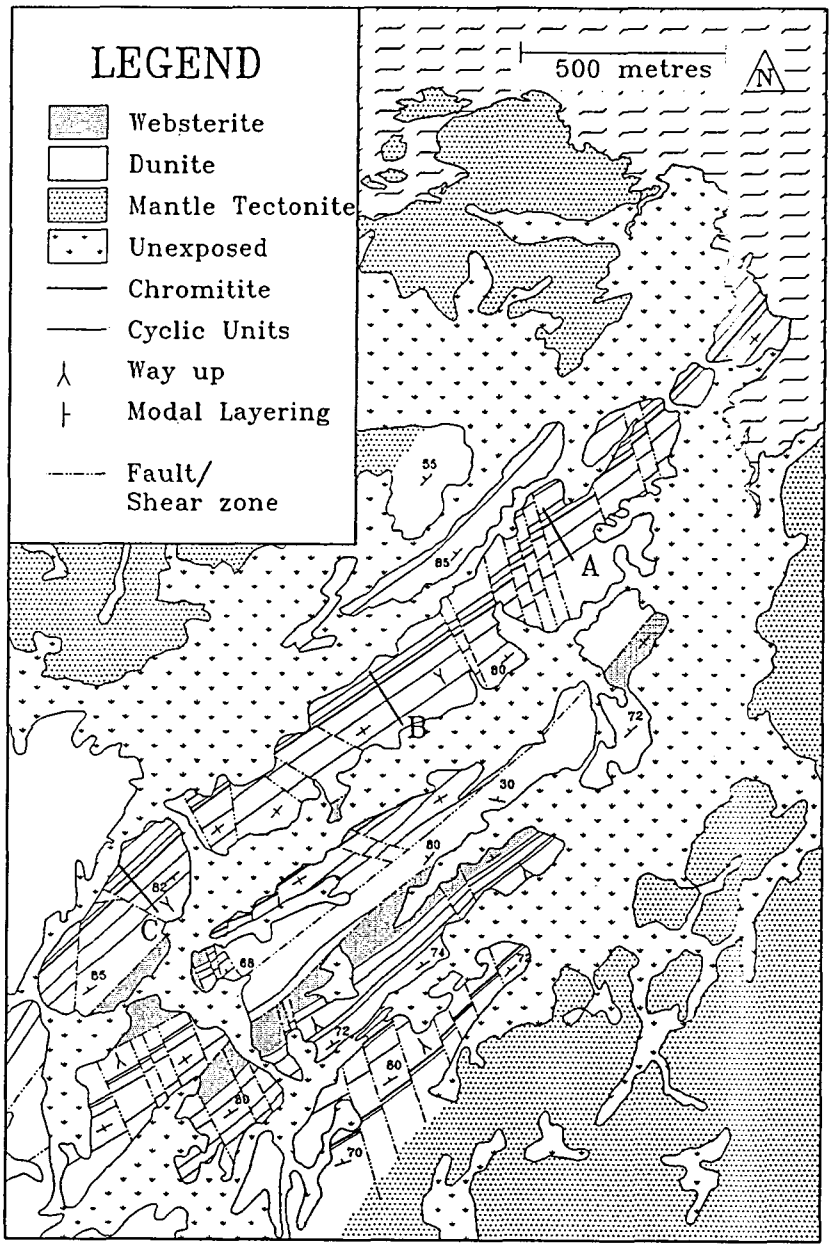

FIG. 3. Detailed map of parts of the ultramafic zone of the layered series which show sub-zones of ol- and ol-pyroxene cumulates. Cyclic units are shown within the ol-cumulate sub-zones where they can be defined in the field. The locations of the main geochemical profiles referred to later in the text are marked by A,B, and C.

her with the very marked bases of some of the units as reliable marker horizons.

A detailed discussion and modelling of these vertical and lateral variations (Pedersen, 1989, Pedersen, in prep) conclude that:

1) The very magnesian olivines ($Fo_{92.5}$) at the base of some of the cyclic units suggest a picritic parental magma for these parts of the layered series.

2) The relatively modest variations in olivine composition from $Fo_{92.5\text{-}85}$ reflect very significant variations in the MgO content of the magma - from ca. 20 to 10 wt%.

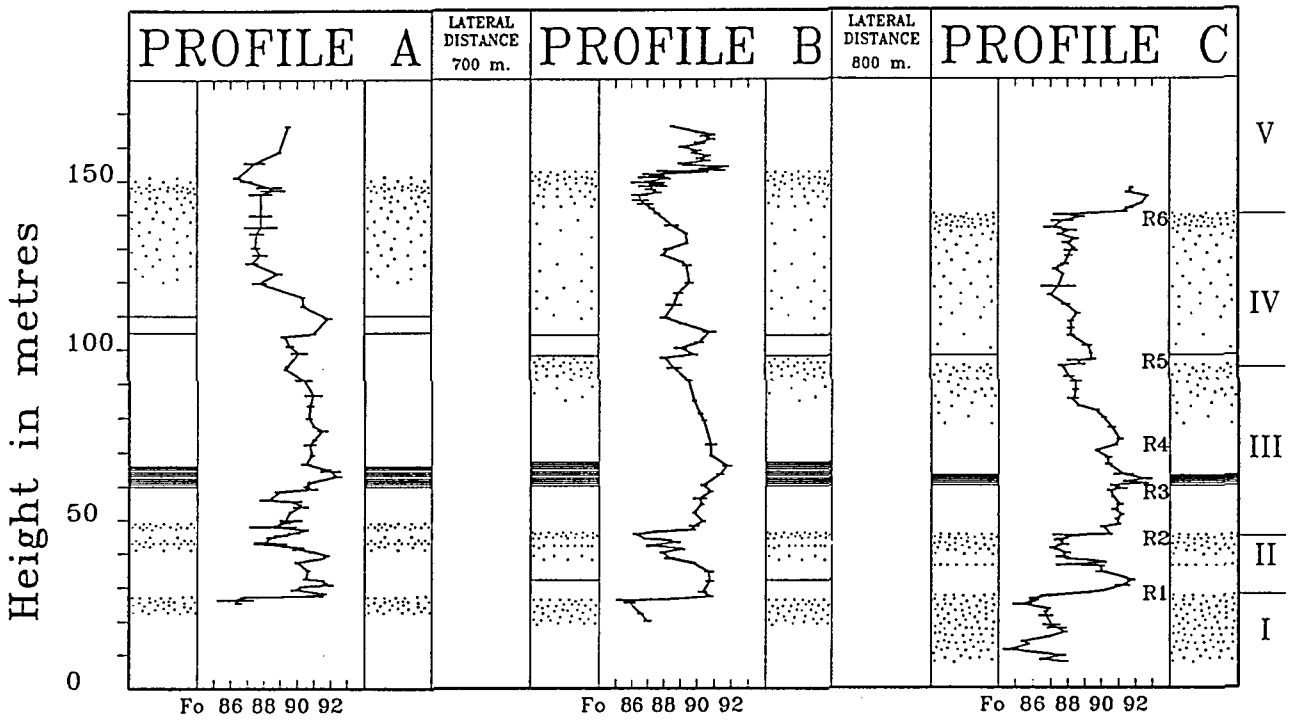

FIG. 4. Cryptic variations across parts of a sub-zone of ol-cumulates. The three profiles are taken across the same cyclic units and are seperated laterally by 700 and 800 metres (for the exact location of the profiles see Fig. 3). Cyclic units that can be defined in the field along profile C are marked with I,II,III,IV and V (some of them are less pronounced along profile A). Cryptic reversals in ol-compositions that can be defined in all three profiles are marked by R1,R2.... (after Pedersen, 1990)

3) The fact that the magma precipitated olivine which is as forsteritic as typical olivine in residual mantle, suggests that the magma could not have formed a plume and mixed extensively with the much more evolved magma further up in the chamber (as is evident from the lateral interfingering of the ultramafic cumulates with gabbros (see Furnes et al. 1988)).

4) The cryptic vertical and lateral variations in the ol-cumulates can be reasonably well explained within the framework of partly intermittent and partly continous influx of picritic magma through a magma fountain, and the formation of hybrid bottom layers which differentiated by olivine fractionation.

PGE Geochemistry

Analytical methods

The rocks were analysed for PGE by inductively coupled mass-spectrometry (ICP-MS) after preconcentration of the precious metals by fire assay. The analyses were carried out by Sheen Analytical Services (Willeton, Australia), and at the Department of Earth Sciences Memorial University of Newfoundland. The analytical procedure at Memorial University is outlined in Jackson et al. (1990). The mean instrumental detection limits at this lab. are reported to range from 0.07ppb for Ir to 0.7ppb for Au. For low level samples the mean blank values are less than 0.15 ppb, and overall method de-

tection limits approach instrumental detection limits (Jackson et al. 1990). Sheen Analytical Services claim slightly higher detection limits, with 0.5 ppb for Pt,Pd,Ru,Rh,Ir and 2ppb for Os and Au, and state that the recovery of Au in Ni-sulphides is not quantitative at levels below 500 ppb.

Three internal standards have been applied to control the precision of the PGE analyses (Appendix I, table 1). A large quantity of unserpentinized dunite was milled and carefully homogenized, and has been analysed routinely together with the samples. The sample yielded mantle values and served as a good measure for the reproducibility of

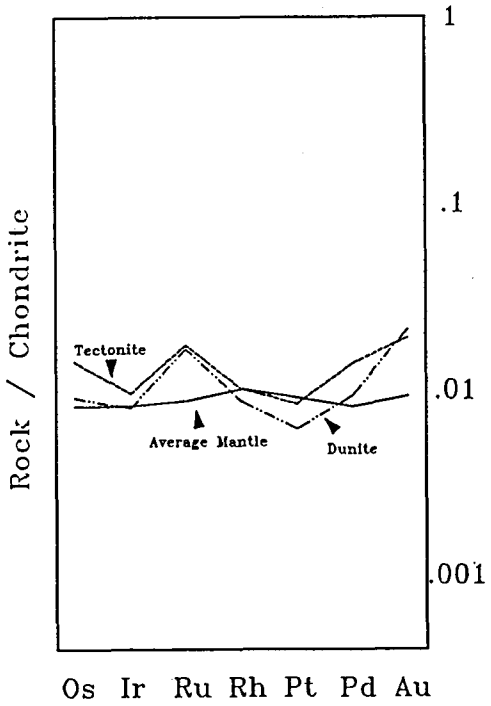

FIG.5. Chondrite normalized PGE-patterns of mantle tectonites and associated dunites.

the base line analyses in this study. The relative standard deviations are less than 20% for Ir, Ru, Rh, and Pt; 37% for Pd and 67% and 88% for Os and Au respectively (Appendix I, table 1). Two samples of komatiite (AX18,90), which were kindly provided by S-J. Barnes, were also analysed routinely. These samples have PGE contents in the intermediate range. AX90 gave relative standard deviations of 10% or better for all the PGE except for Os which gave 22%. The results are less satisfactory for AX18, which can be attributed to a single bad run at Sheen. The results on these samples are also in good agreement with the results obtained by neutron activation (Appendix I, table 1).

Two standards (PTC-1, PTM-1) have been run as a control for peak compositions. Except for Au the results obtained are in good agreement with the recommended values.

Mantle Tectonites

The harzburgites of the Leka ophiolite, which are interpreted to represent depleted mantle tectonite, have very low PGE-contents (Appendix I, table 2) compatible with the values obtained from depleted mantle rocks elsewhere (Barnes et al. 1985). The mantle-normalized PGE-patterns are nearly flat , but contain a slight positive Ru-anomaly which (Fig 5). The dunite dykes and veins that host some of the chromitites studied show PGE-abundances similar to the harzburgites.

Chromitites associated with the mantle tectonites

Chromitites exposed within tabular dunite bodies and within dunite and pyroxenite veins have been sampled and analysed for major elements, S, precious- and base-metals, and the results are listed in table 3 (Appendix I) . The highest content of precious metals found in these rocks is 8500 ppb (PGE + Au), obtained from a ca 10-20 cm

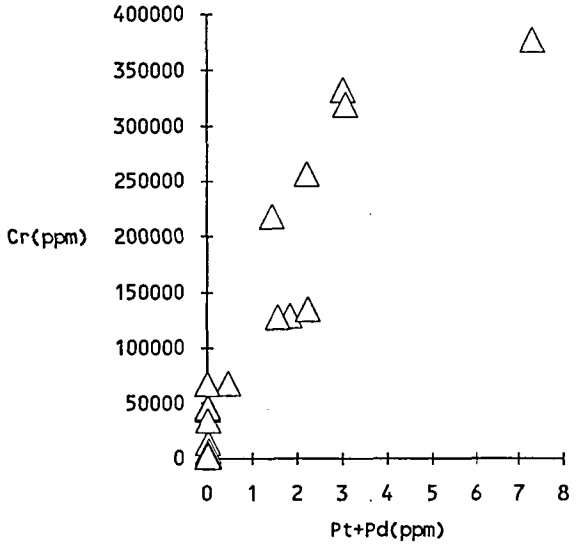

FIG.6.Plot of total PGE against the Cr contents of chromitites hosted within the mantle tectonites

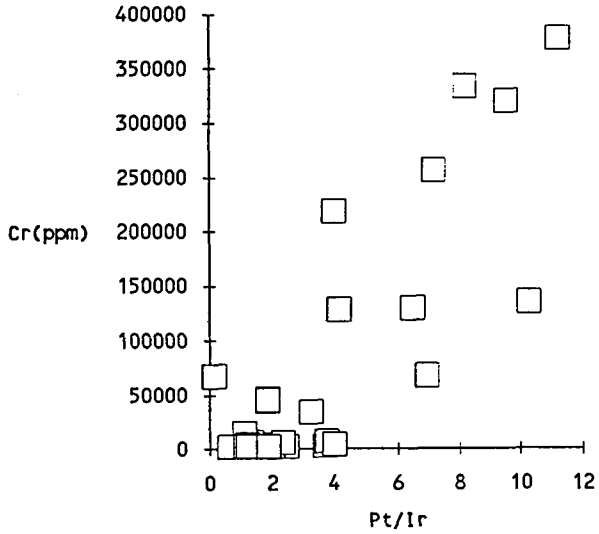

FIG.7. Scattergram of the Pt/Ir ratio against the Cr-content of the chromitites.

thick massive chromitite that can be followed for a few tens of metres. The PGE contents vary, however, considerably between individual samples from this chromitite (from 8510 to 2832 ppb) and the average of 5 samples is 4770 ppb total PGE + Au.

The total PGE contents of the chromitite from the tectonites show a roughly linear relationship with the amount of Cr in the rocks (Fig 6). Disseminated chromitites would therefore be expected to be less PGE-rich than the massive. The increase in PGE with increasing modal abundance of chromite seems not to be proportional for the IPGE and the PPGE, as indicated by the increasing Pt/Ir ratios with increasing Cr contents of the samples (Fig 7). This is also reflected by the chondrite normalized PGE-patterns of the rocks (Fig 8a). While the PGE-depleted rocks have relatively flat PGE-patterns, the enriched rocks show patterns that climb towards Pd. The depleted rocks tend to show a positive Ru-anomaly, while on the other hand many of the enriched samples show a negative Ru-anomaly.

The chondrite normalized patterns of the rocks compare with patterns reported from chromitites from the mantle sequences of other ophiolite complexes (Fig 8b). The PGE depleted patterns are comparable with the PGE-signature of chromitites from the Lewis Hill(Newfoundland) and chromitites from the Thetford Complex show also similarly depleted patterns. The enriched pattern differs from the typical ophiolitic chromitite patterns which tend to be IPGE-enriched, as exemplified on Fig. 8b by chromitites from the White Hills (Newfoundland) and from Harolds Grave within the Unst complex (Shetland). The patterns compare, however, closely with the patterns obtained from the Cliff site on Unst, although the Leka samples are not so rich as the highest grades obtained on Unst.

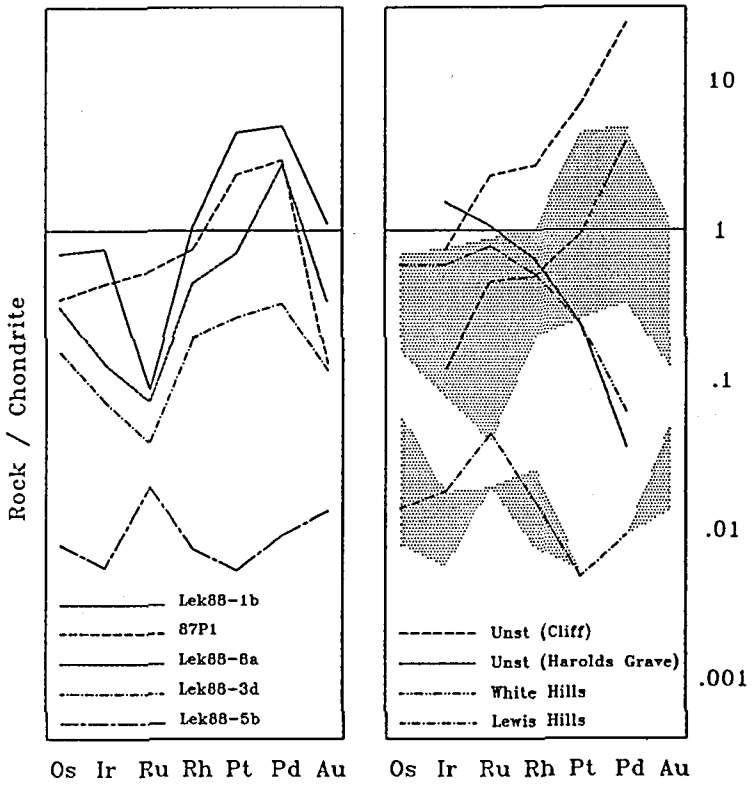

FIG. 8. A) Contrasting chondrite-normalized PGE patterns of chromitites associated with the mantle tectonites. B) Comparison of the PGE-patterns of the Leka chromitites (shaded areas) with other podiform type chromitites (Data from Prichard et al. ,1986; Talkington and Watkinson, 1986).

PGE in the ultramafic zone of the layered series -Variations through cyclic units

The study of the PGE-geochemistry of the cumulate ultramafic rocks has been focused on the sub-zone where cryptic mineral variations had previously been established (Fig 4). Samples that had been collected along profile B to define the cryptic variations in silicate mineral composition were analysed for PGE to give an overall view of the variation in PGE contents through the cyclic units. The results are shown diagrammatically in Fig 9 and listed in table 4 (Appendix I), and demonstrate variations in the PGE content from only a few ppb to above 1ppm total PGE. Although the curves are rather rugged, two pronounced peaks are evident in the IPGE trends. The lowermost is situated, as would be expected, within the main horizon of disseminated chromitite, while the uppermost is located just above the base of the uppermost cyclic unit, where a few thin relatively sulphide-rich chromitite seams are located. The total IPGE content is, however, relatively low in both samples - only of the order of a few hundred ppb. The presence of three peaks in the Pt and Pd curves , two of which yielded more than 1000 ppb of Pt and Pd combined, is more surprising. While the lowermost of these peaks is positioned a metre or two above the top of the main chromitite (R3) the two other are associated with R5 and R6 (Fig 9).

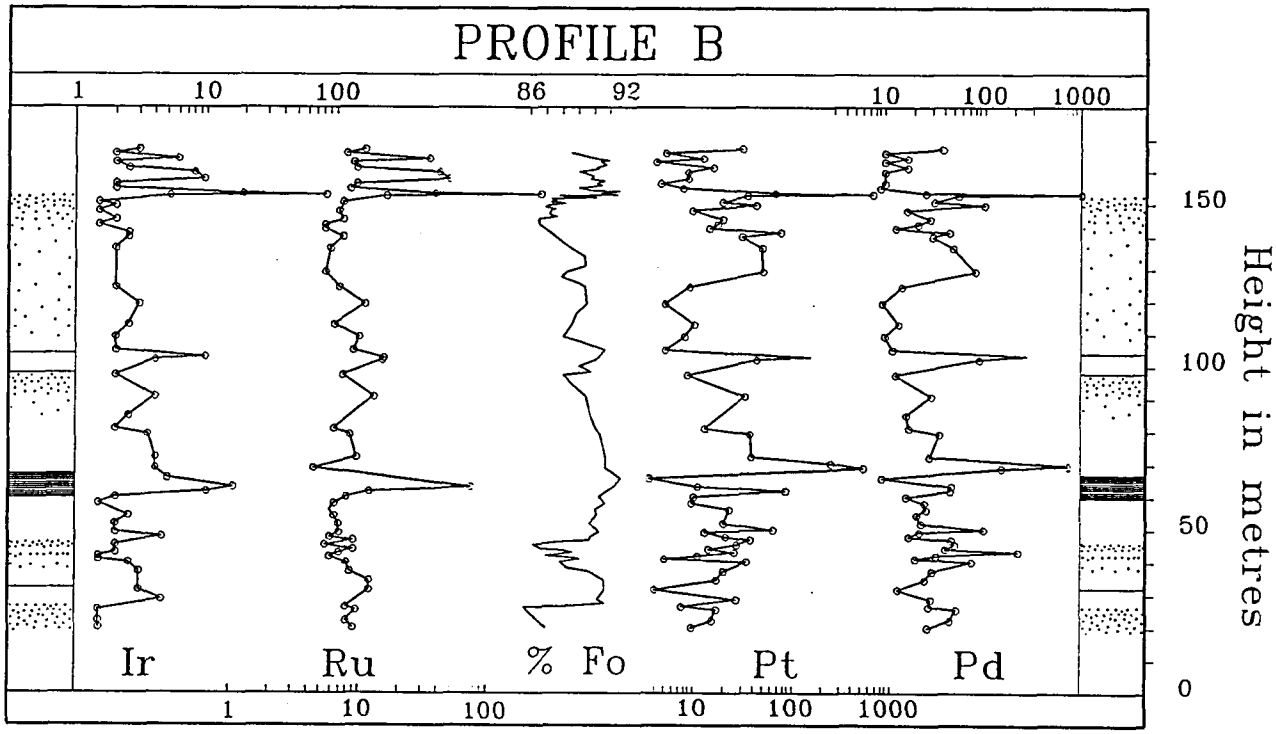

FIG. 9. Variations in PGE with height along profile B.

The bases of four cyclic units and the main chromitite horizon were resampled with short 10-30 metres drill holes. Several cores were also taken across the base of the same cyclic unit to obtain lateral variations in composition. The holes were all taken with ca. 60 degrees inclination to the layering (which is vertical) so that two metres of core represent a one metre section of the rocks. The drill cores were split, and half meter lengths (subsequently meter-lengths) were crushed and analysed. The results are listed in tables 5-16 (Appendix I), and the results are compiled in Fig 10, which shows also the vertical and lateral position of the analysed drill cores.

The results from the drill cores confirm that the PGE contents may fluctuate by an order of two magnitudes across a few metres of the layered rocks. The core-data show also the presence of several PGE-enriched horizons that yield half- and one-meter averages of around 1ppm total PGE (mainly Pt and Pd). The drill core across R6 (88B4 and 88B1), where a sample with around 2ppm PGE had been collected (sample 87P2, Appendix I, table 4), yielded half-meter averages of only a few hundred ppb which suggests that the enriched horizon is very thin and that this horizon had been sampled directly with the hand specimen.

The drill cores across and above the main chromitite horizon show the presence of two Pt and Pd-enriched horizons immediately above the chromitite, and a third 15 to 20 metres above the chromitite which coincides with a minor reversal in olivine compositions (R4). These horizons can be traced

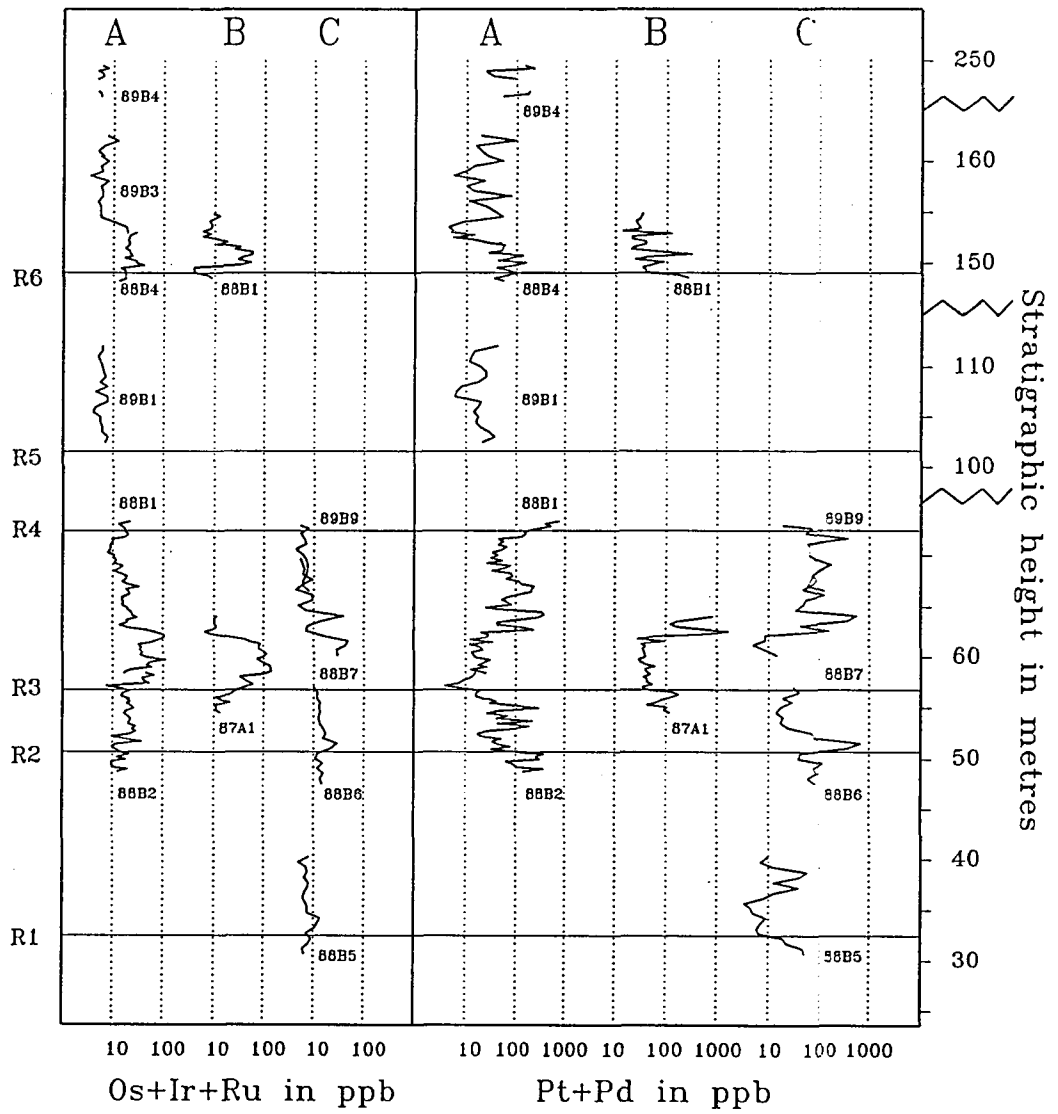

FIG 10.. Compilation of PGE-data from drill-cores taken across the bases of cyclic units along the three major profiles of Fig. 3.

laterally from profile A to B and C - a distance of around 1.5 kilometres (Fig 10). An enriched horizon was also discovered just above R2 (profile 88B6) which also yielded close to 1ppm total PGE over a metre of core.

The variations in the PGE content across and immediately above R2 are shown in more detail in Fig 11 . The change from wehrlite to dunite, which defines the base of the cyclic unit in the field, is reflected in the diagram by a sudden drop from above 10wt% to less than 0.5 wt% CaO about 8 metres above the beginning of the core (the considerable variation in CaO below this level reflects a smaller scale interlayering of dunite and wehrlite). The reversal in composition at the base of the cyclic unit is shown by an increase in the Ni content of the rocks from 800 to above 2000 ppm across three metres of the layered rocks. The PGE enriched horizon (mainly Pt,Pd and Au) is clearly situated at the exact base of the cyc-

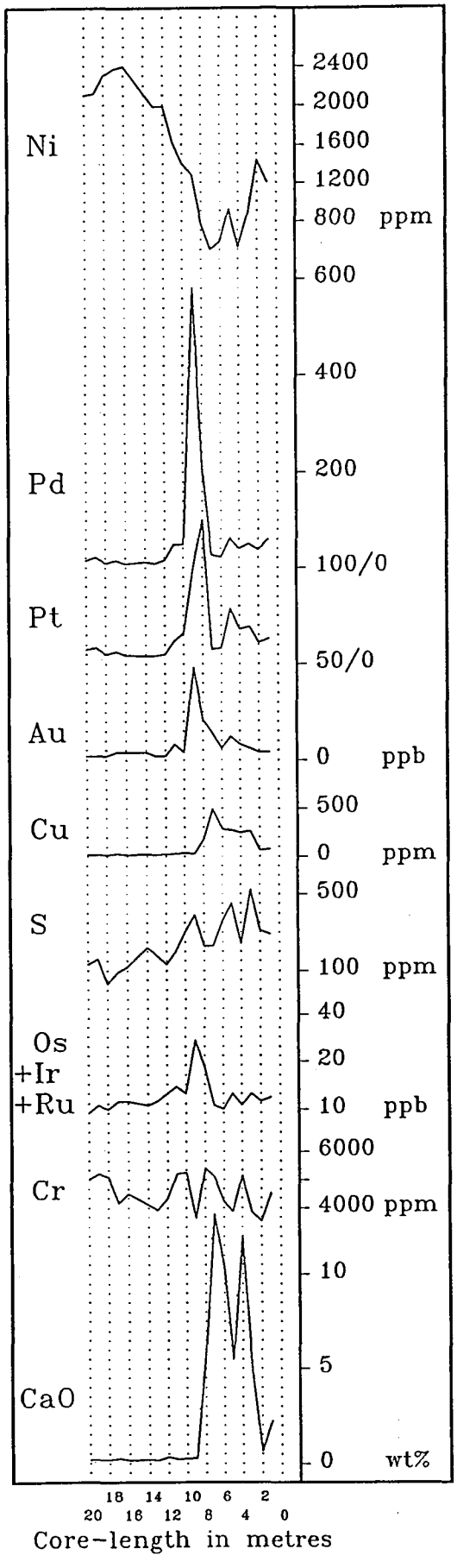

FIG. 11. Compositional variations with height across the base of R2 along profile C (core 88B6).

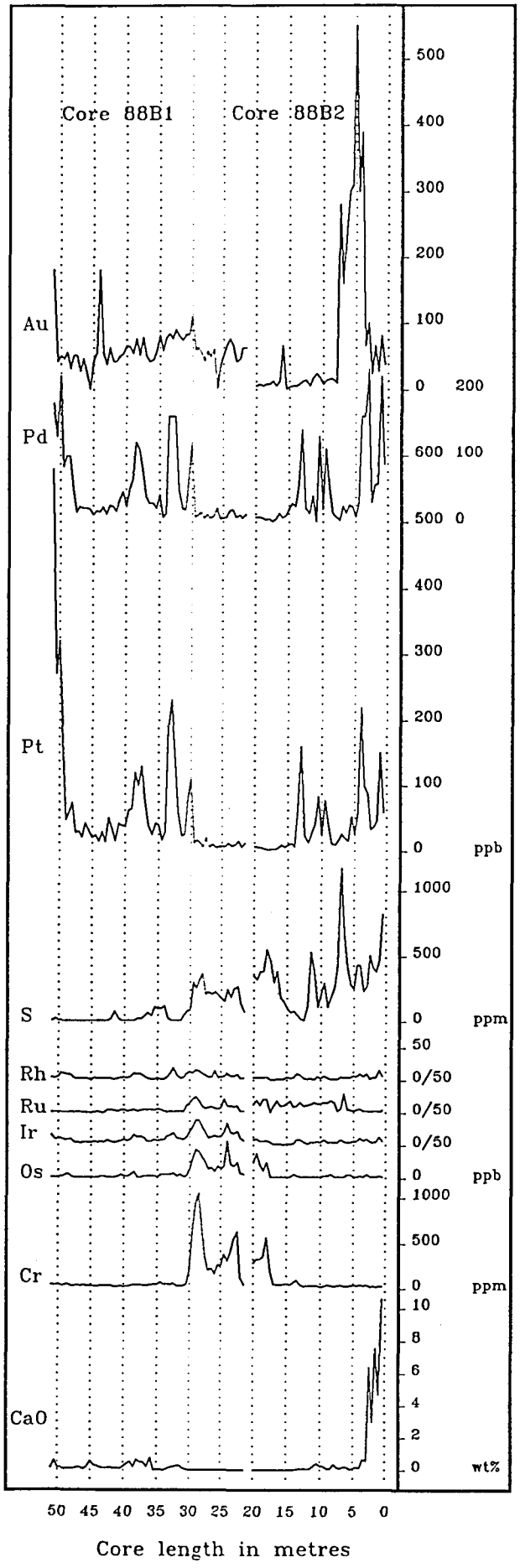

FIG. 12. Geochemical variations with height across and above the main chromitite horizon along profile A (core 88B1 and 88B2).

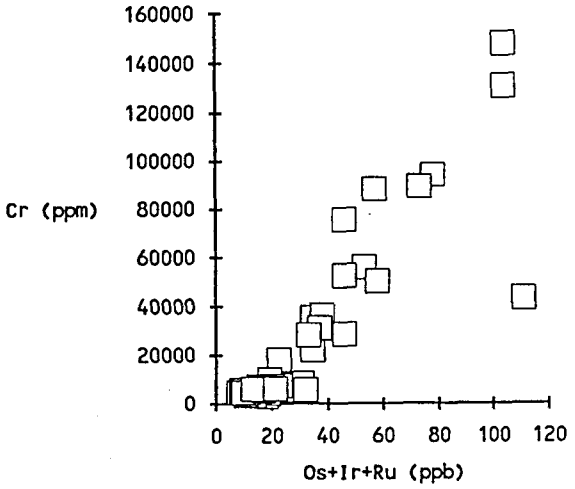

FIG. 13. Diagram that show the systematic increase in the IPGE content with increasing amount of Cr within the main chromitite horizon.

lic unit, and is associated with a minor peak in S.

R2 was also penetrated by core 88B2 taken along profile A (Fig 12). The base of the cyclic unit is again defined on the diagram by the rapid drop in CaO. Peaks in the Pt and Pd trends are also present here at the base of the cyclic unit, and minor peaks are present just below - at a level where the CaO content declines rapidly. A Au enrichment (up to 500 ppb) is present above these peaks. This enrichment cannot, however, be traced laterally, and similar selective enrichment of Au has not been observed in any of the other cores. The local Au enrichment may be related to a minor brittle shear zone, but no detailed study of this Au-anomaly has yet been carried out. Above the Au peak three minor Pt + Pd peaks are present before the main chromitite horizon is intersected as shown on the diagram by a sudden increase in the Cr content.

A hole (88B1) was also drilled from a position just below the base of the chromitite and shows the compositional evolution through this horizon and 10 metres above (Fig 12). The IPGE are enriched in the chromitite horizon and the contents of these elements increase linearly with the Cr content of the bulk rock (Fig 13). Three Pt-Pd peaks are recorded above the chromitite horizon and a fourth is present at the end of the core. These peaks can be traced laterally, and the two lowermost peaks are intersected by drill-hole 87A1(taken along profile B) (Fig 14), and all four peaks are present in cores 88B7 and 89B9 which were drilled along profile C (Fig 10).

Lateral variations in PGE within cyclic units

There appears to be a systematic lateral variation in the Pt/Pd ratio of the three major peaks that are located above the main chromitite horizon. In profile A, which is assumed to have had the most central position in the magma chamber, the peaks are slightly to strongly enriched in Pt relative to Pd with an average Pt/Pd ratio of 1.6 (Fig 15). In profile C, however, the average Pt/Pd ratio of the three peaks is 0.4 or a quarter of that in profile A. A sulphide-rich horizon located at the level of the lowermost of these three PGE peaks can be traced in the field from profile A to B to C. Hand samples from this horizon yielded 137, 1038, 1879 ppb respectively from profiles A, B, C respectively, or an increase in the PGE content towards what we assume are the more distal parts of the intrusion. The Pt/Pd ratio of this horizon seems, however, not to change dramatically (0.33, 0.44 and 0.40) which contradicts the pronounced lateral changes that are observed in the core-data (Fig. 15). Both the total PGE-content and the Pt/Pd ratio of samples from the sulphide-rich horizon that were collected at profile C are compatible with the values obtained for the

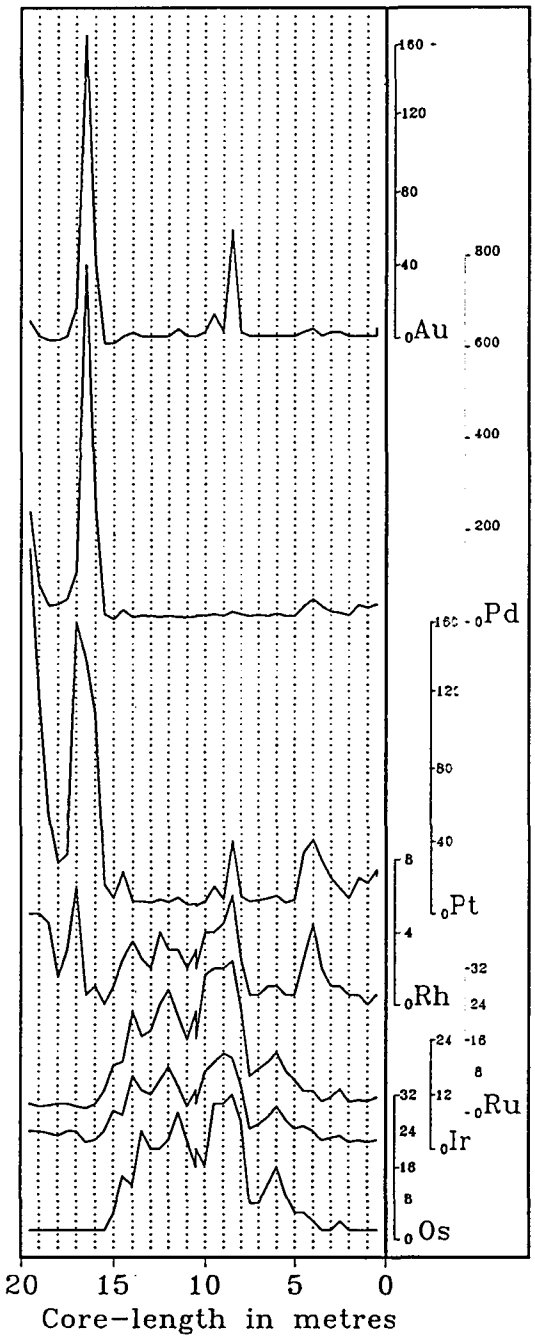

FIG. 14. Variation in PGE contents across the main chromitite horizon in profile B (core 87A1).

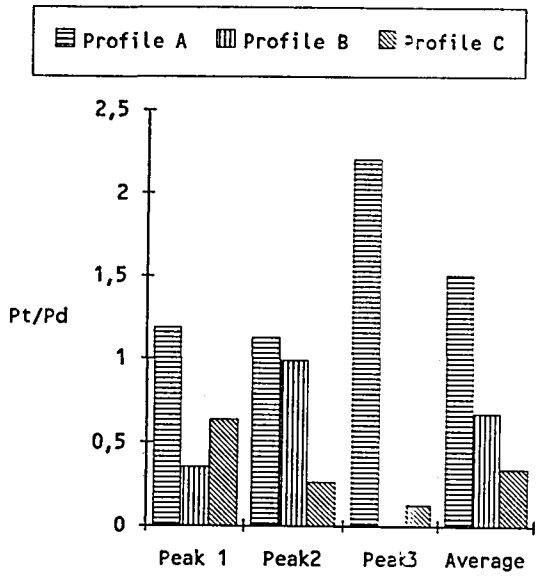

FIG.15. Histogram that show how the Pt/Pd ratio of the three major PGE-peaks above the main chromitite horizon change laterally. For further discussion see text.

lowermost of the three peaks at this location. The reason for the above inconsistency can be found in profile A where the total PGE-content of the sulphide-rich horizon appear to be nearly an order below that of the peak composition in the core (88B1 Fig. 12). It appears therefore that the main PPGE-enrichments along this profile are displaced relative to the sulphide-rich horizon. This relation is shown by the variation of these elements with stratigraphic height (Fig. 12), and it is particularly evident in core 88B1 where the parts that are most enriched in Pt and Pd show the lowest concentration in S (Fig 16). A similar scattergram of the core-data from the hole that was drilled through the base of the uppermost cyclic unit (taken across R6 close to profile A) shows a different picture with the data points spreading out as a fan (Fig 17). The reason for this covariance can be deduced from Fig 18, which shows compositional variation with height across R6. The base of the cyclic unit is here again marked by the sudden decrease in CaO. A meter thick sulphide-rich horizon can be observed in the field a meter above the base of the cyclic unit, and this is depicted in the core as two marked peaks in the S content. Cu is particularly enriched in the uppermost part of this horizon while the lowermost part is enriched in Pd. The main Pt peak occurs, ho-

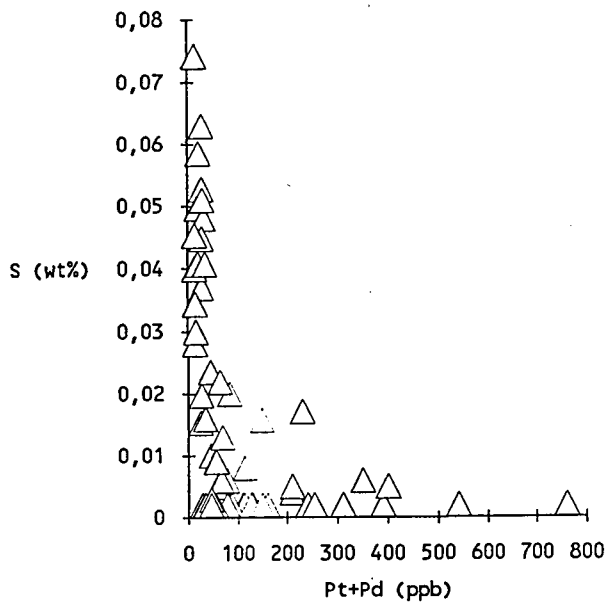

FIG. 16. Diagram that demonstrates the inverse correlation between S and Pt + Pd in core-samples that are taken across and above the main chromitite horizon along profile A (core 88B1)

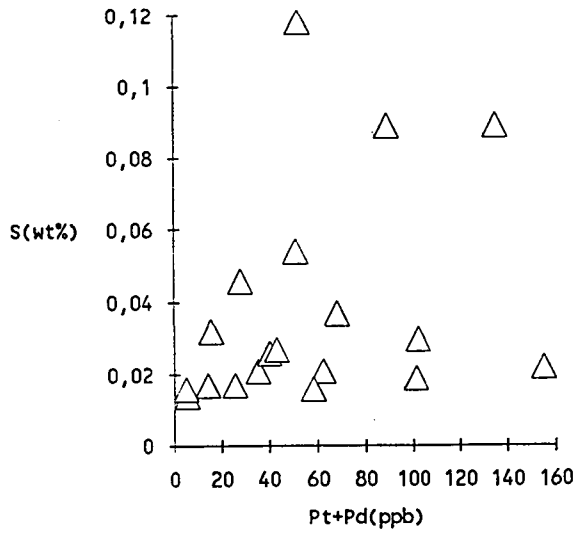

FIG. 17. Variation between S and Pt + Pd in core 88B4 taken across R6 between profile A and B.

wever, below the sulphide horizon. This peak exhibits a Pt/Pd ratio of 2.4 while the peak associated with the sulphide-rich horizon has a Pt/Pd ratio of 0.4, which compares well with the lateral variation in the Pt/Pd ratio observed along the enriched horizons above the main chromitite from profile A to profile C (Fig 15).

The layered series contains both Pt-dominated PGE enrichments, that are not associated with sulphide-enrichments, and Pd-dominated PGE enrichments which are associated with discrete sulphide-rich horizons. The present data suggest that the Pt-dominated enrichments are positioned just below the Pd-dominated, and that they fade towards distal parts of the intrusion, and vice versa for the Pd-dominated enrichments.

Peak-composition of Sulphide-rich horizons

The maximum half- and meter-averages obtained for the Pt- and the Pd-dominated enrichments are of the order of 1ppm for the two elements combined. Hand-samples of 12 sulphide-enriched horizons (maximum S content only 0.6wt%, see Table 19) show that the peak composition of the Pd-dominated enrichments may be above 3ppm total PGE (Table 17). The most enriched samples (89lek9 & 21) were taken from a horizon that is exposed around 30 metres above R6. The second most enriched sample (89lek31) was the only sample taken outside the area studied in detail, and points to the presence of enriched horizon also outside the selected area.

No hand-specimens have yet been taken from the Pt-dominated enriched horizons because their exact locations are difficult to establish in the field, due to the lack of other associated phases such as sulphides or chromite. However, the peak compositions of these horizons would also be expected to

be significantly higher than the half-meter averages obtained from the cores.

Chromitites from the layered series

The disseminated chromitite horizons sampled by drilling yielded low contents both in the PPGE as well as in the IPGE, although modest enrichment in the latter group can be observed through such horizons (Fig 12,14). A number of chromitite horizons were sampled at an initial stage of this study. The sampling was carried out throughout the ultramafic zone of the layered series and the results are listed in table 18. The highest values are obtained in 87P1 and P2, which contrasts with the rest in that they are also enriched in PPGE addition to the IPGE. These samples were taken from a thin chromite seam located a few tens of centimetres above R6 in profile B, and differ from the other samples in that they contain visible sulphides. In the samples that are free of visible sulphides the maximum PGE content is 405 ppb - mainly Ru. The average Ru# (Ru/Os + Ir + Ru) of these samples is 0.51, and is slightly higher than the Ru# obtained from laurite grains in chromitites of the White Hills Peridotite (Ru# 0.46) (Talkinton and Watkinson, 1986) , which suggests that all the IPGE may be confined to laurite grains which have also been identified as inclusions in chromite grains.

Chondrite normalized patterns of the stratabound enriched horizons

Chondrite-normalized patterns of representative samples of the Pt-dominated enrichment, the sulphide-bearing Pd-dominated enrichments as well as of the chromitite horizons are shown in Fig 19

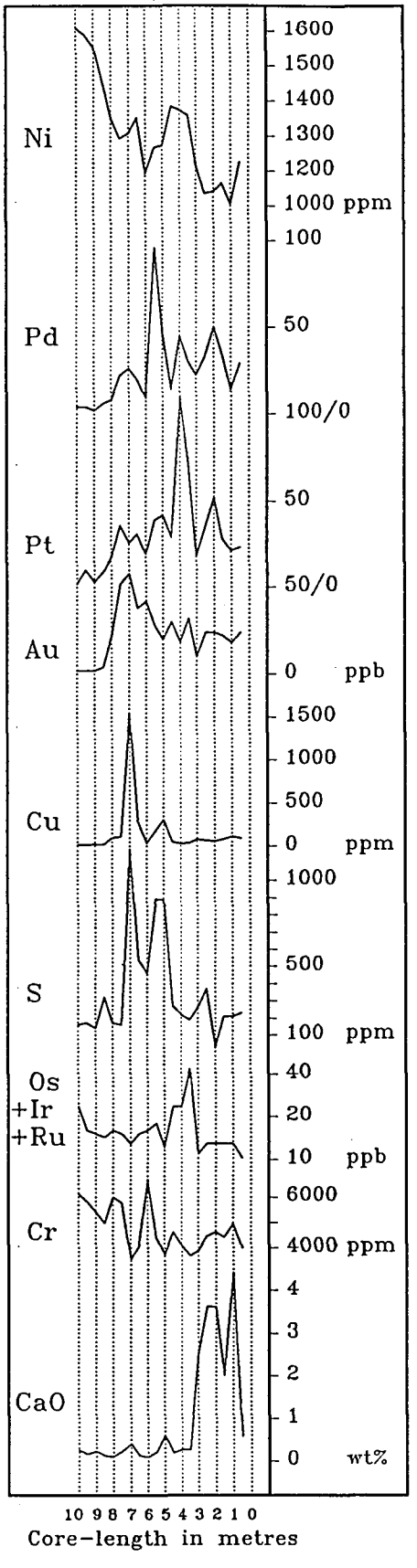

FIG. 18. Geochemical variations with height across R6 (core 88B4)

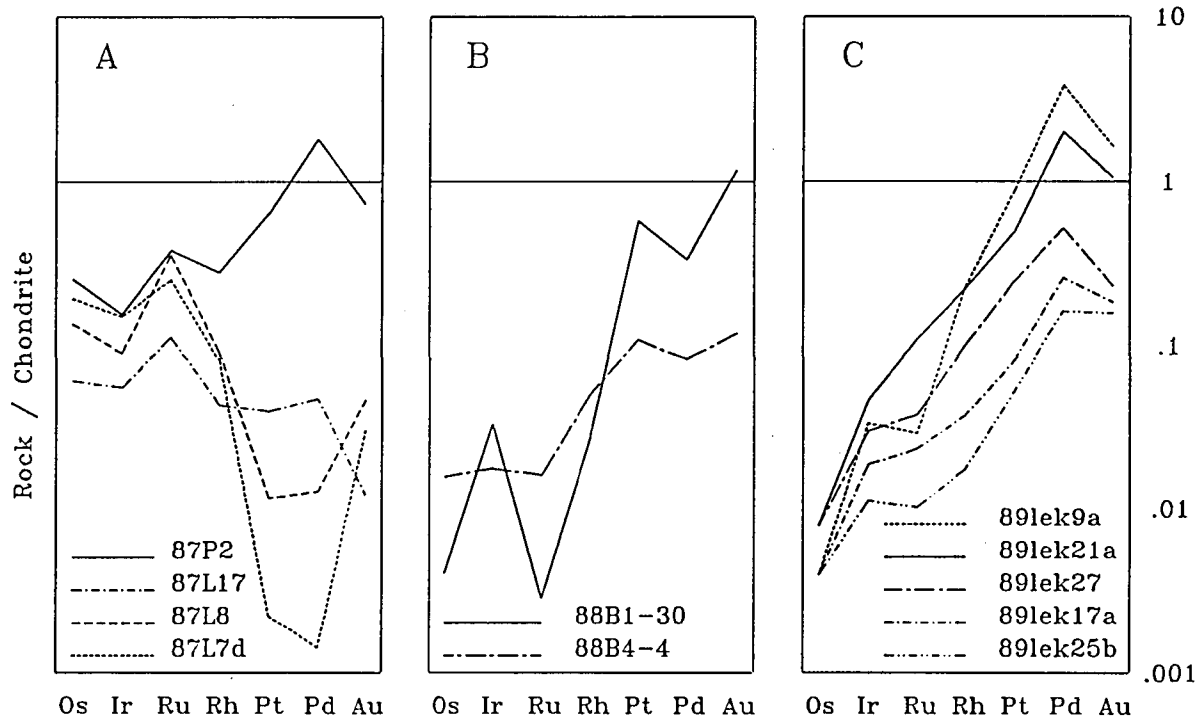

FIG. 19. Chondrite-normalized patterns of the three types of enrichements present within the ultramafic cumulates: a) IPGE-enriched chromitites, b) Pt-dominated enrichments, and c) Pd-dominated enrichments associated with sulphide-rich horizons.

a,b,c respectively. The Pt- and the Pd-dominated enrichments both show PPGE enriched patterns that compare favourably with the patterns of deposits such as the J-M Reef of the Stillwater Complex and the Merensky Reef of the Bushveld Complex (Fig 20). The chromitite horizons show on the other hand IPGE-enriched patterns, similar to the patterns that are reported from the other ophiolite hosted chromitites (Fig 20, Fig 8b). One chromitite horizon, the one containing visible sulphides, deviate from this pattern by having a pattern that can be visualized as a combination of the Pd-dominated pattern of the sulphide rich horizons and the typical pattern of the stratabound chromitites. This pattern compare with the patterns reported from chromitites of the Stillwater Complex (Fig 20).

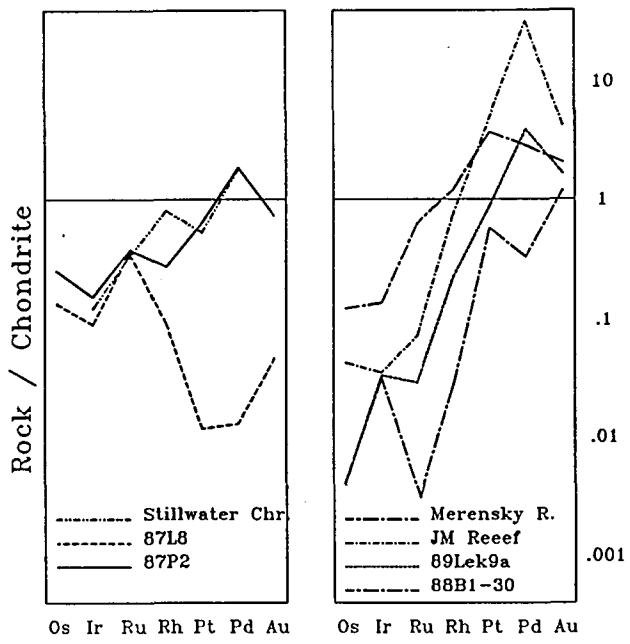

FIG. 20. Comparison of the PGE-patterns of the stratabound chromitites with chromitite from the Stillwater Complex (a), and of the PPGE- enriched horizons

Platinum Group Minerals (PGM) in the PGE-enriched rocks

Methods

PGM have been located in the enriched rocks by B-autoradiography, following the procedure given by Potts (Potts, 1984; Potts & Prichard, 1986). Polished thin sections were cleaned and packed in standard aluminium containers. The sections were radiated for an hour at Institutt for Energiteknikk at Kjeller (Norway) with a thermal flux of $0.8*10^{13}$ neutrons cm^{-2} s^{-2}.

The activated thin-sections were placed on a B-sensitive X-ray film (Fuji-RX) in a dark room were the lights where screened by Kodak GBX-2 safelight filter. The film was exposed for 23 and 48 hours after 14 and 30 days respectively. After exposure the film was developed with Fuji Photosol CD-18 developer for 5 minutes, and CD-40 fixer for 10 minutes (at 20 degrees C).

To discriminate between the B-emitters, two series of autoradiographs were recorded, the first after 14 days of cooling and the last after 30 days. Two parallel exposures are shown in Fig 21, and demonstrate the disappearance of a discrete grain on the last exposure. One of these (the one under the arrow) turned out to represent a Au-Cu alloy and the short halflife (2.7 days) of the B-emitter (^{198}Au) explain the disappearance on the last radiograph. The darker areas on the radiographs represent an image of the chromites which due to the content of B-emitting isotopes (^{60}Co) can be distinguished from the silicate minerals. Due to the contrast between the chromites and silicate minerals, and also between various silicate phases the radiographs are well suited as "maps" to locate the PGM under the scanning electron microscope (SEM) or on the microprobe.

The SEM-work ha been carried out on a Jeol JSM 35. The PGM were searched for in back-scatter mode with an accelerating voltage of 25kV, and the qualitative analyses

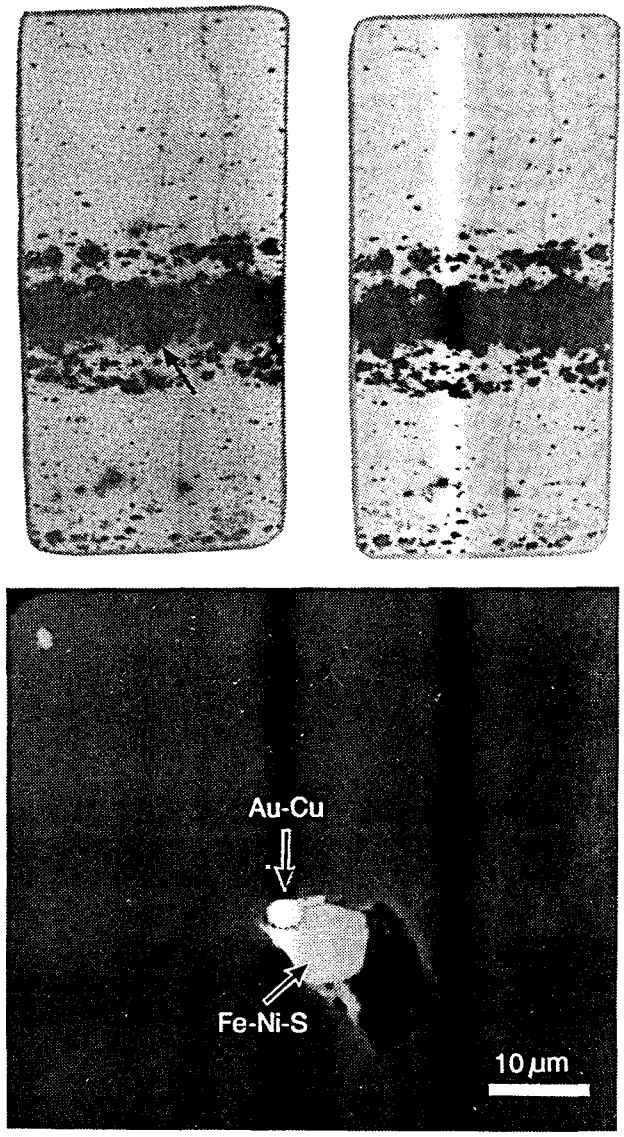

FIG. 21. B-autoradiograph of a stratabound chromitite wich show the presence of a B-emitter (see arrow on A) that dissapear after 30 days of cooling (B). SEM investigation of the chromite grain demonstrated that the B-emitter probably was a small Au-Cu alloy (C).

	Pentlandite		Heazlewoodite		Native Cu	
Weight %	Fe	36.96	Fe	0.40	Fe	0.42
	Ni	28.49	Ni	72.92	Ni	1.01
	Co	0.95	Co	0.01	Co	–
	Cu	–	Cu	–	Cu	98.02
	S	33.96	S	26.98	S	–
	Total	100.40	Total	100.58	Total	99.48
Atom %	Fe	29.77	Fe	0.34	Fe	0.48
	Ni	21.83	Ni	59.30	Ni	1.10
	Co	0.73	Co	0.01	Co	–
	Cu	–	Cu	–	Cu	99.48
	S	47.64	S	40.17	S	–

TABLE 1. Representative analyses of some ore minerals and of native Cu.

Observation	Suggested mineral
Fe,Ni	Awaruite
Fe,Ni,Cu,Te	?
Fe,Cu,S	Chalcopyrite Digenite Valleriite
Ni,As	Orcelite Nickeline
Ni,Sb	Breithauptite
Pb	Native Pb

TABLE 2. Qualitative composition and suggested names for some of the indentified ore minerals.

were done with a Kevex 7000 micro-X energy dispersive X-ray analyser.

Ore-minerals have been analysed quantitatively on an ARL SEMQ microprobe. The analyses were done with an accelerating voltage of 25kV and with a beam-current of 10nA. Metallic standards were chosen for the analyses of Ni, Cu and Co. Arsenopyrite was used as a standard for As analyses, and pyrite for the analyses of S and Fe. Both the SEM and the electron microprobe analyses as well as B-autoradiography were carried out at the University of Bergen.

Ore minerals in the ultramafic zone of the layered series.

Ore minerals occur in small qantitities throughout the ultramafic cumulate pile, but are enriched in the numerous sulphide-rich horizons. Detailed mineralogical work has yet not been carried out on these rocks but pentlandite, heazlewoodite and native copper have been identified and analysed quantitatively, and representative results are listed in table 1. A number of other ore-minerals have been analysed qualitatively on the SEM and their composition and suggested names are given in table 2 .

The paragenesis is dominated by pentlandite. Other Cu-Ni-Fe sulphides and other ore-minerals and native metals are generally associated with the pentlandite, and frequently occur as composite grains. A partial or complete rim of magnetite is often developed around the sulphides.

The ore minerals occur generally interstitially in a serpentine matrix, or in fractures in other minerals such as olivine and chromite. A Fe-Ni sulphide grain is also observed as an inclusion in a chromite grain, where it occur together with a Cu-Au alloy and a silicate inclusion.

Platinum Group Minerals in the Layered Series

The PGM in the layered rocks are observed in two contrasting textural positions:

* PGM present as inclusions in chromite

* PGM associated with sulphides in the stratabound horizons.

Laurite $(Ru,Os,Ir)S_2$ is the most common PGM-mineral found as inclusions within chromitite grains. This mineral has frequently been reported in the same textural position in other ophiolitic chromitites (Johan and Lebel,1978; Johan and Legendre, 1980, Prichard et al., 1981;Talkington et al., 1983; Page et al., 1986) and little attention has therefore been paid to it in this study.

Of the PPGE-enriched horizons only the Pd-dominated have yet been investigated mineralogically. B-autoradiographs of a large number of thin sections from these horizons have recently been recorded, and many of them showed the presence of numerous B-emitters. Systematic SEM work has been carried out on the lowermost Pd-dominate enrichment ecountered in core 87A1 (Fig 14). A set of thin-sections was made from the enriched part of the core and B-autoradiographs of these thin-section revealed a ca 2 cm. thin horizon of B-emitting minerals that parallel the layering in the rocks (Fig 22). SEM studies of these B-emitters show that the emitters were antimonides and tellurides carrying PPGE (Fig 23,24,25). The qualitative composition and the suggested names of the mineral species identified so far are listed in table 3.

Observation	Suggested mineral
Pd,Sb	Mertieite
Pd,Te	Kotulskite Merenskyite Michenerite Telluro- palladinite
Pd,Cu,Pb,Te	?
Pd,Ni,Te	?
Cu,Au,Pd	Metal alloy
Ir,As and Ir,Pt,As	Iridarsenite
Ru,Os,Ir,S	Laurite

TABLE 3. Qualitative composition and suggested names of PGM in stratabound enrichments

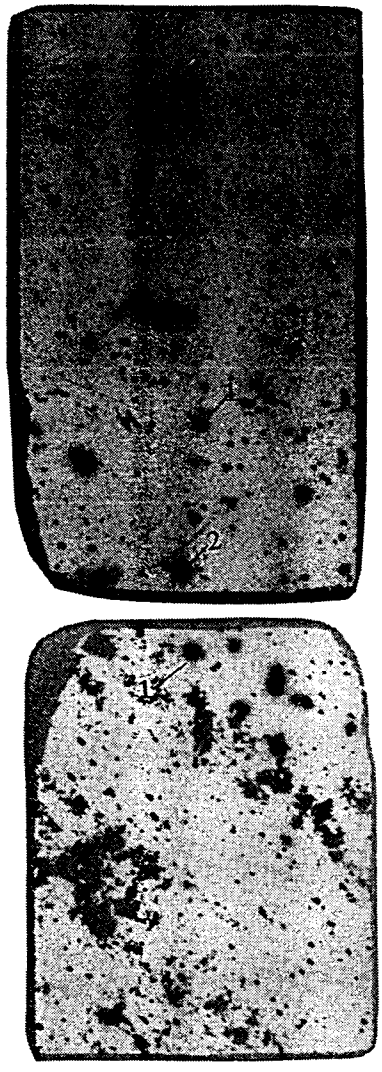

FIG.22. B-autoradiographs taken through the lowermost PPGE enrichment of core 87A1 (see Fig. 14). The autoradiographs document the presence of a two centimetre thick stratabound horizon rich in B-emitters.

Pd-minerals are those most frequently encountered in this horizon which agrees with the bulk-rock composition. Pd occurs generally as antimonides or tellurides (Pd-Sb, Pd-Te, Pd-Cu-Pb-Te, Pd-Ni-Te) but also in

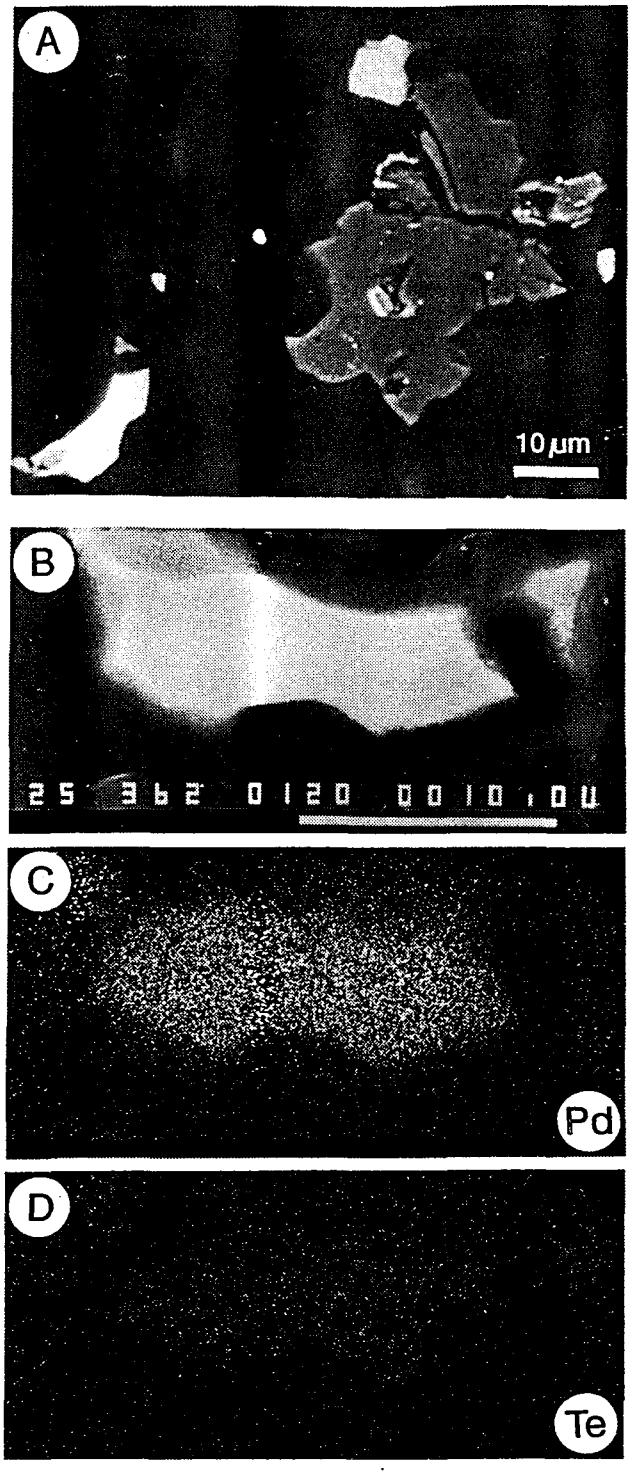

FIG. 23. SEM back-scatter picture of ore-mineral and associated PGM. The two largest white grains are both Pd-Te as shown by the element scans for Pd and Te (C and D).

alloys together with Au and Cu (Fig 24). In the Au,Cu,Pd alloys the ratio between the three elements varies considerably from grains dominated by Pd and Au to grains

FIG. 24. SEM back-scatter picture of Cu-Au-Pd alloy (white), Fe-Ni sulphide (light grey) and chromite (grey).

that are mainly composed of Cu. Grains composed exclusively of Cu-Pd or Cu-Au have also been encountered. The PGM in this horizon are generally 5-10 microns across, but grains up to 25 microns have been observed.

The PPGM in the sections studied are closely associated with Fe-Ni- or other sulphides, with alloys and native metals. The PPGM occur as subhedral inclusions within, or as anhedral grains along, the grain-boundary or in contact with these minerals. In one case a Cu-Au-Pd alloy is observed between two olivine grains, but it seems likely that it has been mobilized from a nearby Fe-Ni sulphide with which similar alloys are associated (Fig 25).

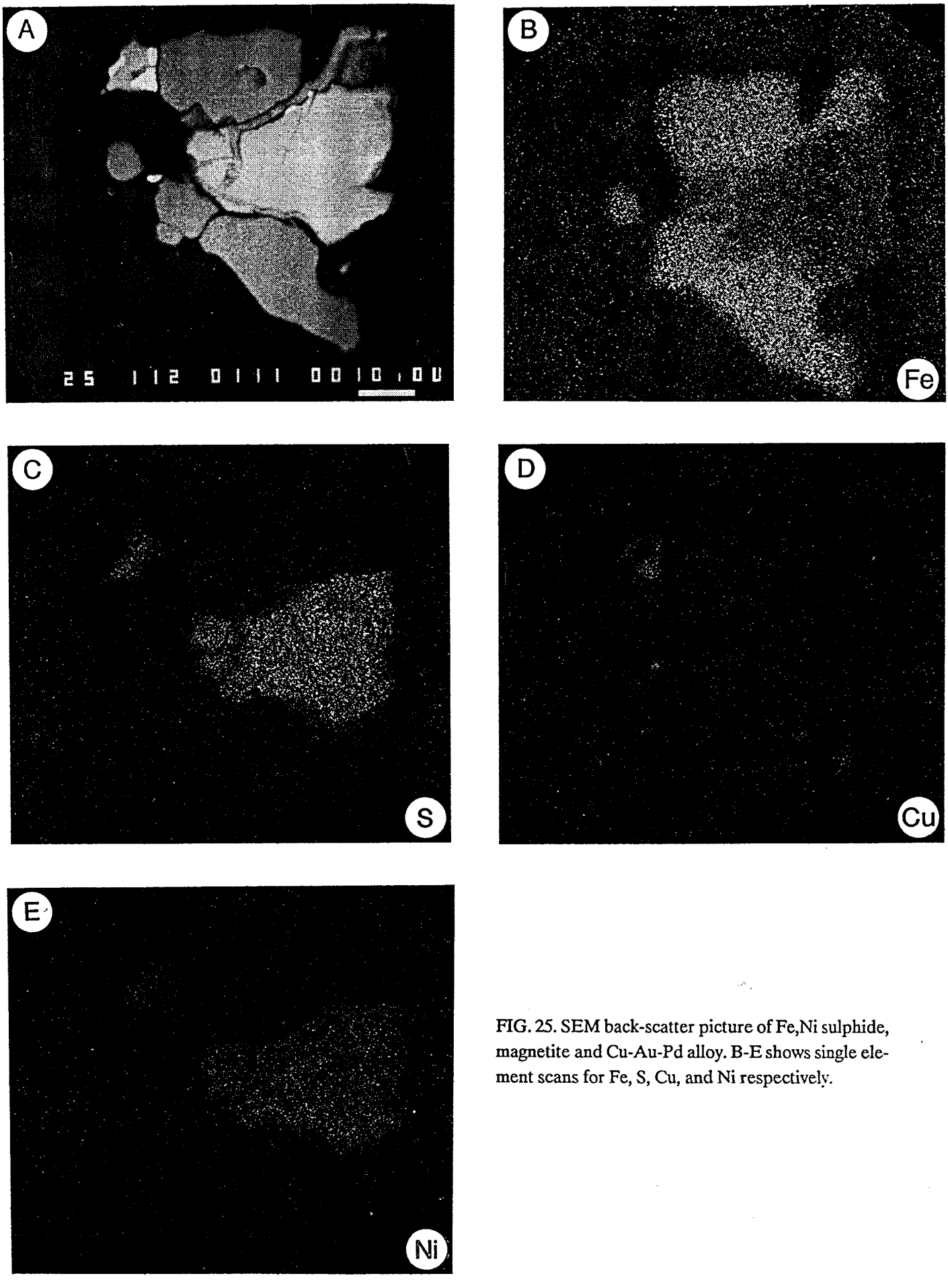

FIG. 25. SEM back-scatter picture of Fe,Ni sulphide, magnetite and Cu-Au-Pd alloy. B-E shows single element scans for Fe, S, Cu, and Ni respectively.

PGM in Chromitites associated with Tectonites.

Samples from the most PGE enriched chromitites have been search for PGM following the same procedure as in the layered series, ie. scanning electron microscopy of thin-sections which appeared promising after B-autoradiography.

Laurite may, as in the layered series, be observed as euhedral grains enclosed within the chromites (Fig 27). They appear more frequently than in the chromitites of the layered series, but as in the latter the grain-sizes are generally less than 10 microns.

PPGM are present as anhedral grains interstitial to the chromites (Fig 26b) or associated with alteration rims around the chromites (ferite-chromite). Pd- and Pt-antimonides, Pt-Cu alloy and native Pt have been identified in addition to laurite (Table 4).

Two unusually large (70 and 150 microns), complex grains have been located with the autoradiographs. While the smaller grain is composed of Pd-Sb and Ni-Sb (Fig 27), the larger grain is composed of one part where Pt-Sb is intergrown with a Pt-Cu alloy, and another part where Pd-Sb is the main component (Fig. 28) . The Pd-Sb seems also to contain some Cu. In addition to the PGM, the larger grain also has domains composed of Ni-Sb and Ni-As.

Observation	Suggested mineral
Ru,Os,Ir,S	Laurite
Pd,Sb	Mertieite
Pt,Cu	Hongshiite
Pt,Sb	Geversite Genkinite ?
Pt	Native Pt

Table 4. Quantitative composition and suggested names of PGM in chromitites associated with mantle tectonites.

Discussion

Chromitites associated with the tectonites

The new data from Leka confirm the findings from the Unst ophiolite which show that podiform chromitites may contain PPGE enriched precious metal deposits. The fact that the enrichments within the mantle tectonites are associated with the chromitites suggest that the reason for these PGE-deposits is to be found in the petrogenesis of the chromitites.

The chromitites show a systematic increase in PGE with increasing Cr content (Fig. 6). This relationship together with higher Pd/Ir ratios in the most PGE enriched rocks (Fig. 7) suggests that the chromites may have acted as a collecter not only of the IPGE, as in the stratabound chromitites, but also of the PPGE. Chromite appear, however, not to be suitable for solid substitution of PGE (Barnes et al. 1985), but they may play a role in the mechanical settling out of the refractory metals which is evident for the IPGE that appear to be confined to discrete euhedral grains of laurites included in the chromites. However, since podiform chromitites (both disseminated and massive) in general are depleted in PPGE, its seems clear that these unusual enrichments only partly can be attributed to a possible chromite control.

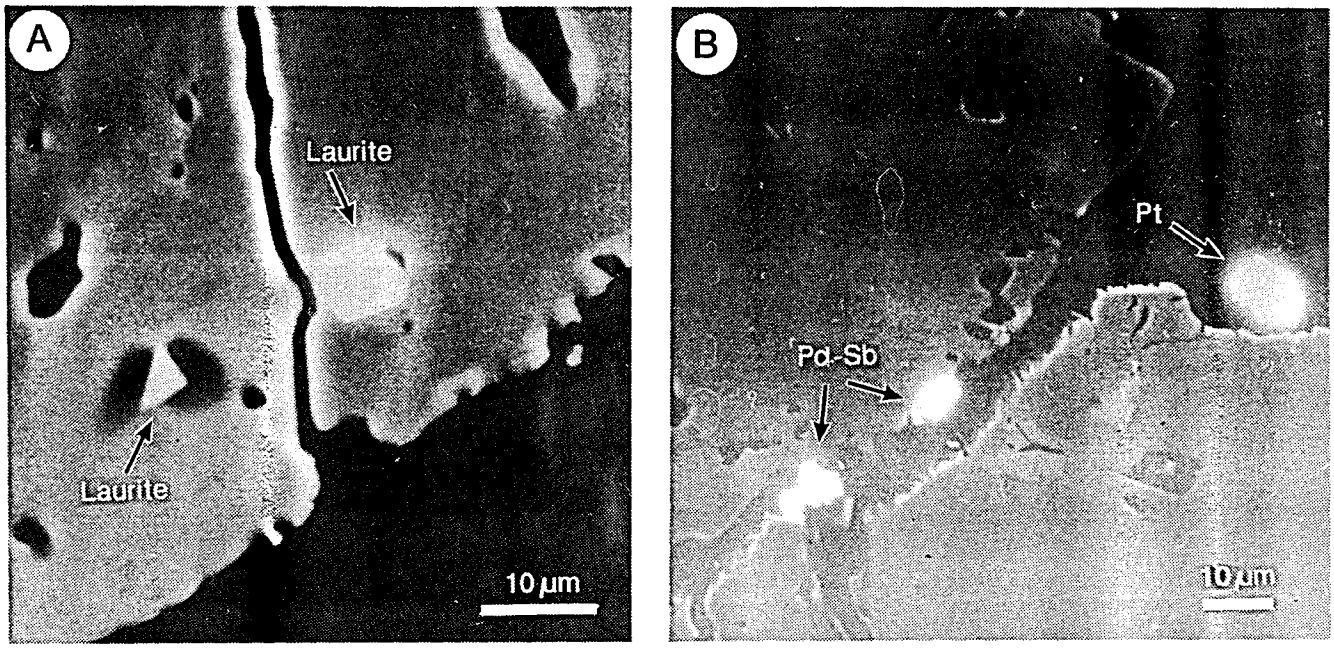

FIG. 26. SEM back-scatter picture of : a) Euhedral laurite (white) in chromite. b) Pd-Sb and native Pt (white) which are positioned interstitially to the chromite grains.

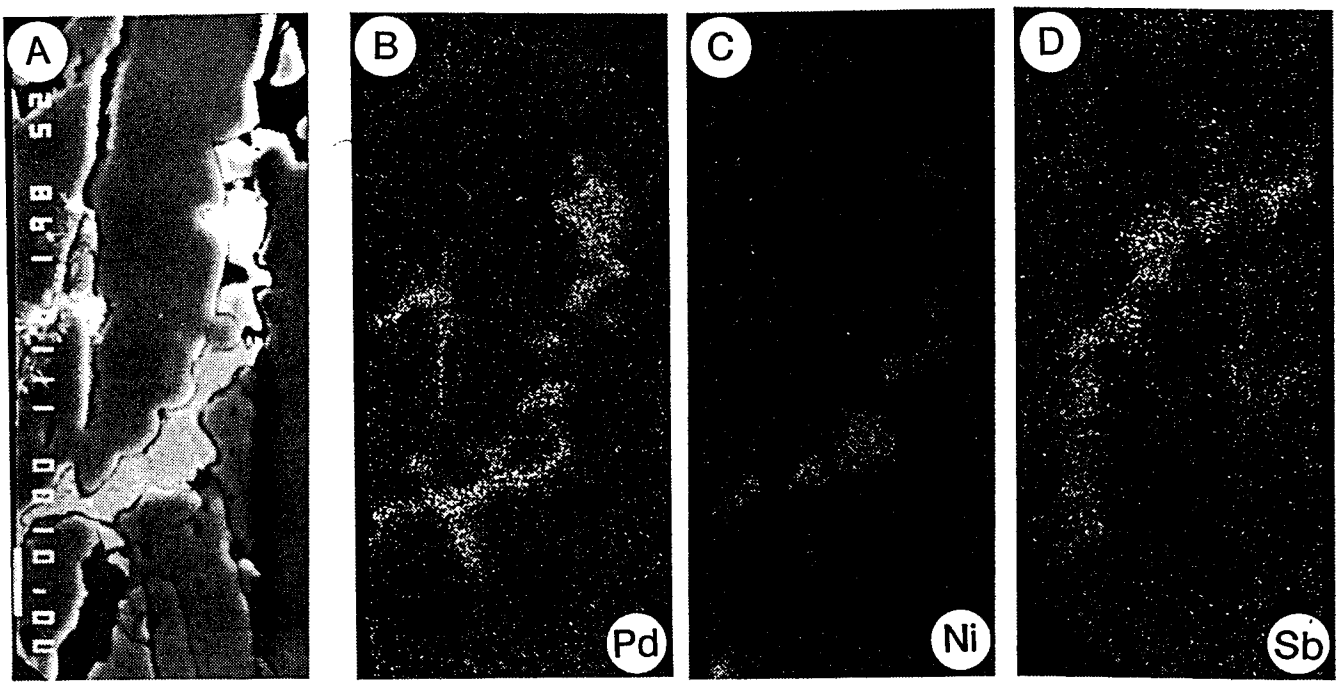

FIG. 27. SEM back-scatter picture of associated Pd-Sb and Ni-Sb grains.

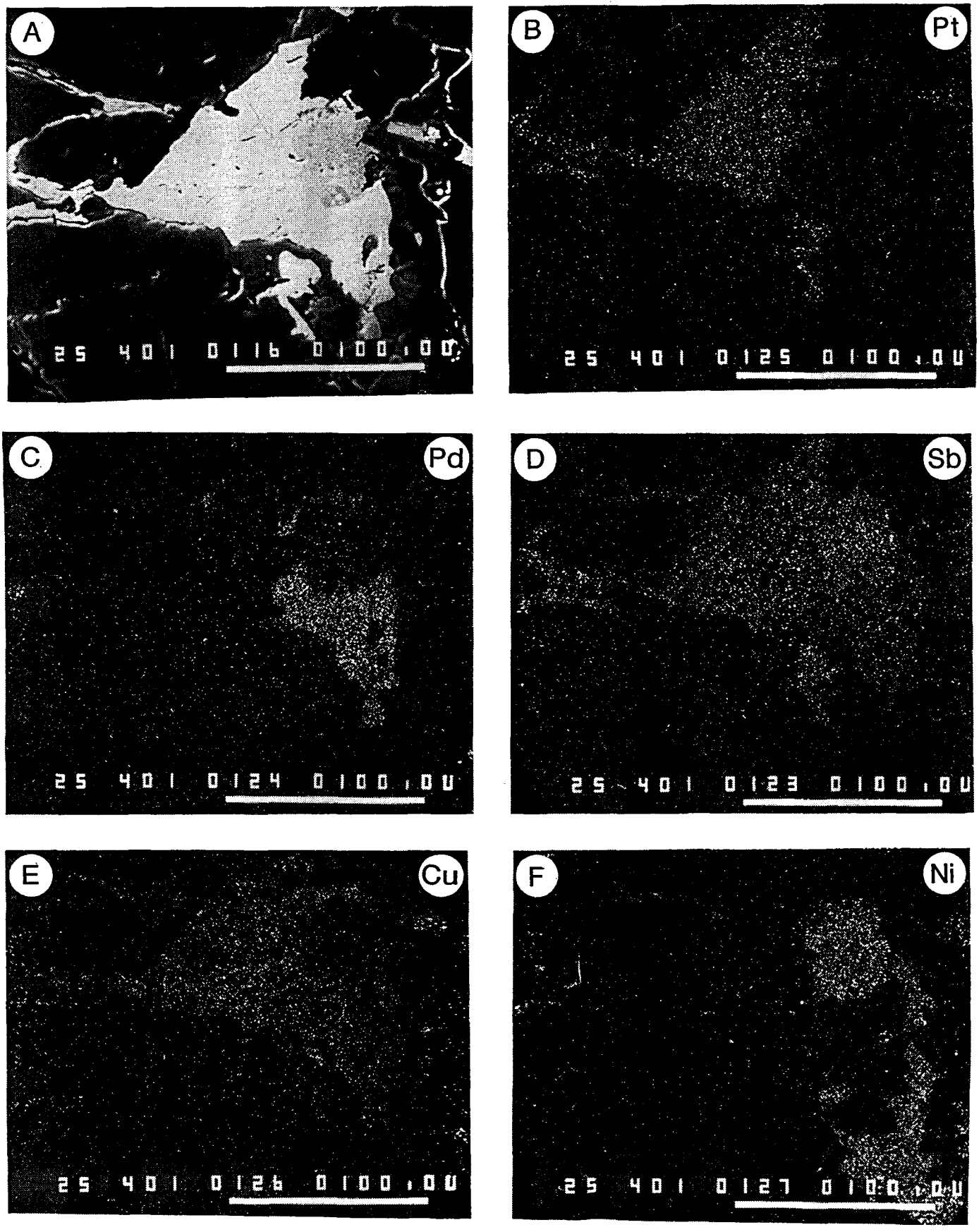

FIG.28. SEM back-scatter picture of composite PGM. B-F show single element scans for Pt, Pd, Sb, Cu, and Ni respectively. The composite grain is composed of domains of Pt-Cu, Pt-Sb, Pd, Sb, Ni-Sb and Ni-As.

The two most enriched chromitites (lek881a,b,c,d,lek87p1 and lek883a,,b,c,d,e) are both hosted in orthopyroxenite veins, while the other samples which are barren except for one (lek88-8a), are associated with tabular dunite bodies and dunite veins. The apperant relationship with orthopyroxenites may be an artefect of the small number of observations, but it may also have importance for understanding these unusual PGE-enrichments.

The orthopyroxenitic veins may represent traces of boninitic magma, which are assumed to be particularly PGE-enriched (Hamlyn et al. 1985). The layered series also shows the crystallization sequence ol-chr-opx-cpx sporadically, instead of the more common sequence of ol-chr-cpx-opx. A Nd-isotope study of these units does not indicate that the more opx-dominated parts of the layered series are related to influx of a more boninitic parental magma (Pedersen et al. in prep), and there seems neither to be ground for suggesting that the orthopyroxenitic veins within the mantle tectonites formed from a boninitic magma either.

The presence of dunite bodies and veins, as well as various pyroxenite veins within the mantle tectonites suggests that the primary magma fractionated to some extent within the conduit system. This is also indicated by cryptic variations in olivine compositions across individual dyke-like bodies, which may be interpreted to reflect the flux of variably differentiated magmas with time (Albrektsen et al., in press) (Fig 29). The more than cotectic proportions of chromitite that have precipitated locally in these bodies can therefore be explained by the mixing of these variably differentiated magmas, in accordance with the interpretation of strat-abound chromitites (Irvine 1977).

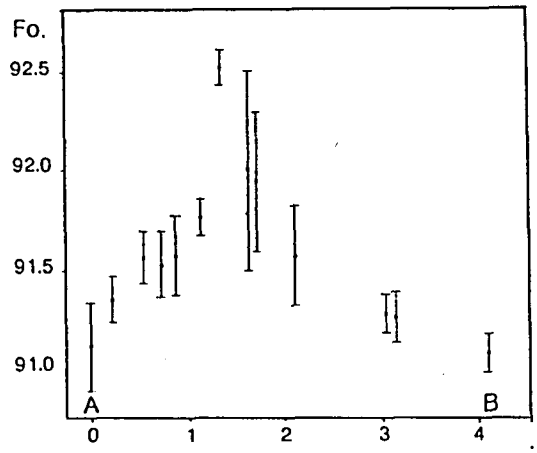

FIG. 29. Cryptic variations in olivine composition across a dunitic dyke within the mantle tectonites. (after Albrektsen et al. in press).

It seems likely that intra-mantle differentiation of the magma may represent a key to understanding these deposits. Differentiation of the magma may saturate the melt in the PGE, and mixing of the variably differentiated melts may induce chromitite precipitation and also the formation of sulphides or other PGE-bearing phases.

Significant intra-mantle differentiation would only be expected to take place within small magma bodies that rise slowly, or become trapped within the mantle. If differentiation of the magma is important for the formation of PPGE-enrichements, one can therefore only expect to find very minor volumes of such enrichments within the mantle sequence.

Parental magma composition

The average PGE-composition of the studied cyclic units in ppb is estimated to be : 3.5(Os), 3.7(Ir), 9.0(Ru), 3.5(Rh), 30.3(Pt), 40.2(Pd), taking both vertical and lateral variations into account. Variations from Fo_{92-87} in extreme ol-adcumulates, have been estimated to reflect ca 20% olivine fractionation (Fig 30). The parental magma to the layered series therefore had a PGE-content of at least 1/5 of the estimated average - ie at least 6 ppb and 8 ppb of Pt and Pd respectively(parental magma is used here to refer to the magma entering the magma chamber, while primary magma denotes the magma that segregated from the partially melting source). The parental magma composition for the Bushveld Complex has been estimated to contain around 15ppb of Pt (Davies and Tredoux, 1985), and a study of the basal series of the Stillwater Complex and associated sills and dykes suggest that the parental magma of this complex contained less than 20ppb of any of the PPGE (Zientek et.al, 1986). The parental magma of the Leka ophiolite seems therefore not to have had significantly lower PGE contents than the parental magma of intracratonic layered intrusions that host major PGE-deposits.

Stratabound enrichments

The PGE-enriched horizons within the layered series on Leka are, as far as we know, the first PPGE enrichments in ophiolites that are documented to be stratabound. The extent to which the mineralization of Ni-Cu-PGE in the Zambales Ophiolite (Abrajano and Bacuta, 1982; Bacuta et al. 1987; Orberger et al. 1987) are of the same type is not clear (i.e. their relationship to chromitites and to hydrothermal processes). The ore- mineralogy of the stratabound enrichments contain sulphur-deficient sulphide such as heazelwoodite as well as native metals. The presence of such phases, and textural relations such as rimming of the sulphides by magnetite, show that the paragenesis has gone through extensive re-equilibration (Lorand, 1987). The presence of native Cu as well as other native metals, suggest reducing conditions during the alteration of the ore-minerals (Eckstrand, 1975), and this alteration may well have been contemporaneous with, and caused by the introduction of reducing fluids during the serpentinisation of the host rock.

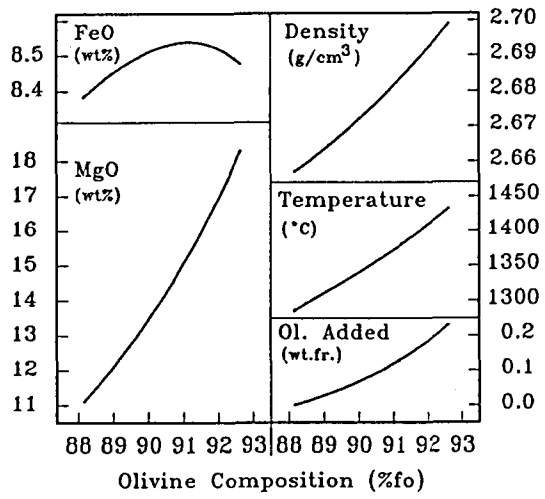

FIG. 30. Modelled variations in FeO, MgO and some physical parametres as a function of increasing degrees of olivine fractionation of a picritic magma (from Pedersen,1990).

It is evident from thin-section studies that the PGE may have been redistributed on a small-scale, but since the enrichments define very thin stratabound horizons that can

be traced for kilometres, a secondary origin related to the hydration and alteration of the rocks seems unlikely. The fact that the stratabound enrichments on Leka occur within extreme olivine adcumulates which show no traces of intercumulus liquid or any late-magmatic hydrous phases, makes it also difficult to attribute the enrichment to percolating late magmatic fluids, which has been suggested to have formed some stratabound enrichments such as the Picket-Pin of the Stillwater Complex (Boudreau and McCallum, 1986).

The enrichments on Leka compare in some respect with PGE-deposits such as the UG-2, Merensky and J-M Reefs of the Bushveld and the Stillwater Complexes in that they occur at the base of cyclic units (Barnes and Naldrett,1985; Kruger and Marsh, 1985; Hiemstra,1986; Irvine et al. 1983). The PGE-collecting phase in the Merensky-type deposits is generally considered to be base-metal sulphide (Naldrett and Cabri, 1976; Campbell and Naldrett 1979; Campbell and Barnes 1984; Naldrett and von Gruenewaldt 1989). This is probably also the case for the Pd-dominated enrichments on Leka which are clearly associated with sulphide-rich horizons. These enrichments show high Pt/S and Pd/S ratios and have similar chondrite-normalized PGE-patterns (except for lower total abundances) to the Merensky and the J-M reefs.

Pt-dominated enrichments appear to be developed just below the Pd-dominated ones, and this type seems to become the dominating type towards the central part of the intrusion. The Pt-dominated type is neither associated with chromite nor with sulphide enrichments. Similar enrichments are not described from the Bushveld or the Stillwater Complexes, but the Sompujärvi mineralization of the Penikat Layered Intrusion (Finland) would also seem to be unrelated to base-metal sulphide-enrichments or chromitites (Alapieti and Lahtinen, 1986), and may be a comparable type of enrichment. The mineralogy of these enrichments on Leka is not yet known, but in the Penikat Layered Intrusion it is characterized by sulphide-free PGM such as sperrylite($PtAs_2$) and isomertieite ($Pd_{11}Sb_2As_2$), as well as various Pd-Pt-Cu-Fe and Pt-Pd-Cu alloys (Alapieti and Lahtinen, 1986).

The main PGE-deposits of layered intrusions are located above the level where plagioclase becomes a cumulus phase, and they are generally considered to be the lowest level at which the magma reached significant and widespread sulphide saturation (Campbell et al. 1983; Irvine et al. 1983; Barnes and Naldrett,1985; Naldrett and von Gruenewaldt, 1989).

The reason for the sudden sulphide saturation is poorly understood but it probably results from magma mixing (Irvine,1977) or a decrease in temperature (Haughton et al. 1974). Campbell et al. (1983) attributed the sudden sulphide precipitation and the formation of Merensky-type deposits to temperature decrease in the influxing magma. The strong PGE enrichment was explained by extraordinary high melt/sulphide ratios (R-factor) so that the sulphides scavenged the PGE from large volumes of magma. The reason for the position of the reefs some distance above the level where plagioclase appears as a cumulus phase was explained by the fact that the resident magma at this stage had become just slightly denser than the

influxing magma (due to an increase in the FeO content of the magma, which have been caused by the plagioclase precipitation). The influxing magma would therefore form a plume and rise into the resident magma column untill it reached the appropriate density-level where it could spread out. Subsequent cooling of the influxing magma would lower the density of the resident magma below that of the underlying resident magma, and result in turnover and the opportunity for the immiscible sulphide droplets to equilibrate with large volumes of magma.

Naldrett and von Gruenewaldt (1989) suggested that the sudden sulphide precipitation was induced by magma mixing and that the reason for the position of the reefs above the level where plagioclase appears lies in the shape of the sulphide solubility curve (Fig 31A). The solubility of sulphide in a silicate magma is to a large extent governed by the temperature and the FeO content of the magma, and a decrease in both lowers the solubility (Haughton et al. 1974; Shima and Naldrett, 1975; Buchanan and Nolan, 1979; Buchanan et al., 1983). It seems therefore likely that the solubility of sulphide in the magma decreases during crystallization of ultramafic cumulates, when the FeO content of the magma should decrease , and that the solubility curve may become flat and even rise after plagioclase appears as a cumulus phase and the FeO concentration starts to increase in the magma (Fig.31A). Mixing of a primitive magma (P) with a resident evolved magma (R) that is crystallizing plagioclase, may therefore re-

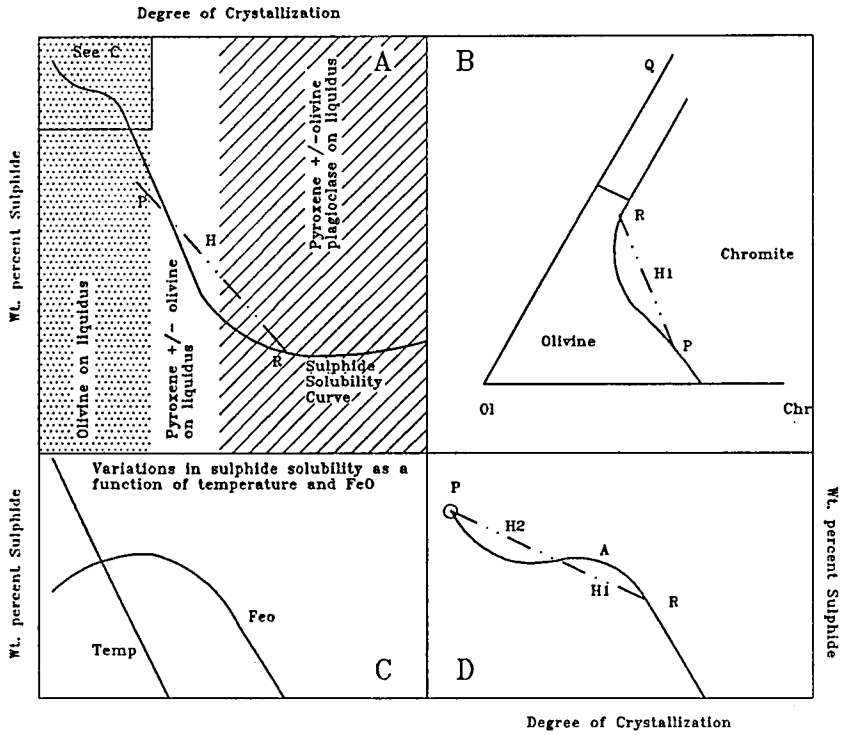

FIG. 31. A) Schematic diagram illustrating assumed evolution in the solubility of iron sulphide with progressive differentiation of basaltic magma (after Naldrett and von Gruenewaldt 1989). B) Phase relations in the system Chromite-olivine-quartz (after Irvine, 1978). C) Schematic diagram illustrating assumed changes in the solubility of sulphide in the magma as a function of variations in the magma-temperature and the FeO content of the magma with progressive differentiation. D) Suggested modifications to the sulphide solubility curve suggested by Naldrett and von Gruenewaldt (1989) (A) which take into account the initial increase in the FeO content of the magma when very magnesian olivines are fractionated

sult in a hybrid magma (H), positioned above the sulphide solubility curve (Fig 31A), and hence give rise to extensive sulphide segregation, which, due to turbulent conditions during mixing may equilibrate with large volumes of magma and scavenge the PGE. However, if the primitive magma mixed with an only slightly more evolved magma, then the hybrid magma might not be positioned above the sulphide solubility curve, and this explains, according to Naldrett and von Gruenewaldt (1989) the general lack of PGE-deposits within the ultramafic zones of layered intrusions.

It may seem illogical that this study has been focussed on the ultramafic zone of the layered series while all the major PGE-deposits within intracratonic layered intrusions are positioned above the level where plagioclase appears as a cumulus phase. MORB and also MORB/IAT-like magmas of comparable ophiolite complexes such as Karmøy(Pedersen,1989), show very low abundances of the PGE (typically less than 0.5 ppb of Pt). The resident magma in the ophiolitic magma chamber from which the gabbroic cumulates formed were therefore probably very depleted in PGE. If a PGE deposit was to form from such a magma an unrealistically high R-factor would be required (ie. if a half-meter thick deposit with 3000 ppb of Pt should form from a magma with 0.3ppb of Pt, all the Pt from a 5000 meter thick column would have had to be scavenged). Our reasoning was therefore that if a PGE-deposit was present in an ophiolite, than the PGE must have been scavenged directly from a more PGE-rich parental magma, and the position of such a deposit could not be governed by whether the sulphides subsequently equilibrated with a large volume of the PGE-depleted resident magma or not. The deposit could, for this reason, just as well be positioned below as above the level where plagioclase appears as a cumulus phase.

The presence of the PGE-enriched horizons within ol-cumulates that appear to have formed from a bottom layer of parental magma (Pedersen, 1989), shows that this reasoning was valid and that the PGE were scavenged from the parental magma shortly after it entered the chamber and before it mixed entirely with the resident magma. The presence of the sulphide-rich horizons within the olivine cumulates studied shows also that sudden and significant sulphide precipitation may take place prior to the appearance of plagioclase as a cumulus phase.

There are therefore grounds for believing that the processes that control PGE distribution in the layered series of ophiolites differ from those of intracratonic layered intrusions. The features that may have a particular importance for understanding the contrasting PGE-distributions are:

1) Widespread and sudden sulphide precipitation occurred repeatedly, and after influx of very primitive parental magma long before plagioclase appeared as a cumulus phase - this appears not to be the case in intracratonic layered intrusions (Naldrett and vo Gruenevaldt, 1989).

2) The stratabound chromitites are depleted in Pt and Pd both within the Leka ophiolite and in ophiolites in general (Page et al. 1986) - chromitites within layered intrusions are generally enriched in PPGE and are of-

ten the host rock of Pt-deposits (ie. the UG-2, Bushveld Complex)

3) Some of the PPGE-enrichments on Leka seem to have a pronounced gradient in Pt/Pd ratio over relatively short distances - similar lateral gradients are not reported from PGE-deposits in layered intrusions.

The discrete sulphide-rich horizons within the ol-cumulates on Leka may have formed due to the influx of sulphide saturated magma containing immiscible sulphide droplets that segregated immediately after the magma entered the chamber. The sulphide precipitation may also have been caused by a drop in temperature of the parental magma after it entered the chamber, but it may be questioned if cooling by thermal diffusion alone could result in the formation of distinct sulphide-rich horizons. Mixing-induced precipitation should not according to Naldrett and von Gruenevaldt (1989) take place, due to the shape of the sulphide solubility curve (Fig. 31A). However, the schematic evolution in sulphide-solubility with progressive differentiation of basaltic magmas may not be entirely valid for cases where very forsteritic olivines initially fractionated from the parental magma. Olivines with Fo_{92} will contain ca. 8wt% FeO, which is below the FeO-content of a reasonable parental magma (9-10wt%). Fractionation of such olivines will therefore initially lead to an increase in the FeO-content of the magma until the FeO-content of the olivines exceeds that of the magma and then start to deplete it in FeO (Fig 30). The sulphide saturation curve may therefore start with a rapid decline before it flattens out and even climbs due to the initial increase in the FeO content of the magma, and will subsequently decline rapidly when both the temperature and the FeO content decrease (Fig 31D). Sudden and widespread sulphide precipitation caused by the blending of magmas may thus be expected to be produced by two circumstances : when primary magma mixes with a resident magma that has undergone plagioclase fractionation for a while (Fig.31A), and when picritic parental magma in equilibrium with very magnesian olivine (Fo_{93-92}) blends with a slightly more evolved magma (in equilibrium with Fo_{90-85})(Fig.31D). The first scenario appear to have resulted in the major PGE-deposits of the world, and the second situation seems to be the petrogenetic framework for the more modest enrichments within the Leka ophiolite.

Chromitites in layered intrusions are considered to have formed as a result of magma mixing (Irvine,1977). Due to the curvature of the olivine-chromite cotectic line, the blending of a magmas positioned somewhere on the olivine-chromite cotectic will result in a hybrid magma positioned within the chromite field, and which consequently will precipitate only chromite (Fig.31B). Blending of magma with very small differences in composition will, according to the phase relations in the system chromite-olivine-quartz, result in a relatively small amount of chromite, while the mixing of melts that have more contrasting compositions may result in the precipitation of larger quantities of chromite.

If the formation of chromitites and enhanced sulphide precipitation are both products of magma mixing then sulphide-rich chromitites enriched in PPGE would be expected to be the result. This is also what is

present in layered intrusions such as the Bushveld and Stillwater Complexes. The sulphide-rich and the chromite-rich horizons are ,however, displaced relative to each other within the cumulates on Leka, with the chromite-rich positioned below the sulphide-rich horizon. This is also reflected in the chondrite-normalized pattern of the PGE content of these rocks. All the analysed stratabound chromitites from Leka, except one, show the typical ophiolitic, IPGE-enriched pattern (Fig 19). The one that is anomalous differs from the other in having visible sulphide and in having a slightly PPGE-enriched pattern which compare with the pattern of chromitites from the Stillwater and the Bushveld Complex (Fig 20). This pattern can be produced by combining the IPGE-enriched pattern of the standard chromitite with the PPGE-enriched pattern of the sulphide-rich horizons, and may be explained by the superposition of a sulphide-rich horizon on a chromitite horizon. This is, however, an exception and generally the sulphide-rich horizons and the chromitites are separated by a few tens of centimetres to a few metres.

If an immiscible sulphide-phase and chromites formed as a consequence of the same mixing event, differing settling velocity between very small immiscible sulphide droplets and larger chromite crystals could possibly explain the separation of the sulphide-rich and the chromite-rich horizons. However, this mechanism cannot easily explain why the relative displacement of these layers should be exclusive to these very magnesian ol-cumulates. If the shape of the sulphide-solubility curve is in principle as outlined in Fig 31 A&D), this relation can readily be explained. Consider first the case where parental magma mixes with a resident magma that has undergone plagioclase crystallization (Fig 31). The assumed shape of the sulphide-solubility curve suggest that the hybrid magma will be positioned above the curve wether the volume of replenishing magma have been small or more substantial.. This may also be the case if a picritic magma mixes with a slightly more differentiated resident magma positioned to the left of point A on the sulphide-solubility curve (Fig 31B). If on the other hand the residing magma is positioned beyond point A, a new influx of magma will initially lead to a sulphide undersaturated hybrid magma (H1), and sulphide saturation will first be achieved after continued influx of picritic magma has brought the hybrid magma above the curve (H2). A similar delay would not be expected for the formation of mixing-induced chromitites (Fig 31B), which hence should develop some distance below the sulphide enrichments.

The lateral gradient in the Pt/Pd ratio of some of the PGE-enriched horizons on Leka may reflect the specific fluid dynamic process that formed the ol-cumulates. The cryptic olivine composition of the units studied can be explained by influx of the parental magma through a magma fountain, within which the parental magma mixed partly with the resident magma before it fell back and spread out as a hybrid bottom layer (Fig.32 D-G). This type of magma influx contrasts with the way the Bushveld Complex is thought to have been replenished when the Merensky cyclic unit formed (Fig.32A-C). The influx through a magma fountain results in a lateral flux of hybrid

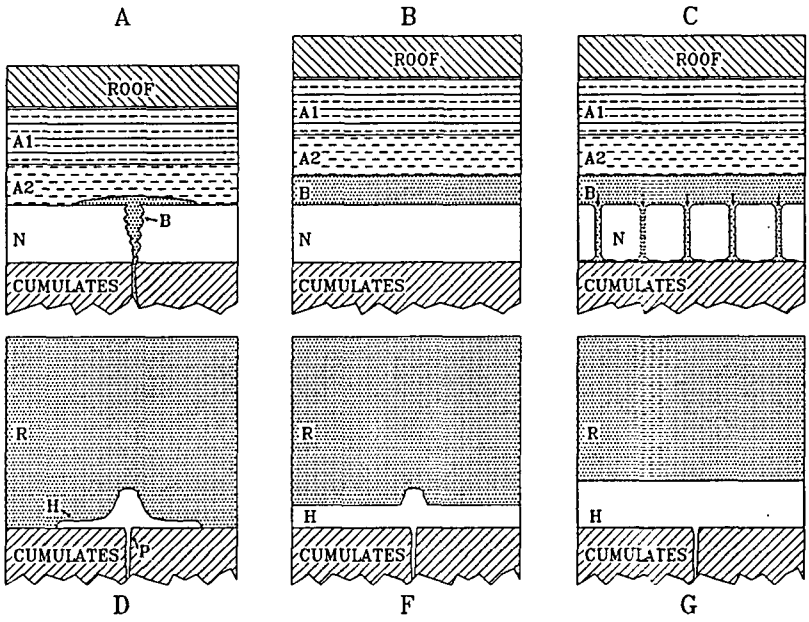

FIG. 32. A-C) Sketch showing a model for the formation of the Merensky Reef (after Naldrett et al. 1986) A) Introduction of a fresh pulse of magma as a turbulent plume, B) the turbulent convection of this pulse and C) downspouting of a mixture of crystals plus sulfides plus entrained liquid to spread out over the crystal pile as the Merensky reef.

D-G) Model for the fluid dynamic processes that appear to have operated during formation of the stratabound enrichements on Leka. D) Introduction of a fresh pulse of picritic parental magma as a magma fountain which partly mixes with the resident magma, E-G) formation of a hybrid bottom layer and mixing-induced precipitation of chromites and subsequently sulphides which scavenged the PGE from the magma. The flux of parental magma across the floor may result in a lateral fractionation of the PGE with the most refractory elements deposited closest to the vent , and this may explain the lateral variation in the Pt/Pd ratio of some of the enriched horizons.

magma across the floor of the chamber (Fig 32D). The refractory metals that precipitate as chromite, PGM, alloys or sulphides may therefore be fractionated laterally, whether these phases were carried by the influxing magma or formed due to magma mixing in the fountain. The thinning of the main chromitite horizon from 5-7 metres thickness in profiles A and B down to a metre thickness in profile C, may be the result of such a lateral fractionation, and the decrease in the Pt/Pd ratio of the PPGE enriched horizon in the same direction may also be explained by such a mechanism.

Fractionation of the PGE

The fractionation of the PGE, as evident from the positive slope of the chondrite-normalized PGE-pattern of terrestrial basalts, can either be attributed to partial melting or to fractional crystallization or a combination of these processes (Barnes et al. 1985). Ophiolite complexes represent a unique possibility to evaluate the effect of various possible mechanisms since both the PGE-contents of the residual source of the magma (mantle tectonites), the cumulates that have been fractionated from the primary magma (podiform chromitites and laye-

red series), and the differentiated basaltic magma (lavas and dykes), can be established.

The PGE composition of dykes assumed to reflect the composition of the axis sequence magma after formation of the ultramafic cumulates, shows an average Pd/Ir ratio of 12 (Pedersen, unpublished data). The stratabound chromitites, which typically yield a Pd/Ir ratio of 0.1, have clearly fractionated the parental magma in the IPGE relative to the PPGE. The sulphide-rich horizons, on the other hand, show a spread in Pd/Ir ratio from less then 10 to above 100 (Fig 33), and the most PPGE-enriched horizons should therefore have fractionated the magma in the PPGE relative to the IPGE, which is reasonable considering that the PPGE partition much more strongly into an immiscible sulphide melt than IPGE (Barnes et al. 1985). However, the average Pd/Ir ratio of

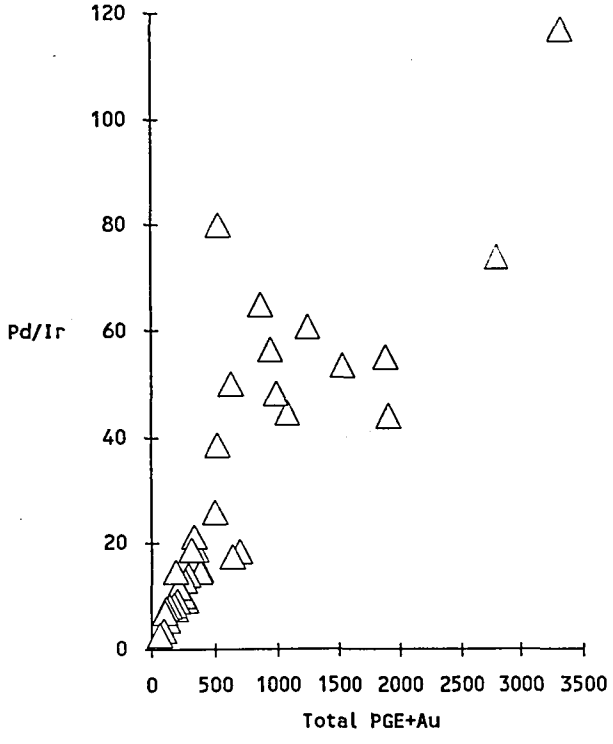

FIG.33. Plot showing variation in the Pd/Ir ratio against the total PGE content of the sulfide-enriched horizons.

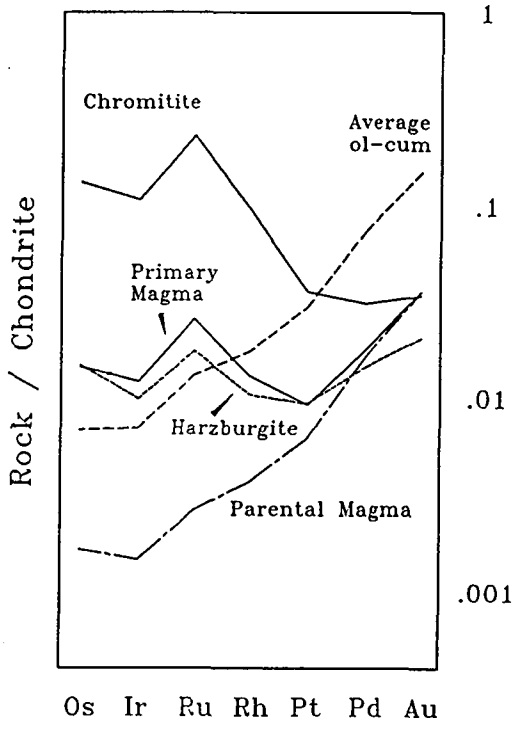

FIG. 34. Chondrite-normalized PGE patterns of the average cyclic units, and estimated parental and primary magma . For further discussion see text.

the all the cumulates studied is ca. 10 - about the same as that of the assumed residual basaltic magma, which suggests that the combined effect of the formation of the various types of PGE-enriched horizons did not lead to any significant fractionation of the PGE. The fractionation of the PGE seems therefore not to have taken place in the magma chamber, and must consequently have occurred during ascent to the magma chamber or during partial melting of the mantle source.

Neither the dunite bodies nor the chromitite schlierens that are assumed to have formed from the primary magma en route to the magma chamber, can account for the fractionation of the PGE because of the insignificant volume of sufficiently PGE-enriched rocks. However, the

PGE-geochemistry of the tectonite-hosted chromitites on Leka is not representative of typical podiform chromitites, which compare in composition with the IPGE-enriched stratabound chromitites on Leka. The PGE-pattern of the mantle-tectonites on Leka can be perfectly modelled from the parental magma composition by adding IPGE-enriched chromitites to the estimated magma composition (Fig 34). However, if we assume chromitites with ca 300 ppb of IPGE (which is a typical content of ophiolitic chromitites, Page et al. 1986), a weight fraction of 0.1 must be added to produce the Pd/Ir ratio of the mantle tectonites. Unless the Cr content of the chromitites is less then 5wt% , ie. low grade disseminated chromitites, the Cr content of the primary magma will be unrealistically high. If very IPGE-enriched chromitites (3000 ppb of IPGE) are considered then a weight fraction of only 0.003 needs to be added to the parental magma to obtain the Pd/Ir ratio of the harzburgite.

The fractionation of the IPGE relative to the PPGE of the parental magma can therefore be accounted for by the formation of podiform chromitites from the primary magma. However, in order to maintain a reasonable Cr-budget, 0.3 to 0.9 wt% of chromitites with IPGE content in the 1-3 ppm range should have fractionated from the primary magma en route to the magma chamber. Such IPGE-enriched chromitites are found in ophiolites, but it may be questioned if they are present in large enough volumes. Present knowledge suggests not, but on the other hand only a very minor portion of the mantle sequence involved in the generation and initial fractionation of the primary melt is exposed within ophiolites.

The estimated parental magma has Pt and Pd contents comparable to the average mantle tectonite on Leka, and the $D_{mantle/crust}$ value for Pt and Pd seems accordingly to have been of the order of 1. This suggests that the fractionation of the PGE in the parental melt is due to depletion of the IPGE and not to enrichment of the PPGE relative to the mantle source. If Ir partitioned very strongly into the residual during partial melting, then the residual mantle would become enriched in Ir by a maximum of 20% relative to the primary source (assuming 20% partial melting). The maximum expected variations in the mantle lithologies are thus at the edge of the precision and accuracy that can be expected from the analyses. A considerably larger database of mantle tectonites which show a wider range in the degree of major element-depletion than is the case for the samples studied, seems therefore necessary to document whether the PGE became fractionated during partial melting or not.

PGE-potential of the Leka ophiolite and application to exploration in ophiolites

The parental magma of the Leka ophiolite appears to have had PGE-contents comparable to that of intracratonic layered intrusions containing economic PGE-deposits. It seems therefore clear that a possible lack of economic deposits in ophiolite complexes should be attributed to the lack of sufficient enrichment of the PGE, and not to PGE-depleted parental magmas. However, significant enrichments of the PGE formed both during ascent of the primary magma through the mantle, and during and immediately after influx of the parental magma into the

magma chamber. The highest contents obtained from the podiform type chromitites are 8500 ppb with an average Pt value of 2500ppb. These values approach ore grade, 3700-4800ppb Pt (Morrissey, 1987), but the volume of these enrichments are insignificant.

The PPGE-enriched stratabound horizons yield a maximum of 3 ppm total PGE + Au (average of 2 samples, 89lek9a,c table 17). Although this is only half of the amount present in the Merensky Reef, the horizon is still highly enriched in PGE. Considering that we have studied only ca 150 metres of cumulates in detail, and that we have discovered one horizon giving 3ppm in hand-samples and several horizons yielding half- and meter-averages of around 1 ppm total PGE + Au, as well as 5-6 other horizons yielding several hundreds of ppb, the chances of finding a stratabound PGE-deposit approaching ore grade within the Leka ophiolite should not be ruled out.

The high number of moderately enriched horizons can, as discussed above, be explained by the fractionation of PGE-rich immiscible base-metal sulphides and/or PGM or alloys immediately after influx of discrete batches of parental magma into the magma chamber. The "R-factor", or the amount of melt that the immiscible sulphides equilibrate with and scavenge the PGE from, is considered to have a major importance for the formation of economic PGE-deposits (Campbell et al. 1983). Magma batches of sufficient volume may therefore be a necessity to form deposits of ore-grade. If a half meter thick enrichment with 4000 ppb of Pt is to form, it would require Pt to be scavenged from at least a 250 metre thick column of parental magma with 8ppb of Pt. The Leka ophiolite complex contains a number of a hundred to several hundred meter thick sub-zones of ol-cumulates which, from mass-balance considerations, must have formed from columns of picritic parental magma that were considerably thicker than a few hundred metres. The magma chamber was therefore periodically refilled with parental magma of sufficiently substantial volume to form PGE-deposits of economic grade. However, the sub-zones studied can be subdivided into several cyclic units and cryptic variation has also revealed the presence of several cryptic cyclic units. The substantial influxes of picritic magma that are reflected by the thick sub-zones of ol-cumulates, seem accordingly not to have entered the magma chamber in one batch, but rather in a series of minor incremental batches and even as a continuous influx of magma over a more substantial period of time (Pedersen, 1989). Thus, instead of one major PGE-enrichment, this type of magma-influx has resulted in a number of more moderately PGE-enriched horizons. Whether this is a general feature of all the major ol-cumulate sub-zones on Leka is, as yet, unknown. Present knowledge suggests that if one of these zones represents a single, or only a couple of macro cyclic units, then PGE-enrichments that approach ore-grade should be expected to be present close to the base of such units.

While the Pt-deposits of layered intrusions are often hosted in chromitites, which therefore are targets for PGE-prospecting, the stratabound chromitites on Leka are poor in PPGE. Studies of a number of other complexes have shown that such Pt- and Pd-de-

pleted chromitites are a general feature of ophiolites (Page et al.1982; Page et al. 1986), and ophiolites complexes have therefore not been regarded as potential platinum sources of economic importance. This study show that the reason for the PPGE-depletion of the stratabound ophiolitic chromitites is probably not related to the **lack** of Pt- and Pd-enrichments in ophiolites, but to the fact that these enrichments are **displaced** relative to the chromitites. In the few cases where they are superimposed on each other the chromitites have PGE-patterns comparable to the chromitites of, for instant, the Stillwater Complex. While the reasons for this relative displacement may be debated, the observation has obvious consequences for the prospecting of stratabound Pt- and Pd-deposits in ophiolites.

The lateral variation in the Pt/Pd ratio of the PPGE enriched horizons, with increasing ratios towards the most central parts of the intrusion has also significanse for prospecting . These lateral gradients suggest that Pt-deposits in ophiolites may be more spatially limited than Pt-deposits of intracratonic layered intrusions. If this also implies that deposits of unusual high grade may be present in ophiolites is yet to be shown, but what seems clear is that Pt-deposits that are not displaceda relative to chromitites, and which are situated within very magnesian olcumulates where the only cyclic units are cryptic, will be difficult to find.

The major PGE-deposits of layered intrusions are located above the level where plagioclase appears as a cumus phase. This level has not been investigated in this study, and to our knowledge not in any other studies of ophiolites either. Our present knowledge does not suggest that these levels should be more favourable for the formation of PGE-deposits than the ultramafic zone studied. Admittedly, however, our knowledge of the layered series of ophiolites, and the magma chamber processes that operated during their formation, is very limited compared with the knowledge available on intracratonic layered intrusions. It should therefore not be excluded that also the mafic zone of the layered series may contain positive surprises with regard to the PGE-potential of ophiolites.

Summary and Conclusions

The study of the PGE-abundances within the Leka Ophiolite Complex has lead to the following conclusions:

1) PPGE-enriched chromitites with a maximum of 8000ppb of PGE + Au are documented to be present within the mantle tectonites. These rocks compare well with PPGE-enriched chromitites within the Unst ophiolite. Intra-mantle differentiation of the primary magma may be one of the processes that control the formation of these enrichments. The low volume of these enrichments, particularly on Leka, but probably also in ophiolites in general, suggest that they do not have any economic potential.

2) The parental magma to the magma chamber of the Leka Layered Series is shown to have had Pt-Pd abundances comparable with that of intracratonic layered intrusions that host major PGE-deposits.

3) The parental magma had a fractionated PGE-pattern when it entered the magma

chamber and no significant fractionation appears to have taken place within the magma chamber. The fractionation may therefore either have taken place by the formation of unusually IPGE-rich podiform chromitites or during partial melting.

4) Three types of statabound enrichment are documented from the ultramafic zone of the layered series: 1) IPGE-enriched chromitites, 2) Pt-dominated enrichments and 3) Pd-dominated enrichments that are associated with sulphide-rich horizons. While IPGE-enriched horizons typically contain a few hundred ppb of IPGE, the Pd-dominated horizons have commonly Pt + Pd contents in the ppm range. Drill holes across the enrichments have shown the presence of several horizons with half- and meter-averages of ca 1ppm of PGE + Au combined, and some of these horizons can be traced for ca 1,5 kilometres.

5) Pd-Pt antimonides,tellurides and arsenides, as well as native platinum have been documented from the enriched rocks, with grainsizes that vary from less than 10 to 150 microns.

6) The PPGE-enriched horizons on Leka are generally displaced relative to the chromitites and this relationship may explain why the ophiolitic chromitites in general are PPGE-depleted.

7) The present data suggest that the Pt-dominated horizons are positioned just below the Pd-dominated horizons and that they fade laterally towards distal parts of the intrusion; the opposite seems to be the case for the Pd-dominated horizons.

8) The enrichments documented are subeconomic, but their presence demonstrates that orthomagmatic statabound Pt-Pd-deposits may be present within ophiolites.

9) Prospecting for stratabound PGE-deposits in ophiolites should not be focused directly on chromitites but just above the chromitites, or if chromitites are not present close to the base of macro cyclic units. Pt may be preferentially enriched laterally towards the central parts of the intrusion.

Acknowledgements

This work has been supported by the Geological Survey of Norway (NGU) directly and with a research grant from the Royal Norwegian Council for Scientific and Industrial Research (NTNF). Dr. R. Boyd is thanked for his support, encouragement and for many valuable discussions. O. Tumyr and M.Tysseland are thanked for assistance with SEM-, microprobe-, and XRF-analyses.

References

Abrajano, T.A., and Bacuta,G.C., 1982, Platiniferous Fe-Ni-Cu sulfides in an Alpine terrane, Zambales, Republic of the Philippines. Geol. Soc. Am., Abstract with Meeting, p. 429.

Alapieti,T.T., and Lahtinen,J.J., 1986, Stratigraphy, petrology, and platinum-group element mineralization of the Early Proterozoic Penikat Layered Intrusion, Northern Finland: Econ.Geol., v.81, p.1126-1136.

Albrektsen,B.A., Furnes,H.,, and Pedersen,R.B., Formation of dunites in the

mantle tectonites, Leka Ophiolite Complex, Norway. (Submitted to Jour. of Geodynamics).

Amossé., Allibert, M., Fischer, W., and Piboule, M., 1987, Étude de l'influence des fugacités d'oxygéne et de soulfre sur la différenciation des platinoïdes dans les magmas ultramafiques-Résultats préliminaires. C.R. Acad. Sci., Paris, v.304, p.1183-1185.

Amossé,J., Allibert, M., Fischer, W., and Piboule, M., 1990, Experimental study of the solubility of platinum and iridium in basic silicate melts-Implications for the differentiation of platinum-group elements during magmatic processes: Chem. Geol., v.81, p.45-53.

Auge,T., 1985, Platinum-group mineral inclusions in ophiolite chromitite from the Vourinos complex, Greece: Can. Mineral., v.23, p.163-171.

Bacuta, G.C., Lipin,B.R., Gibbs,A.K., and Kay, R.W., 1987, Platinum-Group element abundances in chromite deposits of the Acoje Ophiolite Block, Zambales Ophiolite Complex, Phillippine. in Prichard, H.M., Potts,P.J.,Bowles,J.F.W., and Cribb,S.J.,eds., Geoplatinum "87": London-New York, Elsevier, p.361-380.

Barnes, S.J. and Naldrett A.J.,1985, Geochemistry of the J-M (Howland) Reef of the Stillwater Complex, Minneapolis Adit area. I. Sulphide chemistry and sulphide-olivine equilibrium. Econ.Geol., v.80, p.627-645.

Barnes, S.J., Naldrett, A.J. and Gorton, M.P., 1985, The origin of the fractionation of platinum group elements in terrestrial magmas: Chem. Geol., v.53, p.303-323.

Buchanan,D.L., and Nolan,J., 1979, Solubility of sulfur and sulphide immiscibility in synthetic tholeiitic melts and their relevance to Bushveld-complex rocks: Canadian Mineralogist, v.17, p.483-494.

Buchanan,D.L., Nolan,J., Wilkinson,N., and de Villiers,J.P.R., 1983, An experimental investigation of sulfur solubility as a function of temperatures in synthetic silicate melts: Geol. Soc. South Africa Spec. Pub., v.7., p. 383-391.

Boudreau,A.E., and McCallum,I.S., 1986, Investigation of the Stillwater Complex: III. The Picket Pin Pt/Pd deposit: Econ.Geol. v.81, p.1953-1975.

Burkhard, D.J.M., 1987, Ore minerals and geochemistry in the serpentinites of the eastern Central Alps (Davos to the Val Malenco) compared to occurrences in the Klamath Mountains (Calefornia and Oregon). Ph.D. thesis, University of Heidelberg. Geowiss Abh, v.12, p.345p.

Cabri, L.J. (ed.), 1981, Platinum-group minerals: mineralogy, geology, recovery. Special Volume 23, Canadian Institute of Mining and metallurgy.

Campbell,I.H., Naldrett, A.J., 1979, The influence of silicate: sulphide ratios on the geochemistry of magmatic sulphides: Econ. Geol., v.76, p.1503-1506.

Campbell, I.H., Naldrett A.J., and Barnes S.J.,1983, A model for the origin of the platinum-rich sulphide horizons in the Bushveld and Stillwater Complexes: J. Petrol., v.24, p.133-165.

Campbell,I.H., and Barnes,S.J., 1984, A model for the geochemistry of platinum group element deposits in magmatic sulphide deposits: Canadian Mineralogist, v.22, p.151-160.

Chamberlain, J.A., MacLeod, G.R., Trail, J. and Lachance, G.R., 1965, Native metals in the Muskox intrusion: Can. J. Earth Sci., v.2, p.188-215.

Davies,G., and Tredoux,M., 1985, The platinum-group element and gold contents of the marginal rocks and sills of the Bushveld Complex: Econ.Geol. v.80, p. 838-848.

Dickey,J.S.,1975, A hypothesis of origin for podiform chromite deposits: Geochim et Cosmochim Acta, v.39. p.1061-1074.

Dunning,G.R., and Pedersen,R.B.,1988, U/Pb ages of ophiolites and arc-related plutons of the Norwegian Caledonides: Implications for the development of Iapetus: Contrib Mineral Petrol v.98, p.13-23.

Ecstand, O.R.,1975, The Dumont serpentinite: a model for control of nickeliferous opaque mineral assemblages by alteration reaction in ultramafic rocks: Econ. Geol., v.70, p.183-201.

Furnes, H., Pedersen, R.B. and Stillman, C.J., 1988, The Leka Ophiolite Complex, central Norwegian Caledonides: field characteristics and geotectonic significanse. Jour. Geol. soc., London, v.145, p.401-412.

Gain, S.B., 1985, The geological setting of the platiniferous UG-2 chromitite layer on the farm Maandagshoek, Eastern Bushveld Complex: Econ. Geol., v.80, p.925-943.

Gijbels, R., Millard, Jr., H.T, Desborough, G.A. and Bartel, A.J., 1974, Osmium ,ruthenium, iridium & uranium in silicates and chromite from the eastern Bushveld Complex, South Africa: Geochim. Cosmochim. Acta, v.38, p.319-337.

Greenbaum, D.,1977, The chromitiferous rocks of the Troodos ophiolite complex, Cyprus: Econ. Geol., v 72, p.1175-1194.

Hiemstra, S.A.,1985, The distribution of some platinum-group elements in the UG-2 chromitite layer of the Bushveld Complex: Econ. Geol., v.80,p.944-57.

Hamlyn, P.R., Keays,R.R., Cameron, W.E., Crawford, A.J., and Waldron, H.M., 1985, Precious metals in magnesian low-Ti lavas: Implications for metallogenesis and sulfur saturation in primary magmas: Geochim. et Cosmochim. Acta, v.49, p.1797-1811.

Haughton, D.R., Roeder,P.L. and Skinner,B.J., 1974, Solubility of sulfur in mafic magmas: Econ. Geol., v.69, p. 451-467.

Hiemstra, S.A.,1986, The distribution of chalcophile and platinum-group elements in the UG-2 chromitite layer of the Bushveld Complex: Econ. Geol., v.81,p.1080-1086.

Irvine, T.N., Keith D.W. and Todd, S.G., 1983, The J-M platinum-palladium reef of the Stillwater Complex, Montana: II. Origin by double diffusive convective magma mixing and implications for the Bushveld Complex: Econ. Geol., v.78, p.1287-1334.

Jackson,S.E., Fryer,B.J., Gosse,W., Healey,D.C., Longerich,H.P. and Strong,D.F., 1990, Determination of the precious metals in geological materials by inductively coupled plasma-mass spectrometry (ICP-MS) with nickel sulphide fire-assay collection and tellurium coprecipitation: Chemical Geology (in press).

Johan, Z. and Lebel, L., 1978, Origin of chromite layers in rocks of ophiolitic sui-

te. 11th Gen. Meet., Int. Mineral. Assoc., Abstr., v.1, p.51-52.

Johan, Z. and Legrende, O., 1980, Minlogie des platinos dans les chromite massives du feuillet ophiolitique de la Nouvelle Calniee. In: Rm principaux rltats scientifiques et techniques du Service G:ue National. B.R.G.M. (Bur. Rech. GYMin.), Orls, p. 80 (abstract).

Krüger F.J. and Marsh J.S., 1985, The mineralogy, petrology, and origin of the Merensky Cyclic Unit in the Western Bushveld Complex. Econ. Geol. v. 80, 985-974.

Lago, B.L., Rebinowicz,M., and Nicolas,A., 1982, Podiform chromite ore bodies: a genetic model: Jour. Petrology, v. 23, p.103-125.

Legrende, O. and Johan, Z. 1981. Minlogie des platinos dans les chromites massives de ses ophiolitiques: Rapp. Annu. Activitî. (Cent. Natl. Rech. Sci.), Paris, pp. 32-33.

Lorand, J.P., 1985, The behaviour of the upper mantle sulphide component during the incipient serpentinization of "Alpine" type peridotites as illustrated by the Beni Bousera (Northern Morocco) and Ronda (Southern Spain) ultramafic bodies: Tschermaks Mineral. Petrogr. Mitt., v.34, p.183-211.

Lorand, J.P., 1987, Cu-Fe-Ni-S mineral assemblages in upper-mantle peridotites from the Table Mountain and Blow-Me-Down Mountain ophiolite massifs (Bay of Islands, Newfoundland): Their relationships with fluids and silicate melts: Lithos, v.20, p.59-76.

Morrissey,C.J., 1987, Exploration for Platinum: a contemporary viewpoint: In: Prichard H.M., Potts,P.J., Bowles,J.F.W. and Cribb,S.J.,eds., Geo-platinum 87: London-New York, Elsevier Applied Science, p.1-12.

Naldrett,A.J. and Cabri,L.J., 1976, Ultramafic and related mafic rocks: Their classification and genesis with special reference to the concentration of nickel sulphides and platinum group elements: Econ. Geol., v. 71, p. 1131-1158.

Naldrett, A.J., and Lehmann,J.,1988, Spinel non-stoichiometry as the explanation for Ni-,Cu-, and PGE-enriched sulphides in chromitites, in Prichard, H.M., Potts,P.J.,Bowles,J.F.W., and Cribb,S.J.,eds., Geoplatinum "87": London-New York, Elsevier, p.93-110.

Naldrett,A.J. and Von Gruenewaldt,G., 1989, Association of platinum-group elements with chromitite in layered intrusions and ophiolite complexes: Econ. Geol., v.84, p.180-187.

Orberger,B., Friedrrich,G., and Woermann,E.,1987, Platinum-group element mineralization in the ultramafic sequence of the Acoje ophiolite block, Zambales, Philippines: in Prichard, H.M., Potts,P.J.,Bowles,J.F.W., and Cribb,S.J.,eds., Geoplatinum "87": London-New York, Elsevier, p.361-380.

Page, N.J., Pallister,J.S., Brown,M.A., Smewing,J.D., and Hafty,J., 1982, Palladium, platinum, rhodium, iridium, and ruthenium in chromite-rich rocks from the Samail ophiolite, Oman: Canadian Mineralogist, v 20, p. 537-548.

Page, N.J., Aruiscavage,P.J., and Haffty,J., 1983, Platinum-group elements in rocks from the Voikar-Syninsky ophiolite complex, Polar Urals, U.S.S.R.: Mineralium Deposita, v.18, p.443-455.

Page, N.J., and Talkington, R.W., 1984, Palladium, platinum, rhodium, ruthenium and iridium in peridotites and chromitites from ophiolite complexes from Newfoundland: Canadian Mineralogist, v.22, p. 137-149.

Page, N.J., Singer, D.A., Morning, B.C., Carlson, C.A., McDade, J.M. and Wilson, S.A., 1986, Platinum-group element resources in podiform chromitites from California and Oregon: Econ. Geol., v.81: 1261-1271.

Pedersen RB, Furnes H, Dunning GR, 1988, Some Norwegian ophiolite complexes reconsidered: Progress in Studies of the Lithosphere in Norway, Nor. geol. unders., Spec. Publ., v.3, p.80-85.

Pedersen, R.B., 1989, The ultramafic cumulates of the Leka ophiolite (Norway): Constraints on processes in ophiolitic magma chambers. Terra Abstract, v.1, p163.

Pedersen,R.B. and Hertogen, J., 1990, Magmatic evolution of the Karmøy Ophiolite Complex, SW. Norway : Relationships between MORB - IAT - Boninitic - Calc-alkaline and Alkaline magmatism: Contr. Mineral. Petrol., v 104, p.277-293.

Pedersen, R.B., The ultramafic cumulates of the Leka Ophiolite Complex, Norway - constraints on processes operating in an ophiolitic magma chamber (to be submitted to Journal of Petrology)

Potts, P.J., 1984, Neutron activation-induced beta autoradiograpy as a technique for locating minor phases in thin section: application to rare earth element and platinum-group element mineral analysis. Econ. Geol., v.79, p.738-747.

Potts, P.J., 1986, Neutron activation induced beta autoradiograpy as a technique for locating minor phases in thin section: emulsion response characteristics: Material Sciencs Forum, v.7, p.35-44.

Potts, P.J and Prichard, H.M., 1986, Mineralogical application of neutron activation-induced beta autoradiography: the search for gold mineralization, in Gallagher, M.J., Ixer, R.A., Neary, C.R and Prichard, H.M., eds.: The Institution of Mining and Metallurgy, London, Metallogeny of basic and ultrabasic rocks, p.455-465.

Prestvik, T., 1972, Alpine-type mafic and ultramafic rocks of Leka, Nord Trøndelag. Norges Geologiske UndersNlse, v.273, p.23-34.

Prestvik, T. 1980. The Caledonian ophiolite complex of Leka, north central Norway. In: Panayiotou, A. ed., Geological Survey Department, Cyprus, Ophiolites, p.555-66.

Prichard, H.M., Potts, P.J. and Neary, L.R., 1981, Platinum-group-element minerals in the Unst chromite, Shetland Isles: Trans. Inst. Min. Meatl., v.90, p.186-188.

Prichard,H.M., Neary,C.R. and Potts, P.J.,1986, Platinum-group minerals in the Shetland Ophiolite complex. in Gallagher, M.J., Ixer, R.A., Neary, C.R and Prichard, H.M., eds.: The Institution of Mining and Metallurgy, London, Metallogeny of basic and ultrabasic rocks, p. 395-414.

Prichard, H.M., Potts, P.J., Neary, C.R., Lord, R.A. and Ward, G.R., 1987, Development of techniques for the determination of the platinum-group elements in ultramafic rock complexes of potential economic significance: mineralogical studies. Report commissioned by the Eu-

ropean Economic Community Raw Materials Programme.

Shima,H., and Naldrett, A.J., 1975, Solubility of sulfur in an ultramafic melt and the relevance of the system Fe-S-O: Econ. Geol. v.70, p.960-967.

Stockman, M.W. ,1984, Electron microprobe characterisation of minute platinum group mineral inclutions: limits of accuracy. Scanning Electron Microscopy, v.111, p.1097-1109.

Talkington, R.W., Watkinson, D.H., Whittaker, P.J. and Jones, P.C.,1983, Platinum-group-mineral inclutions in chromite from the Bird River Sill, Manitoba: Miner. Deposita, v.18, p.245-255.

Talkington,R.W., and Watkinson,D.H., 1986, Whole rock platinum-group element trends in chromite-rich rocks in ophiolitic and stratiform igneous complexes. in Gallagher, M.J., Ixer, R.A., Neary, C.R and Prichard, H.M., eds.: The Institution of Mining and Metallurgy, London, Metallogeny of basic and ultrabasic rocks, pp.427-440

Talkington, R.W., Watkinson, D.H., Whittaker, P.J. and Jones, P.C. 1984. Platinum-group-minerals and other solid inclutions in chromite of ophiolitic complexes: occurrence and petrological significanse: Tschermaks Mineral Petrogr., v.32, p.285-301.

Von Gruenevaldt, G.,Hatton,C.J., Merlkle,R.K.W., and Gain,S.B., 1986, Platinum-group element-chromitite associations in the Bushveld Complex: Econ. Geol., v.81,p.1067-1079.

Zientek,M.L.,Foose,M.P.,Leung,M.,1986, Palladium, platinum, and rhodium contents of rocks near the lower margin of the Stillwater Complex, Montana: Econ. Geol., v.81, p. 1169-1178.

Table 1 - Standards

KODE	Rock Type	Method /lab.	Os	Ir	Ru	Rh	Pt	Pd	Au
S1	Dunite	ICPMS/Sheen	8,0	8,5	11,0	2,0	4,5	3,0	2,0
S1		ICPMS/Memorial	6,7	5,9	11,4	1,3	3,9	1,7	1,4
S1		ICPMS/Memorial	2,7	7,0	16,9	1,3	3,1	1,6	0,9
S1		ICPMS/Memorial	3,1	7,3	12,7	1,5	4,1	1,9	0,8
S1		ICPMS/Sheen	12,0	7,0	15,0	1,5	3,5	1,5	2,0
S1		ICPMS/Sheen	2,0	5,0	11,0	1,5	3,0	1,0	6,0
S1		Average	5,8	6,8	13,0	1,5	3,7	1,8	2,2
S1		Standard deviation	3,9	1,2	2,4	0,3	0,6	0,7	1,9
S1		Relative standard dev	67,6%	17,7%	18,7%	17,0%	16,3%	37,5%	88,7%
AX90	Komatiite	ICPMS/Sheen	2,0	3,0	14,0	12,0	140,0	270,0	4,0
AX90		ICPMS/Memorial	2,6	3,1	15,8	11,8	132,2	328,7	4,7
AX90		ICPMS/Memorial	1,7	3,2	16,6	12,3	141,8	322,1	4,9
Ax90		Average	2,1	3,1	15,5	12,0	138,0	306,9	4,5
Ax90		Standard deviation	0,5	0,1	1,3	0,3	5,1	32,1	0,5
Ax90		Relative standard dev	22,2%	2,9%	8,5%	2,3%	3,7%	10,5%	10,4%
AX90		Neutron Act. average	2,3	2,7	19,0	12,0	119,0	338,0	5,4
Ax90		Neutron Act. std	0,7	0,2	4,0	1,0	32,0	37,0	0,7
AXD18	Komatiite	ICPMS/Memorial	1,3	1,3	5,5	5,1	58,5	143,7	5,7
AXD18		ICPMS/Sheen	4,0	5,0	12,0	10,0	72,0	160,0	4,0
AXD18		ICPMS/Sheen	2,0	1,5	8,0	5,5	62,0	170,0	4,0
AXD18		ICPMS/Sheen	2,0	1,5	7,5	5,0	56,0	150,0	8,0
AXD18		Average	2,3	2,3	8,2	6,4	62,1	155,9	5,4
AXD18		Standard deviation	1,2	1,8	2,7	2,4	7,0	11,5	1,9
AXD18		Relative standard dev	50,8%	76,6%	33,2%	37,9%	11,3%	7,4%	34,9%
AXD18		Neutron Activation	<9.00	2,4	9,0	10,6	66,0	156,0	37,0
PTC-1		ICPMS/Sheen	310	170	550	630	2700	12000	340
PTC-1		Recommended					3000	12700	650
PTM-1		ICPMS/Sheen	200	340	650	970	5800	8900	1700
PTM-1		Recommended				900	5800	8100	1800

Table 2 - Harzburgite/Dunite/Pyroxenite from Tectonites

Sample #	Rock Type	Lab.	Os	Ir	Ru	Rh	Pt	Pd	Au	Total
lek88-2c	Dunite	Sheen	6,0	4,5	8,5	1,5	8,0	7,5	2,0	38,0
lek88-3f	Dunite	Sheen	2,0	5,0	12,0	2,5	9,5	6,5	2,0	39,5
lek88-4a	Dunite	Sheen	4,0	5,0	10,0	2,0	5,5	4,5	4,0	35,0
lek88-5d	Dunite	Sheen	12,0	6,0	13,0	2,0	8,0	6,0	4,0	51,0
lek88-6b	Dunite	Sheen	2,0	2,5	15,0	1,0	3,0	3,5	6,0	33,0
lek88-7b	Dunite	Sheen	4,0	4,0	9,0	1,5	2,5	1,5	2,0	24,5
lek88-8b	Dunite	Sheen	10,0	4,0	13,0	2,0	15,0	12,0	4,0	60,0
lek88-1e	Harzburgite	Sheen	8,0	6,5	18,0	3,0	24,0	14,0	2,0	75,5
lek88-2d	Harzburgite	Sheen	8,0	6,5	9,0	2,5	13,0	7,5	2,0	48,5
lek88-3e	Harzburgite	Sheen	10,0	6,5	11,0	2,5	8,5	10,0	6,0	54,5
lek88-3g	Harzburgite	Sheen	10,0	5,0	13,0	2,0	8,0	7,0	4,0	49,0
lek88-4b	Harzburgite	Sheen	8,0	4,5	9,0	2,0	9,0	7,5	4,0	44,0
lek88-5e	Harzburgite	Sheen	8,0	7,0	11,0	2,0	8,5	8,5	4,0	49,0
lek88-6c	Harzburgite	Sheen	4,0	4,0	12,0	1,5	5,0	5,0	2,0	33,5
lek88-7c	Harzburgite	Sheen	4,0	3,5	11,0	1,5	6,5	4,0	2,0	32,5
lek88-8c	Harzburgite	Sheen	8,0	4,0	15,0	1,5	4,5	7,5	2,0	42,5
lek88-2b	Pyroxenite	Sheen	2,0	2,0	11,0	1,0	8,0	6,5	2,0	32,5
lek88-5f	Pyroxenite	Sheen	2,0	1,5	9,0	0,5	3,5	3,0	6,0	25,5

Table 3 - Chromitites from Tectonite

Sample #	Lab.	Os	Ir	Ru	Rh	Pt	Pd	Au	Total
lek88-1b	Sheen	360	410	60	210	4600	2700	170	8510
lek87-P1	Sheen	180	240	370	150	2400	1600	20	4960
lek88-1a	Sheen	340	220	56	150	1800	1200	44	3810
lek88-1d	Sheen	240	220	48	160	2100	960	46	3774
lek88-1c	Sheen	210	210	40	140	1500	690	42	2832
lek88-3a	Sheen	400	240	84	300	1000	550	28	2602
lek88-3b	Sheen	270	170	64	210	1100	730	32	2576
lek88-8a	Sheen	180	76	40	80	740	1400	50	2566
lek88-3c	Sheen	370	250	96	270	1000	420	30	2436
lek88-3d	Sheen	80	39	26	39	270	180	18	652
lek88-6a	Sheen	30	14	16	4	2	4	8	78
lek88-2a	Sheen	12	7	9	2	16	9	2	56
lek88-5a	Sheen	4	3	13	2	6	13	2	42
lek88-5b	Sheen	4	3	13	2	6	5	2	34
lek88-7a	Sheen	2	2	13	1	7	2	4	31
lek88-5c	Sheen	4	3	9	2	6	4	2	29

Table 4 - Profile B

Sample #	STRAT	Lab.	Os	Ir	Ru	Rh	Pt	Pd	Au	Total
84-1B	20	Sheen	2,0	1,5	9,0	3,0	9,5	28,0	8,0	61,0
84-2B	22,1	Sheen	2,0	1,5	8,0	3,0	15,0	46,0	8,0	83,5
84-3B	25,4	Sheen	2,0	1,5	9,5	3,5	17,0	54,0	6,0	93,5
84-4B	26,3	Sheen	2,0	2,0	8,0	4,5	7,5	29,0	6,0	59,0
84-5B	28,5	Sheen	2,0	4,5	9,5	9,5	27,0	30,0	6,0	88,5
84-6B	31,6	Sheen	2,0	3,0	12,0	3,0	4,0	14,0	6,0	44,0
84-7B	34,5	Sheen	2,0	3,0	12,0	4,0	17,0	26,0	6,0	70,0
84-8B	37,2	Sheen	2,0	3,0	8,5	6,0	20,0	31,0	6,0	76,5
84-9B	40	Sheen	2,0	2,5	8,0	4,0	34,0	76,0	8,0	134,5
84-10B	40,9	Sheen	2,0	1,5	7,0	2,0	5,0	21,0	4,0	42,5
84-11B	41,9	Sheen	2,0	1,5	6,0	2,5	11,0	34,0	4,0	61,0
84-12B	43,1	Sheen	2,0	2,0	7,0	3,5	26,0	220,0	16,0	276,5
84-13B	44,1	Sheen	2,0	2,0	9,0	3,0	14,0	42,0	2,0	74,0
84-14B	45,5	Sheen	2,0	2,0	5,5	3,0	27,0	52,0	4,0	95,5
84-15B	46,9	Sheen	2,0	3,0	9,0	6,0	37,0	48,0	6,0	111,0
84-16B	47,9	Sheen	2,0	4,5	6,0	7,5	21,0	18,0	4,0	63,0
84-17B	49,3	Sheen	2,0	2,0	7,0	3,5	13,0	23,0	4,0	54,5
84-18B	52	Sheen	2,0	2,0	7,0	3,0	20,0	24,0	4,0	62,0
84-19B	54,5	Sheen	2,0	2,5	6,5	3,5	22,0	22,0	4,0	62,5
84-20B	56,2	Sheen	2,0	2,0	6,0	4,5	23,0	27,0	4,0	68,5
84-21B	58,3	Sheen	2,0	1,5	6,5	2,0	9,5	26,0	6,0	53,5
84-22B	60,2	Sheen	2,0	2,0	8,0	2,5	10,0	17,0	4,0	45,5
84-23B	62	Sheen	6,0	10,0	12,0	16,0	85,0	47,0	6,0	182,0
84-24B	63,4	Sheen	30,0	16,0	75,0	5,5	11,0	48,0	6,0	191,5
84-25B	65,9	Sheen	8,0	5,0	20,0	2,5	3,5	9,5	4,0	52,5
84-26B	68,9	Sheen	4,0	4,0	4,5	6,0	520,0	150,0	130,0	818,5
84-27B	72,2	Sheen	4,0	4,0	9,5	6,0	38,0	29,0	6,0	96,5
84-28B	79,2	Sheen	2,0	3,5	8,5	6,5	36,0	36,0	6,0	98,5
84-29B	81	Sheen	2,0	2,0	6,5	3,0	13,0	18,0	6,0	50,5
84-30B	84,9	Sheen	2,0	2,5	8,5	4,0	18,0	17,0	4,0	56,0
84-31B	90,8	Sheen	4,0	4,0	13,0	4,0	32,0	30,0	6,0	93,0
84-32B	97,4	Sheen	2,0	2,0	7,5	2,0	8,5	13,0	10,0	45,0
84-33B	102	Sheen	6,0	4,0	15,0	5,5	43,0	89,0	42,0	204,5
84-34B	105	Sheen	4,0	2,0	9,0	2,0	5,0	12,0	6,0	40,0
84-35B	109,2	Sheen	2,0	2,0	10,0	2,5	8,0	10,0	14,0	48,5
84-36B	113	Sheen	2,0	2,5	6,5	3,0	10,0	14,0	4,0	42,0
84-37B	119,4	Sheen	4,0	3,0	11,0	2,5	5,0	9,5	4,0	39,0
84-38B	124,6	Sheen	2,0	2,0	7,0	2,5	9,0	15,0	6,0	43,5
84-39B	129,3	Sheen	2,0	2,0	5,5	3,5	49,0	81,0	16,0	159,0
84-40B	136,5	Sheen	2,0	2,5	5,0	3,5	51,0	53,0	4,0	121,0
84-41B	140	Sheen	2,0	2,5	7,5	4,5	30,0	31,0	6,0	83,5
84-42B	141,3	Sheen	2,0	2,5	6,5	4,5	74,0	45,0	6,0	140,5
84-43B	142,6	Sheen	2,0	2,0	5,5	2,5	14,0	13,0	4,0	43,0
84-44B	143,8	Sheen	2,0	1,5	5,5	2,5	17,0	22,0	8,0	58,5
84-45B	145,3	Sheen	2,0	2,0	7,5	3,0	19,0	29,0	8,0	70,5
84-46B	148	Sheen	2,0	1,5	7,0	2,5	9,5	17,0	4,0	43,5
84-47B	149,6	Sheen	2,0	2,0	7,5	3,0	42,0	100,0	10,0	166,5
84-48B	150,7	Sheen	2,0	1,5	7,5	2,5	19,0	32,0	12,0	76,5
84-49B	152,6	Sheen	4,0	5,5	16,0	4,0	34,0	55,0	10,0	128,5
87-P2	153	Sheen	130,0	83,0	260,0	55,0	640,0	1000,0	110,0	2278,0
84-50B	153,3	Sheen	18,0	19,0	38,0	10,0	64,0	26,0	4,0	179,0
84-51B	154,9	Sheen	2,0	2,0	8,5	2,5	7,5	9,0	4,0	35,5
84-52B	156,4	Sheen	2,0	2,0	9,5	2,0	4,5	10,0	6,0	36,0
84-53B	157,8	Sheen	16,0	9,5	49,0	5,5	8,5	10,0	4,0	102,5
84-54B	159,8	Sheen	14,0	8,0	41,0	4,5	8,5	10,0	6,0	92,0
84-55B	161,2	Sheen	4,0	2,5	9,5	4,5	15,0	17,0	6,0	58,5
84-56B	163	Sheen	2,0	2,0	9,0	2,5	4,0	10,0	6,0	35,5
84-57B	164,1	Sheen	8,0	6,0	34,0	4,0	12,0	17,0	4,0	85,0
84-58B	165,8	Sheen	4,0	2,0	8,0	2,5	5,0	10,0	4,0	35,5
84-59B	167	Sheen	4,0	3,0	11,0	5,0	30,0	37,0	6,0	96,0
Average			5,9	4,7	16,0	4,9	39,9	51,5	10,6	133,4

Table 5 - Core 87A1

Core len.	Lab.	Os	Ir	Ru	Rh	Pt	Pd	Au	Total
19,5	Sheen	2,0	4,0	5,0	7,0	200,0	240,0	14,0	472,0
19,0	Sheen	2,0	4,0	3,5	7,0	120,0	82,0	6,0	224,5
18,5	Sheen	2,0	4,0	4,0	6,5	54,0	36,0	4,0	110,5
18,0	Sheen	2,0	3,0	5,0	3,5	28,0	38,0	4,0	83,5
17,5	Sheen	2,0	4,0	5,0	5,0	33,0	51,0	6,0	106,0
17,0	Sheen	2,0	4,0	3,5	8,5	160,0	110,0	22,0	310,0
16,5	Sheen	2,0	2,0	2,5	2,5	140,0	780,0	170,0	1099,0
16,0	Sheen	2,0	2,0	4,5	3,0	110,0	250,0	46,0	417,5
15,5	Sheen	2,0	4,0	12,0	2,0	16,0	17,0	2,0	55,0
15,0	Sheen	6,0	9,0	26,0	3,0	8,5	7,0	2,0	61,5
14,5	Sheen	14,0	8,0	28,0	4,5	23,0	28,0	6,0	111,5
14,0	Sheen	12,0	16,0	56,0	5,5	7,0	11,0	8,0	115,5
13,5	Sheen	24,0	13,0	42,0	4,5	7,0	15,0	6,0	111,5
13,0	Sheen	20,0	12,0	45,0	4,0	6,0	13,0	6,0	106,0
12,5	Sheen	20,0	15,0	60,0	6,0	8,0	12,0	6,0	127,0
12,0	Sheen	22,0	18,0	68,0	5,0	6,5	14,0	6,0	139,5
11,5	Sheen	28,0	14,0	53,0	5,0	9,0	12,0	10,0	131,0
11,0	Sheen	22,0	10,0	40,0	4,0	5,0	11,0	6,0	98,0
10,5	Sheen	16,0	13,0	56,0	5,0	5,5	12,0	6,0	113,5
10,0	Sheen	16,0	17,0	76,0	6,0	7,0	15,0	8,0	145,0
9,5	Sheen	30,0	19,0	80,0	6,0	15,0	17,0	18,0	185,0
9,0	Sheen	30,0	21,0	80,0	6,5	8,0	13,0	8,0	166,5
8,5	Sheen	32,0	20,0	84,0	8,0	40,0	23,0	64,0	271,0
8,0	Sheen	26,0	14,0	57,0	4,5	9,5	17,0	8,0	136,0
7,5	Sheen	8,0	5,0	20,0	2,5	7,0	13,0	6,0	61,5
7,0	Sheen	8,0	6,0	24,0	2,5	7,5	16,0	6,0	70,0
6,5	Sheen	12,0	7,0	28,0	3,0	8,5	14,0	6,0	78,5
6,0	Sheen	16,0	10,0	33,0	3,0	10,0	19,0	6,0	97,0
5,5	Sheen	10,0	7,0	23,0	2,5	6,0	13,0	6,0	67,5
5,0	Sheen	6,0	5,0	18,0	2,5	8,0	13,0	6,0	58,5
4,5	Sheen	6,0	5,0	12,0	4,5	34,0	35,0	8,0	104,5
4,0	Sheen	4,0	4,0	12,0	6,5	41,0	52,0	10,0	129,5
3,5	Sheen	2,0	2,0	6,5	4,0	29,0	35,0	6,0	84,5
3,0	Sheen	2,0	3,0	8,5	3,0	20,0	23,0	8,0	67,5
2,5	Sheen	4,0	3,0	13,0	3,0	14,0	21,0	8,0	66,0
2,0	Sheen	2,0	2,0	6,0	2,5	8,5	15,0	6,0	42,0
1,5	Sheen	2,0	2,0	7,0	2,5	20,0	37,0	6,0	76,5
1,0	Sheen	2,0	2,0	6,5	2,0	17,0	31,0	6,0	66,5
0,5	Sheen	2,0	2,0	8,5	2,5	24,0	38,0	6,0	83,0
Average		10,8	8,1	28,8	4,3	32,8	56,4	13,9	155,1

Table 6 - Core 87B1

ore len.	Lab.	Os	Ir	Ru	Rh	Pt	Pd	Au	Total
0,5	Sheen	2,0	3,0	3,5	5,0	110,0	150,0	14,0	287,5
1	Sheen	2,0	2,0	3,0	3,5	58,0	100,0	8,0	176,5
1,5	Sheen	2,0	1,0	1,0	1,5	17,0	22,0	4,0	48,5
2	Sheen	2,0	1,0	1,0	1,0	15,0	24,0	6,0	50,0
2,5	Sheen	2,0	1,0	1,0	1,0	15,0	19,0	6,0	45,0
3	Sheen	10,0	5,0	20,0	3,0	22,0	31,0	10,0	101,0
3,5	Sheen	12,0	11,0	32,0	8,0	36,0	52,0	10,0	161,0
4	Sheen	8,0	6,0	16,0	3,5	9,5	15,0	4,0	62,0
4,5	Sheen	10,0	7,0	19,0	4,0	20,0	24,0	4,0	88,0
5	Sheen	14,0	12,0	31,0	12,0	170,0	130,0	20,0	389,0
5,5	Sheen	16,0	10,0	31,0	5,5	30,0	41,0	4,0	137,5
6	Sheen	8,0	4,0	14,0	3,5	11,0	10,0	4,0	54,5
6,5	Sheen	10,0	6,0	18,0	3,5	9,0	15,0	6,0	67,5
7	Sheen	2,0	2,0	7,5	1,5	19,0	20,0	6,0	58,0
7,5	Sheen	4,0	4,0	10,0	3,0	22,0	18,0	8,0	69,0
8	Sheen	2,0	2,0	7,0	1,0	7,5	14,0	4,0	37,5
8,5	Sheen	2,0	1,0	3,0	1,5	12,0	9,5	4,0	33,0
9	Sheen	2,0	3,0	3,5	5,5	58,0	65,0	30,0	167,0
9,5	Sheen	2,0	1,0	3,0	2,0	7,0	7,0	4,0	26,0
10	Sheen	2,0	1,0	5,5	2,5	24,0	7,5	2,0	44,5
10,5	Sheen	2,0	1,0	6,0	3,0	24,0	5,0	2,0	43,0
11	Sheen	2,0	1,0	5,5	2,5	22,0	4,5	2,0	39,5
11,5	Sheen	2,0	1,0	5,0	2,5	21,0	5,0	2,0	38,5
12	Sheen	2,0	1,0	6,5	4,0	27,0	3,0	2,0	45,5
12,5	Sheen	2,0	2,0	8,5	3,5	27,0	5,0	2,0	50,0
13	Sheen	2,0	2,0	5,5	3,0	26,0	7,5	4,0	50,0
Average		4,8	3,5	10,3	3,5	31,5	30,9	6,6	91,1

Table 7- Core 8881

Core len.	Lab.	Os	Ir	Ru	Rh	Pt	Pd	Au	Total
30,0	Sheen	2,0	17,0	2,0	5,5	580,0	180,0	180,0	966,5
29,5	Sheen	2,0	9,0	2,0	4,5	270,0	130,0	42,0	459,5
29,0	Sheen	2,0	11,0	2,0	6,0	320,0	220,0	50,0	611,0
28,5	Sheen	4,0	11,0	2,0	12,0	170,0	84,0	46,0	329,0
28,0	Sheen	6,0	9,0	2,0	11,0	48,0	100,0	56,0	232,0
27,5	Sheen	8,0	9,5	2,5	10,0	60,0	100,0	32,0	222,0
27,0	Sheen	4,0	10,0	3,0	9,5	74,0	51,0	52,0	203,5
26,5	Sheen	2,0	5,5	2,0	4,5	29,0	16,0	52,0	111,0
26,0	Sheen	2,0	5,0	3,0	3,0	31,0	24,0	28,0	96,0
25,5	Sheen	2,0	4,5	2,5	3,0	22,0	22,0	46,0	102,0
25,0	Sheen	2,0	5,0	2,0	3,5	43,0	22,0	26,0	103,5
24,5	Sheen	2,0	5,5	1,5	3,5	32,0	21,0	2,0	67,5
24,0	Sheen	2,0	5,0	1,0	2,5	21,0	12,0	44,0	87,5
23,5	Sheen	2,0	6,0	2,5	4,0	25,0	18,0	56,0	113,5
23,0	Sheen	2,0	5,5	3,0	3,0	15,0	16,0	180,0	224,5
22,5	Sheen	4,0	6,0	1,5	3,5	29,0	23,0	54,0	121,0
22,0	Sheen	4,0	5,0	1,5	3,0	14,0	13,0	38,0	78,5
21,5	Sheen	2,0	8,5	5,0	3,5	51,0	25,0	62,0	157,0
21,0	Sheen	2,0	6,5	5,0	3,5	35,0	24,0	42,0	118,0
20,5	Sheen	2,0	4,5	4,0	2,0	16,0	17,0	42,0	87,5
20,0	Sheen	4,0	6,0	3,5	3,5	42,0	35,0	50,0	144,0
19,5	Sheen	6,0	7,5	5,0	4,0	39,0	46,0	54,0	161,5
19,0	Sheen	4,0	9,0	5,0	5,5	39,0	24,0	66,0	152,5
18,5	Sheen	4,0	7,5	3,5	4,5	63,0	50,0	64,0	196,5
18,0	Sheen	6,0	9,0	4,5	6,0	65,0	64,0	54,0	208,5
17,5	Sheen	10,0	17,0	5,0	11,0	120,0	120,0	76,0	359,0
17,0	Sheen	2,0	13,0	3,0	10,0	100,0	110,0	52,0	290,0
16,5	Sheen	2,0	14,0	4,5	10,0	130,0	79,0	78,0	317,5
16,0	Sheen	4,0	12,0	5,0	7,0	74,0	39,0	50,0	191,0
15,5	Sheen	4,0	6,5	5,0	3,5	39,0	28,0	42,0	128,0
15,0	Sheen	4,0	6,0	5,0	2,5	25,0	28,0	44,0	114,5
14,5	Sheen	4,0	8,0	4,0	2,5	42,0	21,0	58,0	139,5
14,0	Sheen	2,0	7,0	6,0	3,0	40,0	41,0	80,0	179,0
13,5	Sheen	6,0	8,0	5,0	2,5	17,0	8,0	58,0	104,5
13,0	Sheen	6,0	8,0	5,0	2,5	29,0	14,0	78,0	142,5
12,5	Sheen	6,0	14,0	3,0	5,5	190,0	160,0	84,0	462,5
12,0	Sheen	6,0	16,0	2,0	11,0	230,0	160,0	76,0	501,0
11,5	Sheen	8,0	19,0	3,5	19,0	150,0	160,0	90,0	449,5
11,0	Sheen	4,0	12,0	2,5	8,0	60,0	49,0	80,0	215,5
10,5	Sheen	6,0	10,0	3,5	3,5	23,0	20,0	74,0	140,0
10,0	Sheen	2,0	8,0	3,5	4,0	25,0	19,0	82,0	143,5
9,5	Sheen	4,0	13,0	2,5	10,0	81,0	68,0	82,0	260,5
9,0	Sheen	14,0	21,0	11,0	13,0	110,0	120,0	110,0	399,0
8,5	Sheen	30,0	28,0	15,0	11,0	12,0	8,5	60,0	164,5
8,0	Sheen	44,0	39,0	21,0	16,0	17,0	11,0	62,0	210,0
7,5	Sheen	40,0	39,0	25,0	14,0	12,0	15,0	54,0	199,0
7,0	Sheen	32,0	28,0	18,0	11,0	6,0	6,5	42,0	143,5
6,5	Sheen	26,0	21,0	11,0	8,0	21,0	12,0	58,0	157,0
6,0	Sheen	14,0	12,0	7,0	5,0	6,0	6,0	48,0	98,0
5,5	Sheen	16,0	13,0	8,0	5,0	10,0	9,5	60,0	121,5
5,0	Sheen	10,0	15,0	9,5	15,0	5,0	22,0	2,0	78,5
4,5	Sheen	18,0	13,0	7,0	4,0	7,5	5,5	36,0	91,0
4,0	Sheen	14,0	14,0	6,5	5,0	7,5	6,5	52,0	105,5
3,5	Sheen	18,0	20,0	8,0	6,0	7,5	7,5	66,0	133,0
3,0	Sheen	56,0	34,0	21,0	11,0	12,0	18,0	76,0	228,0
2,5	Sheen	22,0	20,0	11,0	7,5	8,0	19,0	66,0	153,5
2,0	Sheen	18,0	18,0	10,0	7,5	9,0	8,0	42,0	112,5
1,5	Sheen	24,0	22,0	11,0	9,0	15,0	11,0	46,0	138,0
1,0	Sheen	8,0	11,0	3,5	3,5	6,5	6,0	62,0	100,5
0,5	Sheen	6,0	7,5	3,0	3,0	12,0	12,0	62,0	105,5
Average		9,5	12,6	5,8	6,6	63,2	46,1	60,1	203,8

Table 8 - Core 8882

Core len.	Lab.	Os	Ir	Ru	Rh	Pt	Pd	Au	Total
20,0	Sheen	24,0	8,0	13,0	3,5	7,5	8,0	6,0	70,0
19,5	Sheen	38,0	9,0	19,0	4,0	5,5	8,5	8,0	92,0
19,0	Sheen	20,0	6,0	12,0	3,5	4,5	7,5	6,0	59,5
18,5	Sheen	12,0	6,5	21,0	3,5	4,5	4,5	8,0	60,0
18,0	Sheen	24,0	7,0	21,0	5,5	2,5	5,0	8,0	73,0
17,5	Sheen	2,0	4,5	1,0	0,5	3,5	0,5	12,0	24,0
17,0	Sheen	2,0	1,5	11,0	1,5	3,0	5,5	6,0	30,5
16,5	Sheen	2,0	1,5	18,0	2,0	4,5	14,0	12,0	54,0
16,0	Sheen	2,0	2,0	11,0	1,5	9,0	7,0	66,0	98,5
15,5	Sheen	2,0	1,5	11,0	1,5	6,0	10,0	2,0	34,0
15,0	Sheen	2,0	1,5	18,0	2,5	4,5	18,0	6,0	52,5
15,0	Sheen	2,0	2,0	14,0	4,5	8,5	20,0	4,0	55,0
14,5	Sheen	2,0	2,0	18,0	2,5	12,0	28,0	6,0	70,5
14,0	Sheen	6,0	3,0	9,5	3,5	7,5	23,0	6,0	58,5
13,5	Sheen	4,0	8,5	11,0	9,5	64,0	58,0	8,0	163,0
13,0	Sheen	2,0	8,0	16,0	8,0	160,0	140,0	12,0	346,0
12,5	Sheen	2,0	5,0	11,0	3,0	24,0	21,0	14,0	80,0
12,0	Sheen	2,0	2,5	12,0	2,0	13,0	14,0	6,0	51,5
11,5	Sheen	2,0	4,0	13,0	3,0	27,0	40,0	18,0	107,0
11,0	Sheen	2,0	4,5	16,0	0,5	41,0	0,5	24,0	88,5
10,5	Sheen	2,0	5,5	14,0	5,5	83,0	130,0	18,0	258,0
10,0	Sheen	2,0	4,0	14,0	3,0	24,0	20,0	8,0	75,0
9,5	Sheen	4,0	8,0	16,0	7,0	77,0	110,0	14,0	236,0
9,0	Sheen	4,0	4,5	15,0	4,5	40,0	52,0	16,0	136,0
8,5	Sheen	6,0	4,0	18,0	2,5	11,0	14,0	16,0	71,5
8,0	Sheen	2,0	4,0	16,0	2,0	9,0	8,0	10,0	51,0
7,5	Sheen	2,0	4,5	3,0	2,5	17,0	3,0	280,0	312,0
7,0	Sheen	2,0	8,0	7,0	4,5	26,0	24,0	160,0	231,5
6,5	Sheen	2,0	5,0	29,0	4,0	19,0	14,0	240,0	313,0
6,0	Sheen	2,0	4,5	5,0	4,0	15,0	26,0	300,0	356,5
5,5	Sheen	2,0	4,0	3,5	4,0	53,0	23,0	310,0	399,5
5,0	Sheen	2,0	6,0	3,5	7,0	24,0	8,0	550,0	600,5
4,5	Sheen	2,0	6,5	5,0	6,0	59,0	30,0	300,0	408,5
4,0	Sheen	4,0	11,0	6,0	10,0	220,0	160,0	390,0	801,0
3,5	Sheen	2,0	7,0	3,0	6,5	100,0	160,0	66,0	344,5
3,0	Sheen	6,0	9,0	3,0	10,0	87,0	230,0	100,0	445,0
2,5	Sheen	2,0	5,0	2,5	2,5	33,0	30,0	24,0	99,0
2,0	Sheen	2,0	4,5	3,0	4,0	36,0	56,0	66,0	171,5
1,5	Sheen	2,0	5,0	3,0	4,0	47,0	58,0	28,0	147,0
1,0	Sheen	4,0	13,0	2,5	15,0	150,0	220,0	80,0	484,5
0,5	Sheen	2,0	6,5	4,0	7,5	59,0	87,0	38,0	204,0
Average		5,2	5,3	11,0	4,4	39,0	46,2	79,3	190,6

Table 9 - Core 88B5

Core len	Lab.	Os	Ir	Ru	Rh	Pt	Pd	Au	Total
20	Sheen	2,0	1,5	4,5	1,5	4,5	5,0	4,0	23,0
19	Sheen	2,0	0,5	2,5	0,5	3,0	4,0	4,0	16,5
18	Sheen	2,0	1,0	4,0	1,0	6,0	6,0	6,0	26,0
17	Sheen	2,0	1,5	4,0	2,5	25,0	33,0	6,0	74,0
16	Sheen	2,0	1,0	3,5	2,0	21,0	18,0	6,0	53,5
15	Sheen	2,0	2,5	3,5	3,0	6,5	6,0	4,0	27,5
14	Sheen	2,0	2,0	3,5	2,5	19,0	19,0	6,0	54,0
13	Sheen	2,0	1,0	3,5	1,0	7,0	6,0	4,0	24,5
12	Sheen	2,0	0,5	3,5	1,0	4,5	3,5	6,0	21,0
11	Sheen	2,0	1,0	4,0	1,0	2,0	1,5	4,0	15,5
10	Sheen	2,0	1,0	4,5	1,0	2,0	2,5	6,0	19,0
9	Sheen	2,0	0,5	5,0	0,5	2,5	2,5	2,0	15,0
8	Sheen	2,0	2,5	9,0	1,5	4,0	5,0	2,0	26,0
7	Sheen	2,0	2,5	7,5	1,5	3,5	3,5	2,0	22,5
6	Sheen	2,0	2,0	6,5	1,5	3,5	2,5	2,0	20,0
5	Sheen	2,0	1,5	3,5	2,0	3,5	3,0	2,0	17,5
4	Sheen	2,0	2,0	5,0	2,5	12,0	6,5	2,0	32,0
3	Sheen	2,0	2,5	3,5	3,0	9,5	13,0	2,0	35,5
2	Sheen	2,0	1,0	3,0	1,5	14,0	33,0	6,0	60,5
1	Sheen	2,0	1,0	3,5	1,5	13,0	36,0	36,0	93,0
Average		2,0	1,5	4,4	1,6	8,3	10,5	5,6	33,8

Table 10 - Core 88b6

Sample #	Lab.	Os	Ir	Ru	Rh	Pt	Pd	Au	Total
1	Sheen	2	6	6,5	4	26	58	4	107
2	Sheen	2	6	5,5	3	22	37	4	80
3	Sheen	2	7	6,5	4	39	49	6	114
4	Sheen	2	5	5	4,5	36	39	8	100
5	Sheen	2	6,5	6,5	3,5	57	61	12	149
6	Sheen	2	5,5	3,5	2	16	22	6	57
7	Sheen	2	4,5	5,5	1,5	15	26	14	69
8	Sheen	2	9	11	4	150	210	21	407
9	Sheen	2	8,5	19	5,5	100	580	48	763
10	Sheen	4	7,5	4	7	32	48	4	107
11	Sheen	4	8	5,5	4	24	48	8	102
12	Sheen	2	8	5,5	3	10	14	2	45
13	Sheen	2	6	5	2	8,5	8,5	2	34
14	Sheen	2	6	4,5	2	8	11	4	38
15	Sheen	2	6,5	5	2	6	8	2	32
16	Sheen	2	7	4	2,5	9	8	4	37
17	Sheen	2	7	4,5	2,5	13	15	4	48
18	Sheen	2	5,5	4	2	10	9	2	35
19	Sheen	2	6	4	2,5	17	22	2	56
20	Sheen	2	4,5	3,5	2,5	15	15	2	45
Average		2,2	6,5	5,9	3,2	30,7	64,4	8,0	120,9

Table 11 - Core 88B7

Core len.	Lab.	Os	Ir	Ru	Rh	Pt	Pd	Au	Total
20	Sheen	2,0	0,5	3,0	1,5	27,0	51,0	20,0	105,0
19	Sheen	2,0	0,5	3,0	1,0	32,0	120,0	28,0	186,5
18	Sheen	2,0	1,5	3,0	1,5	34,0	87,0	20,0	149,0
17	Sheen	2,0	1,0	3,0	1,5	27,0	47,0	12,0	93,5
16	Sheen	2,0	2,0	5,5	2,0	47,0	41,0	34,0	133,5
16	Sheen	2,0	2,0	5,0	2,0	43,0	45,0	34,0	133,0
15	Sheen	2,0	1,5	2,5	2,0	33,0	41,0	18,0	100,0
14	Sheen	2,0	1,0	1,5	1,0	18,0	29,0	8,0	60,5
13	Sheen	2,0	3,0	4,5	5,0	77,0	53,0	26,0	170,5
12	Sheen	2,0	2,5	5,0	4,5	36,0	18,0	12,0	80,0
11	Sheen	2,0	1,0	2,0	1,0	17,0	30,0	38,0	91,0
10	Sheen	2,0	1,5	3,5	1,0	16,0	17,0	4,0	45,0
9	Sheen	2,0	12,0	26,0	21,0	250,0	310,0	28,0	649,0
8	Sheen	2,0	4,0	8,0	7,5	120,0	270,0	34,0	445,5
7	Sheen	2,0	1,5	4,0	3,5	28,0	15,0	10,0	64,0
6	Sheen	2,0	1,5	3,5	2,0	55,0	94,0	8,0	166,0
6	Sheen	2,0	2,0	3,5	2,0	61,0	96,0	10,0	176,5
5	Sheen	2,0	3,0	11,0	1,0	4,5	4,0	2,0	27,5
4	Sheen	2,0	10,0	36,0	3,0	4,0	4,5	4,0	63,5
3	Sheen	2,0	9,0	33,0	2,5	2,5	2,5	4,0	55,5
2	Sheen	2,0	6,0	20,0	1,5	5,0	3,5	4,0	42,0
1	Sheen	2,0	5,5	22,0	2,5	6,5	7,5	4,0	50,0
Average		2,0	3,3	9,5	3,2	42,9	63,0	16,5	140,3

Tabel 12 - Core 89B1

Core len.	Lab	Os	Ir	Ru	Rh	Pt	Pd	Au	Total
1	Sheen	2,0	1,0	3,0	1,5	14,0	27,0	6,0	54,5
2	Sheen	2,0	1,0	3,0	1,0	6,0	8,5	8,0	29,5
3	Sheen	2,0	0,5	2,5	0,5	5,0	7,5	8,0	26,0
4	Sheen	2,0	0,5	3,0	1,0	4,0	7,5	8,0	26,0
5	Sheen	2,0	1,5	2,5	1,0	6,5	13,0	8,0	34,5
6	Sheen	2,0	1,0	3,0	1,0	9,5	14,0	6,0	36,5
6	Sheen	2,0	1,0	3,5	1,5	11,0	13,0	8,0	40,0
7	Sheen	2,0	1,0	4,0	1,5	9,5	15,0	6,0	39,0
8	Sheen	2,0	1,0	2,5	1,0	7,5	9,5	6,0	29,5
9	Sheen	2,0	2,0	3,5	1,0	3,0	5,0	8,0	24,5
10	Sheen	2,0	0,5	2,0	0,5	2,0	4,5	10,0	21,5
11	Sheen	2,0	2,0	3,5	1,5	3,5	2,5	4,0	19,0
12	Sheen	2,0	2,0	3,5	2,0	7,5	12,0	4,0	33,0
13	Sheen	2,0	0,5	2,0	0,5	8,0	9,5	2,0	24,5
14	Sheen	2,0	0,5	1,5	0,5	5,5	8,5	4,0	22,5
15	Sheen	2,0	1,0	3,0	1,0	12,0	16,0	4,0	39,0
16	Sheen	2,0	1,5	2,0	1,5	8,0	9,5	4,0	28,5
16	Sheen	2,0	1,0	2,5	1,0	7,0	8,5	4,0	26,0
17	Sheen	2,0	1,0	3,0	1,0	7,5	11,0	4,0	29,5
18	Sheen	2,0	1,5	2,5	1,0	12,0	16,0	4,0	39,0
19	Sheen	2,0	1,5	4,5	1,5	15,0	21,0	4,0	49,5
20	Sheen	2,0	1,5	3,5	1,0	9,0	12,0	4,0	33,0
Average		2,0	1,1	2,9	1,1	7,9	11,4	5,6	32,0

Tabel 13 - Core 89B3

Core len	Lab.	Os	Ir	Ru	Rh	Pt	Pd	Au	Total
20	Sheen	2,0	1,5	4,0	2,5	11,0	8,5	14,0	43,5
19	Sheen	2,0	3,0	7,0	4,0	39,0	54,0	14,0	123,0
18	Sheen	2,0	1,5	3,0	3,0	11,0	4,0	18,0	42,5
17	Sheen	2,0	1,0	2,0	2,0	9,5	9,5	14,0	40,0
16	Sheen	2,0	1,5	3,0	3,0	11,0	14,0	12,0	46,5
16	Sheen	2,0	1,0	2,5	3,0	12,0	13,0	14,0	47,5
15	Sheen	2,0	2,0	4,0	2,5	21,0	30,0	10,0	71,5
14	Sheen	2,0	1,0	2,5	1,5	8,5	5,5	24,0	45,0
13	Sheen	2,0	1,0	3,0	1,5	5,0	5,0	10,0	27,5
12	Sheen	2,0	0,5	1,0	1,5	3,5	2,0	14,0	24,5
11	Sheen	2,0	2,0	4,0	4,5	18,0	4,5	4,0	39,0
10	Sheen	2,0	1,0	2,5	1,5	5,0	5,0	2,0	19,0
9	Sheen	2,0	1,5	2,5	3,5	6,5	7,0	6,0	29,0
8	Sheen	2,0	1,5	2,5	2,5	28,0	48,0	8,0	92,5
7	Sheen	2,0	0,5	2,5	1,0	6,5	4,5	10,0	27,0
6	Sheen	2,0	1,0	2,5	2,0	16,0	8,0	8,0	39,5
6	Sheen	2,0	1,0	2,5	2,0	16,0	8,5	4,0	36,0
5	Sheen	2,0	1,0	2,5	3,0	16,0	13,0	6,0	43,5
4	Sheen	2,0	1,0	2,5	2,5	26,0	26,0	8,0	68,0
3	Sheen	2,0	1,5	7,0	1,0	6,0	2,5	4,0	24,0
2	Sheen	2,0	3,0	13,0	1,5	3,5	1,0	4,0	28,0
1	Sheen	2,0	2,5	14,0	1,5	3,0	3,0	4,0	30,0
Average		2,0	1,4	4,1	2,3	12,8	12,6	9,6	44,9

Table 14 - Core 89B4

Core len.	Lab.	Os	Ir	Ru	Rh	Pt	Pd	Au	Total
1,0	Sheen	2,0	1,0	3,0	3,5	61,0	88,0	22,0	180,5
1,5	Sheen	2,0	1,5	4,5	4,5	85,0	150,0	16,0	263,5
2,0	Sheen	2,0	0,5	2,5	1,0	9,0	15,0	8,0	38,0
4,5	Sheen	2,0	0,5	3,5	1,5	9,5	19,0	8,0	44,0
5,0	Sheen	2,0	0,5	2,5	2,0	34,0	58,0	18,0	117,0
5,5	Sheen	2,0	1,5	2,5	3,0	69,0	99,0	30,0	207,0
6,0	Sheen	2,0	1,0	2,0	3,0	73,0	110,0	42,0	233,0
6,5	Sheen	2,0	1,0	2,5	2,5	77,0	92,0	46,0	223,0
7,0	Sheen	2,0	1,5	2,0	2,5	27,0	26,0	12,0	73,0
Average		2,0	1,0	2,8	2,6	49,4	73,0	22,4	153,2

Table 15 - Core 89B5

Core len.	Lab.	Os	Ir	Ru	Rh	Pt	Pd	Au	Total
7,0	Sheen	2,0	1,0	4,0	1,5	9,5	8,5	6,0	32,5
6,5	Sheen	2,0	2,0	2,0	3,0	33,0	41,0	12,0	95,0
6,0	Sheen	2,0	1,0	1,0	1,5	31,0	49,0	26,0	111,5
5,5	Sheen	2,0	0,5	1,5	1,0	19,0	22,0	34,0	80,0
5,0	Sheen	2,0	1,0	1,5	1,0	18,0	15,0	40,0	78,5
4,5	Sheen	2,0	2,0	3,0	2,5	20,0	12,0	4,0	45,5
4,0	Sheen	2,0	2,0	4,5	3,0	39,0	28,0	6,0	84,5
3,5	Sheen	2,0	0,5	0,5	0,5	12,0	12,0	4,0	31,5
Average		2,0	1,3	2,3	1,8	22,7	23,4	16,5	69,9

Table 16 - Core 89B9

Core len.	Lab.	Os	Ir	Ru	Rh	Pt	Pd	Au	Total
13,5	Sheen	2,0	0,5	3,0	1,5	9,0	9,5	2,0	27,5
13	Sheen	2,0	2,0	4,0	2,0	37,0	35,0	22,0	104,0
12	Sheen	2,0	1,0	2,5	1,0	25,0	27,0	18,0	76,5
11	Sheen	2,0	1,5	3,0	2,0	43,0	330,0	64,0	445,5
10	Sheen	2,0	1,5	3,0	1,5	27,0	33,0	26,0	94,0
9	Sheen	2,0	1,0	1,5	1,0	26,0	35,0	88,0	154,5
8	Sheen	2,0	2,0	2,0	1,0	30,0	32,0	70,0	139,0
7	Sheen	2,0	2,0	3,0	3,0	41,0	50,0	44,0	145,0
6	Sheen	2,0	1,5	4,0	2,0	37,0	140,0	94,0	280,5
5	Sheen	2,0	2,0	3,5	2,0	42,0	60,0	70,0	181,5
4	Sheen	2,0	1,5	3,5	2,0	30,0	41,0	38,0	118,0
3	Sheen	2,0	1,0	3,0	1,5	27,0	39,0	42,0	115,5
2	Sheen	2,0	1,0	3,0	2,0	20,0	37,0	24,0	89,0
1	Sheen	2,0	2,0	4,0	2,5	47,0	81,0	50,0	188,5
Average		2,0	1,5	3,1	1,8	31,5	67,8	46,6	154,2

Table 17 - Sulfide-rich horizons

Sample #	Lab.	Os	Ir	Ru	Rh	Pt	Pd	Au	Total
89lek9a	Sheen	2	18	20	45	890	2100	250	3325
89lek9c	Sheen	8	23	63	42	850	1700	110	2796
89lek21a	Sheen	4	25	75	44	500	1100	160	1908
89lek22	Sheen	2	20	50	27	440	1100	240	1879
89lek31	Sheen	20	63	120	42	550	820	62	1677
89lek21b	Sheen	2	17	41	33	460	910	66	1529
89lek6a	Sheen	20	13	26	14	200	790	180	1243
89lek18a	Sheen	2	13	22	15	360	580	84	1076
89lek21c	Sheen	2	11	29	22	310	530	78	982
89lek2d	Sheen	4	9	20	4	280	480	140	937
89lek1a	Sheen	6	12	28	9	2	780	24	860
89lek5a	Sheen	12	20	39	19	47	370	180	687
89lek27	Sheen	4	16	26	20	250	280	35	631
89lek21d	Sheen	2	7	21	15	200	350	28	623
89lek9b	Sheen	2	4	5	9	140	320	46	526
89lek16	Sheen	2	8	12	4	110	290	94	520
89lek30	Sheen	2	10	17	11	140	260	54	494
89lek11a	Sheen	4	12	16	9	120	180	42	383
89lek28b	Sheen	2	13	19	10	95	190	50	379
89lek8a	Sheen	6	9	10	6	110	160	48	348
89lek13a	Sheen	2	8	8	3	88	160	64	332
89lek26b	Sheen	6	8	9	5	51	150	82	311
89lek17a	Sheen	2	10	16	8	83	140	28	287
89lek24b	Sheen	2	13	30	9	83	120	12	269
89lek29	Sheen	2	10	14	7	73	130	24	260
89lek4e	Sheen	2	9	9	4	62	91	70	246
89lek20b	Sheen	2	9	14	7	63	99	20	213
89lek10a	Sheen	4	8	6	3	58	68	54	200
89lek7c	Sheen	8	8	6	4	41	58	64	189
89lek25b	Sheen	2	6	7	4	54	88	24	185
89lek14a	Sheen	4	9	7	4	44	71	38	176
89lek3a	Sheen	2	10	7	6	27	81	4	137
89lek19a	Sheen	2	7	5	3	38	39	32	125
89lek2a	Sheen	2	7	5	2	3	54	42	114
89lek23a	Sheen	2	7	6	3	25	45	14	102
89lek15	Sheen	2	7	5	2	20	25	34	95
89lek12a	Sheen	2	6	3	2	19	17	16	65

Table 18 - Chromitites Layered Series

Sample #	Lab.	Os	Ir	Ru	Rh	Pt	Pd	Au	Total
87P2	Sheen	130	83	260	55	640	1000	110	2278
87P3	Sheen	58	44	120	39	440	670	100	1471
87L8	Memorial	69,5	48,3	243,4	18,2	11,8	6,9	7,02	405,2
87L21A	Memorial	44,2	36,3	137,5	20,5	96,5	44,5	4,52	384,0
87L7	Memorial	96,8	80,9	174,2	16,1	2,3	0,7	4,82	375,8
87L7-D	Memorial	98,5	80,4	172,0	16,1	2,2	0,8	4,53	374,6
87L1B	Memorial	40,3	57,3	96,7	32,1	92,3	44,0	6,18	368,8
87L10C	Memorial	55,0	41,9	133,5	12,2	12,5	4,7	4,1	263,8
87L20A	Memorial	21,4	30,3	67,8	16,4	61,9	9,3	49,32	256,4
87L3C	Memorial	41,6	37,2	32,8	25,4	81,1	12,8	7,61	238,4
87L17	Memorial	31,0	29,8	77,1	8,6	40,3	25,7	1,86	214,3
87L3B	Memorial	37,6	38,5	69,7	16,8	24,7	10,9	5,74	204,0
87L3B-D	Memorial	39,5	38,0	68,5	16,8	24,7	10,8	5,48	203,8
87L5C	Memorial	51,8	33,2	77,1	8,0	9,7	8,2	4,87	192,9
87L18B	Memorial	34,2	23,5	105,5	7,2	7,6	9,8	2,43	190,1
87L5B	Memorial	31,2	25,9	73,6	7,9	11,1	13,5	3,35	166,6
87L4	Memorial	31,8	34,3	67,8	13,2	6,6	4,0	1,98	159,5
87L5A	Memorial	20,4	33,4	42,6	16,4	12,8	1,9	2,74	130,1
87L15	Memorial	4,1	4,1	7,6	2,4	28,3	44,9	5,77	97,2
87L3A	Memorial	18,3	18,7	32,7	7,0	8,1	1,0	2,83	88,7
87L12	Memorial	4,0	3,0	6,2	1,7	21,8	37,6	13,59	88,0

TABLE 19 XRF-ANALYSES

PRØVE NR.	SiO2	TiO2	Al2O3	FeO	MnO	MgO	CaO	V	Cr	Co	Ni	Cu	Zn	S
89lek1a	37,38	0,02	0,47	10,12	0,14	44,98	0,12	27	8354	141	1673	1360	21	0,097
89lek2a	38,31	0,02	0,23	10,16	0,14	46,38	0,20	19	6173	143	1410	1236	24	0,107
89lek2d	38,30	0,02	0,27	9,89	0,14	46,73	0,15	25	9044	139	1456	366	32	0,035
89lek3a	40,32	0,01	0,13	9,48	0,14	48,48	0,12	14	4298	135	1498	67	21	0,029
89lek4e	37,64	0,02	0,14	11,44	0,16	43,90	0,11	17	4778	151	1313	1706	28	0,125
89lek5a	38,10	0,02	0,26	11,36	0,15	45,36	0,12	28	7924	150	3090	1355	29	0,259
89lek6a	38,31	0,02	0,18	12,10	0,16	44,83	0,20	12	3326	156	2327	2532	22	0,234
89lek7c	38,36	0,01	0,16	11,83	0,16	45,19	0,30	11	2032	156	1601	1929	17	0,133
89lek8a	37,99	0,02	0,25	11,77	0,16	44,13	0,46	18	3511	154	1821	1123	28	0,118
89lek10a	38,20	0,01	0,19	11,80	0,16	44,73	0,53	11	2060	174	2417	2990	14	0,276
89lek11a	36,94	0,02	0,35	12,86	0,16	43,07	0,22	15	3772	161	2133	1595	28	0,236
89lek12a	38,69	0,01	0,14	11,72	0,15	45,37	0,25	13	2937	153	1270	1193	31	0,114
89lek13a	37,90	0,02	0,23	10,40	0,14	44,46	0,32	17	5035	151	2372	1564	24	0,263
89lek14a	38,23	0,02	0,19	12,88	0,17	44,19	0,16	15	3645	156	2066	1912	31	0,238
89lek15	38,40	0,01	0,12	12,33	0,16	45,59	0,21	11	2857	151	1403	855	36	0,044
89lek16	37,25	0,02	0,16	11,49	0,15	44,38	0,20	20	6379	152	1390	897	33	0,093
89lek17a	38,57	0,02	0,16	12,10	0,16	45,02	0,33	26	6238	150	2016	1378	32	0,179
89lek18a	37,05	0,02	0,28	13,14	0,17	43,13	0,41	25	5276	156	2124	1839	33	0,204
89lek19a	37,33	0,01	0,39	11,77	0,15	44,28	0,19	14	3586	154	2428	1183	29	0,209
89lek20b	37,94	0,02	0,16	12,13	0,16	44,57	0,20	16	3773	158	2474	832	33	0,227
89lek21a	36,56	0,02	0,22	12,73	0,16	42,02	0,32	21	5022	170	4778	4602	9	0,636
89lek22	36,52	0,01	0,06	10,70	0,14	43,17	0,22	9	3369	151	4920	1539	22	0,448
89lek23a	37,61	0,01	0,04	10,40	0,14	44,65	0,24	8	2869	141	1496	878	29	0,118
89lek24b	38,17	0,01	0,09	10,91	0,15	45,26	0,19	13	4494	141	1253	1175	27	0,095
89lek25b	37,63	0,02	0,27	12,70	0,16	43,55	0,34	20	4975	158	1972	1005	32	0,281
89lek26b	37,40	0,01	0,07	11,33	0,15	43,46	0,26	6	509	171	1978	4206	2	0,424
89lek27	37,60	0,02	0,58	13,02	0,18	41,23	0,91	33	4478	144	1744	1640	26	0,198
89lek28b	36,13	0,01	0,15	11,24	0,15	41,30	0,25	9	1583	167	2075	3621	3	0,244
89lek29	38,56	0,02	0,14	12,88	0,17	45,47	0,18	18	4499	150	1779	974	36	0,146
89lek30	38,96	0,01	0,07	12,23	0,16	45,76	0,12	5	1267	151	2749	2305	28	0,295
89lek31	40,18	0,02	0,37	10,07	0,15	47,17	0,06	15	2363	154	2956	1662	21	0,163
lek87-P1	27,43	0,29	5,25	23,14	0,28	25,22	<0.01	884	326633	157	288	101	206	0,016
lek88-1a	29,13	0,14	4,65	17,12	0,26	27,38	<0.01	1150	333020	108	588	85	152	0,001
lek88-1c	33,93	0,11	2,88	13,52	0,25	33,59	<0.01	956	256312	102	729	101	146	0,001
lek88-1e	41,48	0,01	0,61	8,79	0,15	40,10	0,64	82	3080	140	2083	133	73	0,001
lek88-2a	40,43	0,01	0,63	10,25	0,19	40,32	0,08	65	2797	181	2213	166	67	0,010
lek88-2c	41,55	0,01	0,82	8,36	0,15	40,65	1,45	83	2372	127	1953	101	61	0,005
lek88-2d	42,81	0,01	0,97	7,60	0,13	38,67	1,48	106	4679	113	1869	152	97	0,001
lek88-3d	41,95	0,05	1,06	9,94	0,25	34,33	<0.01	244	68364	148	1394	471	188	0,001
lek88-3g	42,15	0,01	0,66	8,02	0,15	40,28	0,75	81	2441	132	2005	112	58	0,003
lek88-3e	43,33	0,02	1,04	9,47	0,17	33,22	0,07	97	6826	152	675	246	49	0,001
lek88-3f	41,68	0,00	0,59	8,49	0,14	40,89	<0.01	61	2114	152	2391	119	65	0,001
lek88-4a	39,08	0,01	0,52	10,31	0,18	43,71	<0.01	86	14265	164	1875	80	70	0,007
lek88-4b	42,63	0,01	0,53	7,58	0,14	39,97	0,45	75	2650	127	1981	86	55	0,003
lek88-5a	37,56	0,04	5,39	10,70	0,15	41,47	<0.01	216	46778	111	1849	59	204	0,003
lek88-5b	38,01	0,04	4,98	10,44	0,16	42,50	<0.01	208	44409	118	1903	55	195	0,004
lek88-5c	38,27	0,04	4,80	10,78	0,16	41,17	<0.01	207	46069	125	1968	86	213	0,006
lek88-5d	39,43	0,01	0,37	10,30	0,17	43,22	<0.01	55	2177	172	2463	177	64	0,019
lek88-5f	46,39	0,03	1,41	7,05	0,11	21,54	13,91	193	6337	21	653	125	50	0,001
lek88-6b	40,38	0,00	0,30	9,40	0,17	43,06	<0.01	61	4390	175	2032	117	67	0,006
lek88-7a	38,57	0,04	5,29	9,93	0,13	41,22	<0.01	193	34414	111	1798	210	186	0,001
lek88-7b	41,19	0,01	0,74	8,45	0,15	41,89	<0.01	62	2306	144	2462	114	64	0,007
lek88-8c	42,38	0,01	0,66	7,83	0,15	40,42	0,51	85	2417	134	2040	131	79	0,007
lek88-8b	37,73	0,01	0,60	12,13	0,18	43,44	<0.01	75	7423	182	2375	113	75	0,001
lek88-3b	38,91	0,08	1,62	13,12	0,38	33,07	<0.01	372	129439	155	943	113	295	0,001
lek88-6c	42,78	0,01	0,72	7,53	0,15	39,19	1,20	92	2376	116	1888	136	80	0,001
lek88-1b	27,14	0,16	4,99	18,90	0,27	23,71	<0.01	1255	376691	112	457	66	153	0,001
lek88-1d	30,09	0,14	4,25	17,01	0,26	28,53	<0.01	1098	319695	115	492	49	143	0,001
lek88-2b	43,41	0,03	1,01	8,26	0,14	31,76	8,20	121	4620	67	1239	165	56	0,013
lek88-3a	39,45	0,09	1,64	12,64	0,38	33,59	<0.01	374	128120	157	955	96	290	0,001
lek88-3c	35,09	0,15	2,72	17,36	0,51	30,29	<0.01	543	218434	185	654	124	409	0,001
lek88-5e	44,04	0,01	0,57	6,62	0,14	39,16	<0.01	83	2766	124	1903	75	53	0,001
lek88-6a	38,78	0,03	1,09	12,17	0,22	41,07	<0.01	239	67801	191	1520	125	182	0,004
lek88-7c	42,01	0,01	0,79	8,17	0,14	40,03	0,60	82	2427	133	2128	89	57	0,009
lek88-8a	36,48	0,05	1,19	14,29	0,27	38,29	0,05	300	135124	164	1717	88	378	0,020
88B1-0.5	39,10	0,01	0,36	9,57	0,16	47,54	<0.01	63	6310	179	1823	40	30	0,015

TABLE 19 XRF-ANALYSES

88B2-5.0	38,56	0,01	0,25	11,07	0,18	45,75	0,08	57	5035	202	1392	80	57	0,025
88B2-5.5	38,72	0,01	0,23	10,67	0,17	45,90	0,05	55	4089	194	1483	92	60	0,028
88B2-6.0	38,88	0,01	0,23	10,42	0,17	45,85	0,16	54	3702	191	1494	123	65	0,042
88B2-6.5	38,98	0,01	0,24	10,38	0,18	46,26	0,17	54	3372	195	1479	104	64	0,068
88B2-7.0	38,80	0,01	0,26	10,35	0,17	46,71	0,12	60	5339	190	1587	129	80	0,117
88B2-7.5	38,66	0,01	0,26	10,82	0,17	45,64	0,14	57	4165	193	1633	105	55	0,044
88B2-8.0	39,18	0,01	0,25	10,36	0,17	45,31	0,34	58	3324	192	1543	91	49	0,026
88B2-8.5	38,63	0,01	0,29	11,24	0,18	45,66	0,09	59	4293	212	1516	192	95	0,018
88B2-9.0	38,23	0,01	0,30	11,53	0,18	45,63	0,07	60	5762	203	1465	233	82	0,011
88B2-9.5	38,18	0,01	0,25	12,32	0,19	45,19	0,23	55	3253	230	1453	295	81	0,029
88B2-10.0	38,57	0,01	0,26	11,87	0,19	45,33	0,24	54	2683	232	1448	168	67	0,021
88B2-10.5	38,21	0,01	0,29	12,28	0,19	45,19	0,40	58	3997	228	1419	146	69	0,011
88B2-11.0	38,11	0,01	0,28	12,36	0,19	45,39	0,24	58	4341	234	1580	539	75	0,038
88B2-11.5	38,12	0,01	0,30	12,21	0,18	45,75	0,08	59	4621	231	1485	532	87	0,053
88B2-12.0	38,42	0,01	0,29	11,54	0,18	46,34	0,06	58	4175	224	1538	209	87	0,012
88B2-12.5	38,46	0,01	0,26	11,72	0,19	46,01	0,08	54	3153	230	1430	219	108	0,001
88B2-13.0	38,36	0,01	0,33	11,76	0,18	45,64	0,07	62	6298	220	1278	116	72	0,001
88B2-13.5	38,56	0,02	0,38	10,76	0,18	46,02	0,04	82	13319	187	1271	83	64	0,005
88B2-14.0	39,08	0,01	0,35	10,08	0,17	46,08	0,01	73	8927	182	1338	234	125	0,008
88B2-14.5	39,17	0,01	0,34	9,60	0,16	46,97	0,01	62	5683	174	1377	137	75	0,007
88B2-15.0	38,98	0,01	0,33	9,80	0,16	47,07	0,01	69	7734	176	1417	127	70	0,010
88B2-15.5	39,02	0,01	0,30	9,78	0,16	47,40	0,01	65	6682	183	1542	155	84	0,015
88B2-16.0	39,28	0,01	0,29	9,45	0,16	47,49	0,01	63	6021	179	1572	161	85	0,018
88B2-16.5	39,25	0,01	0,28	9,34	0,16	47,54	0,01	61	5625	173	1675	70	34	0,038
88B2-17.0	38,91	0,01	0,29	9,68	0,16	47,21	0,01	64	6608	171	1763	76	40	0,030
88B2-17.5	38,57	0,03	0,57	9,62	0,16	46,63	0,01	126	27045	145	1760	45	36	0,046
88B2-18.0	36,96	0,06	1,21	10,25	0,17	45,58	0,01	259	79038	113	1380	63	72	0,055
88B2-18.5	38,17	0,04	0,76	9,57	0,16	46,24	0,01	170	48927	125	1628	103	77	0,038
88B2-19.0	38,24	0,04	0,75	9,47	0,16	46,13	0,01	161	45121	124	1652	135	90	0,038
88B2-19.5	37,99	0,04	0,74	9,89	0,16	46,24	0,01	163	45480	133	1662	114	81	0,032
88B2-20.0	38,22	0,03	0,73	9,59	0,16	46,76	0,01	147	39135	132	1779	137	89	0,035
88B4-0.5	39,00	0,02	0,47	13,06	0,18	44,09	0,58	29	3847	143	1205	89	44	0,023
88B4-1.0	41,70	0,03	0,78	10,79	0,15	38,81	4,41	54	4891	114	966	108	35	0,021
88B4-1.5	39,45	0,02	0,50	12,11	0,17	41,72	2,02	40	4097	133	1089	76	44	0,021
88B4.2.0	40,41	0,03	0,64	11,33	0,16	39,68	3,61	52	4408	120	1030	56	42	0,030
88B4-2.5	40,01	0,03	0,52	11,17	0,16	39,66	3,63	53	4189	120	1020	65	35	0,037
88B4-3.0	39,63	0,03	0,45	10,87	0,15	41,68	2,51	41	3331	126	1185	81	29	0,026
88B4-3.5	38,50	0,02	0,31	11,23	0,15	45,29	0,27	17	3012	141	1472	35	35	0,019
88B4-4.0	37,97	0,02	0,29	11,28	0,16	44,52	0,26	17	3604	141	1507	31	38	0,022
88B4-4.5	38,62	0,02	0,26	11,20	0,16	45,68	0,18	20	4403	142	1528	48	40	0,027
88B4-5.0	39,24	0,02	0,53	10,28	0,14	45,37	0,60	17	3138	140	1301	307	23	0,089
88B4-5.5	39,05	0,02	0,44	10,47	0,16	46,18	0,21	17	4065	142	1290	180	24	0,089
88B4-6.0	37,56	0,02	0,37	11,09	0,15	44,74	0,09	22	7393	138	1145	36	40	0,046
88B4-6.5	38,50	0,02	0,24	11,37	0,16	45,27	0,13	15	3611	144	1465	289	34	0,054
88B4-7.0	38,90	0,01	0,30	10,76	0,15	45,52	0,40	16	2854	145	1397	1536	13	0,118
88B4-7.5	38,05	0,02	0,45	10,78	0,15	44,98	0,23	19	6160	142	1348	109	37	0,016
88B4-8.0	37,45	0,02	0,44	10,84	0,15	44,37	0,10	20	6506	142	1466	99	38	0,017
88B4-8.5	37,52	0,02	0,51	11,00	0,15	44,24	0,11	20	4966	140	1668	26	36	0,032
88B4-9.0	37,31	0,02	0,26	11,27	0,15	44,16	0,22	20	5596	141	1863	20	37	0,014
88B4-9.5	37,22	0,02	0,32	11,26	0,15	44,06	0,15	25	6216	138	1930	13	37	0,017
88B4-10.0	37,60	0,02	0,26	11,32	0,15	44,32	0,25	23	6703	137	1974	14	38	0,016
88B6-1	39,05	0,02	0,77	12,34	0,17	40,08	2,24	47	4511	128	1199	71	39	0,029
88B6-2	37,38	0,02	0,33	13,54	0,18	41,04	0,65	25	3510	143	1429	63	43	0,031
88B6-3	40,49	0,03	0,68	9,89	0,14	36,11	4,85	52	3851	106	874	260	25	0,052
88B6-4	46,29	0,04	1,08	6,16	0,11	29,02	11,87	83	5123	47	520	247	12	0,024
88B6-5	42,14	0,03	0,59	8,83	0,13	37,18	5,50	54	3868	99	917	270	23	0,045
88B6-6	45,71	0,03	0,85	5,83	0,10	31,68	10,36	70	4226	48	578	278	11	0,036
88B6-7	46,27	0,04	1,01	4,99	0,09	28,02	13,16	80	5084	29	496	490	7	0,023
88B6-8	41,21	0,03	0,48	7,60	0,12	37,77	5,65	49	5395	85	767	175	19	0,023
88B6-9	38,39	0,02	0,18	10,83	0,15	44,06	0,27	14	3630	140	1279	27	33	0,039
88B6-10	38,37	0,02	0,18	9,95	0,14	44,75	0,26	17	5242	134	1399	29	34	0,030
88B6-11	38,02	0,01	0,10	9,93	0,14	44,62	0,21	15	5217	133	1623	23	31	0,020
88B6-12	38,18	0,02	0,17	9,73	0,13	44,54	0,33	16	4333	130	1987	18	32	0,013
88B6-13	37,16	0,02	0,15	9,52	0,13	43,41	0,17	12	3922	128	1984	14	31	0,018
88B6-14	38,93	0,02	0,14	9,54	0,13	45,92	0,20	13	4104	131	2110	18	31	0,022
88B6-16	38,11	0,01	0,10	9,73	0,13	45,61	0,16	11	4497	132	2391	15	31	0,012
88B6-17	38,15	0,01	0,09	9,64	0,13	45,60	0,26	12	4161	133	2373	26	30	0,009

TABLE 19 XRF-ANALYSES

88B6-18	38,17	0,01	0,11	9,78	0,13	45,74	0,20	13	5086	134	2304	16	33	0,003
88B6-19	37,88	0,02	0,11	9,94	0,14	45,23	0,19	15	5203	134	2115	16	32	0,016
88B6-20	38,29	0,01	0,12	9,70	0,13	45,90	0,19	15	5013	132	2099	14	31	0,013

5. Platinum-group minerals in the Lillefjellklumpen nickel-copper deposit, Nord-Trøndelag,Norway by A.Grønlie, published in Norsk Geologisk Tidsskrift in 1988.

Platinum-group minerals in the Lillefjellklumpen nickel–copper deposit, Nord-Trøndelag, Norway

ARNE GRØNLIE

Grønlie, Arne: Platinum-group minerals in the Lillefjellklumpen nickel-copper deposit, Nord-Trøndelag, Norway. *Norsk Geologisk Tidsskrift*, Vol. 68, pp. 65–72. Oslo 1988. ISSN 0029-196X.

The Lillefjellklumpen Ni–Cu deposit occurs in the Gjersvik Nappe in the Upper Allochthon of the central Norwegian Caledonides. The area has been interpreted by earlier workers as part of an ensimatic island arc of Lower to Middle Ordovician age. The mineralization is associated with a small body of metagabbro occurring at the contact between gabbro and greenstone. The massive sulphide body consists of pyrrhotite, pyrite, pentlandite, chalcopyrite, magnetite and silicates. The average Ni content is 3.6% and the Cu content is 1.2%. The total platinum group element (PGE) content is 5.6 ppm. Pt (1.8 ppm) and Pd (3.1 ppm) accounting for 4.9 ppm. The Pt + Pd/Ru + Ir + Os ratio is 9.8, within the range reported for gabbro related deposits. The average chondrite normalized PGE pattern is similar to that of the Kanichee deposit although Lillefjellklumpen has lower absolute PGE values. Merenskyite is the main platinum-group mineral (PGM), but sperrylite, moncheite and temagamite (?) also occur. The PGM occur as small (<20 μm) inclusions in pyrrhotite and chalcopyrite as well as on grain boundaries. The Lillefjellklumpen deposit probably represents a magmatic sulphide segregation related to a layer 3 (ensimatic) gabbro body later remobilized during a tectonic event and redeposited in its present position.

Arne Grønlie, Norges geologiske undersøkelse, Postboks 3006, N-7002 Trondheim, Norway.

The Lillefjellklumpen Ni–Cu deposit is located in the Grong area, 5 km north of the Skorovas Mine and 200 km NE of Trondheim. The high PGE content of the deposit has been known since Foslie & Johnson Høst (1932), during a noble metal investigation on ores from the Grong area, found Lillefjellklumpen massive sulphides to contain 4 ppm PGE. As no PGE could be found on optical inspection, it was assumed that most of the PGE probably occurred in solid solution within the chalcopyrite lattice. The aim of this investigation was, with the help of the electon microprobe, to try to solve the problem of PGE occurrence and to identify any PGM that might be present. The electron microprobe was chosen because the PGE, if present, obviously had to occur as very small grains and, for identification purposes, as the optical properties of many of the minerals in question are very similar.

The geology of the area has been described by Halls et al. (1977) and by Reinsbakken (1980). The Lillefjellklumpen deposit is situated in the greenstone sequence of the Gjersvik Nappe (Fig. 1), which constitutes the low-grade, uppermost unit of the Seve-Køli Nappe Complex. In the west structurally above the Gjersvik Nappe lie the higher grade rocks of the Helgeland Nappe Complex. To the east are lower tectonic units of the Køli Nappe sequence. To the north and south the Grong area is limited respectively by the Børgefjell basement window and the Grong–Olden basement culmination. The main rocks of the Gjersvik Nappe are gabbro, diorite and trondhjemitic plutons and a sequence of submarine volcanics. The igneous complex is overlain by polymict conglomerates and flysch sediments. According to Reinsbakken (1980) the eruptive sequence is interpreted as an ensimatic island arc, formed to the west of the Fennoscandian continent probably during Lower to Middle Ordovician times, and thrust southeastward onto the Fennoscandian continent during the Silurian.

The Lillefjellklumpen deposit occurs at the boundary between a small metagabbro body and greenstone. Three small gabbros are found to crop out in the vicinity of the deposit (Palmer 1972). The metagabbros are surrounded by a group of greenstones with dykes of quartz keratophyre. The greenstones plot in the OFB and LKT fields of Ti–Zr–Y diagrams and show flat, MORB-like, chondrite-normalized REE patterns (Grønlie & Haugen, in prep.). The REE patterns show a striking similarity to the massive Storøya lava flows of the Leka ophiolite (Prestvik 1985).

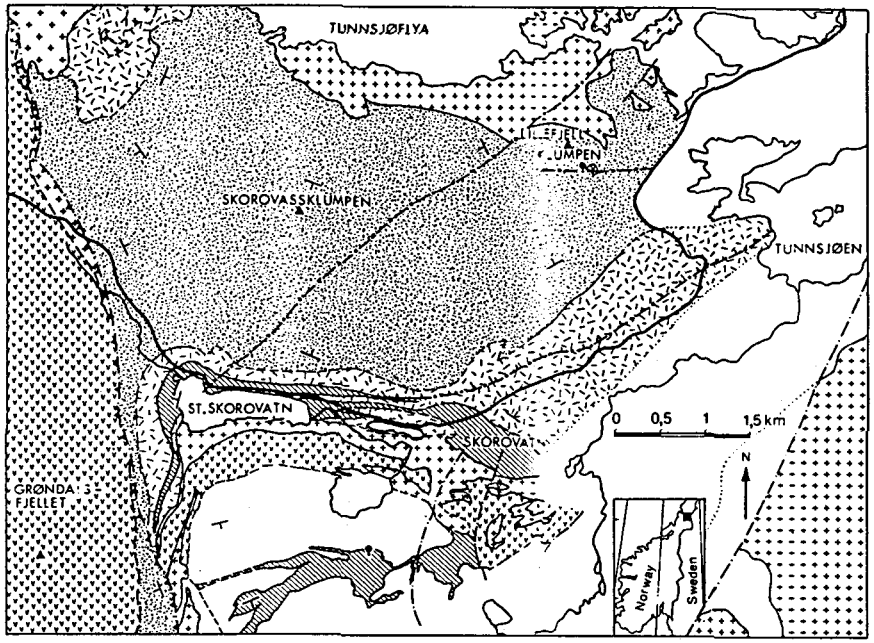

Fig. 1. Simplified geological map of the Lillefjellklumpen–Skorovatn area, based on Halls et al. (1977), Kollung (1979) and A. Reinsbakken (pers. comm. 1984).

Ore geology

The Lillefjellklumpen mineralization consists of an irregular lens of massive sulphides, trending east–west and dipping steeply to the north. The length of the massive sulphide ore is 20 m, and it is up to 2 m wide. The contact against the hanging-wall metavolcanics and the foot-wall metagabbro is always sharp. There are some small angular fragments of greenstone in the ore. Except for the immediate contact zone the sulphide lens is nearly free from gangue minerals. The average Ni content of massive sulphide is 3.6% and the Cu content is 1.2% (Table 1), in good agreement with figures published by Foslie & Johnson Høst (1932); consequently no new modal analyses have been done. Foslie & Johnson Høst estimated the modal composition to be: pyrrhotite (64%), pyrite (15%), pentlandite (12%), chalcopyrite (3%), magnetite (3%) and silicates (2%). There are two distinct ore types, although pyrrhotite is always the most abundant mineral.

1. Pyrrhotite ore, the dominant ore type, consists of pyrrhotite, pentlandite and magnetite. Pyrite and chalcopyrite are not abundant, although pyrite sometimes occurs as rounded grains up to 5 mm across in a groundmass of the other sulphides.
2. Pyrrhotite–chalcopyrite ore occurs less frequently than the pyrrhotite ore. Anhedral chalcopyrite makes up a significant portion of the ground-mass or occurs as a network of veins. This ore type seems to predominate at the margins of the deposit.

The sulphide mineralogy has been described by Foslie & Johnson Høst (1932) and recently by Palmer (1972).

Table 1. Content of Cu, Ni, S (%) and PGE + Au (ppb) in massive sulphide ore.

	Cu	Ni	S	Pt	Pd	Rh	Ru	Ir	Os	Au	Sum PGE + Au
X	1.2	3.6	36.2	1799	3068	214	189	170	139	219	5798
SD	0.9	0.7	2.1	1856	1156	99	100	86	76	445	
N	15	15	15	18	18	10	10	10	10	18	
C1C				1020	545	200	690	540	514	152	

C1C = C1-Chondrites, data from Naldrett (1982).
Cu/Cu + Ni = 0.25 Pt + Pd/Ru + Ir + Os = 9.77.

Platinum-group minerals

Foslie & Johnson Høst (1932) found no discrete PGM with conventional optical methods, but Palmer (1972) recognized one grain of a PGM enclosed in pyrrhotite. The observed PGM, in decreasing order of abundance, are:

Merenskyite (ideal formula $PdTe_2$)
Sperrylite ($PtAs_2$)
Moncheite (ideal formula $PtTe_2$)
Mercurian palladium telluride (temagamite (?) Pd_3HgTe_3)

Merenskyite, ideal $PdTe_2$, general (Pd, Pt, Ni)(Te,Bi)$_2$ is by far the most abundant PGM. The analysed grains are all platinian-bismuthian merenskyite (Fig. 2). The mineral usually occurs as small (<20 μm) hexagonal or rounded grains. The most frequent mode of occurrence is as inclusions in pyrrhotite (Fig. 3) on grain boundaries in pyrrhotite aggregates, or on boundaries between pyrrhotite and chalcopyrite grains. Merenskyite also occurs embedded in late chalcopyrite replacing pyrrhotite (Fig. 4) or exsolved from chalcopyrite (Fig. 3). All observed grains, except one containing a small inclusion of temagamite (?) are apparently homogeneous. Merenskyite forms a complete solid solution series with moncheite (Hoffman & MacLean 1976). Data from Lillefjellklumpen illustrate this (Fig. 2).

Sperrylite, $PtAs_2$, occurs less frequently than merenskyite. The mineral has previously been identified in this ore by Hysingjord (Neumann *1985*). Sperrylite, generally euhedral, is commonly found enclosed in chalcopyrite, but also occurs as inclusions in pyrrhotite.

Moncheite, ideal $PtTe_2$, general (Pt, Pd, Ni)(Te, Bi)$_2$. Only two grains have been identified, only one being large enough for microanalysis. This 10 μm grain occurred embedded in silicates replacing chalcopyrite in type 2 ore. The other, being only 5 μm, occurred at the contact between two pentlandite grains.

Mercurian palladium telluride, occurring as a <5 μm inclusion in merenskyite, again enclosed in pyrrhotite, gave an electron microprobe analysis close to (Pd, Hg)Te. This mineral is probably temagamite (Pd_3HgTe_3). Previously, Buchan (1981) reported an occurrence of kotulskite intergrown with a Pd–Hg–Te mineral, possibly temagamite, from the Fæøy deposit, southwest Norway.

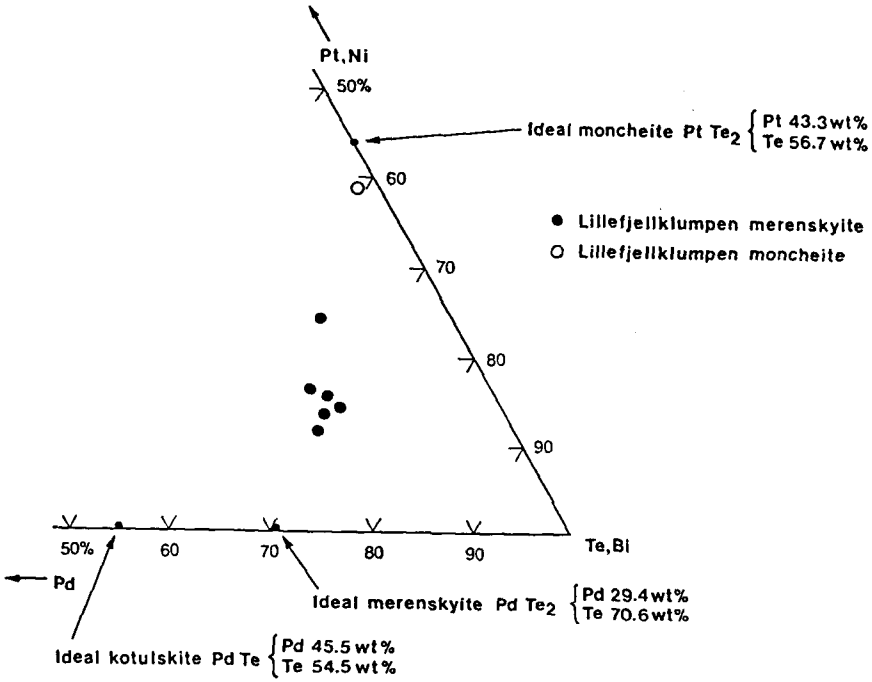

Fig. 2. Compositional variation in Lillefjellklumpen merenskyite and moncheite compared with the ideal mineral compositions.

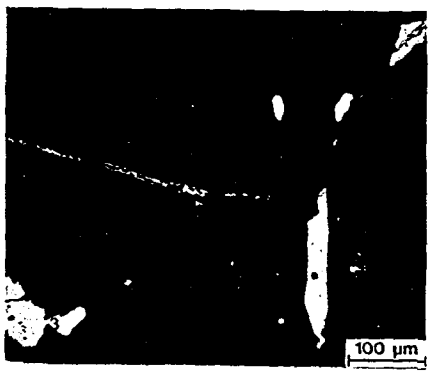

Fig. 3. Three merenskyite grains (white) occurring as: (1) Inclusion in pyrrhotite (dark grey); (2) on grain boundary pyrrhotite/pyrrhotite, and (3) exsolved from chalcopyrite (grey). Backscatter electron image.

Platinum-group element chemistry

Eighteen samples of massive sulphide ore have been analysed for PGE and Au by neutron activation analyses (X-Ray Assay and Chemex Labs., Canada). Cu, Ni and S have been analysed at the Geological Survey of Norway by atomic absorption and fire-assay. The analyses show an average total content of 5.8 ppm PGE + Au, Pd and Pt accounting for 4.9 ppm (Table 1). It is evident (Table 2) that the analyses show a bimodal distribution of Pt and Pd, there being one dominant group where Pd ≫ Pt and one group where Pt > Pd. This roughly reflects the amount of chalcopyrite in the original ore samples, the Pd ≫ Pt group corresponding with the pyrrhotite (type 1) ore and the Pt > Pd group corresponding with the pyrrhotite–chalcopyrite (type 2) ore as defined in a previous section.

Fig. 4. Chalcopyrite (grey) containing euhedral merenskyite (white) replacing pyrrhotite (dark grey). Backscatter electron image.

This is contrary to what one finds at Levack West, Sudbury, where the Cu-rich (28%) stringer ores are more enriched in Pd than Pt, and total PGE-contents are high (Hoffman et al. 1979).

As at Strathcona, the Cu-rich (32%) ore zone is more enriched in Pt than Pd, but the total PGE contents are very low. Cu-rich stringers analogous to those at Levack West, however, were not investigated (Naldrett et al. 1982).

The Levack West stringers do, however, contain more than 20 times as much Cu as Lillefjellklumpen type 2 ore and the ores are therefore not readily comparable. The mechanism of thermal diffusion explaining metal zoning at Levack, favoured by Hoffman et al. (1979), cannot have been operative to the same degree at Lillefjellklumpen, perhaps because of this orebody's small size and tectonic emplacement (see Discussion).

The chondrite normalized PGE pattern (Fig. 5) does show a close similarity to the main trend of the Sudbury ores, suggesting a general genetic similarity.

Discussion

Four main possible origins are considered for the mineralization:

1. The sulphides and PGE represent a magmatic segregation, having settled out of the magma in their present position.
2. The sulphides and PGE represent a magmatic segregation, but settled out of the magma elsewhere and were remobilized during tectonic disturbances, possibly while the sulphides were still fluid.
3. The sulphides and PGE have been mobilized from a lower level in the oceanic crust, the simatic foundation of the Gjersvik island arc, by hydrothermal activity, and deposited in a zone of dilation.
4. The deposit is volcanic exhalative, the sulphides and PGE being leached out of the host rocks by circulatory brines discharged through sea-floor fumaroles and precipitated on the sea floor.

Considering *alternative 1*, this represents the traditional interpretation of the origin of massive Ni–Cu sulphide ores. Cabri & Laflamme (1976) in a study of PGE behaviour in Sudbury ores, maintain that the Pd and Pt bismuth-tellurides concentrated in a Cu-rich liquid fractionated relative to monosulphide solid solution (*mss*), following crystallization of mss and magnetite. The subsequent crystallization of intermediate solid solution (*iss*) with a coexisting liquid rich in Pd–Pt–Te–Bi–Sb on further cooling produced the PGM now observed in the ores. Melting temperatures for $PdTe_2$ (740°C) and $PtTe_2$ (825–900°C) indicate that they would be liquid when *iss* crystallized out of a Cu-rich sulphide melt. At Lillefjellklumpen much of the Pd-Pt bismuth-tellurides, arsenides and Au have fractionated into a Cu-rich liquid, as sperrylite, electrum and much merenskyite are either inclusions in, or found bordering on, chalcopyrite grains. The other Pd–Pt bismuth-tellurides occur either enclosed in pyrrhotite or on grain boundaries in pyrrhotite; this could be interpreted as a trapping of most of the Pd–Pt–Te–Bi elements in the mss structure due to rapid cooling of the sulphides. This could also explain why merenskyite and moncheite are the only Pd–Pt bismuth-tellurides present. Because of later metamorphism the sulphides, however, show no textural evidence of the rapid cooling of the orebody.

Counter to a straightforward magmatic origin is the fact that the gabbro body with which the mineralization is now associated is very small (Fig. 1), and it is unlikely that it could have hosted

Table 2a and 2b. Content of Cu, Ni, S (%) and PGE + Au (ppb) in type 1 and type 2 ore.

Table 2a. Type 1 Ore, Pd ≫ Pt.

Sample no.	Cu	Ni	S	Pt	Pd	Rh	Ru	Ir	Os	Au
8501	0.30	2.53	39.2	290	2900	240	190	190	220	18
8502	1.29	3.07	37.0	710	3100	330	330	290	250	54
8504	1.25	3.52	33.2	580	4100	50	30	30	23	120
8505	0.15	4.33	36.5	460	4600	270	220	210	170	8
8507	0.53	4.04	34.8	1500	3300	180	180	160	110	460
8508	2.26	3.09	39.8	1500	2500	230	210	180	120	300
8510	0.48	4.02	35.6	2100	3400	200	190	180	110	140
SF10	0.22	4.00	37.9	200	4200					<10
1179	—	—	—	<100	4700					<10
1187	—	—	—	1180	3230					1910
1209	—	—	—	455	3600					<10
$\bar{X}$	0.8	3.6	36.8	820	3603	214	193	177	143	275
SD	0.7	0.6	2.2	654	710	87	88	77	77	562

Table 2b. Type 2 Ore, Pt > Pd.

Sample no.	Cu	Ni	S	Pt	Pd	Rh	Ru	Ir	Os	Au
8503	0.53	4.74	36.2	4100	2200	310	280	240	170	15
8506	0.54	2.98	36.5	5900	2900	280	250	210	190	9
8509	1.26	3.46	32.8	5500	4000	45	<21	14	26	350
SF01	2.10	3.10	37.1	1500	1500					250
SF03	2.85	3.01	33.0	700	410					60
SF05	1.11	4.38	37.1	1330	1250					<10
SF07	2.82	3.07	36.0	4330	3330					225
$\bar{X}$	1.6	3.5	35.5	3337	2227	212	180	155	129	131
SD	1.0	0.7	1.8	2128	1265	145	148	123	89	142

the amount of sulphides in question. It is also unlikely that the sulphides originated at this high level position in the body and were deposited together with the volcanic extrusives, the gabbroic (layer 3; Tarling 1981) and ultramafic layers at deeper levels being a more probable setting for a deposit with this Ni and Cu content.

Alternative 2, that the ore is of magmatic origin, but later remobilized by a tectonic disturbance and brought to its present position, possibly while still fluid, seems to be in agreement with mineralogical and textural evidence, and is also able to explain the orebody's present location. As mentioned previously, the trapping of many of the Pd–Pt–Bi–Te elements in the *mss* structure indicates a rapid cooling of the sulphides, possibly after the emplacement of the sulphides in their present position by a tectonic event.

Considering *alternative 3*, the chondrite-normalized PGE and Au pattern (Fig. 5) show that Lillefjellklumpen exhibits a positive slope rather similar to the Sudbury deposits and almost identical with the pattern for the Kanichee deposit which occurs at the base of a tholeiitic layered intrusion (Naldrett 1982). The Pt + Pd/Ru + Ir + Os ratio, which is dependent on this ratio in the silicate magma at time of saturation is 9.8, within the range reported for gabbro-related deposits (Naldrett 1982).

Several ophiolites have recently been investigated with respect to PGE content in rocks and sulphide deposits. Economou & Naldrett (1984) studied the sulphide bodies occurring in ultramafic ophiolitic rocks at Eretria. They suggested that the sulphides and PGE were precipitated by hydrothermal fluids, possibly those responsible

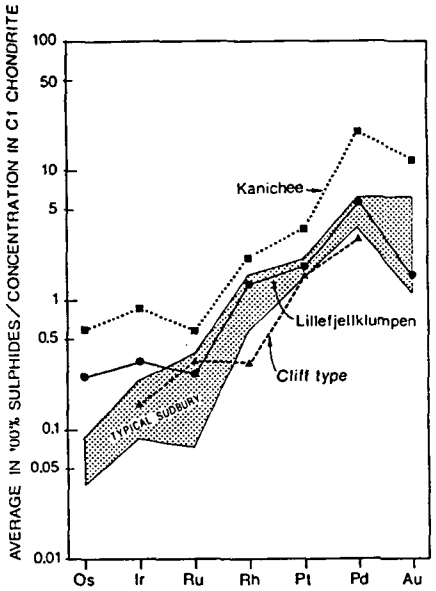

Fig. 5. Chondrite-normalized PGE and Au concentrations for Lillefjellklumpen compared with other gabbro related deposits (Naldrett 1982) and the Cliff deposit (Gunn et al. 1985).

for the serpentinization of the host rocks, and that the source of the metals could have been the ultramafic rocks themselves. In the Unst ophiolite, the Cliff deposit (Gunn et al. 1985) is dominated by Pd and Pt and has a PGE pattern with a positive slope (Fig. 5), being similar to those of the Sudbury deposits, or Lillefjellklumpen. They interpret the Cliff PGM which occur in close association with Ni sulphides and arsenides as being hydrothermal in origin, most likely connected with serpentinization. Fleet et al. (1977) and Fleet & MacRae (1983) have argued that most Ni–Cu deposits have been precipitated by hot aqueous fluids. Using Ir and Pd values as discriminants between different types of Ni–Cu deposits (Keays et al., 1982), the Lillefjellklumpen values for Ir and Pd place this deposit on the trend line for magmatic Ni–Cu deposits (Fig. 6), distinctly removed from hydrothermal or volcanic exhalative deposits, which are very low in Ir. Mineralogically, hydrothermal deposits tend to be highly copper-enriched, like the Eretria deposit (Economou & Naldrett 1984), which has

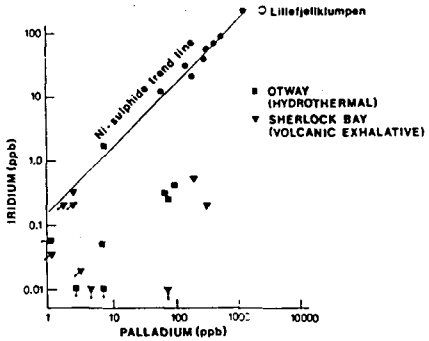

Fig. 6. Pd and Ir contents of major Ni-sulphide deposits of western Australia (Keays et al. 1982) define a Ni-sulphide trend line, close to which analyses from the Lillefjellklumpen deposit plot.

a Cu/Cu + Ni ratio of 0.78 or the New Rambler Mine (McCallum et al. 1976), where Pd and Pt are associated with copper sulphides occurring in shear zones. The Eretria deposit has a chondrite-normalized PGE pattern distinctly different from the Lillefjellklumpen deposit, the Eretria pattern being flat with a pronounced negative Pd anomaly.

Alternative 4, that the metals were leached out of the gabbro and greenstone in the vicinity of the deposit by a hydrothermal cell driven by the igneous activity in the island-arc system, is difficult to evaluate unless one knows the content of PGE in the greenstones and gabbros likely to be affected by the hydrothermal system. Generally MORB have extremely low contents of PGE (Hertogen et al. 1980), and the volcanic exhalative model does not seem to be a likely alternative. Keays et al. (1982) showed that the volcanic exhalative Sherlock Bay Ni–Cu deposit plotted well off the Ir–Ni and Ir–Pd trend line for the other magmatic Ni–Cu deposits on which Lillefjellklumpen plots.

Conclusions

The Lillefjellklumpen deposit probably represents a magmatic sulphide segregation related to an ensimatic gabbro body later remobilized during a tectonic event and redeposited in its present position. The chondrite-normalized PGE

and Au pattern (Fig. 5) shows similarity to the Sudbury deposits and to gabbro-related deposits in general.

Textural and mineralogical evidence indicates that the sulphides could have been fluid when subject to the tectonic event. The orebody was later subject to a small-scale mobilization of silicates and chalcopyrite, particularly affecting the deposit margins, possibly related to the metamorphism of the host rocks.

The main platinum-group mineral is merenskyite, followed by sperrylite and moncheite. Lillefjellklumpen is the only Ni–Cu–PGE deposit described in which merenskyite is the dominant PGM, a fact that could be due to rapid cooling of the liquid sulphides after emplacement. The PGE content, dominated by Pd, is also consistent with a magmatic origin.

Acknowledgements. – I thank Sarah-Jane Barnes, Rognvald Boyd and Jan Sverre Sandstad for invaluable comments on the manuscript and for correcting the English text. Gunnar Juve and Heikki Papunen reviewed the manuscript and gave constructive comments.

Manuscript received October 1986

References

Buchan, R. 1981: Mineralogical examination of 4 samples from Fæoy Ni deposit, Norway. Mineralogy Report No. 1180. Falconbridge Metallurgical Laboratories. 2 pp., unpubl. rep.

Cabri, L. J. & Laflamme, J. H. G. 1976: The mineralogy of the platinum group elements from some copper–nickel deposits of the Sudbury area, Ontario. *Economic Geology 71*, 1159–1195.

Economou, M. I. & Naldrett, A. J. 1984: Sulfides associated with podiform bodies of chromite at Tsangli, Eretria, Greece. *Mineralium Deposita 19*, 289–297.

Fleet, M. E., MacRae, N. D. & Hertzberg, C. T. 1977: Partition of nickel between olivine and sulfide: A test for immiscible sulfide liquids. *Contributions to Mineralogy and Petrology 65*, 191–197.

Fleet, M. E. & MacRae, N. D. 1983: Partition of Ni between olivine and sulfide and its application to Ni–Cu sulfide deposits. *Contributions to Mineralogy and Petrology 83*, 78–81.

Foslie, S. & Johnson Høst, M. 1932: Platina i sulfidisk nikkelmalm. *Norges geologiske undersøkelse 137*, 77 pp.

Gunn, A. G., Leake, R. C. & Styles, M. T. 1985: Platinum-group element mineralization in the Unst ophiolite, Shetland. *Mineral Reconnaissance Programme. Report British Geological Survey No. 73.*

Halls, C., Reinsbakken, A., Ferriday, I. & Rankin, A. 1977: Geological setting of the Skorovas orebody within the allochthonous volcanic stratigraphy of the Gjersvik Nappe. *Spec. Paper No. 7. IMM-Geological Society of London*, 128–151.

Hertogen, J., Janssens, M. J. & Palme, H. 1980: Trace elements in ocean ridge basalt glasses: Implications for fractionations during mantle evolution and petrogenesis. *Geochimica and Cosmochimica Acta 44*, 2125–2143.

Hoffman, E. L., Naldrett, A. J., Alcock, R. A. & Hancock, R. G. V. 1979: The noble-metal content of ore in the Levack West and Little Stobie Mines, Ontario. *Canadian Mineralogist 17*, 437–451.

Hoffman, E. & MacLean, W. H. 1976: Phase relations of michenerite and merenskyite in the Pb–Bi–Te system. *Economic Geology 71*, 1461–1468.

Keays, R. R., Nickel, E. H., Groves, D. I. & McGoldrick, P. J. 1982: Iridium and Palladium as discriminants of volcanic-exhalative, hydrothermal, and magmatic nickel sulphide mineralization. *Economic Geology 77*, 1535–1547.

Kollung, S. 1979: Stratigraphy and major structures of the Grong District, Nord-Trøndelag. *Norges geologiske undersøkelse 354*, 1–51.

Naldrett, A. J. 1982: Platinum-group element deposits. *In* Cabri, L. J. (ed.): Platinum-Group Elements: Mineralogy, geology, recovery. *CIM Special Volume 23*, 197–231.

Naldrett, A. J., Innes, D. G., Sowa, J. & Gorton, M. P. 1982: Compositional variations within and between five Sudbury deposits. *Economic Geology 77*, 1519–1534.

Neumann, H. 1955: The minerals of Norway. *Norges geologiske undersøkelse, Skrifter 68*, 1–278.

Palmer, Q. G. 1972: *The geology of eastern Skorovasklumpen and the geology of the Lillefjellklumpen copper/nickel sulphide assemblage.* B.Sc. thesis, Royal School of Mines, Imperial College, University of London.

Prestvik, T. 1985: Origin of the volcanic Storøya Group, Leka. Results from new geochemical investigations. *Norsk Geologisk Tidsskrift 65*, 237–239.

Reinsbakken, A. 1980: Geology of the Skorovass Mine: a volcanogenic massive sulphide deposit in the central Norwegian Caledonides. *Norges geologiske undersøkelse 360*, 123–154.

Tarling, D. H. 1981: The Crust of the Earth. *In* Smith, D. G. (ed.): *The Cambridge Encyclopedia of Earth Sciences.* Cambridge University Press, Cambridge.